National Library of Canada
Acquisitions and Bibliographic Services Branch
395 Wellington Street
Ottawa, Ontario
K1A 0N4

Bibliothèque nationale du Canada
Direction des acquisitions et des services bibliographiques
395, rue Wellington
Ottawa (Ontario)
K1A 0N4

Your file Votre référence

Our file Notre référence

NOTICE

The quality of this microform is heavily dependent upon the quality of the original thesis submitted for microfilming. Every effort has been made to ensure the highest quality of reproduction possible.

If pages are missing, contact the university which granted the degree.

Some pages may have indistinct print especially if the original pages were typed with a poor typewriter ribbon or if the university sent us an inferior photocopy.

Reproduction in full or in part of this microform is governed by the Canadian Copyright Act, R.S.C. 1970, c. C-30, and subsequent amendments.

AVIS

La qualité de cette microforme dépend grandement de la qualité de la thèse soumise au microfilmage. Nous avons tout fait pour assurer une qualité supérieure de reproduction.

S'il manque des pages, veuillez communiquer avec l'université qui a conféré le grade.

La qualité d'impression de certaines pages peut laisser à désirer, surtout si les pages originales ont été dactylographiées à l'aide d'un ruban usé ou si l'université nous a fait parvenir une photocopie de qualité inférieure.

La reproduction, même partielle, de cette microforme est soumise à la Loi canadienne sur le droit d'auteur, SRC 1970, c. C-30, et ses amendements subséquents.

Canada

EXTENSIONAL SHEAR ZONES AND LITHOTECTONIC DOMAINS IN THE SOUTHWEST GRENVILLE OROGEN: STRUCTURE, METAMORPHISM, AND U-PB GEOCHRONOLOGY OF THE CENTRAL GNEISS BELT NEAR POINTE-AU-BARIL, ONTARIO

by

John W.F. Ketchum

Submitted in partial fulfillment of the requirements
for the degree of Doctor of Philosophy

at

Dalhousie University
Halifax, Nova Scotia
December 1994

ISBN 0-612-08709-3

Name John William Ferguson Ketchum

Dissertation Abstracts International is arranged by broad general subject categories Please select the one subject which most nearly describes the content of your dissertation Enter the corresponding four-digit code in the spaces provided

Geology
SUBJECT TERM

0372
SUBJECT CODE

U·M·I

Subject Categories

THE HUMANITIES AND SOCIAL SCIENCES

COMMUNICATIONS AND THE ARTS
Architecture 0729
Art History 0377
Cinema 0900
Dance 0378
Fine Arts 0357
Information Science 0723
Journalism 0391
Library Science 0399
Mass Communications 0708
Music 0413
Speech Communication 0459
Theater 0465

EDUCATION
General 0515
Administration 0514
Adult and Continuing 0516
Agricultural 0517
Art 0273
Bilingual and Multicultural 0282
Business 0688
Community College 0275
Curriculum and Instruction 0727
Early Childhood 0518
Elementary 0524
Finance 0277
Guidance and Counseling 0519
Health 0680
Higher 0745
History of 0520
Home Economics 0278
Industrial 0521
Language and Literature 0279
Mathematics 0280
Music 0522
Philosophy of 0998
Physical 0523
Psychology 0525
Reading 0535
Religious 0527
Sciences 0714
Secondary 0533
Social Sciences 0534
Sociology of 0340
Special 0529
Teacher Training 0530
Technology 0710
Tests and Measurements 0288
Vocational 0747

LANGUAGE, LITERATURE AND LINGUISTICS
Language
- General 0679
- Ancient 0289
- Linguistics 0290
- Modern 0291

Literature
- General 0401
- Classical 0294
- Comparative 0295
- Medieval 0297
- Modern 0298
- African 0316
- American 0591
- Asian 0305
- Canadian (English) 0352
- Canadian (French) 0355
- English 0593
- Germanic 0311
- Latin American 0312
- Middle Eastern 0315
- Romance 0313
- Slavic and East European 0314

PHILOSOPHY, RELIGION AND THEOLOGY
Philosophy 0422
Religion
- General 0318
- Biblical Studies 0321
- Clergy 0319
- History of 0320
- Philosophy of 0322

Theology 0469

SOCIAL SCIENCES
American Studies 0323
Anthropology
- Archaeology 0324
- Cultural 0326
- Physical 0327

Business Administration
- General 0310
- Accounting 0272
- Banking 0770
- Management 0454
- Marketing 0338

Canadian Studies 0385
Economics
- General 0501
- Agricultural 0503
- Commerce Business 0505
- Finance 0508
- History 0509
- Labor 0510
- Theory 0511

Folklore 0358
Geography 0366
Gerontology 0351
History
- General 0578
- Ancient 0579
- Medieval 0581
- Modern 0582
- Black 0328
- African 0331
- Asia, Australia and Oceania 0332
- Canadian 0334
- European 0335
- Latin American 0336
- Middle Eastern 0333
- United States 0337

History of Science 0585
Law 0398
Political Science
- General 0615
- International Law and Relations 0616
- Public Administration 0617

Recreation 0814
Social Work 0452
Sociology
- General 0626
- Criminology and Penology 0627
- Demography 0938
- Ethnic and Racial Studies 0631
- Individual and Family Studies 0628
- Industrial and Labor Relations 0629
- Public and Social Welfare 0630
- Social Structure and Development 0700
- Theory and Methods 0344

Transportation 0709
Urban and Regional Planning 0999
Women's Studies 0453

THE SCIENCES AND ENGINEERING

BIOLOGICAL SCIENCES
Agriculture
- General 0473
- Agronomy 0285
- Animal Culture and Nutrition 0475
- Animal Pathology 0476
- Food Science and Technology 0359
- Forestry and Wildlife 0478
- Plant Culture 0479
- Plant Pathology 0480
- Plant Physiology 0817
- Range Management 0777
- Wood Technology 0746

Biology
- General 0306
- Anatomy 0287
- Biostatistics 0308
- Botany 0309
- Cell 0379
- Ecology 0329
- Entomology 0353
- Genetics 0369
- Limnology 0793
- Microbiology 0410
- Molecular 0307
- Neuroscience 0317
- Oceanography 0416
- Physiology 0433
- Radiation 0821
- Veterinary Science 0778
- Zoology 0472

Biophysics
- General 0786
- Medical 0760

EARTH SCIENCES
Biogeochemistry 0425
Geochemistry 0996
Geodesy 0370
Geology 0372
Geophysics 0373
Hydrology 0388
Mineralogy 0411
Paleobotany 0345
Paleoecology 0426
Paleontology 0418
Paleozoology 0985
Palynology 0427
Physical Geography 0368
Physical Oceanography 0415

HEALTH AND ENVIRONMENTAL SCIENCES
Environmental Sciences 0768
Health Sciences
- General 0566
- Audiology 0300
- Chemotherapy 0992
- Dentistry 0567
- Education 0350
- Hospital Management 0769
- Human Development 0758
- Immunology 0982
- Medicine and Surgery 0564
- Mental Health 0347
- Nursing 0569
- Nutrition 0570
- Obstetrics and Gynecology 0380
- Occupational Health and Therapy 0354
- Ophthalmology 0381
- Pathology 0571
- Pharmacology 0419
- Pharmacy 0572
- Physical Therapy 0382
- Public Health 0573
- Radiology 0574
- Recreation 0575
- Speech Pathology 0460
- Toxicology 0383

Home Economics 0386

PHYSICAL SCIENCES
Pure Sciences
Chemistry
- General 0485
- Agricultural 0749
- Analytical 0486
- Biochemistry 0487
- Inorganic 0488
- Nuclear 0738
- Organic 0490
- Pharmaceutical 0491
- Physical 0494
- Polymer 0495
- Radiation 0754

Mathematics 0405
Physics
- General 0605
- Acoustics 0986
- Astronomy and Astrophysics 0606
- Atmospheric Science 0608
- Atomic 0748
- Electronics and Electricity 0607
- Elementary Particles and High Energy 0798
- Fluid and Plasma 0759
- Molecular 0609
- Nuclear 0610
- Optics 0752
- Radiation 0756
- Solid State 0611

Statistics 0463

Applied Sciences
Applied Mechanics 0346
Computer Science 0984
Engineering
- General 0537
- Aerospace 0538
- Agricultural 0539
- Automotive 0540
- Biomedical 0541
- Chemical 0542
- Civil 0543
- Electronics and Electrical 0544
- Heat and Thermodynamics 0348
- Hydraulic 0545
- Industrial 0546
- Marine 0547
- Materials Science 0794
- Mechanical 0548
- Metallurgy 0743
- Mining 0551
- Nuclear 0552
- Packaging 0549
- Petroleum 0765
- Sanitary and Municipal 0554
- System Science 0790

Geotechnology 0428
Operations Research 0796
Plastics Technology 0795
Textile Technology 0994

PSYCHOLOGY
General 0621
Behavioral 0384
Clinical 0622
Developmental 0620
Experimental 0623
Industrial 0624
Personality 0625
Physiological 0989
Psychobiology 0349
Psychometrics 0632
Social 0451

TABLE OF CONTENTS

LIST OF FIGURES

CHAPTER 5

CHAPTER 6

LIST OF TABLES

ABSTRACT

A detailed field, structural, metamorphic, and U-Pb geochronologic study of para- and orthogneisses in the Central Gneiss Belt near Pointe-au-Baril, Ontario, provides important constraints on pre-Grenvillian metamorphism and late Grenvillian extensional deformation in the southwest Grenville orogen. The parautochthonous, polyorogenic Britt domain is overlain by the allochthonous Shawanaga domain (affected only by Grenvillian orogenesis) along a Grenvillian thrust detachment that was reactivated as a southeast-directed, ~3 km-wide, ductile extensional shear zone (the Shawanaga shear zone) late in the Grenvillian orogeny. The position of the overprinted thrust detachment is marked by an abrupt change in histories of structural and metamorphic development, felsic plutonism, and mafic dyke emplacement. Extensional displacement on the Shawanaga shear zone and on the smaller Nares Inlet shear zone (within the Britt domain) was contemporaneous with regional folding about axes parallel to the extensional transport direction. A segment of the Britt domain lying between the shear zones was decoupled from this folding event and preserves pre-Grenvillian granulite-facies assemblages and early Grenvillian tectonic fabrics.

Metamorphic *P-T* estimates for pre-Grenvillian granulites are distinct from those obtained from peak- and post-peak metamorphic Grenvillian assemblages in the Britt and Shawanaga domains. Grenvillian *P-T* paths for the domains are also distinct, but both have steep-trajectory segments indicating ~5 kbar of decompression, attributed to tectonic exhumation by extensional shear zones. Pelitic assemblages within the Shawanaga shear zone contain garnet porphyroblasts with strong compositional zoning and record an

'inverted' metamorphic isograd marked by the first appearance of sillimanite in kyanite + K-feldspar assemblages. Preservation of both features appears to be due in part to rapid cooling during extensional exhumation.

U-Pb zircon data from fresh granulite-facies assemblages indicate pre-Grenvillian metamorphism at *ca.* 1450-1430 Ma. Igneous crystallization ages of granitic pegmatite dykes in the Shawanaga shear zone suggest that extensional shearing was waning by 1020 Ma and had ceased by 990 Ma. The time of earlier thrusting is largely unconstrained but it may have occurred at *ca.* 1080 Ma. Concordant to weakly discordant U-Pb titanite analyses from the study area fall into three $^{207}Pb/^{206}Pb$ age groups (1028-1018 Ma, 1008-1000 Ma, and 967-956 Ma) that record initial cooling through the titanite closure temperature (~600°C), followed by at least two localized recrystallization and/or titanite growth events.

The contrasting tectonostratigraphic character and orogenic history of allochthonous and parautochthonous domains documented in this study has implications for the position of the Allochthon Boundary Thrust in the southwest Grenville orogen. The late Grenvillian history of the Pointe-au-Baril area resembles those documented in younger collisional orogens that have undergone important late orogenic extension, suggesting that this region may contain analogous, deep crustal structures that have not yet been exhumed in the younger belts.

ACKNOWLEDGEMENTS

Drs. N.G. Culshaw and R.A. Jamieson co-supervised this study and were both exceptionally generous with their time, insight, financial resources, encouragement, constructive criticism, and good company. To these individuals I owe a great deal of thanks. I particularly appreciate the good advice provided on numerous occasions by Dr. Jamieson and the opportunity to work in the field with Dr. Culshaw and Dr. A. Davidson of the Geological Survey of Canada, both of whom exhibit field skills in high-grade gneiss terranes that are second-to-none. Dr. J.V. Owen of St. Mary's University and Dr. L.M. Heaman of the University of Alberta served on the supervisory committee and contributed greatly toward improving the final version of this thesis, for which I am grateful.

I thank G. Brown and R. MacKay for technical assistance at Dalhousie University and M. Moore, Y.-Y. Kwok, and Drs. L.M. Heaman, T.E. Krogh, F. Corfu, R.D. Tucker, and D.W. Davis for collectively guiding me through the mysteries of U-Pb geochronology during my many visits to the Royal Ontario Museum.

To all my colleagues at Dalhousie University who have made the past few years both pleasurable and memorable, let's move to another university and do it all over again (...or perhaps just the pleasurable and memorable parts)! Highly-deserved accolades go to Charlie Walls and Marcus Tate for answering a plethora of computer questions as I struggled to become a part of the '90's. And last but not least, to Robbie Hicks, for your assistance during all stages of this project, and for simply putting up with me, a very heartfelt thanks.

CHAPTER 1

Introduction

1.1 CONCEPTUAL BASIS OF THE STUDY

The last decade has seen a conceptual revolution in our understanding of the Grenville orogen. This southeasternmost province of the Canadian Shield, long considered an enigmatic metamorphic terrane and poorly studied due to a lack of mineral wealth, is now recognized as the exhumed middle to deep crust of a large, *ca.* 1.2-1.0 Ga collisional orogen. This ~2000 km-long belt of mainly amphibolite and granulite facies gneiss has been compared to modern collisional orogens such as the Himalayas, but many details of Grenvillian orogenesis remain to be established before these comparisons can be fully endorsed.

The geology of the Grenville Province raises a number of important questions concerning the nature of middle and deep crustal deformation and metamorphism in this and other orogenic belts, namely: (*i*) Did ductile thrust zones accommodate significant transport of deep crustal thrust sheets, or was thickening and deformation primarily by widely distributed ductile flow? (*ii*) Do the wide expanses of high-grade rock represent a Grenvillian metamorphic terrane, or were some of these rocks metamorphosed during earlier orogenesis and uplifted with little Grenvillian overprinting? (*iii*) How much of the crust in the Grenville Province is allochthonous, and how much represents reworked Laurentian craton? (*iv*) What was the role, if any, of post-thrusting extension in thinning the crust during and immediately following Grenvillian compressional tectonism?

Questions like these need to be addressed before quantitative comparisons can be made between the Grenville Province and modern collisional orogens.

The present study is based in the Central Gneiss Belt of the western Grenville Province near Pointe-au-Baril, Ontario (Figs. 1.1, 1.2) where these and other questions can be addressed at least on a local scale. Previous work in this area has identified a ductile shear zone between allochthonous and parautochthonous terranes that accommodated both Grenvillian thrusting and extension. This area also preserves pre-Grenvillian metamorphic assemblages that illustrate the nature of the pre-Grenvillian crust and allow Grenvillian and pre-Grenvillian metamorphic assemblages to be contrasted.

1.2 BACKGROUND

The Grenville Province is exposed in Canada from the Labrador coast to central Ontario and as far south as the Adirondack Mountains of northern New York state (Fig. 1.1). Older (Archean and Paleoproterozoic) orogens of the Canadian Shield lie northwest of the Grenville Province whereas the Paleozoic Appalachian orogen and undisturbed Paleozoic cover rocks occur to the southeast.

The Grenville orogen comprises three fundamental parts: (*i*) a Parautochthonous Belt of reworked, polyorogenic, Archean to Mesoproterozoic gneiss that in places can be correlated with rocks in the Grenvillian foreland, (*ii*) an Allochthonous Polycyclic Belt of late Paleoproterozoic and early Mesoproterozoic terranes structurally overlying the Parautochthonous Belt, and (*iii*) an Allochthonous Monocyclic Belt of Mesoproterozoic

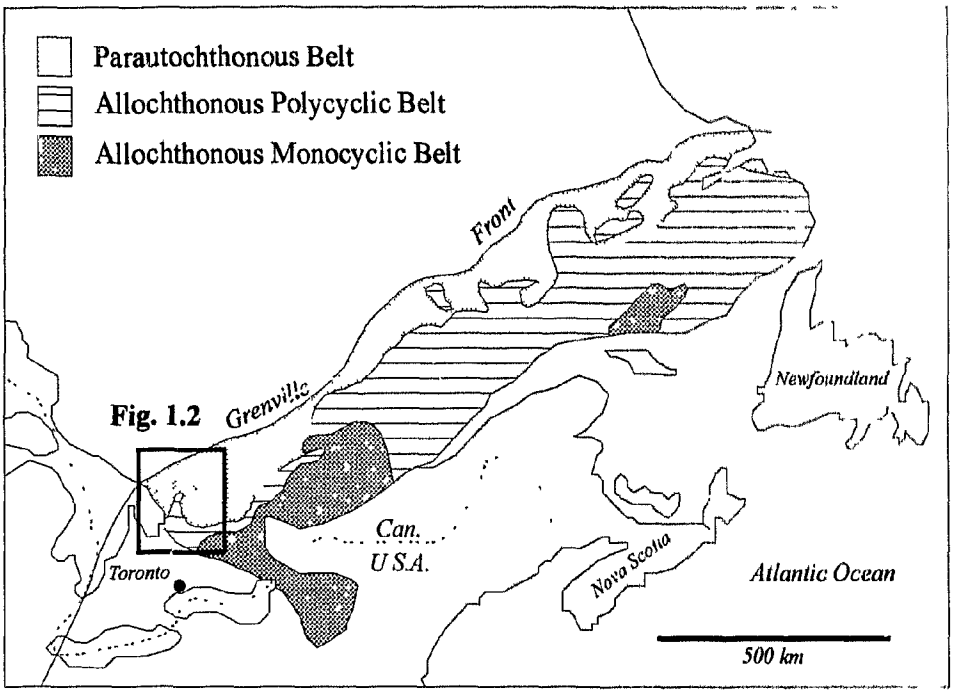

Fig. 1.1. Tectonic map of the Grenville Province showing subdivisions proposed by Rivers et al. (1989). Parautochthonous Belt contains reworked equivalents of Archean to Mesoproterozoic rocks across Grenville Front in foreland. The two allochthonous belts include Paleoproterozoic and Mesoproterozoic polyorogenic (polycyclic) rocks, and Mesoproterozoic units first deformed during the Grenvillian orogeny (monocyclic). Location of Figure 1.2 shown in southwestern part of orogen in Ontario (after Rivers et al. 1989).

terranes structurally overlying the Allochthonous Polycyclic Belt that were deformed and metamorphosed for the first time during the Grenvillian orogeny (Rivers et al. 1989; Fig. 1.1). Northwest-directed thrusting is commonly documented along the orogen-scale tectonic boundaries of the belts and in ductile tectonite zones within the belts. Quantitative estimates of thrust displacement are generally lacking, but significant transport is implied in places where tectonic units have contrasting structural, metamorphic, lithological and/or geophysical characteristics. This relationship indicates that northwest-directed thrusting was likely an important mechanism of Grenvillian crustal thickening and metamorphism (Rivers et al. 1989).

The first-order subdivision of the orogen provides a framework for second-order complexities that have stimulated much research interest. Early studies of geologically distinct, variably-sized, tectonically-bounded crustal segments in the Grenville Province (*e.g.*, Wynne-Edwards 1972; Moore and Thompson 1980; Davidson and Morgan 1981; Davidson et al. 1982; Culshaw et al. 1983; Gower and Owen 1984; Rivers and Nunn 1985; Rivers and Chown 1986; Wardle et al. 1986; Davidson and Grant 1986; Indares and Martignole 1989) formed the basis for the orogen-scale subdivision proposed by Rivers et al. (1989). In Ontario, Davidson and Morgan (1981) and Davidson et al. (1982) recognized that the Central Gneiss Belt (Wynne-Edwards 1972) could be divided into a number of discrete rock packages or *domains,* each bearing a unique combination of lithological, structural, metamorphic, and in some cases geophysical characteristics (Fig. 1.2). The domains were found to be separated by continuous, narrow, ductile high-strain belts with kinematic evidence for northwest-directed thrusting. Culshaw et al. (1983)

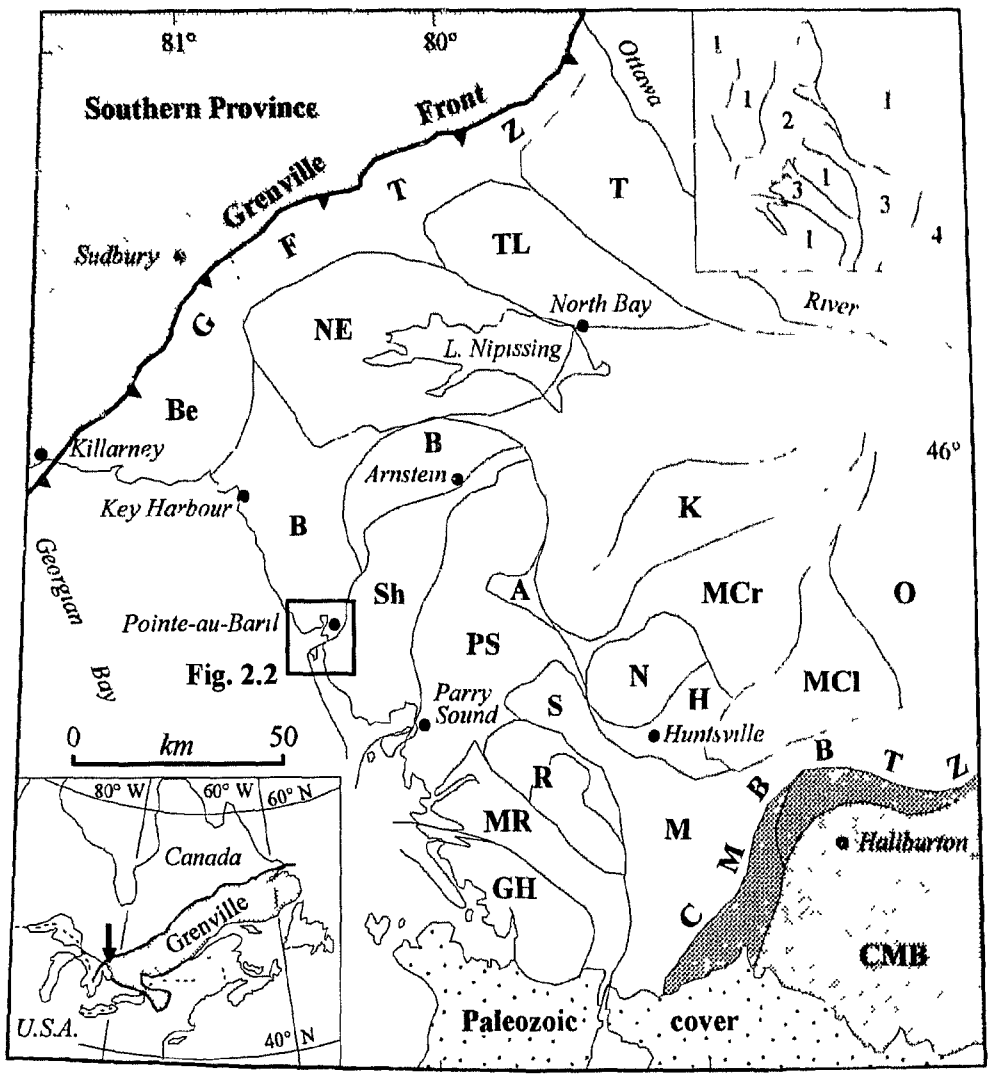

Fig. 1.2. Lithotectonic domains in the Central Gneiss Belt of Ontario, after Davidson and van Breemen (1988), Culshaw et al. (1990), and Easton (1992). Location of study area indicated. Major subdivisions and structures: **GFTZ**, Grenville Front Tectonic Zone; **CMB**, Central Metasedimentary Belt, **CMBBTZ**, Central Metasedimentary Belt boundary thrust zone; **Be**, Beaverstone domain; **Br**, Britt domain; **T**, Tomiko domain; **NE**, Nepewassi domain; **TL**, Tilden Lake domain, **A**, Ahmic domain, **K**, Kiosk domain; **N**, Novar subdomain; **H**, Huntsville subdomain; **MCr**, McCraney subdomain; **MCl**, McClintock subdomain; **O**, Opeongo subdomain; **R**, Rosseau subdomain; **GH**, Go Home subdomain; **S**, Seguin subdomain, **M**, Muskoka domain; **MR**, Moon River subdomain. Numbers (upper inset) indicate structural level (Culshaw et al. 1983). 1 = Parautochthonous Belt, 2, 3 = Allochthonous Polycyclic Belt, 4 = Allochthonous Monocyclic Belt.

assigned these domains to three regional-scale, structurally superincumbent units or 'decks' overlain by a fourth deck comprising the Central Metasedimentary Belt (Wynne-Edwards 1972). These and other characteristics led Davidson et al. (1982) and Davidson (1984*b*) to postulate that a doubling of crustal thickness during continental collision might account for many of the observed crustal features. This work pioneered current tectonic interpretations of the Central Gneiss Belt, now regarded in plate tectonic models (*e.g.*, Windley 1986, 1989; Hanmer and McEachern 1992; Nadeau and Hanmer 1992; McEachern and van Breemen 1993) as the reworked footwall to an overthrust magmatic arc (the Central Metasedimentary Belt) and an unidentified continent to the south. Deck 1 (Fig. 1.2; Culshaw et al. 1983) has been assigned to the Parautochthonous Belt, decks 2 and 3 to the Allochthonous Polycyclic Belt, and deck 4 (the Central Metasedimentary Belt) to the Allochthonous Monocyclic Belt (Rivers et al. 1989).

Despite this conceptual breakthrough, a number of outstanding problems remain in Central Gneiss Belt geology. For instance, the position of the Allochthon Boundary Thrust (the basal thrust to the Allochthonous Polycyclic Belt; Rivers et al. 1989) in Ontario is not rigorously constrained, and in one location where it has been identified (the present study area), shear sense is extensional rather than contractional (Culshaw et al. 1990, 1994; Jamieson et al. 1992). Recent identification of pre-Grenvillian metamorphic mineral assemblages in the parautochthon (*e.g.*, Haggart 1991; Jamieson et al. 1992; Bethune 1993; Corrigan et al. 1994; Ketchum et al. 1994) raises questions on the distribution, extent, and degree of preservation of older assemblages, and on the applicability of earlier thermobarometric studies. The timing and regional extent of plutonic, depositional,

thermal, and deformational events during pre-Grenvillian and Grenvillian orogenesis is not well constrained in much of the Central Gneiss Belt, and the relationship between Grenvillian tectonism and metamorphism is also not entirely clear.

The present study was undertaken to examine some of these problematic features in a portion of the western Central Gneiss Belt along Georgian Bay (Fig. 1.2). The study area straddles the tectonic boundary between the parautochthonous Britt domain and the allochthonous *Shawanaga domain* (new name). Recent work in this region (*e.g.*, Culshaw et al. 1988, 1989, 1990, 1991*a*, *b*, 1994; Jamieson et al. 1992; Ketchum et al. 1993*a*, *b*, 1994) indicates that a thrust-related tectonostratigraphy is preserved despite reactivation of the Allochthon Boundary Thrust as a southeast-directed extensional shear zone late in the Grenvillian orogeny. Extensional shear was accompanied by regional-scale folding about axes parallel to the extensional transport direction. This late orogenic period was also marked by significant exhumation of both the Britt and Shawanaga domains. Pre-Grenvillian and early Grenvillian fabrics and mineral assemblages preserved in the study area escaped late Grenvillian reworking by virtue of the heterogeneous nature of this overprint.

1.3 SCOPE OF THE PRESENT STUDY

The present study, which commenced with fieldwork in August of 1989, considers lithological, structural, metamorphic and geochronological characteristics of the field area as a balanced, multi-disciplinary approach has proven effective in unravelling orogenic histories in complex gneiss terranes (*e.g.*, Passchier et al. 1990). The specific goals of this

thesis are:

1) to establish a detailed field chronology of pre-Grenvillian and Grenvillian orogenic events in the study area.

2) to document lithological variations and differences in plutonic, thermal and tectonic history between allochthonous and parautochthonous rocks.

3) to investigate the origin of pre-Grenvillian and early Grenvillian structures and late Grenvillian folds and extensional shear zones

4) to identify the process(es) that allowed the preservation of pre-Grenvillian mineral assemblages in the southern Britt domain.

5) to document the age and *P-T* conditions of pre-Grenvillian and Grenvillian metamorphic events, and establish *P-T-t* histories for the southern Britt and northern Shawanaga domains.

6) to investigate the relationship between Grenvillian tectonism and metamorphism in the study area.

7) to determine the timing of extensional reactivation of the Allochthon Boundary Thrust.

8) to place some thermochronometric constraints on late orogenic cooling within and to either side of the Allochthon Boundary Thrust.

9) to apply the findings of the study to models of regional-scale orogenic evolution.

In order to attain these goals, a detailed field investigation was carried out and modern methods of structural analysis, thermobarometry and U-Pb geochronology were

applied. The field identification of early Grenvillian and pre-Grenvillan structures and mineral assemblages permits a qualitative and quantitative evaluation of temporally distinct orogenic events, and allows the crustal history of lithotectonic domains to be directly characterized. The principal focus of the study, however, is on the nature and influence of late orogenic extension which occurred deep in the Grenvillian crust. Deep crustal extensional structures and syn-kinematic mineral asemblages have not been widely described or recognized elsewhere in the Grenville Province.

The philosophy behind this investigation is perhaps best summarized by Moore (1986, p. 9), who states that "...work in such relatively new disciplines as precise isotope geochronology, kinematic analysis and refined thermobarometry will reap rich rewards of understanding, *provided* it is closely coordinated with sound mapping."

CHAPTER 2

Lithologies And Field Relations

2.1 INTRODUCTION

Location and Access

The thesis area is located on the eastern shore of Georgian Bay approximately 230 km north-northwest of Toronto, Ontario (Fig. 1.1) and is accessible from Ontario Highway 69. The village of Pointe-au-Baril is situated within the study area (Fig. 2.1).

Rock exposures were examined within a region roughly measuring 20 x 20 km (Fig. 2.1; Fig. 2.2, back pocket). Numerous islands offer excellent shoreline exposure, particularly among outermost islands where overburden and vegetation are sparse or absent. Exposure elsewhere is good, particularly along highways and secondary roads on the mainland where fresh, blasted surfaces are abundant.

Access to most points in the study area is by boat. Marinas and boat launching facilities are located at Bayfield, Pointe-au-Baril, and Nares Inlet. Fuel and supplies are available at these locations and from the Ojibway Hotel (Fig. 2.2). Marked boat channels are maintained by the Canadian Coast Guard and by local cottager associations, making navigation relatively straightforward. The waters of Georgian Bay, however, are renowned for numerous shoals and caution must be exercised when operating out of the marked channels. Large waves can make small boat travel hazardous among the outer islands, within Shawanaga Bay, and along the approaches to Nares Inlet. These areas are best avoided during stormy conditions. Many islands are privately owned but large tracts

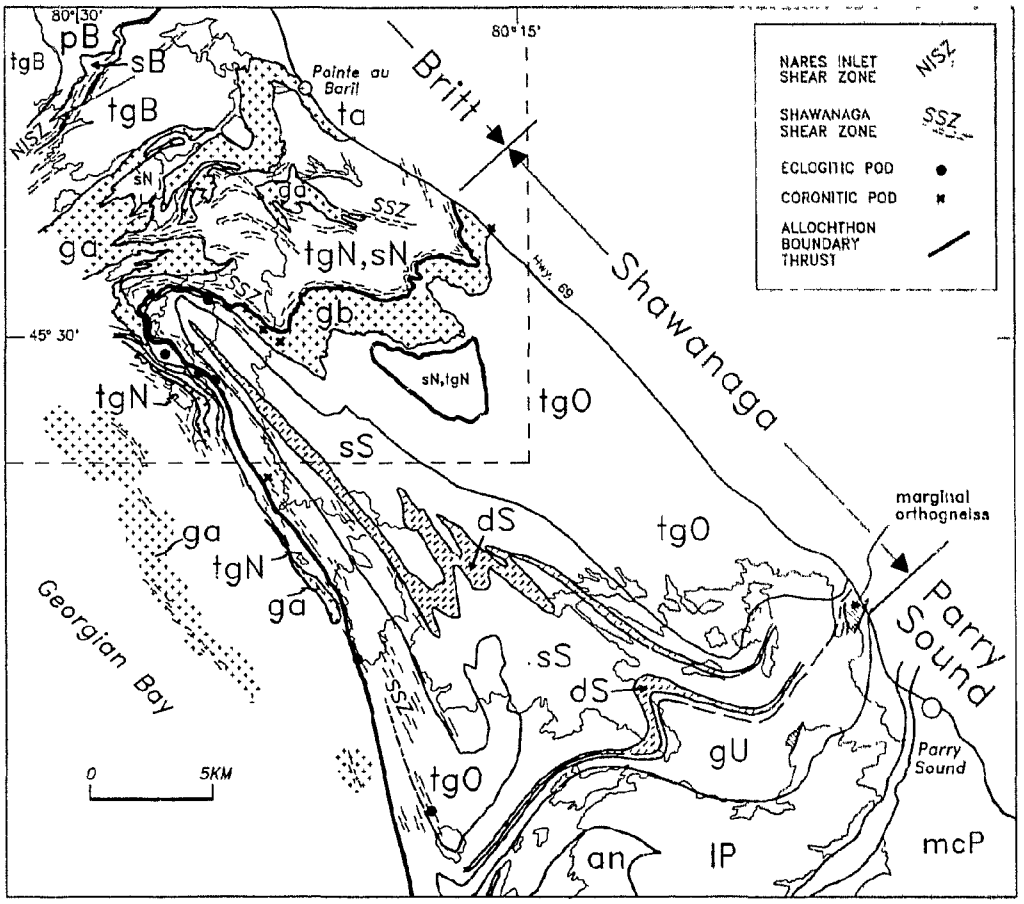

Bayfield Gneiss Association
tgB, pB - orthogneiss
sB - paragneiss

Nadeau Island Gneiss Association
tgN - orthogneiss
sN - paragneiss, mafic supracrustal gneiss

Ojibway Gneiss Association
tgO - orthogneiss

Sand Bay Gneiss Association
sS - paragneiss
dS - Dillon schist

Monocyclic Plutons
ga, ta - Pointe-au-Baril complex
gb - Shawanaga pluton

Unnamed Gneiss Association
gU - orthogneiss, paragneiss

Parry Sound Domain
lP -Lighthouse gneiss association
mcP - McLaren Island gneiss association
an - anorthosite

Fig. 2.1. Geological map of the Pointe-au-Baril - Parry Sound region (after Culshaw et al. 1994; see Fig. 1.2 for location). Extent of Britt, Shawanaga, and Parry Sound domains indicated. Study area (Fig. 2.2 - back pocket) indicated by dash-dot rectangle.

of the mainland and numerous smaller islands remain crown land.

Previous Work

Despite ease of access and superb rock exposure, little was known of the geology of the Pointe-au-Baril area until the regional reconnaissance studies of Davidson and Morgan (1981) and Davidson et al. (1982). This work not only provided details of local geology but established a tectonic framework for the Central Gneiss Belt in western Ontario. Details of the regional tectonic evolution of the Central Gneiss Belt are outlined in Chapter 1.

Davidson and Morgan (1981) recognized that tracts of migmatized orthogneiss and paragneiss underlying the Britt domain (which includes the Shawanaga domain by their definition) were intruded by granitoid plutons prior to further deformation and metamorphism. Metamorphic grade was estimated at middle to upper amphibolite facies and a predominant northwest structural grain and late, northwest-trending folds were documented. South of Pointe-au-Baril, Davidson et al. (1982) mapped a 2-3 km-wide zone of straight gneiss and mylonite extending from Georgian Bay to the village of Arnstein (Fig. 1.2). This zone was considered to be internal to the Britt domain and not a domain-bounding shear zone. Davidson et al. (1990) named this structure the Central Britt shear zone.

Culshaw et al. (1988, 1989) investigated the Pointe-au-Baril area during 1:50,000 scale mapping of the eastern shore of Georgian Bay. This work confirmed many of the earlier findings of Davidson and Morgan (1981) and Davidson et al. (1982) and

contributed additional information on lithology, tectonometamorphic history, and location of structural boundaries. The Central Britt shear zone was found to contain kinematic evidence for top-to-the-southeast extensional displacement, and a smaller, southeast-directed, extensional mylonite zone was mapped eight kilometres to the northwest in Nares Inlet (Fig. 2.1, 2.2). Map units in the Britt and Shawanaga domains were grouped into distinctive rock packages on the basis of commonly affiliated rock types with a shared geological history, and the term gneiss association was introduced to describe them.

The tectonic history of the Pointe-au-Baril area was described by Culshaw et al. (1990, 1994) and Jamieson et al. (1992). These workers recognized that lithotectonic terranes with contrasting histories of plutonism, structural and metamorphic development, and mafic dyke emplacement are juxtaposed along a regional décollement lying within the central Britt shear zone. Furthermore, the lithologic character, tectonometamorphic history, and U-Pb age of rocks structurally above the décollement indicate an allochthonous origin (Culshaw et al. 1994). This work yielded a revised position for the Allochthon Boundary Thrust in the western Central Gneiss Belt (initially placed along the Parry Sound shear zone by Rivers et al. 1989) and demonstrated that the boundary thrust was reactivated as an extensional shear zone in this region.

It is evident from the above that a revised nomenclature is required for this area of the Central Gneiss Belt. The allochthonous lithotectonic domain lying structurally above the décollement and bounded on the east by the Parry Sound domain (termed the southern Britt domain by some workers) is herein called the *Shawanaga domain* in order to

distinguish it from underlying parautochthonous rocks of the Britt domain. The structural boundary separating these domains is termed here the *Shawanaga shear zone* rather than the Central Britt shear zone (Davidson et al. 1990) as the latter name implies lithologic and tectonometamorphic continuity across this zone. Tuccillo et al. (1992) named this structure the Pointe-au-Baril shear zone but this term is not recommended here as the town of Pointe-au-Baril lies several kilometres north of the shear zone (Fig. 2.2).

Gower (1992) presented structural data from the Shawanaga and Parry Sound domains indicating the presence of three northeast-verging, superincumbent fold nappes. Two of the recumbent nappes contain Shawanaga domain lithologies while the third comprises structurally lowest units of the Parry Sound domain. The nappes were suggested to have been emplaced during early, northeast-directed thrusting and modified subsequently by northwestward thrusting and folding about northwest-trending axes. Although early, regional-scale folds are known to occur in the Shawanaga, Parry Sound, and Moon River domains (*e.g.*, Schwerdtner 1987; Culshaw et al. 1989, 1994), many of the fold closures shown in Gower's (1992) down-plunge projection were inferred from the data of Culshaw et al. (1989) but were not identified in the field. Further mapping is required to test this hypothesis.

The metamorphic evolution of the Pointe-au-Baril area has been documented by several workers. Needham (1987, 1992) described metamorphic and relict igneous mineral assemblages in two metabasite bodies within the Shawanaga shear zone (Frederic Inlet metagabbros; Fig. 2.2). Both bodies contain retrogressed eclogite that re-equilibrated for the last time in the upper amphibolite facies. Compositionally similar rocks preserving this

metamorphic history, termed 'meta-eclogite' by Grant (1987), have been documented elsewhere in the Central Gneiss Belt (*e.g.*, Grant 1987, 1989; Davidson 1990, 1991; Culshaw et al. 1991*a*) where they commonly occur within shear zones.

Northeast of Frederic Inlet in the Britt domain, Tuccillo et al. (1990) documented strong chemical zonation in metapelite garnet porphyroblasts. Pressure-temperature (*P-T*) estimates from a single sample indicate a Grenvillian *P-T* history dominated by isothermal decompression. However, Tuccillo et al. (1992) abandoned this interpretation in light of U-Pb garnet data suggesting growth of porphyroblast cores at *ca.* 1450 Ma. Maximum pressure estimates obtained from core compositions were attributed to pre-Grenvillian metamorphism whereas lower pressure rim compositions were attributed to Grenvillian metamorphism. However, Grenvillian pressures reported by Tuccillo et al. (1992) are 2-3 kbar lower than regional estimates for the Britt domain (Anovitz and Essene 1990).

Jamieson et al. (1992) documented distinctive metamorphic histories for gneiss associations lying north and south of the Shawanaga shear zone, consistent with a regional tectonic model proposed by Culshaw et al. (1990; see above). They emphasized that parautochthonous rocks locally preserve Grenvillian and pre-Grenvillian mineral assemblages of similar grade, and that reliable *P-T* estimates of known age were difficult to obtain from these rocks.

Geochronological investigations in the Pointe-au-Baril area employing the U-Pb, Rb-Sr, $^{40}Ar/^{39}Ar$, and Sm-Nd isotopic systems span more than two decades. A summary of U-Pb ages for the Central Gneiss Belt and Grenville Front Tectonic Zone is presented in Chapter 5 and is not repeated here. The earliest published geochronological data are Rb-Sr

whole-rock ages of *ca.* 1800 Ma for a paragneiss sample collected near Pointe-au-Baril (Krogh and Davis 1969, 1970*a*, 1971). This age was suggested to date a high-grade metamorphic event with younger mineral isochron ages providing evidence for a partial isotopic resetting during Grenvillian orogenesis. Culshaw et al. (1991*b*) reported $^{40}Ar/^{39}Ar$ cooling ages of 964 ± 5 Ma for hornblende and 904 ± 3 Ma for muscovite from a sample collected in the study area. These data were combined with other $^{40}Ar/^{39}Ar$ ages obtained by the authors in the Britt domain to constrain a time-temperature curve indicating erosionally-controlled post-orogenic cooling.

Dickin and McNutt (1989, 1990) reported Sm-Nd data for the Central Gneiss Belt including T_{DM} ages of 1.98-1.46 Ga for five samples from the Pointe-au-Baril - Parry Sound region. Samples with oldest model ages (1.98-1.86 Ga) were collected north of and within the Shawanaga shear zone whereas samples with younger ages (1.64-1.46 Ga) were obtained south of this zone. Similar variations in T_{DM} were observed by Dickin and McNutt (1990) across tectonic boundaries elsewhere in the Central Gneiss Belt, providing broad support for the domainal subdivisions proposed by earlier workers.

Seismic data from lines 30 and 31 of the Lithoprobe Abitibi-Grenville transect (White et al. 1994) constrain the crustal structure of the Britt and Shawanaga domains. A prominent southeast-dipping zone of high reflectivity extending beneath the Parry Sound domain was interpreted as the Shawanaga shear zone (White et al. 1994), supporting the interpretation of this structure as a regional décollement (Culshaw et al. 1990, 1994).

2.2 GEOLOGY OF THE POINTE-AU-BARIL AREA

The description of lithologies given below for the Pointe-au-Baril area combines the unit names of Culshaw et al. (1988, 1989, 1994) with observations made during the present study. The concept of gneiss associations (Culshaw et al. 1988, 1989; see above) provides a useful framework for describing rocks in this area. Rock units and gneiss associations with a polyphase history of metamorphism and deformation are termed polycyclic whereas those with a history of only Grenvillian tectonism and metamorphism are termed monocyclic (*e.g.*, Rivers et al. 1989). Youngest plutons in the study area have a monocyclic history even though some occur within polycyclic gneiss associations.

All rocks in the study area have been metamorphosed to granulite or amphibolite facies. For the purpose of brevity, the prefix 'meta' is dropped from most lithology names. Orthogneiss compositional names given below are based on visual estimates of modal mineralogy. Terminology for highly strained rock follows that of Davidson et al. (1982) and Hanmer (1988). Rocks for which the term mylonite (*e.g.*, White et al. 1980) may be inappropriate but which are of unequivocal tectonic origin are described as gneissic tectonite (Davidson 1984*a*, *b*).

Polycyclic Gneiss Associations of the Britt Domain

Bayfield Gneiss Association

The Bayfield gneiss association (Culshaw et al. 1988, 1989) extends from the Britt pluton (10 km north of the study area) to the Pointe-au-Baril plutonic complex (Figs. 2.1, 2.2). These bounding plutons both consist of *ca.* 1.46 granitoid orthogneiss (van Breemen

et al. 1986; Culshaw et al. 1994). The study area encompasses only the southern half of the Bayfield gneiss association.

The predominant Bayfield association lithology in the study area is a grey, migmatitic, tonalite to granodiorite orthogneiss with a homogeneous, streaky appearance suggesting a deformed plutonic texture (unit tgB, Fig. 2.2). Numerous, centimetre-size lenses of polycrystalline feldspar in these rocks may represent highly recrystallized and deformed feldspar phenocrysts. Sparse granite, leucogranite, and amphibolite layers up to several metres wide are locally present. All rock types contain elongate amphibole porphyroblasts and minor, recrystallized garnet porphyroblasts.

The tonalite gneiss hosts a large body of pink, fine-grained, biotite granite to leucogranite gneiss (unit pB, Fig. 2.2) containing layers of similar but slightly more mafic composition. Rare feldspar augen in some units may represent strained phenocrysts. Compositional layering (gneissic banding?) is poorly developed but a strong foliation defined by fine, biotite-rich laminations is characteristic. Pink, coarser-grained, centimetre-width granitic layers with magnetite porphyroblasts may represent transposed leucosomes. Garnet and amphibole are relatively uncommon in these rocks. The biotite granite gneiss strongly resembles bodies of pink leucogranite gneiss that locally intrude the Bayfield association (Culshaw et al. 1988). Both the biotite granite and the smaller leuocogranite bodies appear to predate *ca.* 1460 Ma felsic plutonism in the Pointe-au-Baril area (see below).

Structurally overlying the biotite granite gneiss is a belt of supracrustal gneiss centred on Nares Inlet (unit sB, Fig. 2.2). This unit contains a variety of migmatitic,

quartzofeldspathic and feldspathic paragneisses. Contact relations with orthogneiss are obscured by high-strain fabrics, particularly within the Nares Inlet shear zone which generally follows the southeast margin of the supracrustal belt. Lithologies include pelitic and semi-pelitic gneiss, leucocratic gneiss, quartzite, and less abundant quartz-free rocks including garnet-feldspar gneiss and biotite-magnetite gneiss. Pelitic gneiss contains kyanite ± sillimanite ± staurolite, and quartz-free lithologies may contain corundum, staurolite, and/or kyanite. The presence of aluminous minerals is typically indicated in these rocks and in other pelitic gneisses within the study area by the presence of violet-pink garnet (*e.g.*, Davidson et al. 1982). Muscovite, chlorite, and epidote are retrograde phases.

Nearly all paragneisses in Nares Inlet are characterized by garnet-bearing leucosomes which may also contain kyanite. Some strongly deformed, leucocratic, aluminosilicate-bearing gneiss layers may represent highly transposed and recrystallized leucosomes. Most of these layers are K-feldspar-rich, particularly those that contain kyanite.

At least three generations of cream-coloured, granitic leucosome are present in the Bayfield association. South of the Nares Inlet shear zone, early stromatic leucosomes in a contorted gneissic foliation are preserved in low strain areas within northeast-striking straight gneiss (Fig. 2.3*a*). Straight gneiss development was accompanied by the generation of a second set of leucosomes which were mainly transposed into the gneissic banding. Where strain levels were highest, a third leucosome generation formed in the necks of boudined gneissic foliation (Fig. 2.3*b*).

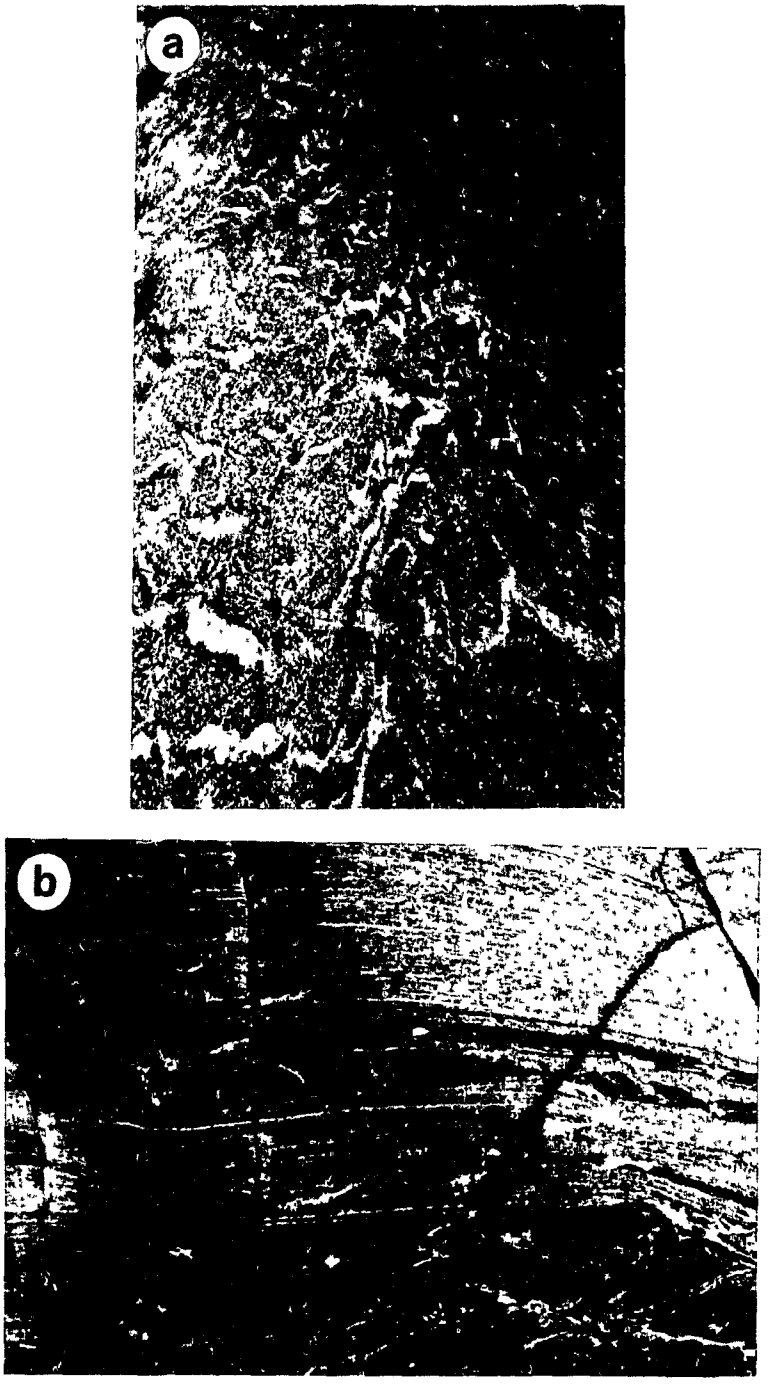

Fig. 2.3. The Bayfield gneiss association. **a)** Pre-Grenvillian leucosomes parallel to a contorted early foliation in megacrystic granodiorite orthogneiss. NE-striking Grenvillian foliation (perpendicular to dominant leucosome trend) poorly developed here. **b)** NE-striking Grenvillian straight gneiss with leucosomes of two early generations transposed and a third generation occupying necks of boudined foliation. Note back-rotation of boudined mafic layer in centre of view indicating dextral shear (outcrop surface parallel to lineation, perpendicular to foliation).

The oldest leucosomes are cut by amphibolite dykes (*e.g.*, Fig. 3.14*c*) that are tentatively correlated with the 1238 Ma Sudbury swarm (see below). This relationship indicates that the oldest leucosomes are pre-Grenvillian. Second generation leucosomes are absent near the margins of these dykes suggesting that their development may have been locally suppressed by fluid migration into the anhydrous dykes during Grenvillian metamorphism.

U-Pb geochronological data for the Bayfield gneiss association are presented by Krogh et al. (1993*a*) and Culshaw et al. (in prep.). Zircons from a sample of migmatitic tonalite orthogneiss indicate igneous crystallization at 1739 ± 34 Ma (sample GC89-117; Fig. 5.2). No other primary crystallization ages or constraints on the timing of sedimentation are currently available for the Bayfield gneiss association.

Nadeau Island Gneiss Association

The Nadeau Island gneiss association lies structurally above the Bayfield gneiss association (Fig. 2.2). This rock package resembles the Bayfield association but contains a higher proportion of supracrustal gneiss and, unlike the Bayfield gneiss association, is cut by granitoid rocks of the Pointe-au-Baril complex (Culshaw et al. 1988).

Rocks of plutonic parentage in the Nadeau Island gneiss association (unit tgN, Fig. 2.2) include tonalite, granodiorite, and biotite granite gneiss. Leucocratic varieties of granodiorite and granite are also locally observed (Needham 1987; Culshaw et al. 1988). Small bodies of biotite-bearing leucogranite intrude the Nadeau Island association but appear to predate emplacement of the Pointe-au-Baril complex. Hornblende forms ubiquitous porphyroblasts in tonalite gneiss, particularly in leucosomes; garnet

porphyroblasts are less abundant.

A wide variety of supracrustal gneisses, some of unequivocal sedimentary parentage, occur within the Nadeau Island gneiss association (unit sN, Fig. 2.2). Predominant lithologies include biotite ± garnet pelitic and semipelitic gneiss, and garnet + clinopyroxene + biotite + amphibole calc-silicate gneiss. Less abundant quartzofeldspathic lithologies (some pelitic) include graphitic gneiss, muscovite + biotite gneiss, and quartz + K-feldspar leucogneiss with isolated biotite-rich lenses. Muscovite is retrograde in most supracrustal lithologies but locally occurs as a matrix phase (*cf.* Needham 1992). Aluminous minerals noted in pelitic assemblages in the present study include kyanite, sillimanite, staurolite, corundum, and spinel.

Two distinctive, commonly interlayered, supracrustal rock types occur in the northern Nadeau Island association. These are amphibole + biotite + plagioclase ± orthopyroxene ± clinopyroxene mafic gneiss, and quartz-free, corundum-bearing gneiss. The mafic gneiss regularly contains calc-silicate layers and pods up to 1 m wide with epidote-rich interiors and plagioclase + amphibole + ilmenite ± garnet ± clinopyroxene margins. Unzoned calc-silicate layers dominated by plagioclase and clinopyroxene are also common. Some layers contain idioblastic clinopyroxene porphyroblasts up to 7 cm long within quartzofeldspathic veins. A number of calc-silicate pods also exhibit a folded older gneissic foliation (Fig. 2.4*a*). The mafic gneiss locally hosts discontinuous layers of muscovite-biotite schist up to 1-2 m wide. This rock package is of particular interest as it locally preserves pre-Grenvillian granulite facies mineral assemblages dated at *ca.* 1450-1430 Ma (Ketchum et al. 1994; Chapter 5).

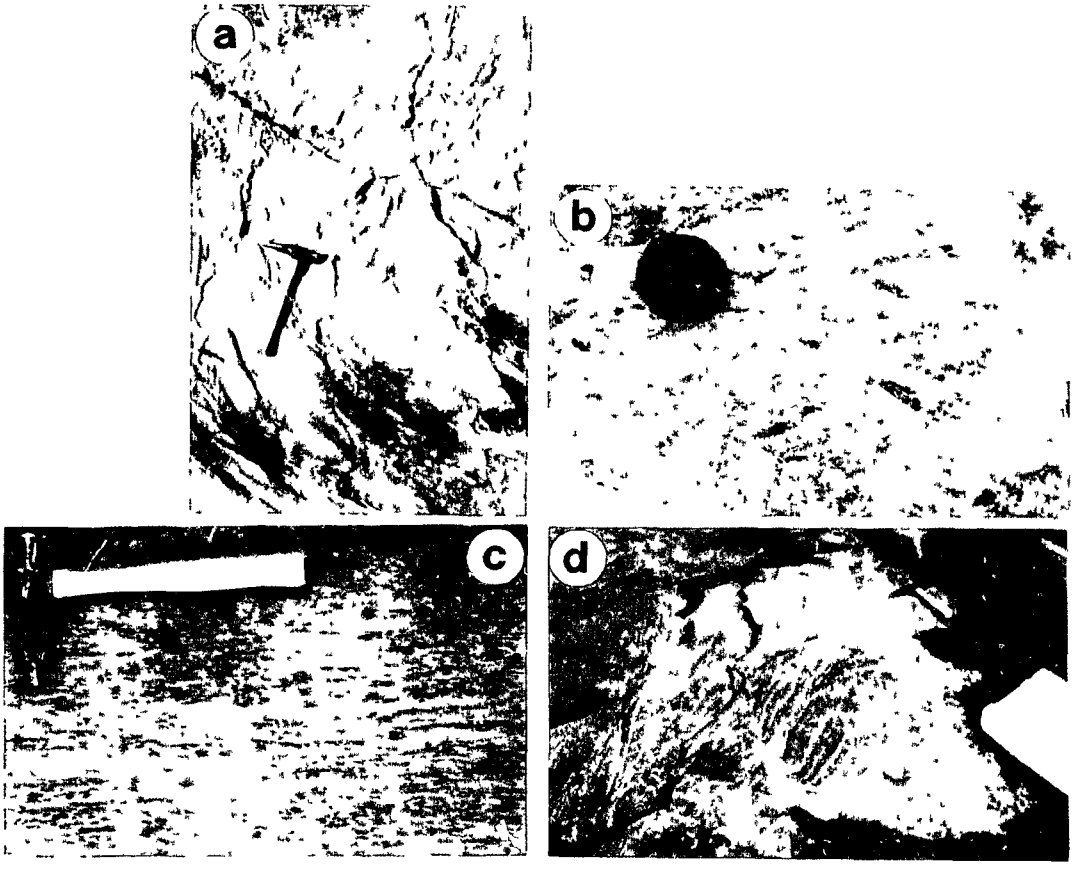

Fig. 2.4. The Nadeau Island gneiss association **a)** Folded, early gneissic foliation preserved in calc-silicate pods hosted in mafic supracrustal gneiss. Pods derived from boudined calc-silicate layers. **b)** Corundum porphyroblasts in sub-silicic biotite paragneiss overgrowing an early migmatitic foliation. Note K-feldspar-rich leucosome cutting foliation in upper right corner, and thin leucocratic halos around corundum, interpreted as zones of biotite consumption during corundum growth. **c)** Foliated version of b). Dark knots are kyanite-sillimanite intergrowths after corundum porphyroblasts **d)** Strain gradient in migmatitic tonalite orthogneiss. Folded early gneissossity is dissected by leucosome-filled, axial planar shears subparallel to high-strain foliation of Shawanaga shear zone (visible on left).

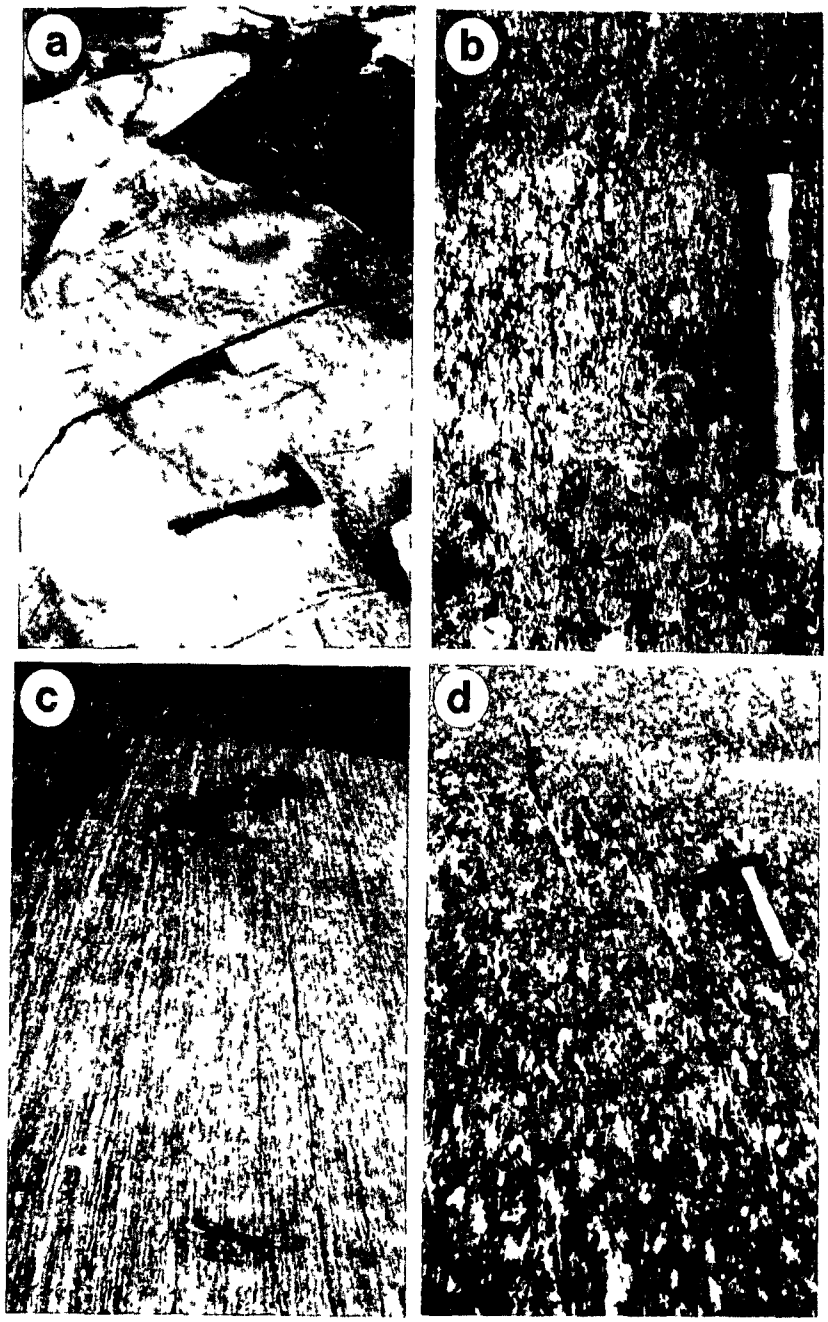

Fig. 2.6. Monocyclic granitoid plutons **a)** Xenoliths of Nadeau Island gneiss in weakly foliated, megacrystic granite of the Pointe-au-Baril complex. Elongate xenolith alignment on left may be due to magmatic flow. **b)** Megacryst-rich unit (left) in Pointe-au-Baril complex granite (outcrop partly obscured by lichen) Tectonic foliation shallowly cross-cuts igneous layers **c)** Migmatitic granodiorite gneiss of the Shawanaga pluton with K-feldspar augen derived from megacrysts **d)** Contorted leucosomes and thin, discordant leucosomes in Shawanaga orthogneiss.

Spatially associated with mafic supracrustal gneiss are distinctive layers of a pink to dark grey, quartz-free biotite gneiss. Corundum porphyroblasts up to 3 cm long overgrow an early migmatitic foliation, and K-feldspar-rich leucosomes hosting corundum porphyroblasts also cut this fabric (Fig. 2.4*b*). Leucocratic, K-feldspar-rich halos typically surround corundum porphyroblasts and are interpreted as zones of biotite consumption during solid-state corundum growth (Fig. 2.4*b*; *cf.* Best 1982, p. 361), possibly by a reaction such as:

$$\text{Biotite} = \text{K-feldspar} + \text{Corundum} + \text{Ilmenite} + H_2O$$

Embayed porphyroblasts with biotite overgrowths appear to indicate the opposite reaction during later metamorphism. Magnetite and ilmenite are common in these rocks.

Moderate deformation of corundum-bearing gneiss has produced a gneissic tectonite in which corundum is replaced by kyanite-sillimanite lenses (Fig. 2.4*c*). In higher-strain zones, these lenses are up to 10 cm long and in places are completely disaggregated into small aluminosilicate knots. Lithologies with these characteristics (but lacking corundum) are also found in the belt of supracrustal gneiss forming the southern margin of the Nadeau Island association (Fig. 2.2), indicating that corundum growth may not have been restricted to the north of this association.

Another distinctive Nadeau Island supracrustal lithology crops out among the outer islands and shoals west of Shawanaga Island (Fig. 2.2). These are migmatitic, semi-pelitic gneisses with a contorted foliation and a uniform fine grain size, in contrast to other supracrustal rocks which typically exhibit a coarser grain size in leucosomes. Predominant minerals include quartz, plagioclase, K-feldspar, and biotite; garnet is a minor

phase. The semi-pelite locally grades to a K-feldspar-rich leucogneiss with mafic lenses rich in biotite, sillimanite, and garnet. The similarity of this unit to supracrustal lithologies in the Key Harbour area of the northern Britt domain (Fig. 1.2) led Culshaw et al. (1989) to suggest that elements of the Key Harbour gneiss association are found west of Shawanaga Island. While this remains a possibility, scattered occurrences of this rock type throughout the Nadeau Island association indicate that comparable lithologies may occur in both associations.

At least two generations of quartzofeldspathic leucosome are present in the Nadeau Island gneiss association. Contorted, cream-coloured leucosomes and younger stromatic leucosomes are locally observed in orthogneiss. As for the Bayfield gneiss association, the younger generation likely formed during Grenvillian transposition and high-strain fabric development. Evidence of this is observed in strain gradients adjacent to the Shawanaga shear zone where folded, older gneissic foliations are cut by spaced, leucosome-filled, axial planar shears (Fig. 2.4*d*). Toward the shear zone, these axial planar shears become more numerous and eventually form the penetrative shear zone fabric.

Original contact relationships between Nadeau Island orthogneiss and supracrustal gneiss are everywhere obscured by tectonic transposition. However, rare enclaves of supracrustal gneiss in orthogneiss suggest that plutonism post-dated supracrustal deposition and initial deformation and metamorphism. In one locality where a pelitic gneiss enclave is hosted by granodiorite orthogneiss, a crystallization age of 1606 ± 2 Ma was obtained for the latter (U-Pb zircon; Culshaw et al. in prep.).

Monocyclic Gneiss Associations of the Shawanaga Domain

Ojibway Gneiss Association

The Ojibway gneiss association (unit tgO, Fig. 2.2) overlies the Shawanaga pluton and extends southeastward to within a few kilometres of the Parry Sound domain (Fig. 2.1). This rock package was not designated a separate association in early studies (Culshaw et al. 1988, 1989) but was distinguished and characterized in later works (*e.g.*, Culshaw et al. 1991*a*, 1994).

The predominant lithology in the Ojibway association is a pink to grey, migmatitic, granodiorite to tonalite orthogneiss in which leucosomes become progressively more abundant toward the southeast (Culshaw et al. 1989, 1991*a*). Isolated concordant layers of granite gneiss and amphibolite are also observed. Biotite, amphibole, and garnet are the primary mafic constituents of Ojibway orthogneiss, but garnet is largely absent at higher structural levels to the southeast. Titanite and epidote are common accessory phases. Supracrustal rocks appear to be absent from this association. In contrast with Britt domain lithologies, rocks of the Ojibway gneiss association contain only a single leucosome generation of presumed Grenvillian age .

Two samples of Ojibway tonalite gneiss from a single outcrop have been dated by U-Pb geochronology (Culshaw et al. in prep.). The combined data yield a zircon upper intercept age of 1466 ± 11 Ma which is considered the best estimate for crystallization of the plutonic protolith (Culshaw et al. in prep.), and a *ca.* 1050 Ma lower intercept age reflecting Grenvillian metamorphism. These data indicate that the tonalite crystallized approximately 140 M.y. after early plutonism in the Bayfield and Nadeau Island gneiss

associations. However, Ojibway plutonism is coeval with intrusion of megacrystic granite of the Pointe-au-Baril complex and Shawanaga pluton (see below).

Sand Bay Gneiss Association

The Sand Bay gneiss association (unit sS, Fig. 2.2) overlies the Ojibway association and extends from the Shawanaga shear zone to near the western margin of the Parry Sound domain. Only a narrow, unnamed gneiss association (unit gU; Fig. 2.1) of granodiorite gneiss, minor supracrustal rocks, and *ca.* 1346 Ma granitic orthogneiss ('Marginal orthogneiss' of van Breemen et al. 1986) separates Ojibway and Sand Bay lithologies from the Parry Sound domain (Culshaw et al. 1994).

In contrast to the Ojibway gneiss association, Sand Bay gneisses are largely supracrustal. A distinctive paragneiss suite including migmatitic quartzofeldspathic gneiss, plagioclase-quartz-biotite schist, quartzite, calcareous gneiss, amphibolite, and rare marble is characteristic (Culshaw et al. 1989, 1991*a*). The present study area encompasses only a portion of the Sand Bay association and not all of these lithologies are found. On the east side of Shawanaga Island, a highly-strained package of pink, biotite-bearing leucogneiss interlayered with amphibole-biotite gneiss at lowest structural levels (Fig. 2.5*a*) is overlain by quartz-rich paragneiss with magnetite and muscovite porphyroblasts. Amphibolite and amphibole-plagioclase-quartz ± garnet ± epidote gneiss are more abundant at higher structural levels where they are interlayered with pink quartzofeldspathic gneiss and leucogneiss. Epidote-rich pods similar to those in mafic supracrustal rocks of the Nadeau Island association are locally present in some mafic lithologies. Rare, coarse-grained mafic

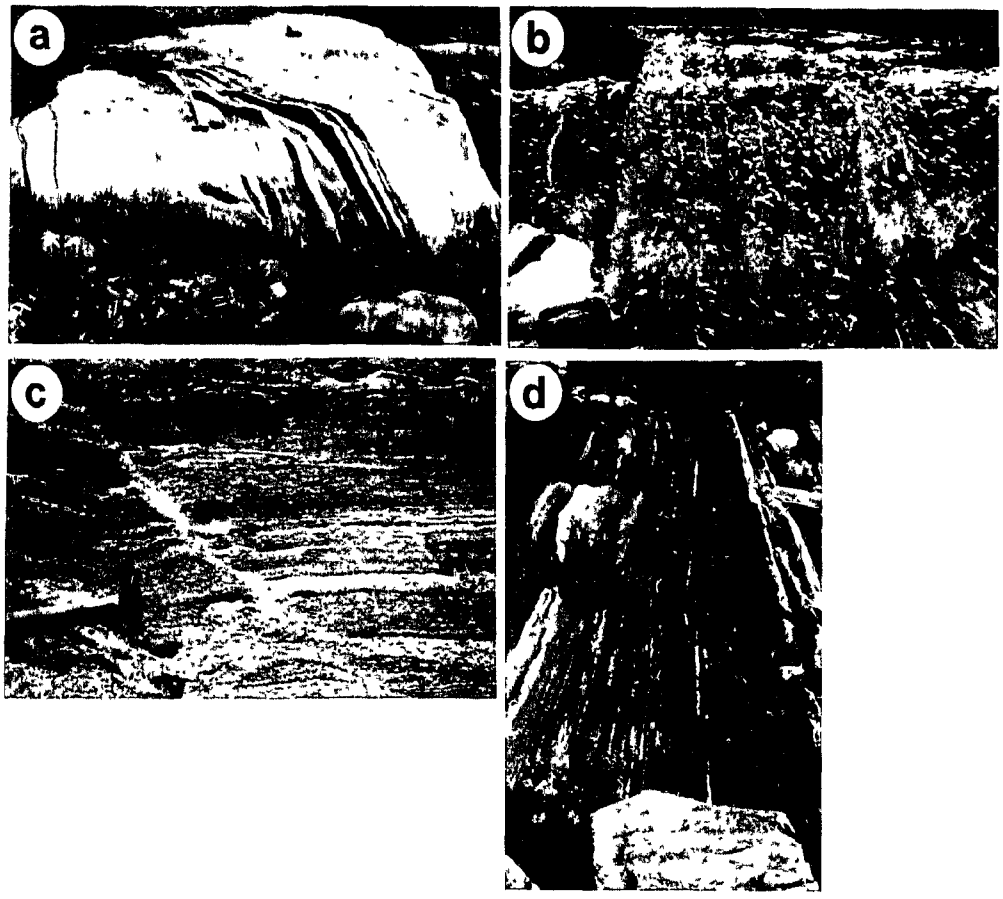

Fig. 2.5. The Sand Bay gneiss association. **a)** Pink, biotite-bearing leucogneiss with concordant biotite amphibolite layers, at lowest structural level of the association. **b)** Shallowly discordant leucosomes in amphibolite gneiss. Leucosome trend is likely axial planar to the Shawanaga synform which folds the Ojibway and Sand Bay associations. **c)** Late, discordant leucosome cutting older leucosomes and fabrics in paragneiss within the Shawanaga shear zone. Discordant vein may be related to late extensional movement on the shear zone **d)** Straight, biotite-rich, quartzofeldspathic paragneiss (Dillon schist) with stretched quartz pods and minor leucogneiss layers.

pods in amphibolite gneiss contain accessory chalcopyrite, pyrite and malachite. Accessory minerals in Sand Bay rocks include titanite, ilmenite, epidote, allanite, calcite, and tourmaline.

With the exception of some mafic lithologies, all units contain abundant leucosomes hosting porphyroblasts of muscovite, magnetite, amphibole, and clinopyroxene. Leucosomes are completely transposed in high-strain fabrics of the Shawanaga shear zone but preserve a systematic cross-cutting relationship with gneissic foliations in lower strain areas (*e.g.*, Fig. 2.5*b*), perhaps representing an axial planar orientation to large-scale folds. These are Grenvillian leucosomes (Culshaw et al. 1994) of a single generation, although sparse examples of a younger generation possibly associated with late movement on the Shawanaga shear zone (Fig. 2.5*c*) hint at a more complex metamorphic history.

A distinctive unit of the Sand Bay association can be traced from the study area for several tens of kilometres to the southeast where it outlines the folded internal structure of the Shawanaga domain (Fig. 2.1; Culshaw et al. 1994). This unit is a grey, quartzofeldspathic rock (Fig. 2.5*d*) containing biotite in proportions that warrant designation as a schistose gneiss (unit dS, Fig. 2.2). Culshaw et al. (1989) named this unit the Dillon schist and noted the presence of quartz pods and common accessory phases epidote, scapolite, and apatite. In the study area, quartz pods are generally elongate (Fig. 2.5*d*), and decimetre-scale granitic pods with accessory tourmaline, epidote, apatite, muscovite, titanite and chloritized biotite are also present. The Dillon schist locally grades to a dark grey, homogeneous, amphibole-biotite quartzofeldspathic rock.

U-Pb geochronological data demonstrate that rocks of the Sand Bay gneiss association are among the youngest in the Central Gneiss Belt (Krogh 1991; Krogh et al. 1993*a*; Culshaw et al. in prep.). Single-grain analyses of detrital zircon from a quartz-rich paragneiss ~120 m above the contact with the Ojibway association indicate deposition after 1417 ± 5 Ma, the age of the youngest grain. At a higher structural level, detrital zircon ages from the Dillon schist suggest deposition during or after *ca.* 1390-1360 Ma. Lithological characteristics and the U-Pb data tentatively suggest deposition of mature, quartz-rich clastic sediments, followed by deposition of immature volcanogenic sediments. Interlayered felsic and mafic paragneisses typical of the Sand Bay association may represent a bimodal, rift-related volcanic suite (Culshaw et al. in prep.). The age data indicate that *ca.* 1466 Ma Ojibway orthogneiss is overlain by younger Sand Bay lithologies either along an unconformity or a tectonic contact (Culshaw et al. 1994).

Monocyclic Granitoid Plutons

Davidson and Morgan (1981) described a suite of granitoid plutons in the Britt domain which cut migmatitic gneisses but are themselves variably deformed and metamorphosed. Regional mapping by Davidson et al. (1982) outlined two sheet-like masses in the Pointe-au-Baril area (Fig. 2.1) and several others in the northern Britt domain. These plutons are now known to occur throughout the Central Gneiss Belt and comprise a volumetrically important crustal component. Granite, granodiorite, and tonalite are characteristic compositions of this suite (Davidson et al. 1982; Culshaw et al. 1988; Nadeau 1990; van Breemen and Davidson 1990). U-Pb data (summarized in Chapter 5)

indicate igneous crystallization primarily between 1470 Ma and 1380 Ma, with younger ages obtained for several granitoid plutons in the Parry Sound domain (Wodicka 1994).

Monocyclic granitoid rocks in the Pointe-au-Baril area are assigned to the Pointe-au-Baril complex (Culshaw et al. 1988) and the Shawanaga pluton (Davidson et al. 1982). These bodies are described in detail below.

Pointe-au-Baril Complex

The Pointe-au-Baril granitoid complex (units ga, ta; Fig. 2.2) forms a significant component of the Nadeau Island gneiss association and occurs only in this association. The complex consists of a number of intrusive bodies separated by screens of country rock. Individual bodies are irregular in plan where finite strains are low but form narrow, elongate sheets within the Shawanaga shear zone. In addition to exposures in the eastern and central study area, Pointe-au-Baril granite is found on the Blackbill Islands (Fig. 2.2) and on the outermost islands between Pointe-au-Baril and the entrance to Parry Sound (Fig. 2.1; Culshaw et al. 1989). The spatial distribution of granite suggests the presence of a large, folded plutonic complex mainly covered by water.

Rocks of the Pointe-au-Baril complex range from tonalite to granite to quartz monzonite. K-feldspar megacrystic varieties predominate, with megacrysts up to 3 cm long. Plagioclase megacrysts are also locally observed, some which are strongly recrystallized and rimmed by fine-grained garnet (*cf.* Needham 1992). In high-strain areas, some non-megacrystic varieties are demonstrably the product of extensive recrystallization and tectonic degradation of a megacrystic protolith. Much of the Pointe-au-Baril complex,

however, contains wholly or partly recrystallized feldspar augen, making identification straightforward.

The two principal rock types of the complex are megacrystic tonalite gneiss (unit ta) and megacrystic granite gneiss (unit ga); both typically contain metamorphic biotite, amphibole, and garnet. These rock types generally occur in separate plutonic masses (Fig. 2.2) suggesting temporally distinct intrusive events. U-Pb zircon data appear to confirm a diachronous emplacement history. Analyses from granite and granodiorite gneiss (GC89-120, -122, -128; Fig. 5.2) define a discordia line with an upper intercept age of 1460 + 12/-8 Ma, interpreted as the age of igneous crystallization (Culshaw et al. in prep.). Megacrystic tonalite gneiss southeast of Pointe-au-Baril (TK84-92; Fig. 5.2) was emplaced at 1430 ± 17 Ma (Krogh et al. 1993*a*).

Angular to sub-rounded xenoliths of Nadeau Island orthogneiss and paragneiss are locally abundant in the Pointe-au-Baril complex (Fig. 2.6*a*). Mafic supracrustal gneiss with calc-silicate pods forms a common xenolith type readily distinguished as a Nadeau Island lithology (see above). Strongly foliated xenoliths of this type in mildly deformed granite indicate that not all high-strain fabrics post-date intrusion of monocyclic plutons. Less abundant enclave types not recognized as Nadeau Island lithologies include quartzite, metagabbro, and mafic-ultramafic rock with igneous layering (see below). Nearly all xenoliths contain a migmatitic gneissic foliation that predates granitoid plutonism Along the margins of granitoid bodies, original contact relationships with Nadeau Island gneiss are generally obscured by tectonic transposition.

Apart from a recrystallized plutonic texture, only a few primary magmatic features

are evident in the Pointe-au-Baril complex. Examples include metre-scale igneous layers defined by variations in megacryst abundance that likely indicate multiple magma injections (Fig. 2.6*b*), and flow alignment of xenolith long axes in weakly deformed granite (precluding a tectonic origin for the alignment; Fig. 2.6*a*).

The Pointe-au-Baril complex is weakly migmatitic and, in lower strain areas (*e.g.*, northwest of the Ojibway Hotel; Fig. 2.2), preserves granulite facies mineral assemblages. Orthopyroxene-bearing megacrystic granite is characterized by a grey to 'greasy green' appearance and is typically massive to weakly foliated. Feldspar megacrysts in these rocks commonly exhibit a purple hue and crystal-plastic deformation features (*e.g.*, undulose extinction, bent albite and deformation twins). Orthopyroxene is typically a relict phase in these rocks and is in contact with or rims metamorphic clinopyroxene (Chapter 4), indicating that both pyroxenes are metamorphic. Scattered occurrences of granulite-facies granite northwest of the Ojibway Hotel (Fig. 2.2) are spatially associated with mafic granulite xenoliths. Needham (1992) reported similar rocks of the Pointe-au-Baril complex on Hertzberg Island that appear to lie in the strain shadow of a competent mafic gneiss body (Fig. 2.2).

As outlined in Chapter 5 and by Ketchum et al. (1994), granulite facies assemblages preserved in low strain areas of the Nadeau Island gneiss association crystallized at *ca.* 1450 Ma. In light of the spatial association of charnockitic granite and orthopyroxene-bearing Nadeau Island gneiss, it is reasonable to assign granulite facies assemblages of the Pointe-au-Baril complex a similar age. This interpretation contrasts with that of Culshaw et al. (1988) who suggested that the Pointe-au-Baril complex was

only metamorphosed during the Grenvillian orogeny. However, both the Shawanaga pluton and Pointe-au-Baril complex are considered here to be monocyclic as neither contains evidence of deformation prior to Grenvillian orogenesis, and leucosomes within them appear to be entirely Grenvillian.

Shawanaga Pluton

The Shawanaga pluton (unit gb, Fig. 2.2) forms an elongate body between the Nadeau Island and Ojibway gneiss associations. The map pattern of this pluton highlights the northwest-trending, kilometre-scale folds that are the predominant structural feature in this region (Fig. 2.1). In the study area, the Shawanaga pluton narrows from several kilometres thick in the east to tens of metres thick in the west and southwest. This pluton appears to pinch out east of Hertzberg Island (Fig. 2.2) although Davidson et al. (1982) noted similar rocks to the south (assigned to the Pointe-au-Baril complex by Culshaw et al. 1989). Davidson et al. (1982) traced the Shawanaga pluton 20 km northeast of the study area. This body therefore forms a narrow but continuous, sheet-like mass at least 50 km long.

According to Davidson et al. (1982), the Shawanaga pluton consists of dioritic, tonalitic, granitic, and garnet-rich syenitic orthogneiss. Not all of these lithologies are recognized in the study area, in part because Davidson et al. (1982) included units that Culshaw et al. (1994) assigned to the Ojibway gneiss association. The pluton as outlined in Figure 2.2 consists predominantly of migmatitic, garnet-amphibole-biotite granodiorite gneiss with minor granite and leucogranite gneiss. K-feldspar megacrystic varieties are

present but megacrysts are generally not abundant. Relict garnet porphyroblasts up to 1 cm in diameter are rimmed by amphibole and biotite. These porphyroblasts are a distinctive feature of Shawanaga orthogneiss but are not everywhere present. Although resembling units of the Pointe-au-Baril complex, the Shawanaga pluton is distinctly more migmatitic and less megacrysytic, lacks country rock enclaves, and generally contains more garnet and amphibole porphyroblasts. Accessory titanite, allanite, apatite and zircon are also more abundant in this body than in the Pointe-au-Baril complex.

Nearly all exposures of Shawanaga orthogneiss in the study area lie within the Shawanaga shear zone. Megacrystic and non-megacrystic varieties have been reduced to homogeneous, streaky augen gneiss and straight gneiss, respectively (Fig. 2.6*c*). Leucosomes are generally transposed but in one lower strain area (Fig. 2.6*d*), contorted, irregular leucosomes appear to be transected by weakly discordant stromatic veins. However, no distinctive contacts were observed between these leucosome sets, suggesting either that they formed coevally or that the local stress field varied during a single metamorphic event. The stromatic veins have a similar orientation to discordant leucosomes in the Sand Bay gneiss association (Fig. 2.5*b*) and may be axial planar to the Shawanaga synform (Fig. 3.2).

U-Pb zircon analyses from a sample of granodiorite orthogneiss collected at the site of Figure 2.6*d* are colinear with discordant zircon analyses from Pointe-au-Baril complex granite. An upper intercept age of 1460 +12/-8 Ma for the combined data is interpreted as the igneous crystallization age of both plutonic masses (Culshaw et al. in prep.).

Mafic Plutonic Rocks and Dykes

Mafic plutonic rocks in the study area consist of (*i*) map-scale plutonic masses, (*ii*) layered mafic-ultramafic xenoliths in the Pointe-au-Baril complex, (*iii*) variably deformed and metamorphosed discordant mafic dykes, (*iv*) an unmetamorphosed diabase dyke of the *ca.* 590 Ma Grenville swarm, (*v*) isolated, metre- to decametre-scale tectonic enclaves, and (*vi*) concordant amphibolite layers of uncertain parentage. All of these forms are present in the parautochthon (Bayfield and Nadeau Island gneiss associations) but only some are found in the allochthon (Ojibway and Sand Bay gneiss associations). The above classification merely provides a convenient framework for describing mafic plutonic rocks in the study area and does not imply a unique magmatic-tectonic history for each. In fact, as outlined below, the ability to confidently assign metabasites to a specific period of dyking or plutonism is severely hampered by the heterogeneity and overall intensity of tectonic and metamorphic overprints. In this regard, preliminary whole-rock analyses (A. Davidson, unpublished data) indicate that geochemical studies may prove effective in distinguishing metabasite suites.

Mafic Plutons

Four large mafic plutonic units are shown in Figure 2.2. Metagabbro and amphibolite masses are located at the southwest end of Nares Inlet and west of Shawanaga Landing, respectively, and two closely spaced metagabbro bodies are found in Frederic Inlet. All have undergone tectonic modification along their margins such that

original contact relationships with host rocks are obscured. It is not known whether these bodies were intruded into their host rocks or were emplaced by tectonic processes. The structural setting of some, however, make it difficult to envisage an entirely tectonic derivation.

Nares Inlet Metagabbro. The Nares Inlet metagabbro (Fig. 2.2) is hosted by granitic orthogneiss of the Bayfield gneiss association. A smaller pluton to the northeast may be continuous at depth with the larger body or may constitute a separate pluton. Both contain medium- to coarse-grained metagabbro derived from a gabbronorite precursor. Mineral textures indicate a mixture of metamorphic and relict igneous minerals in these rocks. Igneous orthopyroxene and clinopyroxene are rimmed and partly replaced by metamorphic amphibole, and granoblastic plagioclase aggregates mimic the form of igneous plagioclase laths. Fine-grained garnet overgrows plagioclase-rich domains and rims amphibole overgrowths on pyroxene. Garnet and amphibole are typically separated by a thin 'moat' of recrystallized plagioclase, indicating migration of garnet grain boundaries into plagioclase domains (Whitney and McLelland 1973). Accessory minerals include ilmenite, apatite, and biotite.

Granulite facies recrystallization of the Nares Inlet pluton is indicated by the presence of granoblastic orthopyroxene and clinopyroxene that are texturally distinct from their relict igneous counterparts. Granulite facies assemblages are overprinted by amphibolite facies assemblages at the pluton margin where a gneissic foliation is observed. Boundaries between gneissic amphibolite and little-deformed metagabbro are commonly sharp (Fig. 2.7*a*).

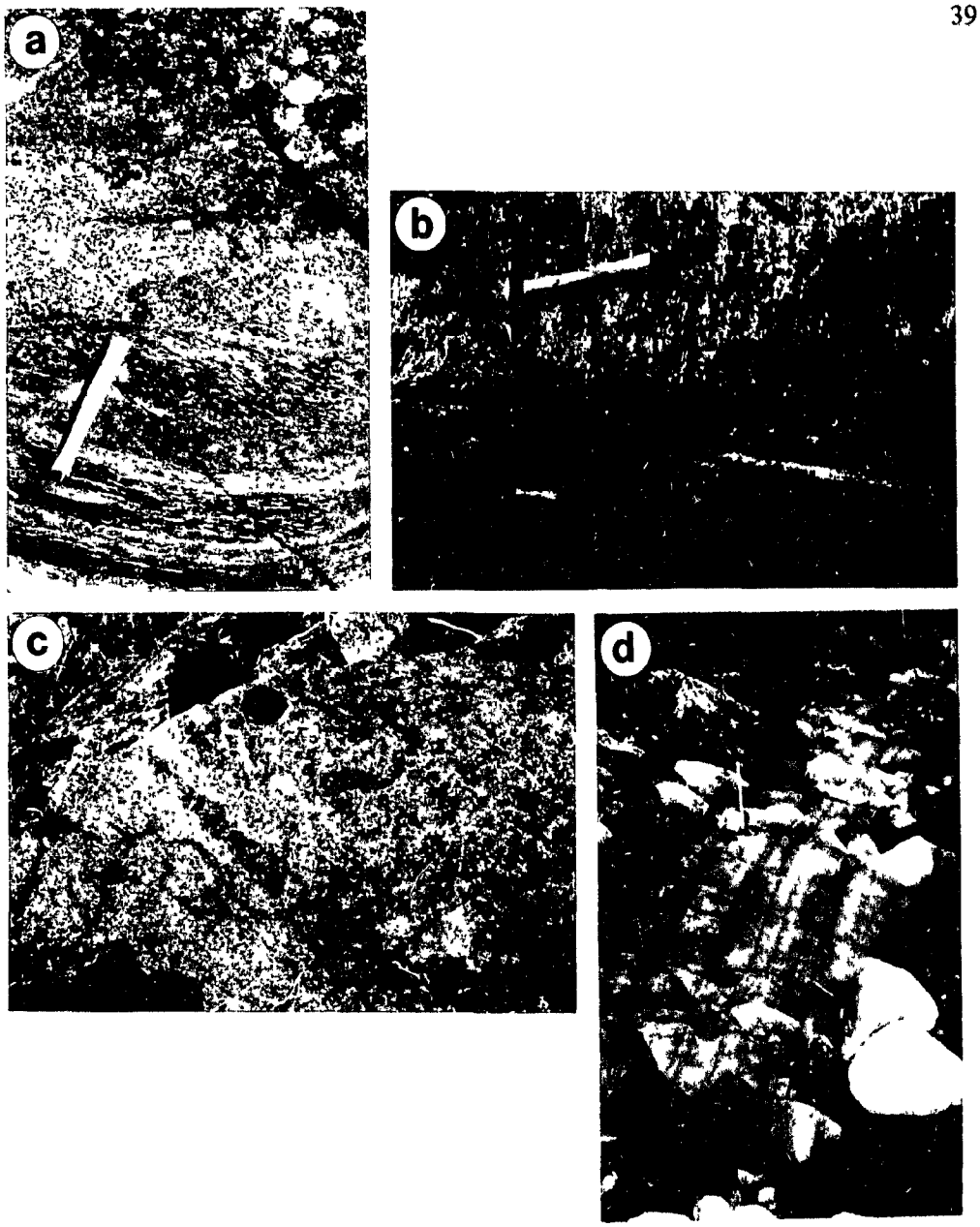

Fig. 2.7. Mafic plutonic rocks. **a)** Abrupt strain gradient between unfoliated metagabbro and sheared, migmatitic amphibolite derived from metagabbro near the margin of the Nares Inlet pluton. **b)** Narrow internal shear zone in the Leaming Island body of the Frederic Inlet metagabbros. Coronitic metagabbro is reduced to foliated, garnet-clinopyroxene amphibolite. **c)** Coarse-grained garnet metaclinopyroxenite ('meta-eclogite') with wispy, plagioclase-rich layers in the Leaming Island body. **d)** Layered mafic-ultramafic xenolith in the Pointe-au-Baril complex, Barclay Island.

The northwest margin of the Nares Inlet pluton is overprinted by mylonitic fabrics of the Nares Inlet shear zone (Fig. 2.2). Penetrative high-strain fabrics of this zone extend for only a few metres or tens of metres into the body.

Shawanaga Landing Metabasite. This body crops out a few hundred metres west of Shawanaga Landing as an irregular mass (Fig. 2.2). It is thoroughly metamorphosed and lacks relict igneous textures and minerals. Only one locality near the margin of the metabasite was visited. Here, the predominant rock types are heterogeneously deformed, fine- to medium-grained amphibolite, and garnet amphibolite cut by leucocratic veins. The abundance of fine-grained garnet and coarse, idioblastic amphibole in these rocks appears to increase with increasing intensity of tectonic fabric. A biotite amphibolite examined in thin section contains sericitized plagioclase and accessory quartz, Fe-Ti oxide, apatite, zircon, and allanite. The lack of relict igneous minerals and textures suggests that the Shawanaga Landing metabasite is an older, more thoroughly recrystallized plutonic body than the Nares Inlet metagabbro.

Frederic Inlet Metagabbros. Two metagabbroic bodies located southwest of Shawanaga Island are distinct from all other metabasic rocks in the Pointe-au-Baril area. These are the Frederic Inlet metagabbros (Fig. 2.2), mapped and studied in detail by Needham (1987, 1992). Both bodies lie within the Shawanaga shear zone and are hosted by straight and porphyroclastic gneiss of the Nadeau Island association. The proximity and along-strike position of the bodies suggest that they may represent a tectonically disrupted larger plutonic mass (Needham 1992).

Needham (1987, 1992) examined the field setting, petrology, chemistry, and *P-T*

evolution of the Frederic Inlet metagabbros and a summary of this work (employing Needham's terminology) is presented here. The Leaming Island body and the smaller Twin Domes metagabbro (Fig. 2.2) contain a number of mafic and ultramafic rock types preserving a wealth of igneous and metamorphic textures. The principal units are olivine metagabbro, garnet peridotite, orthopyroxene-clinopyroxene metagabbro, hornblende-plagioclase metagabbro, garnet-clinopyroxene metagabbro, garnet metaclinopyroxenite, and hornblende-biotite metagabbro. Hornblende-biotite metagabbro mainly occurs as a foliated marginal phase. Igneous layering, defined by modal variations in plagioclase, is locally preserved in pluton interiors within otherwise massive, subophitic metagabbro. Intense tectonic fabrics overprint these units near pluton margins and within discrete, sharp-walled, internal shear zones (*e.g.*, Fig. 2.7*b*).

Whole rock geochemical data indicate that the metagabbros crystallized from two distinct magmas. Garnet metaclinopyroxenite and hornblende-biotite metagabbro protoliths crystallized from an evolved magma enriched in iron (Fe series; Needham 1992) whereas all other rock types crystallized from a primitive liquid enriched in calcium and magnesium (Mg series). There is no chemical evidence to suggest a genetic link between these magmas, and no contact relationships indicating relative emplacement age were observed.

Metamorphism has produced a variety of corona and symplectic textures, many of which have been previously documented in the southwest Grenville Province (*e.g.*, Davidson et al. 1982; Davidson and Grant 1986; Grant 1989; Davidson 1990). Metamorphism of olivine gabbro in Frederic Inlet has produced distinctive corona

textures. Relict igneous olivine is rimmed by metamorphic orthopyroxene, clinopyroxene, amphibole, and garnet in a core-to-rim sequence. Where corona-forming reactions are more advanced, olivine is completely replaced by granoblastic orthopyroxene. A wealth of disequilibrium textures in these and other rocks collectively demonstrate a lack of complete metamorphic re-equilibration in the 'dry,' rheologically competent, mafic and ultramafic units. However, unlike similar textures described in metabasites from the southwest Grenville Province, corona assemblages in the Frederic Inlet metagabbros are interpreted as the product of reactions between olivine and clinopyroxene-spinel symplectite rather than between olivine and plagioclase. Needham (1992) suggested that igneous plagioclase reacted to form clinopyroxene-spinel symplectite during an early stage of metamorphism that preceeded corona development.

The presence of garnet metaclinopyroxenite or 'meta-eclogite' in the Frederic Inlet metagabbros provides information on the conditions of this early metamorphism. This rock type has been documented in several localities throughout the Central Gneiss Belt (Davidson et al. 1982; Culshaw et al. 1983, 1989, 1991*a*; Grant 1989; Davidson 1991) where it commonly forms an internal unit of tectonized mafic bodies in domain-bounding shear zones. Although containing plagioclase and lacking omphacitic clinopyroxene, reaction textures and mineral chemical data suggest that the meta-eclogites are re-equilibrated relics of eclogite *sensu stricto* (Davidson 1990). Plagioclase and diopside are interpreted as products of omphacite breakdown during decompression from eclogite facies. The garnet metaclinopyroxenites described by Needham (1987, 1992) resemble meta-eclogites in the southwest Grenville Province and indicate an early episode of high

pressure metamorphism. This is consistent with metamorphic textures in garnet peridotite from the Frederic Inlet metagabbros suggesting reaction of primary garnet and olivine to form orthopyroxene-spinel symplectite ($P_{minimum}$ ~ 16 kbar; Needham 1992), and by the breakdown in other rocks of igneous plagioclase to form clinopyroxene-spinel symplectite. Metastable preservation of these metamorphic assemblages and textures likely reflects a combination of slow reaction kinetics and reduced water activity in the rheologically competent mafic rocks (*e.g.*, Grant 1989; Indares 1993). Meta-eclogites in the Central Gneiss Belt thus appear to provide a window on high pressure tectonometamorphic events prior to widespread re-equilibration in the amphibolite to granulite facies.

A critical question, not yet resolved, concerns the age of eclogite-facies metamorphism in the Central Gneiss Belt. Was it an early Grenvillian metamorphic event or was it pre-Grenvillian? Do the eclogite-facies tectonic enclaves document a period of *in situ* metamorphism (Davidson 1990) or do they carry exotic metamorphic assemblages transported from depth along ductile shear zones (Grant 1989)? Resolution of these questions is critical to unravelling the tectomometamorphic evolution of the Central Gneiss Belt.

A traverse across the western portion of the Leaming Island body (Fig. 2.2) was made during the course of the present study. The traverse crossed from weakly foliated hornblende-plagioclase metagabbro and garnet metaclinopyroxenite in the interior to strongly foliated hornblende-biotite metagabbro at the margin. Field observations and petrography show that (*i*) massive, subophitic, coronitic metagabbro derived from an olivine + clinopyroxene + plagioclase igneous assemblage is reduced to

garnet-clinopyroxene amphibolite within discrete high-strain zones in the interior of the Leaming Island body (Fig. 2.7*b*), (*ii*) garnet metaclinopyroxenite ranges from fine-grained with modal variations in clinopyroxene defining a centimetre-scale (igneous?) layering, to coarse-grained with plagioclase-rich layers defining a weak metamorphic foliation (Fig. 2.7*c*). Amphibole is common in this rock and plagioclase may be completely replaced by sericite and epidote. Titanite and ilmenite are matrix accessory phases, and rutile occurs as inclusions in clinopyroxene and garnet. Clinopyroxene is riddled with exsolved plagioclase blebs. (*iii*) Garnet-biotite amphibolite near the margin of the body contains amphibole poikiloblasts and vermicular quartz exsolved from plagioclase grains. Macroscopically, this rock preserves few clues as to the identity of its igneous precursor.

Exposures of garnet metaclinopyroxenite were also examined at a locality in the Twin Domes body. Here, the rock is massive and fine- to medium-grained, with abundant garnet and clinopyroxene intergrown with weakly recrystallized amphibole poikiloblasts. Plagioclase is moderately sericitized, and titanite rims ilmenite. Where hydration of this unit has produced garnet amphibolite, centimetre-size, idioblastic scapolite porphyroblasts with quartz inclusions are locally observed, and smaller titanite porphyroblasts are rimmed by intergrowths of amphibole and ilmenite. No other rock types were examined in the Twin Domes body.

Layered Mafic-Ultramafic Xenoliths in the Pointe-au-Baril Complex

Metabasic xenoliths preserving relict igneous textures and layering occur at three localities in the Pointe-au-Baril complex (Fig. 2.2). The xenoliths range from 2 to 40 m in

longest dimension and are characterized by rhythmically alternating layers of subophitic metagabbro and a clinopyroxene-rich ultramafic rock. Ultramafic layers are generally several centimetres thick whereas metagabbro layer widths are measured on the decimetre- to metre-scale.

A 10 x 40 m xenolith hosted by megacrystic tonalite on Barclay Island (Fig. 2.2) was examined in detail. Planar igneous layering is well developed in this body (Fig. 2.7*d*) and layer contacts are sharp. Metagabbro is highly recrystallized but preserves a relict subophitic texture. Igneous clinopyroxene is epitaxially overgrown by metamorphic amphibole, and igneous plagioclase laths are partly replaced by scapolite. Biotite-amphibole aggregates are locally present; both of these minerals also overgrow Fe-Ti oxides. Idioblastic garnet porphyroblasts commonly decorate amphibole-plagioclase contacts.

Locally, the metagabbro contains coarse-grained plagioclase oikocrysts enclosing well-preserved igneous orthopyroxene and clinopyroxene with only thin, discontinuous rims of amphibole. Orthopyroxene crystals are crowded with minute spinel inclusions and are locally recrystallized to a mosaic of spinel-free, granoblastic grains rimmed by columnar amphibole.

Ultramafic layers in the Barclay Island xenolith contain a relict clinopyroxene + olivine + orthopyroxene igneous assemblage with superimposed corona textures. Olivine relicts are successively mantled by columnar orthopyroxene and a very fine-grained symplectite (amphibole-clinopyroxene?). An additional symplectic mantle of garnet and an unidentified phase occur where olivine-consuming reactions have gone to completion; this

symplectite also rims relict igneous clinopyroxene. Pale brown amphibole overgrows clinopyroxene, and opaque oxides are mantled by biotite. Rutile and green spinel comprise accessory phases; the latter also forms rare overgrowths on olivine.

The origin of mafic-ultramafic xenoliths in the Pointe-au-Baril complex is uncertain. Although they resemble lithologies of the Frederic Inlet metagabbros, the latter lack the well-developed, rhythmic, mafic-ultramafic layering that is characteristic of the xenoliths. It is therefore suggested that the layered xenoliths represent fragments of a deep-level mafic-ultramafic body which does not crop out in the Pointe-au-Baril area.

Metabasic Dykes

At least four metamorphosed mafic dyke suites are present in the study area. Three suites are recognized in the parautochthonous Bayfield and Nadeau Island gneiss associations (Culshaw et al. 1994) whereas only a single suite confined to the Sand Bay gneiss association has been identified in the allochthon. Discussion is restricted here to metabasic layers for which an intrusive origin can be unequivocally demonstrated; concordant amphibolite layers that may or may not represent transposed dykes are described later.

Parautochthon. The oldest dykes in the parautochthon are foliated, migmatitic, biotite-garnet amphibolites that shallowly cross-cut their host rocks (Fig. 2.8*a*). Emplacement of this suite pre-dates intrusion of *ca.* 1460-1430 Ma plutons. These dykes are readily distinguished from younger dykes by their gneissic foliation and the presence of trondhjemitic veins that locally preserve relict orthopyroxene porphyroblasts. Vein

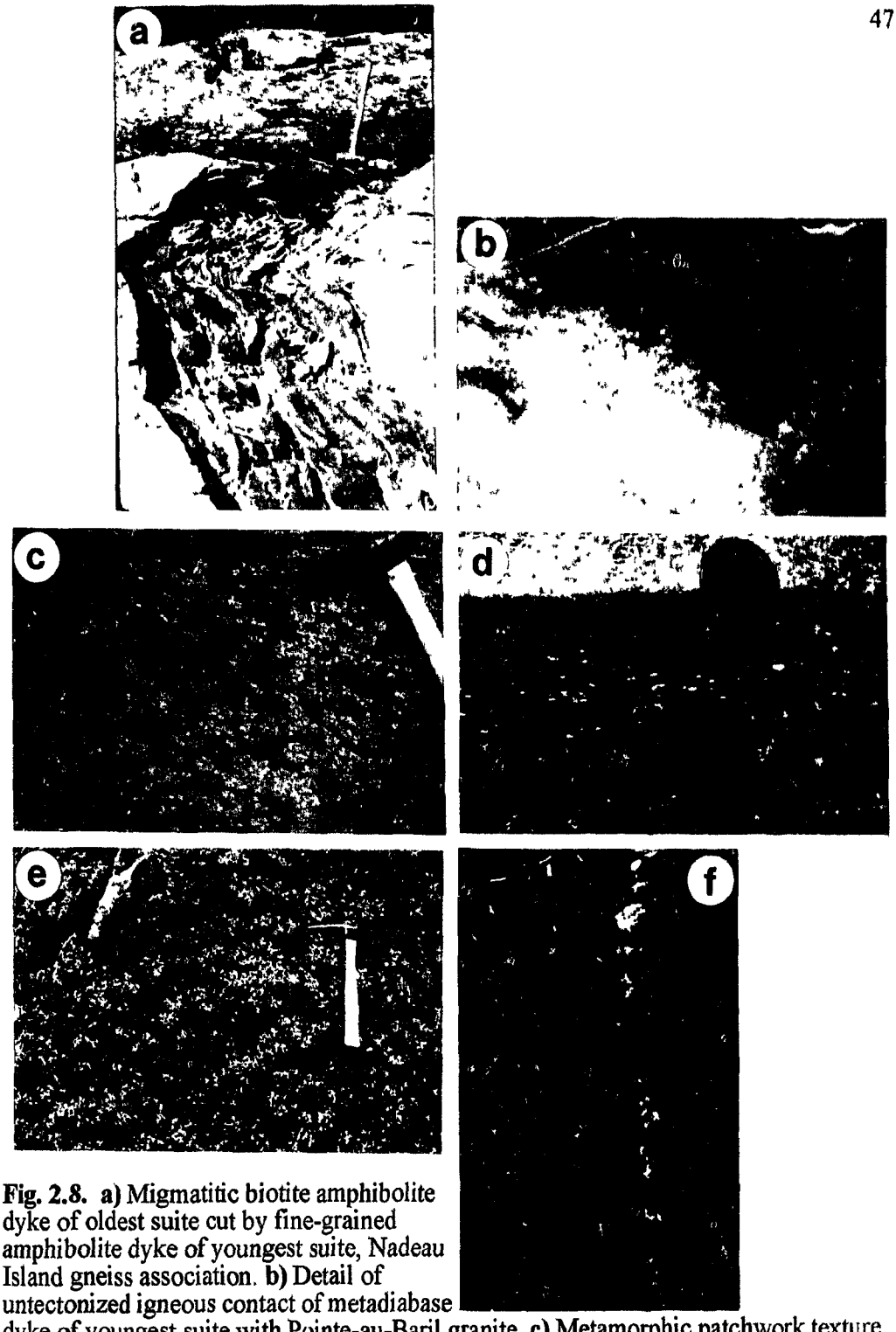

Fig. 2.8. **a)** Migmatitic biotite amphibolite dyke of oldest suite cut by fine-grained amphibolite dyke of youngest suite, Nadeau Island gneiss association. **b)** Detail of untectonized igneous contact of metadiabase dyke of youngest suite with Pointe-au-Baril granite. **c)** Metamorphic patchwork texture and **d)** plagioclase phenocrysts in amphibolite dykes of youngest suite, Bayfield gneiss association. **e)** Raised clinopyroxene oikocrysts in a recessively weathered matrix, coronitic olivine metagabbro body in Shawanaga pluton. **f)** Syn-volcanic(?) amphibolite dyke with intrusive apophyses in supracrustal gneiss, Sand Bay gneiss association.

generation is suggested here to be synchronous with *ca.* 1450 Ma granulite-facies metamorphism (Chapter 5). Grenvillian tectonometamorphic activity has led to a variable metamorphic overprint and has imparted much of the gneissic, amphibolite-facies fabric displayed by this suite.

The period beween emplacement of *ca.* 1460-1430 Ma granitoid plutons and latest Grenvillian metamorphism was marked by intrusion of at least two mafic dyke suites in the parautochthon. These dykes serve as monitors of Grenvillian strain and metamorphism as their emplacement post-dates pre-Grenvillian orogenic events (Culshaw et al. 1988). Where strongly metamorphosed, both dykes suites are characterized by garnet-biotite amphibolite with few mineralogical or textural differences to distinguish them. However, where Grenvillian overprinting is weak, distinctive textural and compositional differences can be discerned. For example, at a locality ~1 km southeast of Lookout Island (Fig. 2.2), an amphibolite dyke of the older suite lacks igneous textures and minerals despite a comparatively low level of Grenvillian strain. This dyke is cut by a north-striking, 2 m-wide, metadiabase dyke of the younger suite that preserves primary clinopyroxene and plagioclase and a subophitic texture. Metamorphism has resulted in growth of abundant, fine-grained garnet in plagioclase-rich domains and amphibole-biotite overgrowths on igneous clinopyroxene and Fe-Ti oxides. Metamorphic clinopyroxene is also present in this dyke.

Metamorphic and relict igneous textures in the younger dyke resemble those observed in metadiabase dykes of the *ca.* 1238 Ma (Krogh et al. 1987) Sudbury swarm (A. Davidson, written communication 1993). Variably deformed and metamorphosed

members of this suite are documented up to 45 km southeast of the Grenville Front in Ontario (*e.g.*, Davidson and Bethune 1988; Bethune and Davidson 1988; Bethune 1989, 1993; Corrigan 1990; Jamieson et al. 1995). Geochemical data (A. Davidson, unpublished data) for the younger dyke described above and an identical body along Pointe-au-Baril channel (Fig. 2.8*b*) tentatively support correlation of these dykes with the Sudbury swarm. Culshaw et al. (1994) also suggested that the youngest dykes in the Britt domain near Pointe-au-Baril could be correlated with Sudbury metadiabase.

Within the study area, a number of metadiabase dykes of the youngest suite have textural and mineralogical characteristics that mark intermediate stages of the progressive transformation of metadiabase to garnet amphibolite. This metamorphic transformation is characterized by early destruction of relict subophitic textures as amphibole rims on Fe-Ti oxide and igneous clinopyroxene coarsen, and as metamorphic garnet, amphibole, biotite, and pyroxenes become more abundant. This stage may have taken place at granulite facies as several dykes contain granoblastic orthopyroxene in the equilibrium assemblage. Amphibolite facies hydration along the margins of these dykes represents a more advanced stage of transformation and is marked by the development of centimetre-scale domains rich in garnet, biotite, and altered clinopyroxene, bounded by an anastomosing network of amphibole-rich domains (termed here *patchwork texture*; Fig. 2.8*c*). Within some dykes the transition from metadiabase in the core to garnet amphibolite with patchwork texture along the margins is sharp, suggesting that diffusion of fluids into the dyke occurred along a discrete hydration front.

The end product of deformation and metamorphism of the youngest dyke suite is a

homogeneous, fine-grained garnet amphibolite. Patchwork textures in precursors are obliterated by continued recrystallization, by deformation, or may not have initially formed. Where deformation has not completely homogenized the patchwork texture, the dykes have a distinctive striped appearance formed by flattening of the amphibole-rich domains.

In addition to the above characteristics, a few dykes of the youngest suite contain small (<1 cm), recrystallized plagioclase phenocrysts that typically occupy dyke margins (Fig. 2.8*d*). Youngest dykes are also locally distinguished by an absence of Grenvillian leucosome in adjacent host rocks. This feature suggests that during Grenvillian metamorphism, dyke hydration was accomplished by migration of fluids from adjacent host rocks into the dyke, thereby depleting the host of fluids necessary for leucosome development.

In summary, although strongly metamorphosed dykes of the two youngest suites are not readily distinguished from one another, specific combinations of textural and mineralogical characteristics can in some cases serve to distinguish them. Cross-cutting relationships provide the best means of identifying these suites, but it should be cautioned that cross-cutting relationships are locally observed among dykes of the youngest suite. This characteristic further supports correlation of these dykes with the Sudbury swarm as diachronous intrusion of Sudbury diabase is indicated by field, geochronological, and geochemical data from both sides of the Grenville Front (*e.g.*, Bethune 1993).

Allochthon. Cross-cutting mafic dykes observed in the parautochthon have not been identified in the allochthonous Shawanaga domain. Although there are scattered

amphibolite layers in the Shawanaga pluton and Ojibway gneiss association that could be dykes, no discordant relationships were observed between these layers and their host rocks.

Rare, garnet-bearing amphibolite layers in the Sand Bay gneiss association preserve intrusive apophyses that unequivocally demonstrate their origin as dykes. Members of this suite were examined at a locality on the east shore of Shawanaga Island (Fig. 2.8*f*). Here, the dykes are narrow (≤30 cm) and concordant to a weak foliation in their amphibole + plagioclase ± garnet paragneiss host rocks. They are medium grained and are mineralogically similar to their host rocks, varying in only a greater abundance of amphibole. Deformation and metamorphic recrystallization appear to have influenced dykes and host rocks alike as both have comparable metamorphic textures and grain size. This contrasts with amphibolite dykes in the parautochthon which are finer grained than their host rocks and have a less extensive tectonometamorphic history. Correlation of the Sand Bay suite with dykes in the parautochthon is therefore ruled out. The possibility that these dykes were emplaced during *ca.* 1400-1300 Ma volcanic activity in the Sand Bay association (N.G. Culshaw, personal communication 1993) requires testing by U-Pb and geochemical methods.

Diabase of the Grenville Dyke Swarm

A single outcrop of medium-grained, pristine diabase with no evidence of metamorphism or deformation was discovered in Nares Inlet during the present study (Fig. 2.2). This outcrop coincides with a prominent east-northeast-trending lineament mostly

filled by water and swamp. The contact of the diabase with quartzofeldspathic gneiss of the Bayfield association was not observed.

The diabase weathers reddish brown and is pale green on fresh surfaces. Subophitic intergrowths of medium-grained plagioclase and clinopyroxene, and numerous small plagioclase laths ophitically enclosed by clinopyroxene, are observed in thin section. Olivine is partly to completely replaced by brown serpentine.

The diabase bears all the field and petrographic characteristics of tholeiitic diabase of the *ca.* 590 Ma (Kamo et al. 1991) Grenville dyke swarm (Fahrig and West 1986). These dykes trend easterly and are thought to be related to the earliest stages of Iapetan rifting (Kumarapeli 1993). The Grenville dykes resemble weakly metamorphosed Sudbury diabase but can be distinguished from them by a number of field and thin section criteria (see Bethune and Davidson 1988). Based on field and petrographic evidence, it is likely that the Nares Inlet diabase is part of a previously undocumented dyke of the Grenville swarm.

Tectonized Mafic Bodies

A variety of deformed metabasic bodies are found throughout the study area, particularly within ductile high-strain zones. These bodies range from less than a metre to several tens of metres in longest dimension. Contacts with host gneisses are invariably tectonic and intrusive relationships, if once present, are not preserved. The bodies exhibit a variety of metamorphic and relict igneous textures but all have amphibolite margins. Although their parentage is in many cases unclear, most undoubtedly formed by the

tectonic disaggregation of larger, competent metabasite bodies during ductile deformation of their quartzofeldspathic host rocks. Repetition of pods of a distinctive composition along strike locally attests to this process. The pods are derived from metagabbro plutons, mafic dykes, and concordant amphibolite layers.

Included in this category are bodies of coronitic olivine metagabbro belonging to a *ca.* 1170 Ma (Davidson and van Breemen 1988) suite that is widespread in the Central Gneiss Belt (*e.g.*, Davidson et al. 1982, 1985; Davidson and Grant 1986; Grant 1987; Davidson 1991). Individual bodies of this suite are typically less than 1 km in longest dimension and are found as isolated masses or in clusters, often near or within domain-bounding shear zones (Davidson and Grant 1986). Where undeformed or only mildly deformed, metagabbro retains a subophitic igneous texture and exhibits metamorphic coronas formed by reaction of primary olivine and Fe-Ti oxide with igneous plagioclase (Davidson and van Breemen 1988). Coronas typically comprise an outward succession of polycrystalline orthopyroxene, clinopyroxene, (±amphibole), and garnet on olivine, and polycrystalline biotite, amphibole, and garnet on Fe-Ti oxide (Davidson 1991). The coronas are thought to have formed during metamorphic recrystallization in the interval 1060-1030 Ma, the age of zircon mantles on primary baddeleyite (Davidson and van Breemen 1988; van Breemen and Davidson 1990; Heaman and LeCheminant 1993). A thorough discussion of field relationships and petrographic characteristics of this suite is given by Davidson (1991).

Coronitic olivine metagabbro in the Pointe-au-Baril area displays many, if not all, of the characteristics of the *ca.* 1170 Ma suite. Scattered tectonic enclaves of coronite up

to tens of metres long are observed in the Shawanaga pluton and Ojibway gneiss association (Fig. 2.2). Some metagabbro bodies contain clinopyroxene oikocrysts up to 7 cm in diameter which impart a distinctive mottled appearance in outcrop (Fig. 2.8*e*). Olivine is partly to completely replaced by orthopyroxene or brown serpentine. Where intensely recrystallized, coronite is reduced to fine-grained garnet amphibolite with vestiges of subophitic texture.

A coarse-grained metagabbro body located approximately 10 km south of Pointe-au-Baril on Highway 69 (Fig. 2.2) is typical of little-deformed coronite. U-Pb dating of primary baddeleyite and zircon indicates igneous crystallization of this body at 1152 ± 2 Ma (Heaman and LeCheminant 1993), in contrast to emplacement ages of *ca.* 1170 Ma indicated for coronites up to 130 km east of the Pointe-au-Baril area (Davidson and van Breemen 1988). Reasons for this discrepancy are not immediately apparent, but if the U-Pb data accurately reflect igneous crystallization age, a minimum 20 M.y. emplacement interval for this suite is suggested.

Coronitic metagabbro bodies in the study area are restricted to the Shawanaga domain (excluding the Sand Bay gneiss association) and many of these lie within the Shawanaga shear zone. This is consistent with Davidson's (1991) observation that coronite is absent north of the Shawanaga shear zone, and with the additional observation (Davidson and Grant 1986) that coronites generally lie within or near the boundaries of lithotectonic domains. Differences in whole-rock geochemistry (A. Davidson, unpublished data) preclude the possibility that youngest dykes north of the shear zone (tentatively correlated with the 1238 Ma Sudbury swarm; see above) belong to the *ca.* 1170 Ma

coronite suite. Olivine-bearing rocks of the Frederic Inlet metagabbros have comparable corona textures but are geochemically and mineralogically distinct from coronite (Needham 1992). These data support the hypothesis (Davidson 1991; Bethune 1993; Culshaw et al. 1994) that the Shawanaga shear zone separates regions with distinctive mafic intrusive suites. The regional tectonic significance of this structural boundary is discussed in Chapter 6.

Concordant Amphibolite Layers

Allochthonous and parautochthonous rocks in the study area regularly contain centimetre- to metre-width, concordant layers of amphibolite and amphibolite gneiss. These layers are generally traceable for several tens of metres. The moderate to high strain state of their host rocks suggests that their concordance is mainly due to tectonic transposition. In some localities, the concordant sheets have a similar width and composition to nearby discordant amphibolite dykes, suggesting derivation from dykes. However, it is unlikely that all concordant amphibolite layers in the study area formed exclusively by dyke transposition. The amphibolite layers may in some cases represent deformed sills, highly attenuated tectonic enclaves, or even original strata.

Pegmatite Dykes

Granitic pegmatite dykes intrude all units in the study area. The pegmatite dykes range from unrecrystallized, straight-walled discordant sheets to highly tectonized concordant layers that in some places have been completely disaggregated into trains of

feldspar porphyroclasts.

Three sets of pegmatite dykes were documented in the Frederic Inlet area by Needham (1992). The oldest dykes are strongly deformed within the Shawanaga shear zone and are cut by synkinematic pegmatites that have undergone rotation and progressive boudinage. The youngest dykes cut shear zone fabrics and older dykes alike, and form straight-walled, pristine intrusive sheets.

Field observations made during the course of this study are consistent with the observations of Needham (1992). A dyke from each of the above suites (Fig. 5.6) has been dated by U-Pb geochronology in order to constrain the timing of extensional shear on the Shawanaga shear zone. The results of this work (Chapter 5) indicate that the three suites are Grenvillian and were emplaced in the interval 1042-988 Ma.

Rare, strongly recrystallized pegmatite dykes cutting Nadeau Island lithologies may belong to a pre-Grenvillian suite as their degree of recrystallization is greater than that observed in Grenvillian pegmatites.

2.3 SUMMARY

1) The study area is underlain by parautochthonous rocks of the Britt domain and structurally overlying allochthonous rocks of the Shawanaga domain (new name). These lithotectonic domains are separated by the extensional Shawanaga shear zone (new name) which accommodated early, northwest-directed thrusting prior to top-side-down to the southeast reactivation during the Grenvillian orogeny. The Shawanaga shear zone is the site of Allochthon Boundary Thrust (Rivers et al. 1989) in the western Central Gneiss

Belt.

2) Parautochthonous rocks in the study area belong to the polycyclic Bayfield and Nadeau Island gneiss associations (Culshaw et al. 1988). These associations contain a variety of ortho- and paragneisses which were deformed and metamorphosed prior to emplacement of megacrystic granite and tonalite of the Pointe-au-Baril complex and intrusion of at least three mafic dyke suites. All were deformed subsequently during the Grenvillian orogeny. Polycyclic orthogneisses were emplaced at *ca.* 1740 Ma and *ca.* 1605 Ma, and the megacrystic granitoid plutons at *ca.* 1460-1430 Ma. Youngest dykes in the parautochthon have petrographic and geochemical characteristics suggesting that they may belong to the *ca.* 1238 Ma Sudbury dyke swarm.

3) Allochthonous rocks in the study area belong to the monocyclic Ojibway and Sand Bay gneiss associations. The Ojibway association comprises *ca.* 1460 Ma orthogneiss whereas the Sand Bay association consists of supracrustal gneiss with protolith ages younger than *ca.* 1420 Ma. The Shawanaga pluton is a *ca.* 1460 Ma megacrystic granitoid body that resembles the Pointe-au-Baril complex in the Britt domain but is assigned to the Shawanaga domain. Mafic dykes do not penetrate from the Britt domain into the Shawanaga domain. The Shawanaga domain appears to have been deformed and metamorphosed only during the Grenvillian orogeny.

4) In addition to mafic dykes, other metabasic rock types in the study area include metagabbro, *ca.* 1170-1150 Ma coronitic metagabbro, sparse meta-eclogite, unmetamorphosed *ca.* 590 Ma diabase, and layered mafic-ultramafic enclaves in granite orthogneiss. Small metagabbro and amphibolite bodies (plutons?) are documented in the

Britt domain. Coronitic metagabbro is restricted to the allochthonous Shawanaga pluton and Ojibway gneiss association. Meta-eclogite occurs in the Frederic Inlet metagabbros and in small tectonic enclaves within the Shawanaga shear zone. An outcrop of fresh diabase in Nares Inlet is correlated with the *ca.* 590 Ma Grenville dyke swarm. Rare, layered mafic-ultramafic enclaves are found in the Pointe-au-Baril complex.

5) Granitic pegmatite dykes range from undeformed to strongly deformed within the Shawanaga shear zone.

CHAPTER 3

Structural Zones, Folds, And Extensional Shear Zones

3.1 INTRODUCTION

A large portion of the Grenville Province is underlain by rocks of Archean to Mesoproterozoic age that were ductilely deformed and metamorphosed at high grade prior to ~1.2-1.0 Ga Grenvillian reworking (*e.g.*, Rivers et al. 1989). These rocks are generally dominated by Grenvillian tectonic elements and in many places preserve little evidence of older ductile deformation events. However, older gneissic fabrics and structures are preserved in some areas due to the lack of a thorough Grenvillian overprint (*e.g.*, Gower and Owen 1984; Corrigan et al. 1994). A similar appearance of temporally distinct gneissic fabrics may cause difficulty in distinguishing the relative contributions of pre-Grenvillian and Grenvillian deformation to finite strain. This distinction is vital, however, in the interpretation of structural, metamorphic, and geochronologic data, and in the construction of tectonic models of Grenvillian and pre-Grenvillian orogenesis.

Recent work in the Central Gneiss Belt (*e.g.*, Corrigan 1990; Haggart 1991; Jamieson et al. 1992; Bethune 1993; Corrigan et al. 1994; Ketchum et al. 1994) and elsewhere in the orogen (*e.g.*, Gower and Owen 1984; Thomas et al. 1986; Indares and Martignole 1989; Scott et al. 1993; Connelly and Heaman 1993) has amply demonstrated that pre-Grenvillian tectonic and metamorphic elements survive at a variety of scales. The Pointe-au-Baril area (Fig. 3.1) is one area where pre-Grenvillian structures and metamorphic assemblages are preserved (Jamieson et al. 1992; Ketchum et al. 1994;

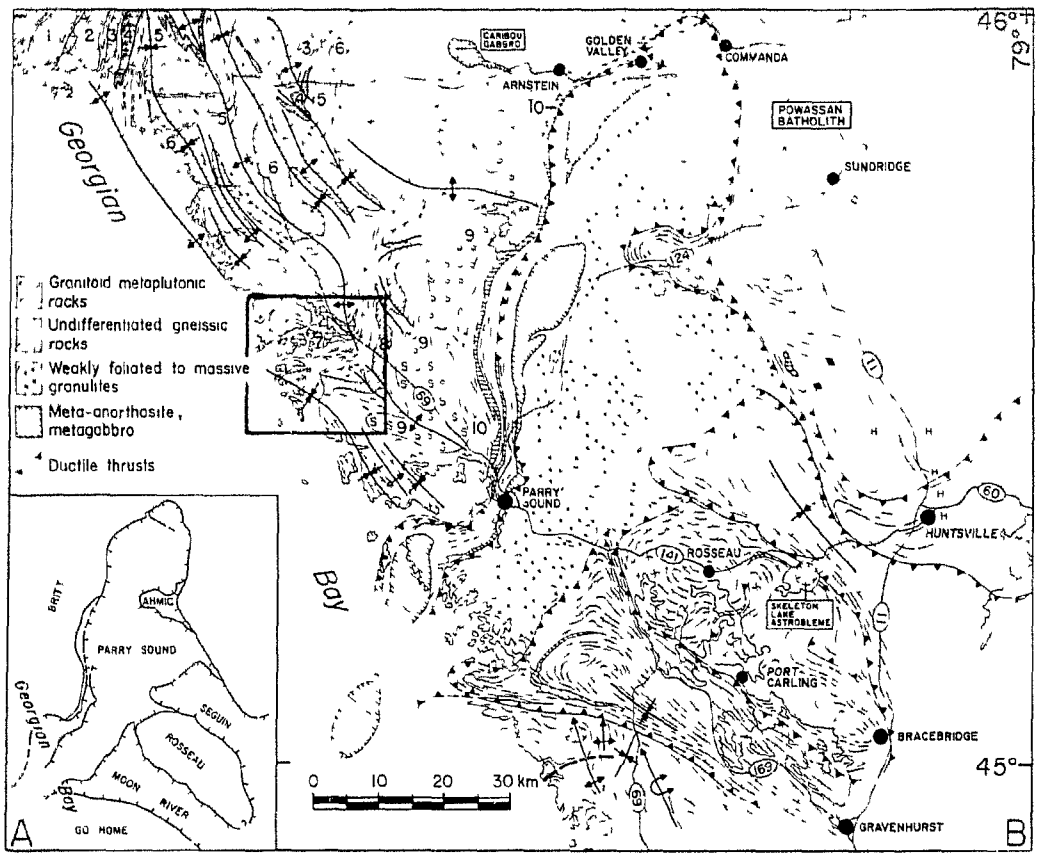

Fig. 3.1. Regional lithotectonic map of SW Central Gneiss Belt showing major lithologic units, domains and subdomains (inset), and hinge trace of km-scale, NW-trending antiforms and synforms. Study area indicated by box. Britt pluton is labelled 6, Shawanaga pluton is labelled 8 (from Schwerdtner 1987, after Davidson et al. 1982).

Culshaw et al. 1994), providing a rare opportunity to study features of the pre-Grenvillian crust in the interior of the southwest Grenville Province. The complex tectonic history of the Pointe-au-Baril region (*e.g.*, Davidson et al. 1982; Culshaw et al. 1988, 1989; 1994) and a heterogeneous late Grenvillian deformation have resulted in a zonal distribution of geometrically and temporally distinct structures and tectonic fabrics. In this chapter, six structural zones preserving elements of this protracted history are delineated in the study area. The Shawanaga and Nares Inlet shear zones are also examined in detail, particularly with regard to their extensional displacement history and the interaction of folding and southeast-directed extensional shear. As outlined below, these shear zones appear to have played a key role in the preservation of pre-Grenvillian tectonic and metamorphic elements.

Regional Structural Framework

In the Central Gneiss Belt of Ontario, pre-Grenvillian tectonic elements in parautochthonous rocks have been variably overprinted during Grenvillian orogenesis whereas polyorogenic deformation in allochthonous domains has not been demonstrated. This contrasts with the well-established polyorogenic character of a number of allochthonous domains in the eastern Grenville Province (*e.g.*, Wardle et al. 1986). The possibility that allochthonous rocks lying north of the Central Metasedimentary Belt in Ontario are monocyclic (*i.e.*, affected only by Grenvillian orogenesis) requires further investigation. This observation tentatively points to variations in the pre-Grenvillian tectonic history of allochthonous terranes along the length of the Grenville orogen (*e.g.*,

Rivers et al. 1993).

Regional-scale structures in the western Central Gneiss Belt include narrow but laterally continuous ductile shear zones with thrust-sense kinematic indicators (*e.g.*, Davidson et al. 1982; Culshaw et al. 1983) and upright, close to tight folds with variably plunging, northwest-trending axes (*e.g.*, Davidson and Morgan 1981; Davidson et al. 1982; Schwerdtner 1987; Culshaw et al. 1991*a*, 1994) (Fig. 3.1). Ductile shear zones, particularly those within parautochthonous rocks, are both internal and external to lithotectonic domains and are likely to have formed over an extended period of Grenvillian (and possibly earlier) orogenesis (Davidson et al. 1982; Culshaw et al. 1983, 1988; Easton 1992; Nadeau and Hanmer 1992; Jamieson et al. 1995). In contrast, the northwest-trending folds appear to be late Grenvillian structures (Davidson and Morgan 1981; Culshaw et al. 1994) as they deform shear zones and related tectonic fabrics of presumed Grenvillian age. These folds are coaxial with a regional, southwest-plunging finite stretching lineation. Schwerdtner (1987) labelled them as 'set-2' Grenvillian structures that overprint an older generation of set-1 isoclinal folds (restricted to allochthonous domains?; Culshaw et al. 1994) but are themselves reworked by open to close, east- to northeast-trending folds of set-3. A recent hypothesis is that regional-scale, isoclinal folds of set-1 were formed during early northeastward stacking of fold nappes prior to northwest-directed thrusting (Gower 1992). However, fold closures shown by Gower (1992) in the Pointe-au-Baril and Parry Sound areas were not conclusively demonstrated in the field, leaving the validity of this model in doubt. Dome-and-basin map patterns observed in the southern portion of the Central Gneiss Belt are attributed to

interference of set-2 and set-3 folds (Schwerdtner 1987). This map pattern appears to be more common in allochthonous than in parautochthonous domains.

The kinematic framework of set-2 folds remains a subject of considerable debate. Schwerdtner (1987) proposed that the northwest-trending folds formed by buckling in response to intermittent east-west compression and transcurrent shear during temporary locking of thrust displacement on the Grenville Front (see his Fig. 24*b*). This model requires rotation of the folds from an initial north-south orientation to a northwest-southeast orientation. Gower (1992) presented alternative models in which these folds formed either during northeast-southwest compression or during northeast-directed extension in a transpressional regime. In contrast, Culshaw et al. (1994) suggested that northwest-trending folds in the Britt and Shawanaga domains formed during southeast-directed extensional shear on the Shawanaga shear zone and did not undergo significant hinge rotation. The folds were considered to be "a"-type folds (*e.g.*, Malavieille 1987) that nucleated with axes subparallel to the flow direction during combined extensional shear and wrench shear. Resolution of the controversy surrounding the origin of the regional northwest-trending fold set awaits further detailed study but is addressed in this chapter by examination of folds in the Shawanaga shear zone that appear to be congruent minor structures.

The ages of shear zones, folds, and tectonic fabrics in the Central Gneiss Belt have been partly constrained by U-Pb geochronology. The oldest-known gneissic fabrics in the parautochthon are observed in the Key Harbour area of the Britt domain (Fig. 1.2) and formed prior to 1694 Ma (Corrigan et al. 1994). These fabrics appear to be rarely

preserved elsewhere in the Britt domain (N. Culshaw, personal communication 1994). A younger deformation event at *ca.* 1470-1450 Ma accompanying high-grade metamorphism and voluminous felsic plutonism is indicated in by U-Pb data in parts of the Grenville Front Tectonic Zone (Haggart et al. 1993; Bethune 1993) and Central Gneiss Belt (Krogh et al. 1993*a*). Tectonic fabrics related to this event have only been confidently identified near the Grenville Front (Haggart et al. 1993; Bethune 1993) and possibly in the study area (see below).

Widespread structural reworking and juxtaposition of allochthonous and parautochthonous rocks is considered a manifestation of Grenvillian thrust tectonics (Rivers et al. 1989), although it is increasingly being recognized that late orogenic extension may have played a significant role in modifying the thrust-related crustal architecture of the Central Gneiss Belt (*e.g.*, Culshaw et al. 1994; Jamieson et al. 1995). Extension within collisional orogens is a natural consequence of crustal thickening (Dewey 1988) and has been documented in orogenic belts world-wide. Grenvillian thrusting within the Central Gneiss Belt, Grenville Front Tectonic Zone, and Central Metasedimentary Belt Boundary Zone occurred episodically between *ca.* 1190 Ma (McEachern and van Breemen 1993) and *ca.* 980 Ma (Haggart et al. 1993). A southeastward or 'break-back' migration of latest thrusting in the southern Central Gneiss Belt is suggested by U-Pb ages for syn-kinematic pegmatite veins within major shear zones (*e.g.*, Nadeau and Hanmer 1992). However, displacement on some shear zones is known to have occurred intermittently, and it is not always clear if a dated movement phase corresponds to a major displacement event. Furthermore, some of the data incorporated in this model, such as the

ca. 1160 Ma thrusting age for the Parry Sound shear zone (van Breemen et al. 1986) have recently been reinterpreted in light of new data. Wodicka (1994) has suggested that *ca.* 1160 Ma tectonism in the Parry Sound domain represents an early phase of deformation and that final emplacement of this domain did not occur until *ca.* 1120-1080 Ma. Additional geochronology, in conjuction with detailed mapping and structural analysis, is required to confirm a regional-scale break-back migration of latest thrusting.

Syn- to late orogenic extension within the Central Gneiss Belt in the interval 1040-1020 Ma (Nadeau 1990; Ketchum et al. 1993*a*, *b*; Culshaw et al. 1994) resulted in reactivation of the Allochthon Boundary Thrust as a 3 km-wide, southeast-directed displacement zone (the Shawanaga shear zone). This period also saw the regional development of upright, northwest-trending folds (Culshaw et al. 1994). Ductile deformation in the Central Gneiss Belt after this interval was largely confined to minor readjustments of the crust and ductile folding of gneissic fabrics adjacent to *ca.* 990 Ma pegmatite dykes (*e.g.*, Corrigan 1990). In contrast, thrusting in the Grenville Front Tectonic Zone continued until *ca.* 980 Ma (Haggart et al. 1993)

The structural history of the western Central Gneiss Belt was closed by minor displacement on steep, east- and northeast-striking brittle faults (Schwerdtner and Waddington 1978; Culshaw et al. 1988). These faults have kilometre-scale spacings and strike lengths of several tens of kilometres. Displacements are generally on the order of several tens to hundred metres with south-side-down documented in several localities (*e.g.*, Lumbers 1971; Culshaw et al. 1988).

Tectonic Significance of Gneiss Types

It is important to recall the tectonic significance of several gneissic rock types common to the Grenville Province and other deeply eroded orogens and to adopt a terminology that adequately reflects their tectonic character. Workers in Ontario (*e.g.*, Davidson et al. 1982; Davidson 1984*a*; Hanmer 1988; Nadeau and Hanmer 1992) have qualitatively demonstrated the relationship between finite strain and these gneissic fabrics. For example, uniformly fine- to medium-grained rocks with pronounced and remarkably continuous, millimetre- to metre-thick gneissic layering, termed 'straight gneiss' (Davidson et al. 1982; Hanmer 1988), are thought to be products of high ductile strain(s). Medium-grained varieties of this rock type typically represent recrystallized equivalents. The continuous layering characteristic of straight gneiss is demonstrably the result of extreme transposition and attenuation of folds, discordant veins, tectonic inclusions, and/or compositional layering in the protolith. Rocks of similar aspect but with isolated porphyroclasts and tectonic inclusions ('porphyroclastic gneiss;' Hanmer 1988) are also the product of intense deformation. Both gneiss types can be described as mylonite. Straight gneiss and porphyroclastic gneiss (and their recrystallized equivalents) are common in regional-scale ductile shear zones in the Grenville Province. The non-coaxial nature of strain in these zones is demonstrated by indicators of shear-induced vorticity such as asymmetric winged porphyroclasts, C-S fabrics, and back-rotated boudins (*e.g.*, Simpson and Schmid 1983; Passchier and Simpson 1986; Hanmer 1986; Hanmer and Passchier 1991).

Vast tracts of gneiss lying between the shear zones are also dominated by gneissic

tectonites (Davidson et al. 1982), but structures and tectonic fabrics in these rocks gernerally indicate lower strain levels than in the shear zones. Hanmer (1988) employed the terms 'regular gneiss' to describe a well-layered rock in which low-angle discordant features are visible only on surfaces perpendicular to both lineation and foliation, and 'irregular gneiss' to denote a less-strained equivalent in which discordant features are visible on all surfaces perpendicular to layering. These terms are somewhat unfortunate as straight and porphyroclastic gneisses may, in lower strain settings or for certain combinations of L and S (normally L>S), preserve low-angle discordant features. However, all of the above terms will be retained here and clarified where necessary.

3.2 STRUCTURAL ZONES IN THE POINTE-AU-BARIL AREA

Basis of Subdivision

The five structural zones defined in the study area are mainly distinguished by unique combinations of planar and linear fabric orientations. Structural zones are outlined in Figure 3.2 and orientation data are plotted on equal-area, lower-hemisphere stereonets in Figure 3.3. As will be demonstrated, each zone contains structural elements that record portions of a complex, polyorogenic deformation history. The diversity of fabric orientations mainly reflects the heterogeneous nature of extensional reworking of pre-Grenvillian and early Grenvillian fabrics. Although primarily defined by unique combinations of fabric orientation, the zonal subdivision may also reflect variations in gneiss type, metamorphic assemblage, and/or strain intensity of gneissic fabrics. Zone boundaries range from sharp to gradational and coincide with shear zones, limits of

tectonic overprinting, and cryptic structural boundaries. As will be shown, the structural data presented below support the presence of juxtaposed allochthonous and parautochthonous terranes with contrasting orogenic histories in the Pointe-au-Baril area (Culshaw et al. 1994).

Description of Structural Zones

Zone 1

Zone 1 extends from the northern border of the map area to the structurally highest level of the Nares Inlet shear zone (Fig. 3.2). This zone is one of two structural domains lying completely within the Bayfield gneiss association. Regular gneiss is abundant in this structural zone northwest of the straight and porphyroclastic gneisses that characterize the Nares Inlet shear zone.

Zone 1 foliations mainly dip moderately toward the southeast, east and northeast, defining a diffuse cluster of poles to foliation (Fig. 3.3). Finite extension lineations, defined by one or more of mineral alignments, long axes of mineral aggregates and tectonic inclusions, and (in the Nares Inlet shear zone) rod and mullion structures, mainly plunge gently to moderately northwest and southeast. Minor fold axes and bisectors to sheath folds in the Nares Inlet shear zone have a similar orientation to these lineations. Some stretching lineations near the top of the Nares Inlet shear zone plunge shallowly southwest and northeast. Although parallel to lineations in the adjacent zone 2 (see below), these are included in zone 1 as they accompany high strain foliations that overprint zone 2 fabrics. No overprinting relationships were observed along the lower boundary of the Nares Inlet

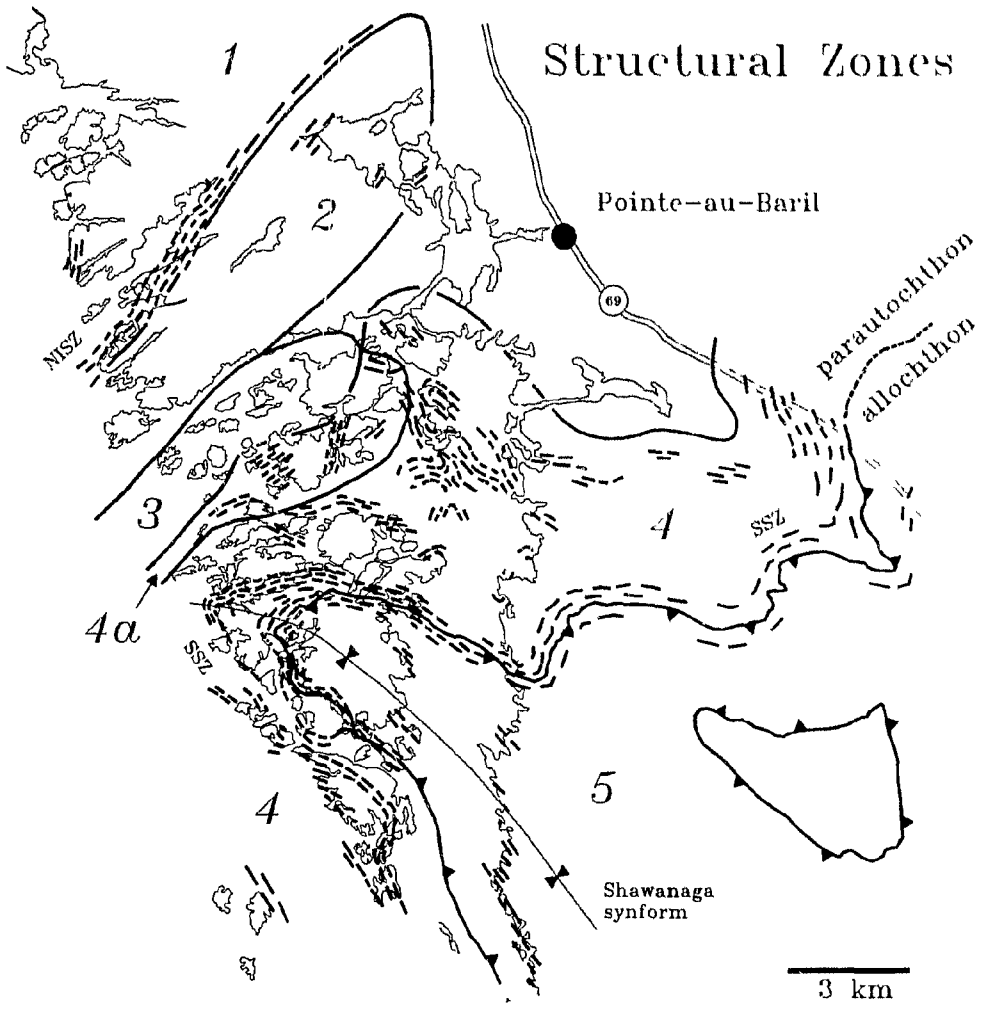

Fig. 3.2. 1-5 = structural zones in the study area (see text for details). Dashed lines indicate trend of high-strain foliation in the extensional Nares Inlet (NISZ) and Shawanaga shear zones (SSZ). Barbed line is position of former thrust detachment between parautochthon and allochthon, after Culshaw et al. (1994)

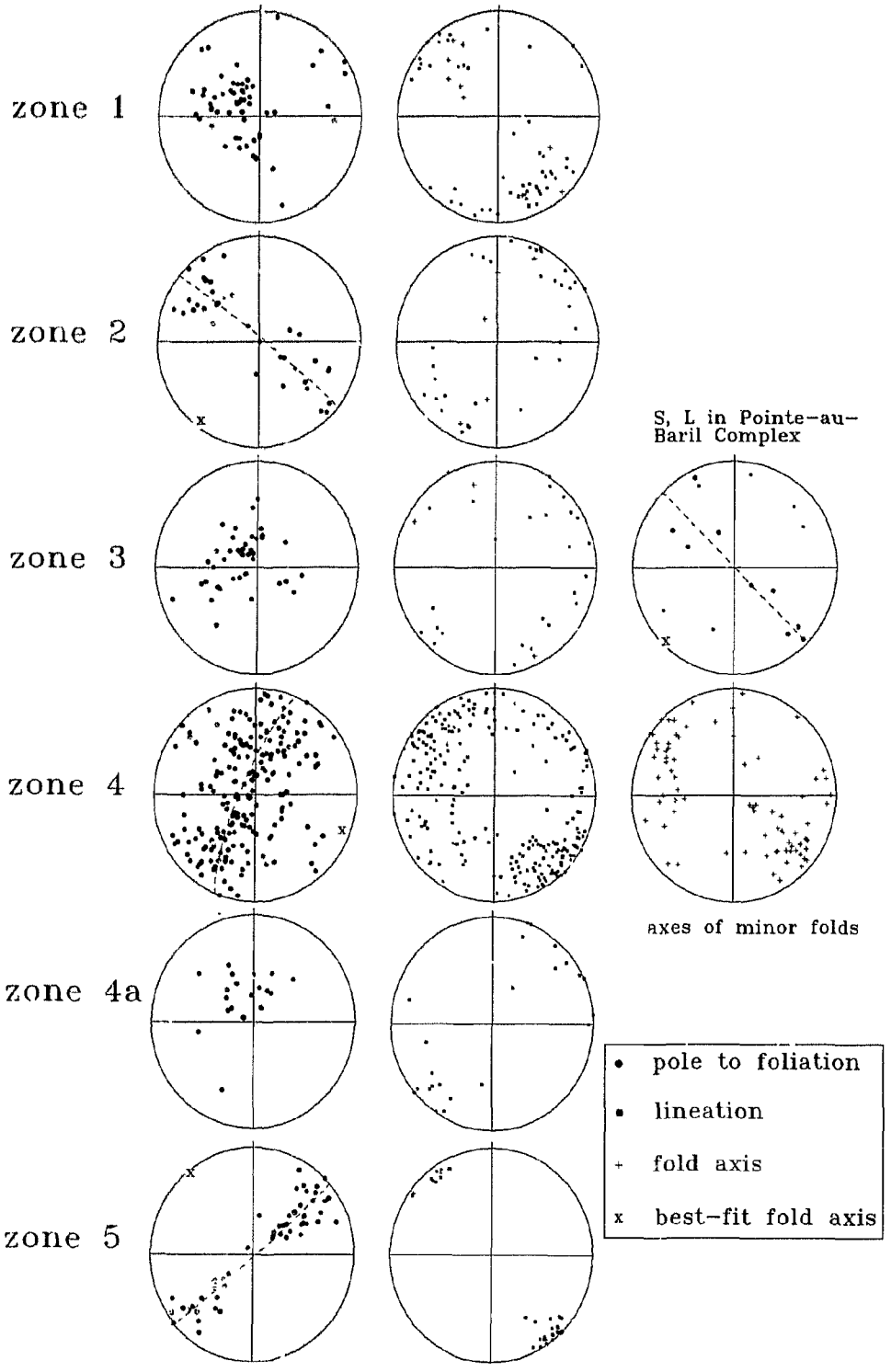

Fig. 3.3. Structural data for the six structural zones defined in the study area (Fig. 3.2). Lower-hemisphere, equal-area projections.

shear zone which appears to mark a continuous strain gradient between regular gneiss and mylonite.

Zone 2

Zone 2 extends from the structural top of the Nares Inlet shear zone to the northwest edge of the Pointe-au-Baril complex (Fig. 3.2) and mainly comprises Bayfield association straight gneiss. Older, contorted gneissic foliations are locally observed where straight gneiss fabrics are poorly developed. Rare kinematic indicators in straight gneiss indicate that a component of dextral shear accompanied fabric development (Fig. 2.3*b*).

Foliation and lineation orientations in zone 2 are atypical of the Britt domain which is generally characterized by shallowly-plunging, northwest-trending folds and a gently southeast-plunging stretching lineation (Davidson et al. 1982; Culshaw et al. 1988). In contrast, zone 2 straight gneisses strike northeast and dip moderately to steeply northwest and southeast. Poles to foliation define a girdle suggesting the presence of map-scale, northeast-trending folds with subhorizontal axes (Fig. 3.3). However, large fold closures were not observed in the field and may not be present if the stereonet pattern merely reflects local variations in dip. Lineations and rare minor fold axes have shallow to moderate plunges mainly toward the northeast and southwest.

The northeast-striking straight gneiss foliation in zone 2 can be traced offshore to the Blackbill Islands (Fig. 2.2) in submerged shoals visible on air photographs. Inland from Georgian Bay, northwest-trending folds progressively overprint the northeast structural grain of zone 2, resulting in a narrowing and pinching out of this domain west of Highway

69 (Fig. 3.2). Zone 2 fabrics are preserved at the north end of Sturgeon Bay but are reworked to the south in a kilometre-scale, southeast-plunging synform-antiform pair outlined by the map trace of the Pointe-au-Baril complex (Fig. 2.1).

Zone 3

Zone 3 constitutes the smallest structural domain in the study area. Termed the "low-strain area" by Ketchum et al. (1994), this zone contains migmatitic supracrustal gneiss of the Nadeau Island association intruded by weakly deformed granite of the *ca.* 1460 Ma Pointe-au-Baril complex. Regular and irregular gneiss are abundant although finer-grained, L=S to L>S straight gneiss is present in discrete high-strain zones. Zone 3 is bordered to the south and east by the Shawanaga shear zone. Its northern border is placed at the contact of the Pointe-au-Baril complex with the Bayfield gneiss association. The northern boundary marks an abrupt decrease in the intensity of zone 2 straight gneiss fabrics.

It is instructive in zone 3 to distinguish fabric attitudes in supracrustal gneiss from those in Pointe-au-Baril complex granite. Supracrustal gneiss dips shallowly to moderately in all directions, defining a diffuse central cluster of poles to foliation (Fig. 3.3). Lineations also show a variety of shallowly-plunging orientations. In contrast, foliations in granite invariably strike northeast with shallow to steep northwest and southeast dips, and lineations plunge shallowly in the northeast and southwest quadrants. Fabric attitudes in granite are identical to those observed in zone 2 straight gneiss, suggesting that structural elements of this zone are also present in zone 3. However, the tectonic event(s) that

formed the zone 2 straight gneisses did not penetratively overprint fabrics in Nadeau Island supracrustal gneiss of zone 3.

Zone 4

Zone 4 encompasses units of the Nadeau Island gneiss association lying within the Shawanaga shear zone. Although this structural domain could be expanded to include a region of broadly folded gneiss near Pointe-au-Baril with similar fabric attitudes (unlabelled area in Fig. 3.2), this lower strain area is excluded as it is instructive to analyse shear zone fabrics independently (see below). Zone 4 contains a high proportion of S>L straight and porphyroclastic gneiss but includes lower strain areas of regular and irregular gneiss.

Gneissic layering throughout zone 4 is warped at outcrop- to map-scale by shallowly northwest- and southeast-plunging, upright, open to tight folds. Several map-scale synforms in straight and porphyroclastic gneiss at the north end of Shawanaga Inlet are overturned toward the southwest. The folds share a range of axial orientations (mainly from east-southeast to southeast), resulting in a broad girdle of poles to foliation with a shallowly east-southeast-plunging, best-fit axis (Fig. 3.3). The trend of this axis closely matches the axial trace of the Shawanaga synform in the parautochthon (Fig. 2.2).

Stretching lineations throughout zone 4 are weakly to strongly developed. Many highly-strained, fine-grained rocks are S>L tectonites with a weak lineation, but strong lineations are commonly observed within leucosomes and in Pointe-au-Baril megacrystic granite. Considerable scatter in the orientation of stretching lineations, with maxima in the

northwest and southeast quadrants, is apparent for zone 4 (Fig. 3.3). Axes of minor folds mirror this distribution but with fewer northeast and southwest trends. Shear-sense criteria (*e.g.*, Simpson and Schmid 1983; Hanmer and Passchier 1991), discussed in detail below, indicate southeast-directed extensional shear for all orientations of foliation (Culshaw et al. 1994).

A structural subdomain is apparent in the Shawanaga shear zone immediately south of zone 3. Labelled zone 4*a* (Fig. 3.2), this subdomain extends from the north end of Shawanaga Inlet southwestward to the limit of outer islands and is characterized by moderately southeast- to southwest-dipping straight gneiss with shallowly northeast- and southwest-plunging lineations (Fig. 3.3). Rare kinematic indicators suggest sinistral movement on northeast-striking shear planes, although extensional kinematic indicators like those in zone 4 are locally observed. The southern and eastern boundaries of zone 4*a* are placed where mylonites with a southeast-plunging stretching lineation replace zone 4*a* fabrics. However, northeast- and east-striking gneisses with a low-rake stretching lineation are locally observed throughout zone 4, suggesting that zone 4*a* fabrics are patchily preserved in the larger domain.

Field observations and the stereonet patterns indicate considerable structural and kinematic complexity for parautochthonous rocks in the Shawanaga shear zone. The nature of this complexity is discussed in detail later in this chapter.

Zone 5

Zone 5 extends from the upper contact of the Nadeau Island gneiss association to

the southern boundary of the map area. This zone is underlain by the Shawanaga pluton and the allochthonous Ojibway and Sand Bay gneiss associations. The base of zone 5 has been suggested to mark the location of a basal detachment to allochthonous units overthrust from the southeast during Grenvillian orogenesis (Culshaw et al. 1990, 1994; Jamieson et al. 1992). However, Culshaw et al. (1994) tentatively assigned the Shawanaga pluton an independent tectonic status as its inherent characteristics do not clearly indicate affinity with either allochthonous or parautochthonous rocks.

Medium-grained straight and porphyroclastic gneiss of the Shawanaga shear zone is abundant at lower structural levels of zone 5, giving way to less intensely deformed rocks at higher levels. Although shear fabrics throughout the Shawanaga shear zone consistently indicate top-to-the-southeast displacement, planar and linear elements in zone 5 yield strikingly different stereonet patterns from those in zone 4 (Fig. 3.3). Foliations are folded about horizontal, northwest-trending axes and stretching lineations plunge shallowly northwest and southeast without exception. When compared with orientation data from zone 4, the geometric simplicity of zone 5 structures, along with a notable difference in a best-fit fold axis orientation, is curious given that both zones are part of the same kinematic framework.

Significance of the Structural Zones

Structural subdivisions have been made at a variety of scales throughout the Central Gneiss Belt. For example, Culshaw et al. (1983) showed that lithotectonic domains could be grouped into regional-scale, superincumbent structural units interpreted

as major thrust sheets. Both the domains and larger crustal units were distinguished in part by distinctive orientations of tectonic elements. Smaller scale examples include a variety of structural zones in the Parry Sound domain that carry structures and fabric orientations distinctive from those in their neighbouring zones (*e.g.*, Jamieson et al. 1992; White and Flagler 1992; Gower 1992; Wodicka 1994). In all of these studies, the proposed subdivisions partly or wholly reflect differences in structural history or indicate strain partitioning during regional deformation.

Structural zones defined in the Pointe-au-Baril area share many of the distinguishing characteristics of structural zones noted elsewhere in the Central Gneiss Belt. Although the zones are not entirely bounded by ductile shear belts in the manner of lithotectonic domains and subdomains, shear zones and cryptic tectonic boundaries have played an important role in the evolution and preservation of distinctive structural regions in the Pointe-au-Baril area.

Zone 1

Zone 1 is part of a larger structural domain (Culshaw et al. 1991*a*, fig. 4, stereonet *b*) extending from the Nares Inlet shear zone northward to the edge of the Britt pluton (Fig. 3.1). As zone 1 encompasses only the southwest limb of a large synform and the Nares Inlet shear zone, poles to foliation do not mimic the broad, poorly-defined girdle of the larger domain. Fabric orientations similar to those of zone 1 are widely observed throughout the Central Gneiss Belt (*e.g.*, Culshaw et al. 1983) and have generally been attributed to regional deformation accompanying thrust stacking of lithotectonic domains.

It has been noted, however, that upright, symmetrical folds with axes parallel to the regional transport direction are not compatible with northwest-directed thrusting (Schwerdtner 1987; Gower 1992) but may have formed as buckle folds during east-west compression (Schwerdtner 1987) or as "a"-type folds during northwest-southeast extensional flow (Culshaw et al. 1994). Whatever their tectonic significance, folded gneissic fabrics of zone 1 appear to be primarily Grenvillian. Planar and linear fabric orientations in the extensional Nares Inlet shear zone are similar to those in lower-strain rocks northwest of this zone.

Zone 2

The northeast structural grain and shallowly northeast- and southwest-plunging lineations of zone 2 represent an entirely different deformation regime to that of zone 1. Steeply dipping, S>L straight gneisses, possibly folded about subhorizontal, northeast-trending axes and containing evidence for dextral shear, are overprinted both by northwest-trending folds and fabrics of the Nares Inlet shear zone. The tectonic significance of the straight gneiss is unclear.

Amphibolite dykes with 'patchwork' texture (Chapter 2) and recrystallized plagioclase phenocrysts, equated with the youngest mafic dyke suite in the Britt domain, are strongly transposed in zone 2 straight gneiss. If these dykes belong to the 1238 Ma Sudbury swarm as tentatively indicated by field and geochemical data (Culshaw et al. 1994; A. Davidson, unpublished data; Chapter 2), then the straight gneisses must have formed after 1238 Ma but prior to regional northwest folding and extensional

displacement on the Nares Inlet shear zone. Given this bracket, it is tempting to speculate that the straight gneisses are preserved from an early phase of Grenvillian orogenesis, perhaps related to northwest transport of thrust sheets over the parautochthonous Britt domain. It is not known, however, if zone 2 fabrics retain their original orientations. Alternatively, zone 2 straight gneiss may be related to northeastward tectonic transport suggested by some workers (*e.g.*, Gower 1992) to be an important element of early Grenvillian deformation in the Central Gneiss Belt. Similar northeast-trending lineations within older Grenvillian foliations in the Parry Sound domain are thought to have formed during orogen-parallel extension that was broadly coeval with northwest-southeast compression (Wodicka 1994).

Zone 3

A variable orientation of planar and linear elements and local preservation of pre-Grenvillian, granulite-facies mineral assemblages in zone 3 reflects the lack of a penetrative Grenvillian tectonometamorphic overprint. This structual domain preserves pre-Grenvillian gneissic fabrics from at least two episodes of deformation. The oldest fabrics pre-date intrusion of the Pointe-au-Baril complex at *ca.* 1460 Ma and are readily observed in enclaves of migmatitic Nadeau Island gneiss in weakly-deformed granite (Fig. 2.6*a*). The degree to which these fabrics are preserved in supracrustal gneiss is generally not apparent, but in some localities, leucosomes formed during later granulite facies metamorphism remain discordant to the early fabrics, suggesting that these fabrics are at least locally well preserved.

Rare exposures of strongly deformed, orthopyroxene-bearing mafic supracrustal gneiss indicate that a second period of deformation took place during granulite-facies metamorphism at 1450-1430 Ma. Little is known of the nature or extent of this deformation or the degree to which fabrics of this age are preserved in amphibolite-facies rocks. Based on evidence from the Grenville Front Tectonic Zone in Ontario, Bethune (1993) has suggested that orogeny at *ca.* 1470-1450 Ma was coeval with widespread granitoid plutonism. It is possible that the Pointe-au-Baril area was also tectonically active at this time, but given the low-strain state of the Pointe-au-Baril complex in zone 3, tectonism must have mainly preceded *ca.* 1460 Ma intrusion of granite.

Grenvillian deformation in zone 3 formed a weak, northeast-striking foliation with low-rake stretching lineations in granite, and variably overprinted and reoriented older fabrics in supracrustal gneiss. Grenvillian tectonic fabrics are confidently identified in supracrustal rocks where granulite-facies gneiss is transposed into moderately- to strongly-foliated, amphibolite-facies gneiss, and where outcrop-scale shear zones contain southeast-plunging mineral lineations and kyanite-sillimanite aggregates after corundum (Fig. 2.4*c*). The minor shear zones may indicate local development of extensional shear fabrics that dominate zone 4 (kinematic indicators not observed). However, field observations indicate that a penetrative Grenvillian deformation is largely absent from zone 3. This is best illustrated by mafic dykes of the youngest (Sudbury?) suite which preserve relict igneous minerals and cut older fabrics.

Zone 4

Zone 4 is dominated by structures and fabrics formed during southeast-directed extensional displacement on the Shawanaga shear zone. Less common tectonic elements include sinistral kinematic indicators in northeast-striking gneiss (zone 4*a*), and northeast-southwest trending lineations and minor folds. The sequence of tectonic events responsible for all these fabrics is best illustrated at the eastern end of zone 4*a* where northeast-striking straight gneiss is overprinted by mylonite with northwest-southeast lineations and kinematic evidence for extensional shear. This indicates that an episode of sinistral transcurrent shear on northeast-striking shear planes preceeded top-side-down to the southeast displacement on the Shawanaga shear zone. Combined with tectonostratigraphic evidence for early thrusting along a detachment embedded in the Shawanaga shear zone (Culshaw et al. 1994) and preservation of thrust-sense kinematic indicators along strike near the village of Arnstein (Fig. 3.1; Ketchum et al. 1993*a*, *b*), this suggests that the Shawanaga shear zone accommodated at least three kinematically distinct movement phases. This polyphase kinematic history undoubtedly contributed to the geometric complexity observed in zone 4. The movement history of the Shawanaga shear zone is discussed in greater detail later in this chapter.

Zone 5

Straight and porphyroclastic gneisses of zone 5 are clearly the product of extensional displacement on the Shawanaga shear zone. As in zone 4, these rocks are folded about upright, northwest-trending, subhorizontal axes parallel to a well-developed

stretching lineation. Both the folds and lineations are suggested to have formed during regional northwest-southeast ductile flow accompanying extensional shear (Culshaw et al. 1994).

The geometrical simplicity of fabric elements in zone 5 is at odds with the complex structural geometry of zone 4 despite the fact that both are part of the Shawanaga shear zone. This suggests either that extensional shear strain was partitioned across the zone 4-5 boundary, or that zone 5 did not share the full structural history of zone 4. Reactivation of the thrust décollement during extension could have partitioned strain across the zone 4-5 boundary, but displacement dominated by slip within a narrow detachment zone is considered unlikely as the high metamorphic grade would have favoured broadly distributed ductile shear (*e.g.*, Ramsay 1980). The lack of a common structural history is implicit in the model of the Ojibway - Sand Bay assemblage as an allochthonous thrust sheet that overrode a polyorogenic, parautochthonous footwall (Culshaw et al. 1994) and is suggested here as the most likely reason for the disparity of fabric attitudes across the zone 4-5 boundary.

Structural data from the Shawanaga pluton indicate greater similarity with overlying allochthonous units than with underlying parautochthonous rocks. Combined with the presence of *ca.* 1170-1150 Ma coronitic metagabbro bodies in the pluton (also found in the Ojibway gneiss association), this favours assignment of the Shawanaga pluton to the allochthonous assemblage.

Preservation of Pre-Grenvillian and Early Grenvillian Structures

As outlined above, pre-Grenvillian and early Grenvillian tectonic elements dominate zones 2, 3, and 4*a* whereas fabrics and structures in zones 1, 4, and 5 are mainly the product of late Grenvillian deformation. The relative absence of Grenvillian deformation in a crustal segment bounded by extensional shear zones points to a fundamental link between the shear zones and preservation of older fabrics. As the crustal block outlined by zones 2, 3, and 4*a* lacks the northwest-trending folds that characterize the Britt and Shawanaga domains, this strongly suggests that the shear zones were active during late Grenvillian folding and decoupled this block from adjacent crustal segments that were undergoing penetrative deformation (Ketchum et al. 1994). Shear zone decoupling has also been invoked by Coward (1984) in the Limpopo Belt of southern Africa to account for the absence in the footwall of a fold set that deforms hanging wall units.

The proposed decoupling model is corroborated by field evidence along the northwest boundary of zone 2. Here, a gradual northeastward decrease in both the width and strain intensity of the Nares Inlet shear zone coincides with an increase in the number of southeast-and northwest-plunging minor folds that warp the straight gneiss of zone 2. This progressive "dying out" of the shear zone suggests a northeastward decrease in the amount of extensional displacement accommodated by the zone, which may have led to less efficient decoupling in the northeast, allowing northwest trending folds to develop in zone 2.

3.3 THE SHAWANAGA SHEAR ZONE

As outlined above, the Shawanaga shear zone is a kinematically and geometrically complex, regional-scale structure that last accommodated southeast-directed extensional displacement. The geometric complexity of this structure is principally due to a polyphase movement history and a heterogeneous extensional overprint.

Only a few workers have previously studied the Shawanaga shear zone in any detail. The zone was initially described by Davidson et al. (1982) as a continuous, curvilinear belt of mylonite and straight gneiss. These authors traced this >100 km-long structure from Georgian Bay to northeast of the village of Arnstein (Fig. 3.1). Culshaw et al. (1989) first recognized that the Shawanaga shear zone contained kinematic evidence for extensional shear. Shortly thereafter (Culshaw et al. 1990) these authors proposed that a basal detachment to allochthonous thrust sheets (Shawanaga, Parry Sound, Moon River, Seguin, and northern Rosseau domains), some forming a "duplex-like structure," was embedded in the Shawanaga shear zone. Northwest-directed thrusting on the detachment created a sharp tectonostratigraphic break between adjacent gneiss terranes that was preserved during southeast-directed extensional reactivation of the zone. Thrust fabrics were not recognized within this structure near Pointe-au-Baril and were likely overprinted during later tectonism (Culshaw et al. 1994), but were noted along strike near Arnstein (Fig. 3.1; Ketchum et al. 1993*a*, *b*).

Based on this and other evidence it appears that the Shawanaga shear zone marks the location of the Allochthon Boundary Thrust (Rivers et al. 1989) in the western Grenville orogen. This zone was reactivated at *ca.* 1020 Ma (Ketchum et al. 1993*a*;

Chapter 5) during an episode of late orogenic extension, possibly in response to thermal weakening of the mid- to lower crust (Culshaw et al. 1990, 1994; Ketchum et al. 1993*b*). That this late tectonic activity is due to crustal extension rather than crustal shortening (*i.e.*, extensional rather than normal faulting) is suggested by the likelihood, based on field (Culshaw et al. 1990, 1994) and seismic reflection data (White et al. 1994), that the Shawanaga shear zone is a crustal scale feature and therefore cannot represent a reoriented compressional structure such as a folded back-thrust (Wheeler and Butler 1994).

Structural and kinematic data presented earlier in this chapter suggest that although extensional shear fabrics dominate the Shawanaga shear zone in the Pointe-au-Baril area, older fabrics related to strike-slip movement on northeast shear planes are locally preserved. Sinistral movement has not previously been documented for the Shawanaga shear zone. The kinematic history of the Shawanaga shear zone thus appears to involve early, northwest-directed thrusting, followed by sinistral strike-slip movement, followed by southeast-directed extension. Whether these kinematic events are part of a progressive deformation or occurred as temporally distinct events is not known. All movement phases are suggested here to be Grenvillian in the absence of contrary evidence.

In this section, kinematic indicators, microstructures, and folds within the Shawanaga shear zone are examined in detail, and possible reasons for the complex kinematic history of this zone are discussed. Much of the discussion involves tectonic elements formed during the latest, extensional phase of movement on the Shawanaga shear

zone as these elements are dominant and provide insights on the nature of ductile extensional flow in collisional orogens.

Kinematic Indicators

Kinematic indicators in the Shawanaga shear zone include rotated winged porphyroclasts and inclusions (Hanmer and Passchier 1991), C-S fabrics (Berthé et al. 1979), shear band foliations (White et al. 1980), and asymmetrical pull-aparts (Hanmer 1986); examples of each are illustrated in Figure 3.4. The asymmetry of folded marker horizons (*e.g.*, mafic dykes) is generally consistent with the sense of shear deduced from other criteria but was not employed as a kinematic indicator due to potential problems associated with their use (*see* Wheeler 1987; Hanmer and Passchier 1991). By far the most abundant shear-sense indicators in the Shawanaga shear zone are δ-type winged feldspar porphyroclasts (Fig. 3.4; Passchier and Simpson 1986).

Figure 3.5 shows some of the locations of unambiguous shear-sense indicators and the orientation of their associated high-strain fabrics. As noted by Culshaw et al. (1994), kinematic indicators overwhelmingly demonstrate extensional, top-side southeast displacement for all orientations of foliation. In the Pointe-au-Baril area where the Shawanaga shear zone is folded about shallowly southeast- to east-southeast-plunging axes, shear-sense is mainly dextral on northeast-dipping foliations, sinistral on south-and southwest-dipping foliations (both observed in subhorizontal outcrop surfaces), and top-side-down on southeast-dipping foliations (observed in subvertical outcrop surfaces). This relationship is illustrated in stereographic form in Figure 3.6 with poles to foliation

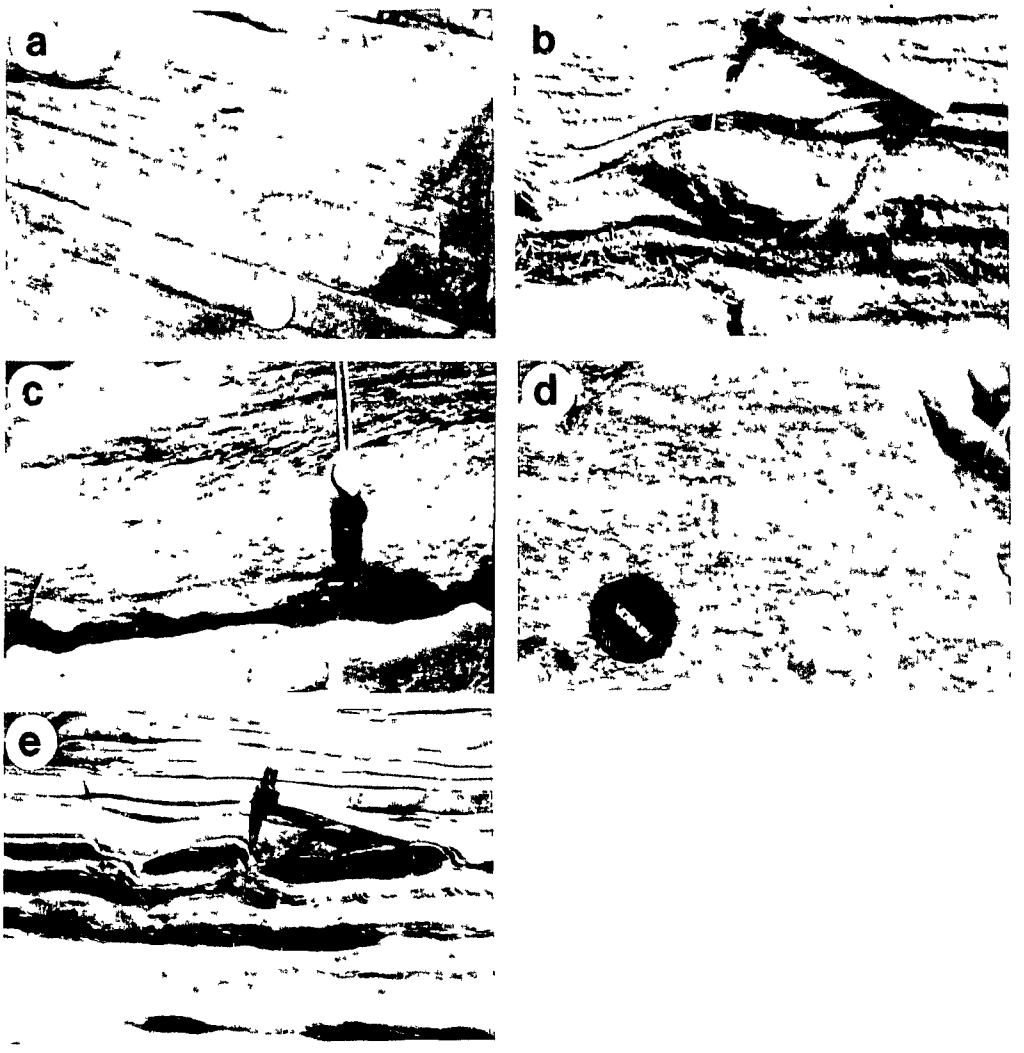

Fig. 3.4. Kinematic indicators in the Shawanaga shear zone **a)** δ-type winged feldspar porphyroclast. **b)** rotated calc-silicate tectonic inclusion (tails derived from pressure shadow material). **c)** C-S fabrics. **d)** extensional shear band foliation in megacrystic granite. **e)** back-rotated, asymmetrical pull-apart in concordant mafic layer. All outcrop surfaces shown are parallel to finite stretching lineation and perpendicular to foliation Dextral shear indicated in b) and e), sinistral shear in d), and top-side-down to SE in a) and c).

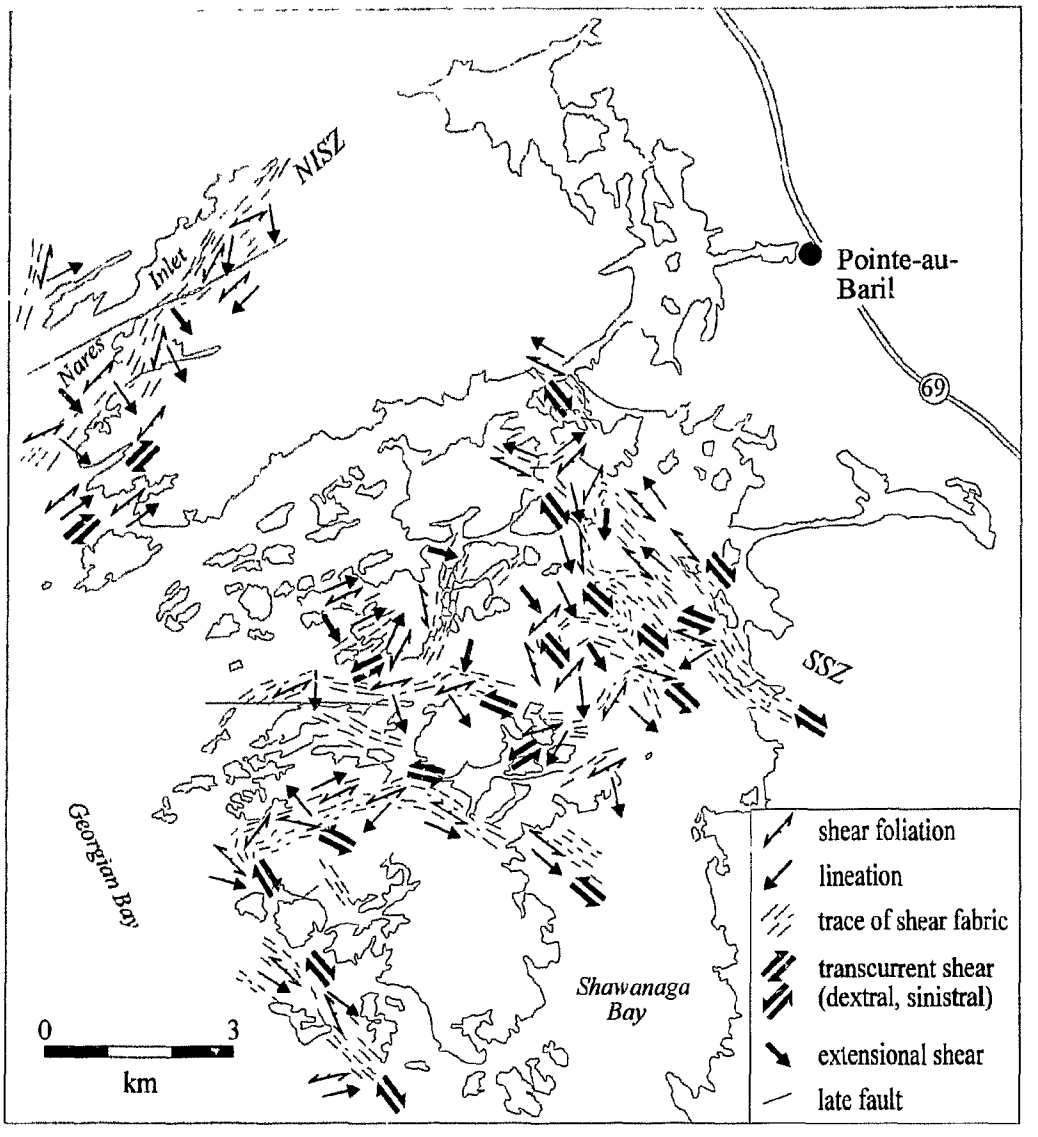

Fig. 3.5. Location of some of the kinematic indicators (primarily δ porphyroclasts) observed in the Nares Inlet (NISZ) and Shawanaga shear zones (SSZ). Shear sense is mainly dextral on NE-dipping foliations, sinistral on SW-dipping foliations, and top-side to the southeast on SE-dipping foliations.

ornamented according to shear-sense. Inspection of Figure 3.6 reveals that several steeply northeast-dipping foliations contain sinistral kinematic indicators, suggesting northwest-directed thrusting However, overturned folds are evident at several localities where this relationship is observed, indicating that all northeast-dipping planes with sinistral shear-sense may lie within overturned folds. These kinematic indicators are unlikely to be relics of early thrusting as extensional shear fabrics can be continuously traced into regions where an apparent thrust sense is observed.

Finite extension lineations within zone 4 of the Shawanaga shear zone do not entirely conform to a tectonic history dominated by penetrative, northwest-southeast extensional ductile flow. Lineations in dextrally sheared tectonite mainly plunge shallowly northwest and southeast whereas those accompanying sinistral shear foliations plunge in the northwest, southwest, and southeast quadrants (Fig. 3.6). The anomalous southwest-plunging lineations (orthogonal to the extensional transport direction) mainly occur in moderately to steeply south-dipping gneiss Southeast-to south-dipping foliations with top-side-down shear sense typically contain a southeast-plunging stretching lineation, but in some localities a low-rake lineation is observed (Fig. 3.6).

Two points need to be addressed concerning the relationships noted above. First, the anomalous southwest-plunging lineations are almost entirely associated with sinistrally sheared gneissic tectonite. These rocks kinematically and geometrically resemble tectonites in zone 4*a* suggesting that their fabrics survive from an earlier, sinistral transcurrent shear event and are not related to extension. The transcurrent shear fabrics appear to be preserved within discrete lenses that escaped extensional reworking.

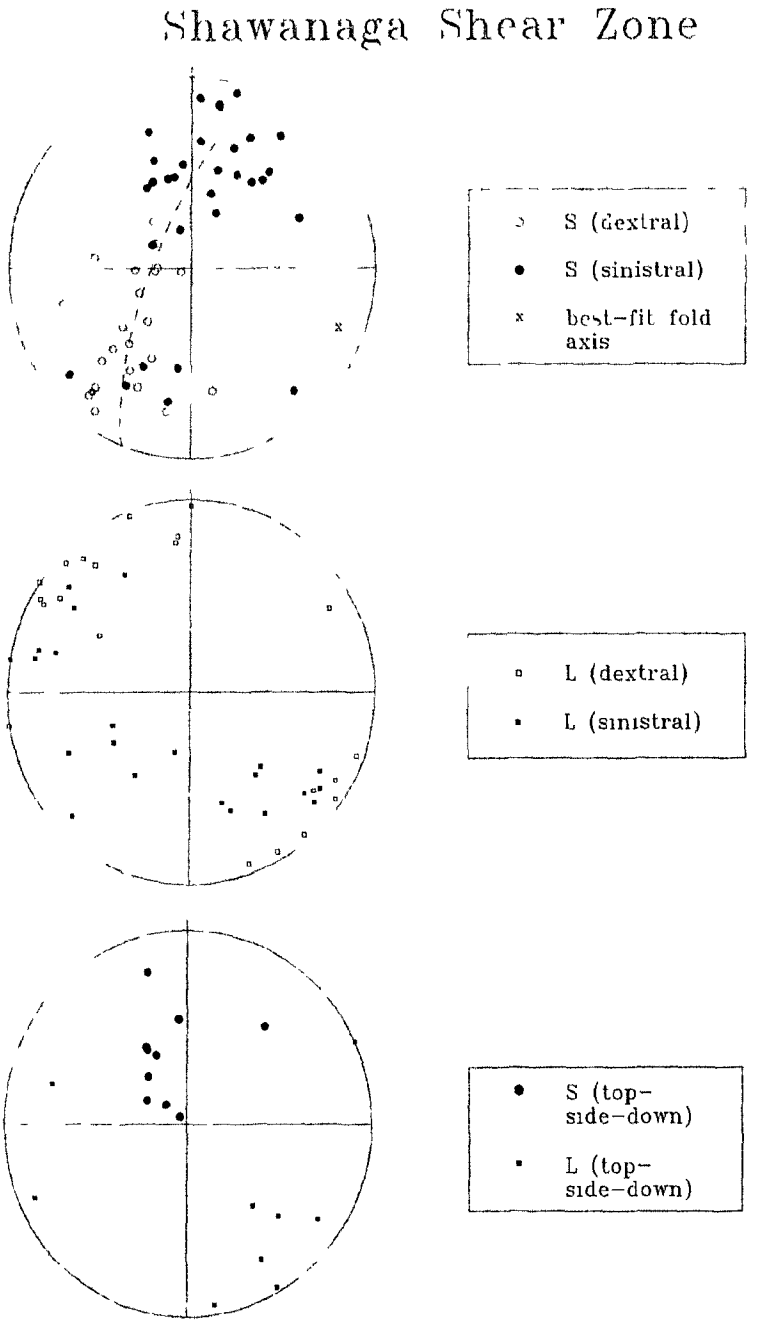

Fig. 3.6. Structural data for the Shawanaga shear zone (zone 4) from where kinematic indicators were observed. See text for discussion of data.

Second, a number of top-side-down porphyroclasts with a well-developed asymmetry are hosted by tectonites with a lineation parallel to the porphyroclast rotation axes. This is in contrast to the general observation, both in this and other studies (*e.g.*, Passchier and Simpson 1986), that porphyroclast asymmetry and tails are well developed only when the viewing surface is perpendicular to the shear plane (foliation) and parallel to the shear direction (lineation). Lineations that parallel the rotation axes of non-coaxial strain have been noted in other ductile shear zones (*e.g.*, Lister and Price 1978, Hanmer and Ciesielski 1984; Nadeau and Hanmer 1990) and are attributed to mechanisms such as transpression (Sanderson and Marchini 1984) near a shear zone buttress, or to the simultaneous operation of thrusting and transcurrent shear within discrete segments of a single zone. In the Shawanaga shear zone, top-side-down porphyroclasts with rotation axes parallel to the finite extension lineation are rare and are unlikely to indicate the systematic operation of one of these mechanisms. Preservation of these lineations from an earlier deformation event (perhaps sinistral shear) is therefore considered a more likely explanation to account for their low-rake orientation.

Geometry of δ-type Winged Porphyroclasts

With the kinematic and geometric framework of the Shawanaga shear zone established, it is instructive to examine the geometry of rotated winged porphyroclasts in order to comment on the nature of ductile extensional flow. The non-coaxial nature of strain in this zone is amply demonstrated by numerous indicators of shear-induced vorticity (*e.g.*, Fig. 3.4). Whether flow approximated to ideal simple shear or non-ideal

shear (simple shear plus a component of pure shear) can be deduced by the overall geometry of δ-type porphyroclasts (Hanmer 1990; Hanmer and Passchier 1991). Those with tails that mainly lie within a reference plane parallel to the shear plane that contains the rotation axis (in-plane geometry; Fig. 3.7) are suggested to indicate a component of extension within the flow plane (*i.e.*, non-ideal shear). Porphyroclasts with tails that cross the reference plane (stair-stepping geometry) indicate a strain regime approximating to ideal simple shear. Passchier et al. (1993) note that δ–type porphyroclasts with stair-stepping geometry are rarely documented in the literature, implying that ideal simple shear is atypical of solid-state flow in shear zones.

In the Shawanaga shear zone, most δ–type porphyroclasts indicating top-side-down movement have stair-stepping geometries whereas those indicating dextral or sinistral shear mainly have in-plane geometries (Fig. 3.8). This variation is particularly evident in folded mylonitic fabrics at the north end of Shawanaga Inlet where stair-stepping varieties are commonly found in fold hinge zones and in-plane varieties are found along fold limbs. This observation suggests that the top-side-down porphyroclasts formed in an ideal simple shear regime whereas porphyroclasts in fold limbs underwent non-ideal shear. As all these porphyroclasts indicate southeast-directed extension, a model that accounts for local and systematic variations in flow regime during a progressive deformation must be invoked.

Based on field relations noted above, a model in which strain was partitioned between hinge zones and limbs during syn-kinematic folding may best account for the

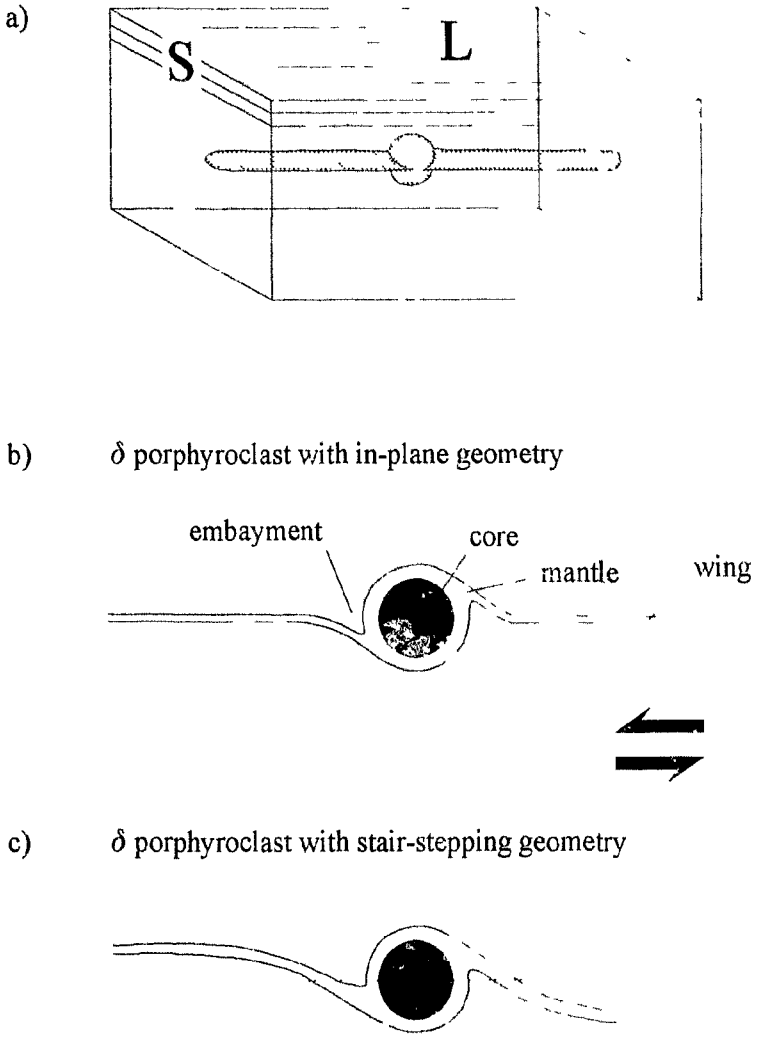

Fig. 3.7. a) Schematic 3-dimensional view of winged porphyroclast in mylonite Wings lie within foliation (S) parallel to lineation (L). In surfaces perpendicular to S and parallel to L, δ porphyroclasts have either an in-plane (**b**) or stair-stepping geometry (**c**) depending on whether tails cross a reference plane lying parallel to foliation and containing the porphyroclast rotation axis. Sinistral shear sense indicated for both porphyroclasts (after Passchier et al. 1993).

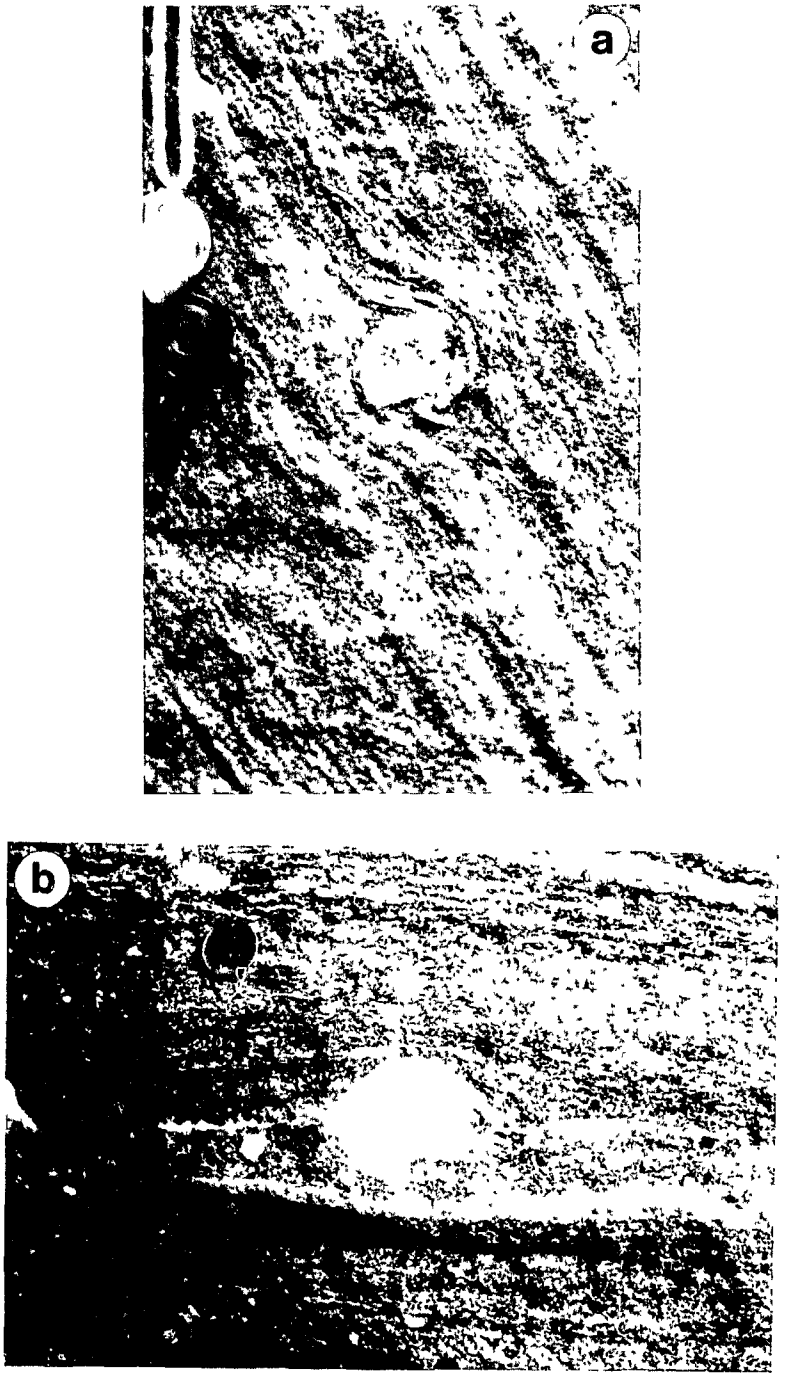

Fig. 3.8. Geometry of δ-type porphyroclasts in the Shawanaga shear zone. **a)** Top-side-down porphyroclasts commonly exhibit stair-stepping whereas sinistrally **(b)** and dextrally rotated porphyroclasts mainly have in-plane geometries (see also Fig. 3.7.).

observed variation in porphyroclast geometry. It is suggested that southeast-directed extensional flow initiated on an unfolded shear zone that had previously accommodated both thrust and strike-slip displacement. Regional folding about the extensional transport direction during this event (Culshaw et al. 1994) and progressive tightening of these folds may have led to increased resistance to continued displacement (*e.g.*, Mancktelow and Pavlis 1994) and migration or cessation of extensional shear. The contrasting porphyroclast geometries suggest that extensional shear initially ceased in the hinge zones when the strain regime approximated to ideal simple shear, and at a later time in the fold limbs when it had evolved to non-ideal shear. This model implies that δ-type porphyroclasts with stair-stepping were initially formed in the fold limbs and were modified to in-plane geometries during later non-ideal shear.

The model described above is consistent with the general observation from other shear zones that syn-kinematic folds regularly preserve older fabrics in their hinge zones whereas fold limbs are strongly deformed (*e.g.*, Ghosh and Sengupta 1987). This model is also consistent with the rotation of an inclined structure to shallower dips as extension proceeded. Such a rotation is a natural consequence of crustal thinning and is postulated here for the Shawanaga shear zone which is a gently-dipping, regional-scale structure (Culshaw et al. 1994). The shear zone would be subject to an increased component of vertical pure shear flattening (expected at deep crustal levels) across the shear plane with progressive rotation to shallower dips, which may have led to a transition from ideal simple shear to non-ideal (pure) shear.

Microstructure

A distinctive variation in microtexture and late metamorphic mineral growth is evident within the Shawanaga shear zone between parautochthonous rocks of the Nadeau Island gneiss association (zone 4) and allochthonous rocks of the Ojibway and Sand Bay gneiss associations (zone 5). Strongly sheared rocks of zone 4 regularly display a variable but generally fine to very fine grain size, irregular grain boundaries, and an abundance of intragranular strain features in quartz (*e.g.*, undulatory extinction, deformation bands, subgrains). Feldspars also show undulatory extinction. Straight grain boundaries and triple junctions are generally not observed in these rocks. In contrast, allochthonous rocks within the shear zone exhibit a granobiastic-polygonal texture with gently curved to straight grain boundaries, a less variable and coarser grain size, and an absence of intragranular strain in quartz and feldspar. A strong foliation is generally not apparent on the thin section scale in granoblastic rocks but is readily apparent in outcrop. Exaggerated grain growth has modified some zone 5 rocks but is not observed in zone 4. Most allochthonous lithologies contain a higher proportion of biotite, muscovite, chlorite, calcite, and sericitized plagioclase than do their parautochthonous counterparts. Muscovite commonly overgrows a biotite-defined foliation.

The contrasting microstructures within the Shawanaga shear zone are comparable to those noted by Wodicka (1994) between the Parry Sound and Parry Island thrust sheets, and by Nadeau and Hanmer (1992) between the Novar thrust sheet and the Huntsville thrust zone. In both of these studies an important tectonic boundary is

postulated to separate the contrasting microstructural regions.

At least two explanations can be advanced to account for the disparity of microstructures in the Shawanaga shear zone; both are likely to have contributed to the development and preservation of the domain-specific microtextures. First, mineral assemblages and microstructures in allochthonous rocks clearly indicate that recovery, recystallization, and post-kinematic mineral growth modified the straight and porphyroclastic gneisses of zone 5. Abundant chlorite, muscovite, and sericitized feldspar strongly suggest that late metamorphic fluids played an important role in shaping the microtextural and mineralogical character of these rocks. An influx of heat and fluid into allochthonous rocks following extensional shear may have contributed to recovery and new mineral growth.

In contrast, microstructures in parautochthonous rocks indicate that recovery and late recrystallization were not pervasive. Preservation of high temperature metamorphic mineral assemblages and intragranular strain features in these rocks suggests that they cooled rapidly during and/or following extensional shear and were relatively uninfluenced by late metamorphic reactions. This interpretation is consistent with the tectonic setting of parautochthonous rocks which were tectonically unroofed during extensional shear. Heat from the cooling parautochthon may have driven fluid convection and retrograde metamorphism in the overlying allochthon (*cf.* Reynolds and Lister 1987). Significant differences in thermal and fluid regime may therefore have contributed to the microtextural and mineralogical variations observed in allochthonous and parautochthonous rocks.

Second, it is evident that allochthonous and parautochthonous assemblages are

distinctive both in lithology and tectonometamorphic history. Perhaps most importantly, the Nadeau Island gneiss association underwent at least two episodes of high-grade pre-Grenvillian metamorphism whereas the Ojibway and Sand Bay gneiss associations were metamorphosed only during the Grenvillian orogeny (Culshaw et al. 1991*a*, 1994). This suggests that prior to the onset of extensional shear, allochthonous and parautochthonous rocks already had contrasting microtextures inherited from earlier events. It is possible that extensional shear influenced these rock packages unequally due to differences in starting material. In addition, bulk compositional differences and earlier dehydration of the parautochthon during pre-Grenvillian metamorphism may have inhibited 'convergence' toward a uniform microstructure within the shear zone. Significant variations in bulk composition (mica-rich versus mica-poor lithologies) and tectonometamorphic history (monocyclic versus polycyclic) represent potentially important controls on microtextural development in allochthonous and parautochthonous rocks.

Folds in the Shawanaga shear zone

Folded fabrics of the Shawanaga shear zone dominate the map pattern in structural zones 4 and 5. Zone 4 contains a predominant, shallowly east-southeast- to southeast-plunging fold set with wavelengths measured on the metre- to kilometre-scale. In zone 5, these folds are subhorizontal with southeast-trending axes and mainly constitute map-scale structures. Zone 5 folds are coaxial with the regional southeast-trending stretching lineation whereas those in zone 4 generally trend at a

shallow angle counter-clockwise to this lineation. Folding of this lineation is evident in some but not all minor folds of this set in zone 4 (*e.g.*, Fig. 3.9*b*).

Kilometre-scale folds in zone 5 and parts of zone 4 are coaxial, and in places continuous with, northwest-trending folds outside of the shear zone (Fig. 3.1). These folds have open to close, symmetrical profiles and gently plunge northwest or southeast. Many smaller-scale, upright, symmetric and asymmetric folds throughout the Shawanaga shear zone are congruent with the regional structures (*e.g.*, Fig. 3.9*a*). However, a number of east-southeast-plunging folds in zone 4, particularly those near the base of the shear zone at the north end of Shawanaga Inlet (Fig. 2.2), do not have the geometric form of the minor folds. These structures instead have northeast-dipping axial surfaces, and a number of synforms are overturned toward the southwest. Given their geometric similarity with the upright folds, however, they are considered to be coeval structures.

An older generation of tight to isoclinal folds is also observed in the Shawanaga shear zone. These are mainly outcrop-scale structures that are deformed by and are often coaxial with the northwest-trending folds, creating a type 3 interference pattern (Ramsay 1967; Fig. 3.9*c*). The refolded isoclines may have formed by rotation and tightening of rare, northeast- and southwest-trending, shallowly-plunging minor folds preserved in zone 4*a* and in lower strain areas of zone 4, although no direct evidence for this kinematic history was observed. Sheath folds with variably-oriented bisectors, mainly observed near the allochthon-parautochthon boundary (Fig. 3.9*d*), may also represent modified early folds. The kinematic significance of the older folds is not known but they may be associated with early movement(s) on the Shawanaga shear zone. Mylonite and

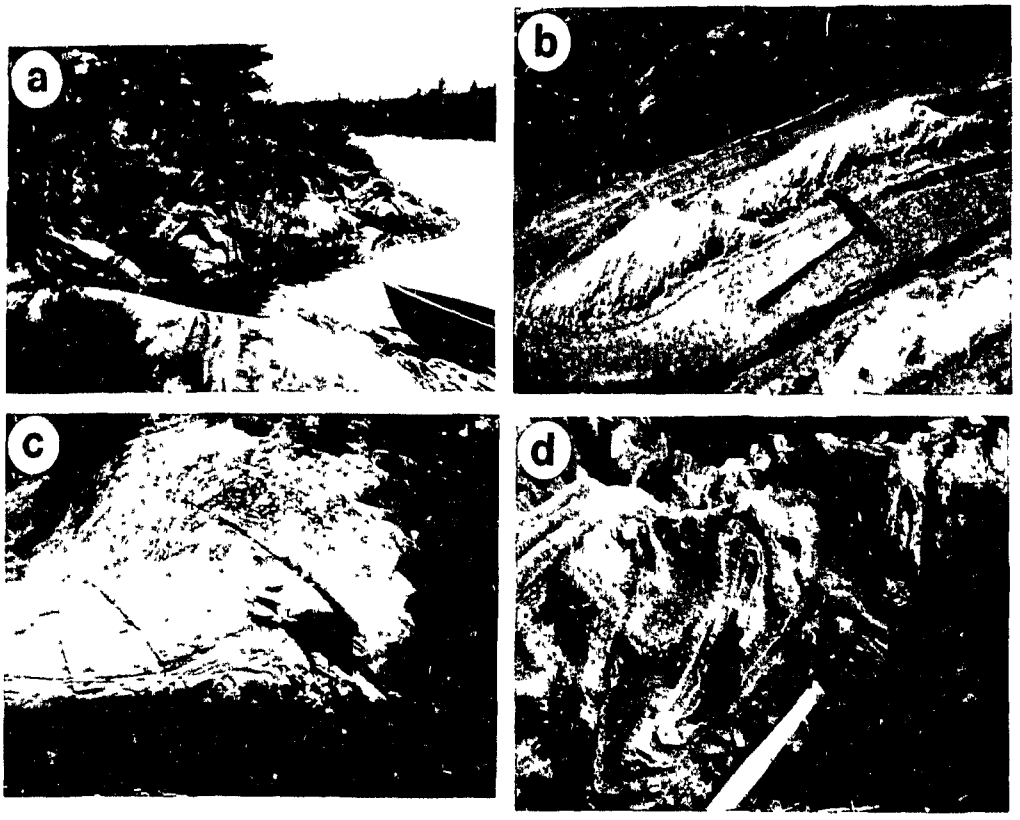

Fig. 3.9. Folds in zone 4 of the Shawanaga shear zone. **a)** Subhorizontal, upright, close and tight minor folds that warp extensional shear fabrics. Minor folds are congruent with km-scale, NW-trending folds. **b)** Moderately plunging minor fold from locality shown in a). Note older lineation in leucocratic layer folded in manner similar to that depicted in Fig. 3.14*a*. **c)** Gently inclined, isoclinal, early fold within upright, gently ESE-plunging antiform of the dominant fold set. Folds are coaxial, yielding a type 3 interference pattern (Ramsay 1967). **d)** Small-scale, subhorizontal sheath folds near the allochthon-parautochthon boundary.

porphyroclastic gneiss tightly folded about a southeast-dipping hinge surface at the east end of Pollard Island (Fig. 2.2) may represent a large-scale example of an early fold.

Regional folding about northwest-trending axes was followed by local development of subhorizontal, northeast-trending open folds. These third generation structures are conspicuous where they interfere with second generation folds, creating a type 1 (dome-and-basin) interference pattern (Ramsay 1967). Metre-scale dome-and-basin folds are commonly observed in the Shawanaga shear zone within the hinge zone of the Shawanaga synform. Schwerdtner (1987) described late, northeast-trending, kilometre-scale folds in the Central Gneiss Belt that form dome-and-basin structures where they intersect northwest-trending folds. Late-stage folds in the present study area may represent equivalent structures. A tectonic window within the Ojibway gneiss association containing rocks of the Nadeau Island gneiss association (Fig. 3.1) may have formed by interference of northeast- and northwest-trending antiforms. The kinematic significance of the late folds is also uncertain, but one possibility is that they formed late in the extensional shear history during layer-parallel shortening in the transport direction.

Geometric Analysis

Structural data from the intensely folded region at the north end of Shawanaga Inlet were examined in detail to determine possible mechanisms of fold development. The folded mylonitic gneisses found in this region are kinematically linked to the Shawanaga shear zone in that top-side-southeast displacement is indicated for all fabric orientations. Data from a gently overturned synform on Mackey Island and an upright antiform on

Eldorado Island (Figs. 2.2, 3.10*a*, 3.11*a*) were analysed in order to investigate the attitudes of linear and planar fabric elements within individual folds. The folds, both with widths of several tens to hundreds of metres, are roughly cylindrical and plunge gently east-southeast (Mackey Island synform) and southeast (Eldorado Island antiform). Both folds contain linear fabric elements with approximate great circle distributions (Figs. 3.10*b*, 3.11*b*) suggesting that folded older lineations are present (Hobbs et al. 1976; Ghosh and Chatterjee 1985). However, the apparent great circle patterns may be fortuitous if not all lineations formed coevally, as has been suggested above for fabric elements in the Shawanaga shear zone.

To further investigate the pattern of folded lineations within the Eldorado and Mackey Island folds, form surface maps were constructed for each following the method of Ghosh and Chatterjee (1985). These maps are useful for analysing the influence of folding on earlier-formed lineations and can potentially provide information on both the pre-folding orientation of these lineations and on the mechanism of folding. Within shear zones they can yield information on fold nucleation and rotation history during progressive ductile shear (Ghosh and Sengupta 1987). The form surface maps are created by stereographically unrolling a folded layer and its associated linear elements about the fold hinge. Form surface maps for the folds considered here (Figs. 3.10*c*, 3.11*c*) are not rigorously constructed as lineation measurements were not taken from a single folded layer. Nevertheless, they are reasonable approximations to true form surface maps as lineation data were obtained across a relatively narrow structural interval.

The Eldorado Island fold is an upright, close, symmetrical antiform that plunges

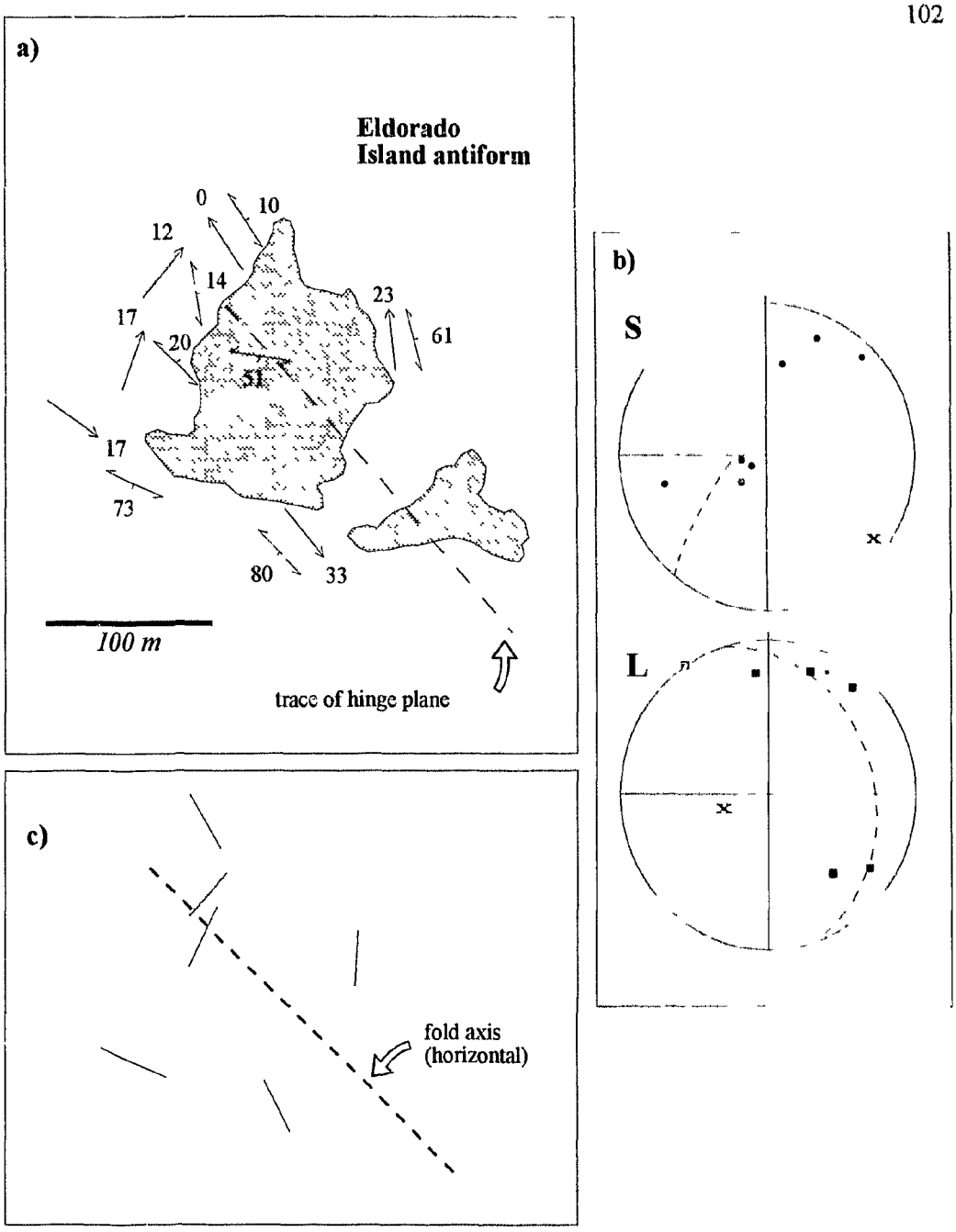

Fig. 3.10. Structural analysis of an upright antiform exposed on Eldorado Island in the Shawanaga shear zone (zone 4) See Figure 2.2 for location **a)** Structural data. **b)** Lower-hemisphere, equal-area stereonet plots of lineation (L) and poles to foliation (S). **c)** Form surface map (Ghosh and Chatterjee 1985) of lineations created by stereographically unfolding fold. Lineations are as they would appear on the unfolded surface.

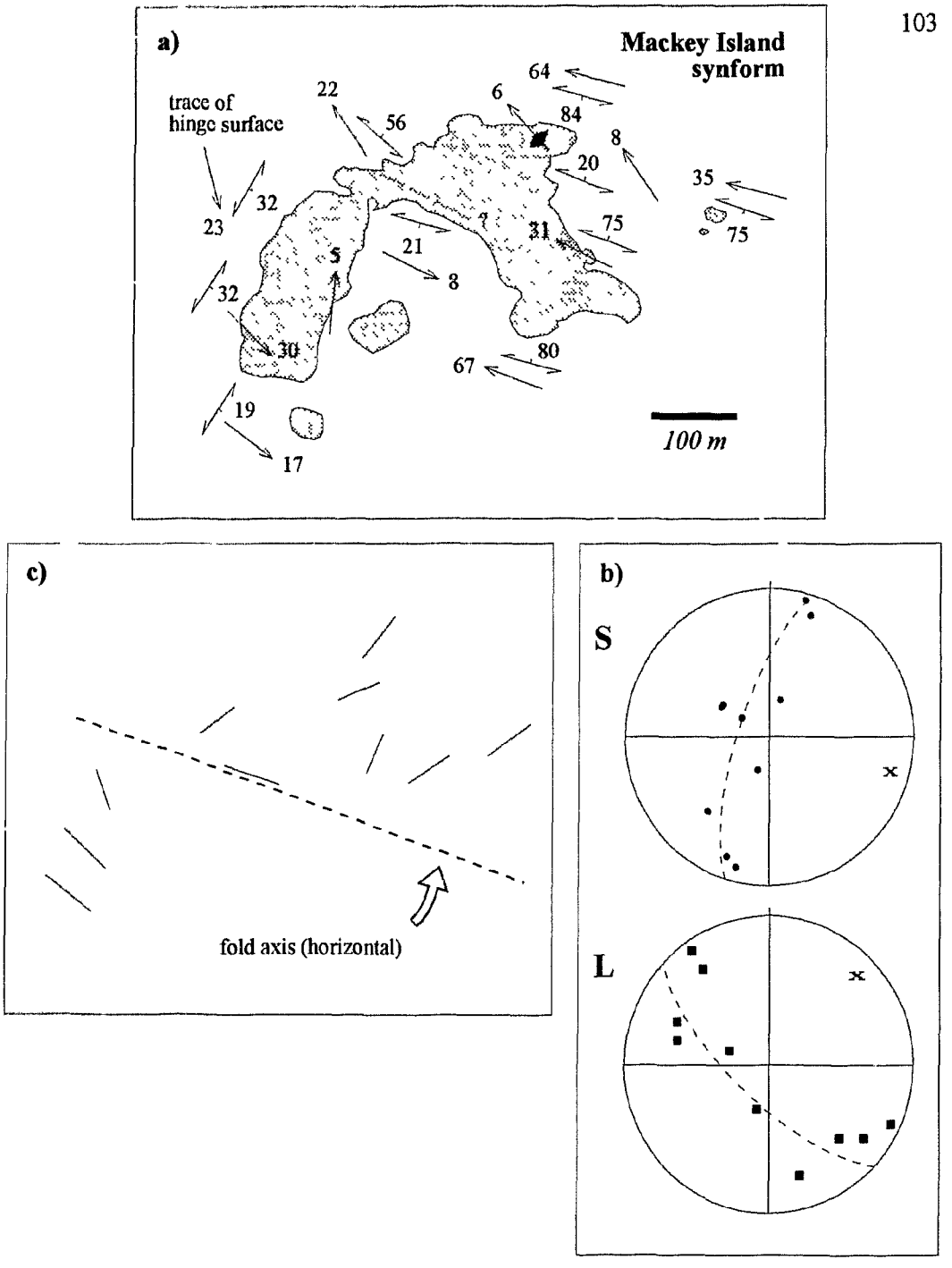

Fig. 3.11. Structural analysis of an overturned synform exposed on Mackey Island in the Shawanaga shear zone (zone 4). See Figure 2.2 for location. **a)** Structural data. **b)** Equal-area, lower-hemisphere stereoplots of lineations (L) and poles to foliation (S). **c)** Form surface map of the fold (see caption to Fig. 3.10).

gently southeast. Its form surface map shows fold limb lineations trending at a shallow to moderate angle to the fold axis, and high-angle lineations in the hinge zone (Fig. 3.10*c*). In contrast, the form surface map of the open to close, gently overturned, east-southeast plunging synform on Mackey Island shows a large variation in lineation trend across the fold hinge and a single axis-parallel lineation in the hinge zone (Fig. 3.11*c*). With the exception of the axis-parallel lineation in the Mackey Island synform, both form surface maps are typical of shear zone folds which nucleate at a high angle to the transport/lineation direction and rotate toward this direction with continued shear (Ghosh and Sengupta 1987).

Strongly rotated folds in shear zones are expected to have tight to isoclinal profiles and axial planes sub-parallel to the mylonitic foliation (Ghosh and Sengupta 1987). However, the open to close profiles of the Eldorado and Mackey Island folds and their transverse axial planar orientations contrast with the expected geometry of strongly rotated folds in the Shawanaga shear zone. This suggests that these folds were not significantly rotated during extensional shear (*cf.* Culshaw et al. 1994).

High-angle lineations in the hinge of the Eldorado Island antiform (suggesting substantial fold rotation) may be preserved from an earlier deformation event, perhaps the same one that formed northeast-trending lineations in zone 4*a*. Further study of the relationship of these lineations to those in the fold limbs is required to test this hypothesis. Although the variation in lineation trend across the hinge of the Mackey Island synform suggests fold rotation, the absence of high-angle lineations in the hinge zone does not support rotation through a large angle. This raises the possibility that folding and partial

realignment of older, northeast-trending lineations during extensional shear accounts for the form surface pattern of lineations in the Mackey Island synform. This would indicate that reorientation of an older lineation dominated over development of a new lineation during extensional shear. Extensional shear fabrics are typically S>L in the Shawanaga shear zone, tentatively supporting this hypothesis.

The Mackey Island fold contains L=S to L>S tectonites in the hinge zone and S>L tectonites in the fold limbs. The hinge zone fabrics suggest that a significant component of axial stretching accompanied fold development. This general relationship is noted in several other localities at the north end of Shawanaga Inlet where transitions from straight gneiss to tightly folded straight gneiss are accompanied by an increase in the intensity of the axis-parallel stretching lineation. Hinge-parallel stretching on a regional scale has been suggested to indicate widespread northwest-southeast ductile flow during extension (Culshaw et al. 1994).

A Model of Fold Development

Sanderson (1982), Coward and Potts (1983), Ridley (1986), and Ridley and Casey (1989) have outlined a general model of fold development in ductile thrust zones which may account for the orientation and geometry of folds in the Shawanaga shear zone and the apparent lack of significant fold rotation. This model describes fold initiation and growth in regions where a gradient in thrust displacement exists in a direction perpendicular to the transport direction. Differential movement resulting from this gradient gives rise to a component of wrench shear on planes at right angles to the thrust plane

(Fig. 3.12). Both thrust- and wrench-shear planes, however, share a common slip direction and the resulting total strain is a simple shear on inclined shear planes. Strain regimes of this type are expected where displacement dies out at the lateral tips of shear zones (Sanderson 1982; Coward and Potts 1983) and where rheological heterogeneities within shear zones cause local variations in strain rate (Platt 1983; Ridley 1986).

Coward and Potts (1983) suggest that folds trending obliquely to the transport direction can develop in combined thrust-wrench shear regimes by buckling of the early-formed thrust foliation. The general form of these folds and amount of rotation they undergo depends on the total finite strain as well as the thrust/wrench shear ratio (Coward and Potts 1983; Ridley 1986). Weakly asymmetric, upright to moderately inclined folds with open profiles and axis-parallel lineations may develop where wrench shear dominates the strain regime (Ridley 1986; Ridley and Casey 1989). These folds can nucleate with axes subparallel to the transport direction and do not undergo substantial rotation.

There is no kinematic reason why the model described above cannot equally apply to an extensional shear-wrench shear couple. Two geometric characteristics of the Shawanaga shear zone suggest that wrench shearing may have been important during southeast-directed extension. On a regional scale, the dextrally sheared western limb of the Shawanaga synform represents a lateral ramp to extensional shear. If this synform developed during regional, syn-extension folding about northwest-trending axes (Culshaw et al. 1994), the resultant wrench shear component created at this ramp may have resulted in folding of extensional shear fabrics west of the synform hinge. This provides a mechanism of forming the east-southeast trending folds in zone 4 that are oblique to both

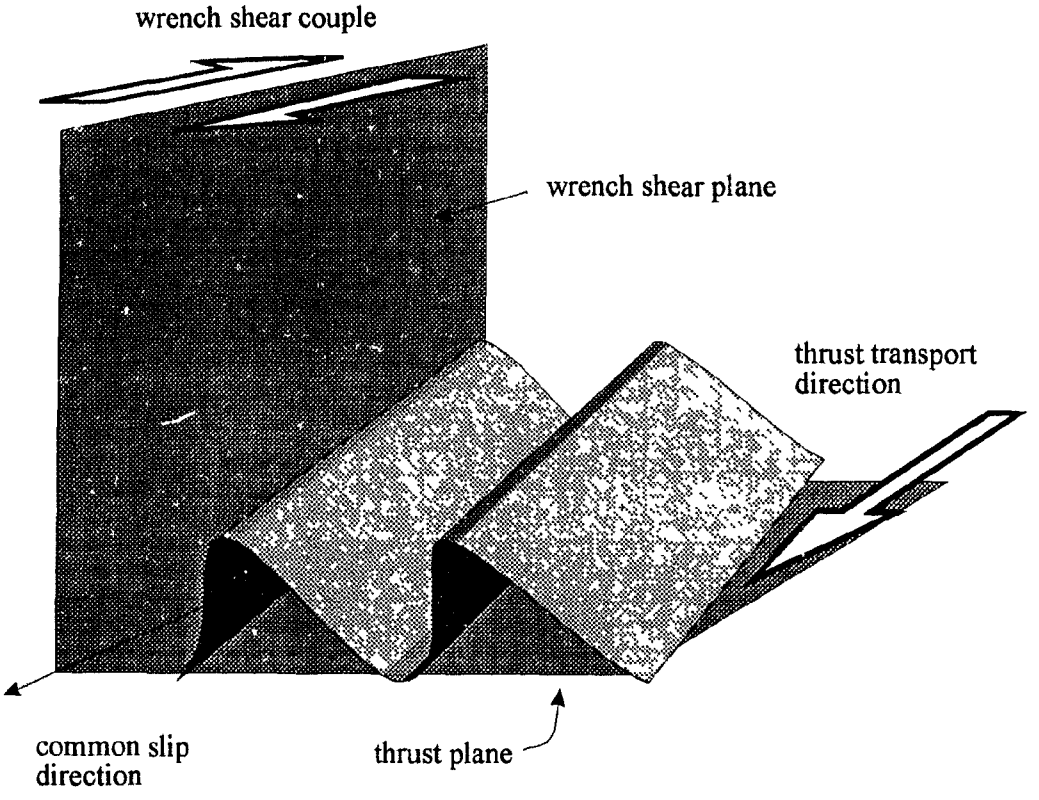

Fig. 3.12. Schematic 3-dimensional view of folds formed in combined thrust-wrench shear (after Coward and Potts 1983; Ridley 1986; Ridley and Casey 1989). Differential slip on thrust plane in a direction perpendicular to the transport direction gives rise to a wrench shear on planes at right angles to the thrust plane, but with the same slip direction.The thrust-wrench shear couple causes buckling of the early thrust fabrics. These folds are commonly asymmetric with a consistent vergence and have axes subparallel to the lineation/transport direction They need not have undergone a large rotation to obtain their depicted orientation. Folds shown above have similar profiles to those in the Shawanaga shear zone within areas where a wrench shear component may have been significant.

the kilometre-scale folds and the southeast lineation/transport direction. Growth of these moderately oblique folds without significant rotation should yield northwest-plunging lineations on northeast-dipping surfaces and southeast-plunging lineations on southwest-dipping surfaces (Fig. 3.13*a*). This is the pattern observed in zone 4 of the Shawanaga shear zone (Fig. 3.13*b*) and supports a model of fold development without significant rotation. Variable reorientation of older lineations, development of new transport-parallel lineations (Culshaw et al. 1994), and overturning of fold limbs during syn-folding shear can account for much of the scatter in lineation attitude observed in zone 4.

On a local scale, pervasively folded, high-strain fabrics at the north end of Shawanaga Inlet may have formed in a wrench shear regime created by a constriction in flow past the eastern end of zone 3. The open to close profiles, southwestward vergence, and concentration of folds east and southeast of this little-deformed zone (Figs. 2.2, 3.2) are consistent with a large dextral wrench component during extensional shear. Culshaw et al (1994) suggested that the region of older fabrics and pre-Grenvillian metamorphic assemblages between the Britt and Nares Inlet shear zones (*i.e.*, structural zones 2 and 3) acted as a resistant block during extension, resulting in nucleation of kilometre-scale northwest-trending folds at the northeast edge of this block. These folds are outlined by the map trace of the Pointe-au-Baril complex and, unlike the majority of kilometre-scale folds, have northeast-dipping hinge planes. Folds at the north end of Shawanaga Inlet have a similar form to the large-scale folds, suggesting that they formed by a similar process.

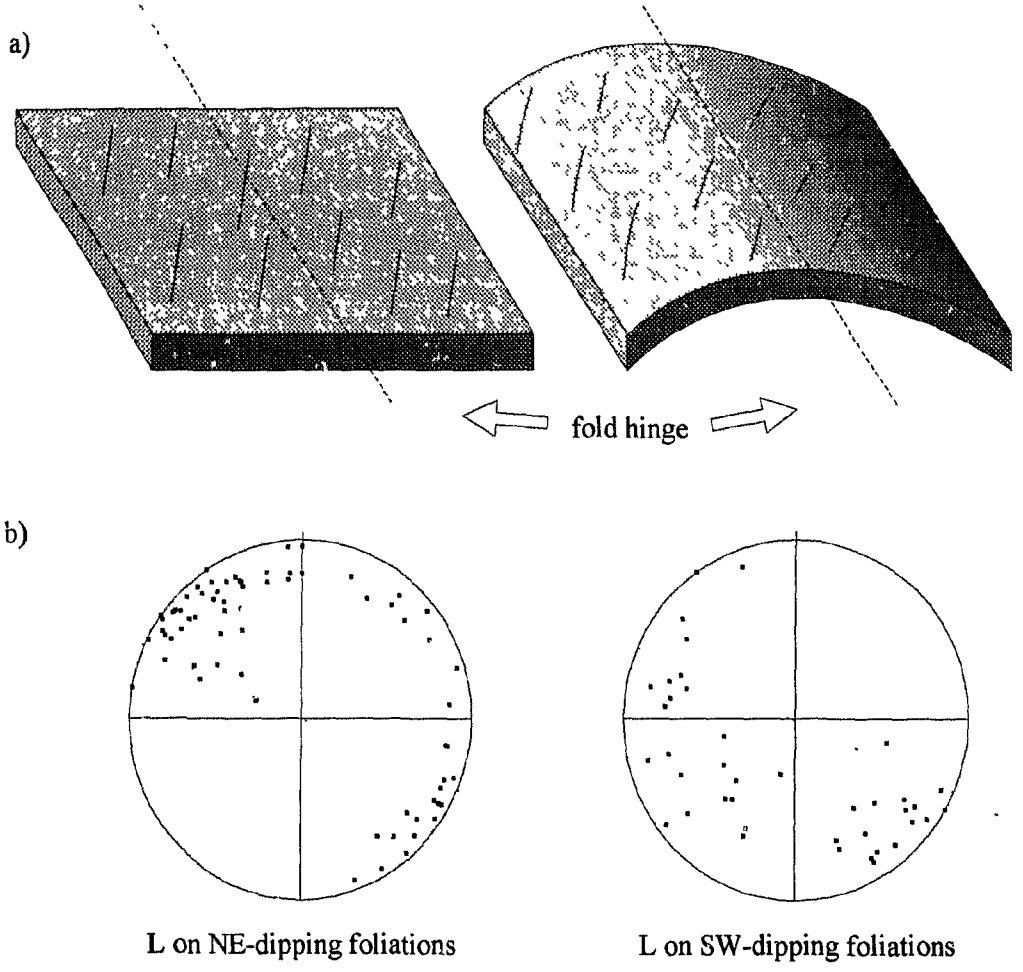

Fig. 3.13. **a)** Schematic diagram illustrating effect of folding a linear fabric about an oblique, subhorizontal axis Lineations will plunge in opposite directions to either side of fold hinge. **b)** Lineations in zone 4 of the Shawanaga shear zone plotted with respect to foliation dip. Dotted lines indicate trend of best-fit fold axis for zone 4 foliations. Maximum lineation concentrations in the northwest sector for foliations dipping toward the northeast strike (270-360°) and in the southeast sector for foliations dipping toward the southwest (strike 090-180°) suggest that the shear zone lineation was folded in the manner depicted in a). That these lineations have a similar trend to the regional lineation suggests that the folds did not undergo substantial rotation during their development

3.4 THE NARES INLET SHEAR ZONE

The Nares Inlet shear zone is a shallowly to moderately southeast-dipping extensional shear zone of variable width that lies structurally beneath the Shawanaga shear zone. The zone lies entirely within the Bayfield gneiss association and coincides with a belt of metasedimentary gneiss along part of its length (Culshaw et al. 1988). Along the Georgian Bay coast the Nares Inlet shear zone is marked by a 300 m-thick succession of mylonite gneiss. Shear fabrics can be traced ten kilometres northeast of here to Highway 529 (Fig. 2.2) where an outcrop of north-striking, fine-grained straight gneiss with millimetre-scale tectonic layering and a moderately north-northeast-plunging lineation marks its location. The shear zone progressively narrows toward the northwest and is probably <100 m wide where it crosses Highway 529. The Nares Inlet shear zone could not be located in roadcut exposures east of this location on Highway 69 and may die out before reaching this highway.

Northwest of the Nares Inlet shear zone along Highway 529, stretching lineations plunge mainly toward the northwest whereas southeast of this structure, lineations mainly have southeasterly plunges. Along Georgian Bay the shear zone also marks a change in lineation attitude, but here northwest- and southeast-plunging lineations structurally beneath the zone are replaced by low-rake, northeast-trending lineations above it (Fig. 2.2). The marked lateral variation in lineation attitude in the hanging wall of the Nares Inlet shear zone may reflect the progressive overprinting of zone 2 straight gneiss by northwest-trending folds (see *Preservation of Pre-Grenvillian and Early Grenvillian Structures*).

The Nares Inlet shear zone resembles the Shawanaga shear zone in that it contains unambiguous kinematic indicators (mainly δ-type winged porphyroclasts; Fig. 3.14*a*) and accommodated southeast-directed extensional shear in the upper amphibolite facies. It differs from the Shawanaga shear zone in that it shows no evidence of earlier thrusting and is not strongly folded. Finite extension lineations within the zone, defined by elongate mineral aggregates and alignment of amphibole grains, plunge with few exceptions toward the southeast. Bisectors of sheath folds in mylonite (Fig. 3.14*b*) are coaxial with this lineation. Open, gently-plunging, northeast-trending folds locally warp the shear fabrics but are mainly outcrop-scale structures. These may be equivalent to third generation folds noted in the Shawanaga shear zone (see above).

Garnet amphibolite dykes of the youngest suite in the Britt domain (tentatively correlated with the 1238 Ma Sudbury swarm; Chapter 2) are strongly transposed within the Nares Inlet shear zone but retain cross-cutting relationships in lower strain enclaves (Fig. 3.14*b*, *c*). Metamorphic patchwork textures (Chapter 2) in the transposed dykes are highly deformed, indicating that dyke metamorphism and hydration preceeded extensional displacement. The timing of extensional shear is unconstrained but kinematic similarity with the Shawanaga shear zone and an absence of northwest-trending folds between these zones suggests that they are broadly contemporaneous structures. Culshaw et al. (1988) noted that northeast-trending folds within the Nares Inlet shear zone overprint northwest-trending folds at the base of this zone, suggesting that extensional shear post-dated folding of the Shawanaga shear zone. Although fold interference patterns of

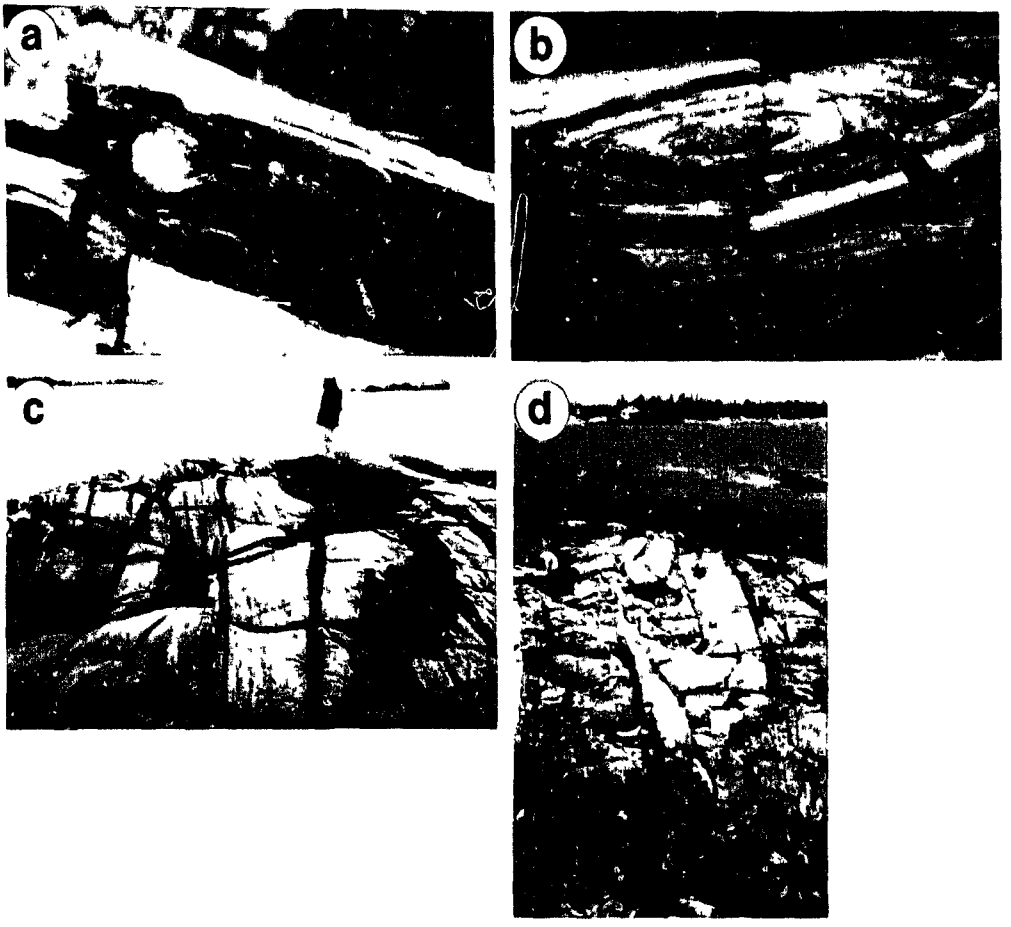

Fig. 3.14. Structural features of the Nares Inlet shear zone. **a)** δ-type winged feldspar porphyroclast indicating top-side-down to the SE displacement **b)** sheath fold in mylonite gneiss, looking down finite stretching lineation. **c)** lower strain zone in which latest dyke generation preserves cross-cutting relationship with pre-Grenvillian gneissosity and leucosomes. **d)** mylonite gneiss containing wide, isoclinally folded, strongly recrystallized dyke (dark) of latest suite.

this type were not observed, the planar geometry of the Nares Inlet shear zone broadly supports syn- to post-folding extensional shear. As noted earlier, syn-kinematic folding of the Shawanaga shear zone may have greatly decreased the ability of this zone to accommodate tectonic transport. The possibility that extensional displacement may have been transferred to the Nares Inlet shear zone after locking of the Shawanaga shear zone remains to be thoroughly investigated, but is strongly suggested by the position of the smaller zone structurally beneath the only segment of the Shawanaga shear zone known to be strongly folded.

3.5 DISCUSSION

Structural Zones

The six discrete structural zones identified in the study area collectively preserve a considerable record of tectonic events in the Pointe-au-Baril area. Oldest gneissic foliations in the Britt domain are migmatitic and pre-date emplacement of the *ca.* 1460 Ma Pointe-au-Baril complex. High-grade metamorphism and tectonic activity at *ca.* 1450-1430 Ma (Chapter 5) is indicated by scattered occurrences of strongly deformed granulite-facies gneiss preserved in zone 3. Grenvillian tectonism was marked by early development of northeast-trending straight gneiss (preserved in zone 2), followed by regional folding and extensional displacement on the Shawanaga and Nares Inlet shear zones. Microtextures in zone 4 of the Shawanaga shear zone indicate that recovery and recrystallization were not effective in modifying extensional shear fabrics, suggesting that rapid post-kinematic cooling may have occurred.

A similar tectonic history is documented in the Key Harbour area of the northern Britt domain where Grenvillian high-strain zones anastomose around lower strain panels preserving fabrics from at least two pre-Grenvillian tectonometamorphic episodes (Corrigan et al. 1994). Here, the oldest gneissic fabrics formed prior to 1694 Ma, and a second tectonometamorphic event occurred between 1694 Ma and 1456 Ma. Grenvillian tectonism in the northern Britt domain involved both thrusting and extensional deformation (Jamieson et al. 1995). This tectonic history is fully compatible with the polyorogenic history of the parautochthon documented in the Pointe-au-Baril area.

In contrast, tectonic elements in structural zone 5 of the Shawanaga domain indicate a less protracted deformation history than for parautochthonous rocks. The simple geometric distribution of fabric elements in zone 5 reflects the absence of older orthogonal fabrics that in the Britt domain were variably reoriented during latest Grenvillian deformation. Microtextures in the Shawanaga shear zone above the allochthon-parautochthon boundary suggest that recovery, recrystallization, and exaggerated grain growth strongly modified these rocks. Pre-extension folds and straight gneisses were documented outside of the study area in the southern Shawanaga domain but were not observed in the Britt domain, providing further evidence of contrasting tectonic histories for these crustal slices (Culshaw et al. 1994). These early folds and straight gneisses may reflect the thrust emplacement history of the Shawanaga domain (Culshaw et al. 1994).

This study has shown that identification of distinct structural regions, whether it be at the scale of lithotectonic domains or within individual outcrops, should be a primary goal of mapping in the Central Gneiss Belt as it provides a means of refining the regional

Grenvillian tectonic framework. Any presumption that gneissic fabrics in this region are entirely Grenvillian needs to be carefully evaluated now that pre-Grenvillian structures and mineral assemblages have been identified (*e.g.*, Jamieson et al. 1992; Corrigan et al. 1994; Ketchum et al. 1994).

Extensional Shear Zones and Transport Direction-Parallel Folds

Amphibolite-facies shear zones in the Pointe-au-Baril area accommodated southeast-directed, top-side-down displacement late in the orogenic history of the Central Gneiss Belt. The Shawanaga shear zone was the site of earlier northwest-directed thrusting and is postulated to mark the site of the Allochthon Boundary Thrust in the western Grenville Province. Extensional reactivation of the Allochthon Boundary Thrust was coeval with kilometre- to metre-scale folding about axes parallel to the extensional transport direction. In contrast, the Nares Inlet shear zone was not deformed by these folds and preserves no evidence for early thrusting, suggesting that it formed late in the extension/folding history but before significant regional cooling.

The Nares Inlet and Shawanaga shear zones bound a crustal segment (zones 2, 3, and 4*a*) lacking a strong, late Grenvillian structural and metamorphic overprint. Extensional movement on these shear zones served to decouple the intervening block from adjacent crustal segments that were deformed by northwest-trending folds, the principal regional expression of late Grenvillian tectonism. Although Culshaw et al. (1994) showed that the Shawanaga and Nares Inlet shear zones may join at depth, the intervening block is not completely fault-bounded as the Nares Inlet shear zone dies out in the northeastern

study area and does not link with the Shawanaga shear zone. This distinction is important as it demonstrates that the block is not 'exotic' (*i.e.*, tectonically transported to its present position carrying evidence of a distal metamorphic event), but rather provides us with a snapshot of the structural and metamorphic character of the parautochthonous crust prior to Grenvillian orogenesis.

Davidson et al. (1982) mapped a large region of granulite-facies gneiss in the footwall of the Shawanaga shear zone west of Arnstein (Fig. 4.1). Tectonite zones appear to encircle this region (Fig. 1.2) implying that it may constitute an 'exotic' crustal block. However, by analogy with their along-strike counterparts near Pointe-au-Baril, these granulites may also be pre-Grenvillian. This hypothesis could be tested by detailed field and petrographic studies in conjunction with U-Pb dating If the granulites west of Arnstein are pre-Grenvillian, then by what mechanism were older fabrics and metamorphic assemblages preferentially preserved in the immediate footwall of the Shawanaga shear zone? Decoupling from regional Grenvillian deformation by concurrent movement on the bounding shear zones could also be invoked for the granulites west of Arnstein, but the need for a more general model is indicated by the preservation of pre-Grenvillian titanites in the footwall of the Nares Inlet shear zone (Ketchum et al. 1992, Krogh et al. 1993*a;* Chapter 5). It appears likely that late Grenvillian strain was strongly partitioned into the extensional shear zones, resulting in a low strain level in adjacent footwall rocks.

Extensional displacement on the Shawanaga shear zone was coeval with local development of upright, northwest-trending folds in both the Britt and Shawanaga domains (Culshaw et al. 1994). Evidence from the study area supporting this hypothesis

includes (*i*) the unfolded crustal segment between extensional shear zones suggesting that the shear zones were kinematically active during folding, (*ii*) a correlation between the abundance of northwest trending folds in zone 2 and the width and strain intensity of fabrics in the adjacent Nares Inlet shear zone, (*iii*) top-side southeast kinematics for all orientations of folded fabric in the Shawanaga shear zone, and (*iv*) fold orientations and forms implying nucleation and growth during combined extensional-wrench shear on the Shawanaga shear zone.

Mancktelow and Pavlis (1994) examined extensional shear zones near Death Valley in the Basin and Range Province, U.S.A., and in the Simplon region of the Swiss Alps. Both of these zones are characterized by (*i*) the presence of a brittle detachment surface within the shear zone that separates footwall from hanging wall rocks, (*ii*) upright folds in footwall rocks with axes parallel to the extensional transport direction, (*iii*) prolate finite strain geometries within fold hinges and flattening strains along fold limbs, and (*iv*) younger extensional shear fabrics that are less strongly folded than older fabrics. In both areas, earlier crustal thickening events formed a strongly layered anisotropic crust. Compressional foliations and structures were subsequently exploited by extensional ones, and all were warped into transport-parallel folds during extensional displacement.

The structural evolution of the Simplon and Death Valley regions bears a strong resemblance to the late orogenic history of the Pointe-au-Baril area. The main differences between these regions and the Pointe-au-Baril area are that syn-kinematic ductile folds developed both above and below the Shawanaga shear zone, and a discrete, brittle detachment did not form between footwall and hanging wall units. These discrepancies

can be attributed entirely to differences in crustal level. The Central Gneiss Belt exposes deep crust (>30 km depth), in contrast to the middle and upper crustal levels represented by the Simplon and Death Valley examples, respectively. Extension ceased on the Shawanaga shear zone at its currently exposed level before it was exhumed into the brittle regime, prohibiting development of a discrete detachment surface. Extensional deformation occurred while both allochthonous and parautochthonous domains were at high metamorphic grade, with the result that ductile folding was not restricted to footwall lithologies. It is possible that the Shawanaga shear zone represents a lower crustal analogue to the mid- and upper-crustal detachment zones described for extended orogenic crust by Mancktelow and Pavlis (1994) and numerous other authors. This topic is discussed further in Chapter 6.

Mancktelow and Pavlis (1994) attributed transport-parallel, upright folds in the Death Valley and Simplon regions to a component of shortening perpendicular to the extension direction. This horizontal shortening was suggested to reflect compression within a regional kinematic framework of transcurrent shear or lateral extrusion. Both tectonic environments permit fold nucleation and growth about axial planes at right angles to the active extensional fault. In the Central Gneiss Belt, there is no compelling evidence to indicate a regional tectonic setting of transcurrent shear or lateral extrusion during late orogenic extension. However, a transcurrent shear model has been proposed to account for fold development during earlier northwest-directed thrusting (Schwerdtner 1987). It is possible that the northwest-trending folds may have initially formed during compression and were amplified during extension (*cf.* Abassi and Mancktelow 1990), but much further

structural study is needed to verify this hypothesis, particularly in the northern Britt domain where northwest-trending folds are abundant (Fig. 3.1). Evidence outlined above and by Culshaw et al. (1994), however, suggests that at least some of the northwest-trending folds formed during combined wrench and extensional shear in a ductile flow regime characterized by pre-existing anisotropies (*i.e.*, tectonic layering), rheological heterogeneity, and laterally variable flow.

3.6 SUMMARY

1) The Pointe-au-Baril study area can be divided into six structural zones with unique combinations of planar and linear fabric attitudes. Five structural zones have been defined in the parautochthonous Britt domain and one in the allochthonous Shawanaga domain. Structural zones in the Britt domain collectively preserve a record of pre-Grenvillian and Grenvillian orogenic events whereas the structural zone in the Shawanaga domain only exhibits fabrics and structures of Grenvillian age.

2) A structural zone within the Shawanaga shear zone contains kinematic evidence for sinistral displacement on northeast-striking shear planes. These fabrics pre-date top-side-southeast extensional shear, and in conjunction with evidence for early northwest-directed thrusting, indicate that the Shawanaga shear zone had a polyphase Grenvillian movement history.

3) A crustal lozenge bounded by the Shawanaga and Nares Inlet shear zone preserves pre-Grenvillian fabrics and granulite-facies mineral assemblages, and lacks northwest-trending, metre- to kilometre-scale folds. It is postulated that the bounding

extensional shear zones decoupled this block from a late regional Grenvillian deformation that was principally expressed by folding about northwest-trending axes.

4) Northwest-trending fold development was coeval with extensional displacement on the Shawanaga shear zone. Folded shear zone fabrics contain kinematic evidence of top-side-southeast displacement for all orientations of foliation. Decametre-scale, upright and weakly overturned folds near the base of this zone have systematic, moderately oblique trends to the extensional transport direction and are thought to have formed during combined extensional-wrench shear. This model of fold development, which may have widespread application in the western Central Gneiss Belt (Culshaw et al 1994), does not require significant fold rotation during extensional shear, consistent with the open to close profile of these folds.

5) The Nares Inlet shear zone accommodated top-side-southeast extensional displacement and is a later structure than the Shawanaga shear zone. This zone may have formed after extensional displacement was no longer possible on the strongly folded Shawanaga shear zone. It is postulated that extensional shear was transferred from the Shawanaga shear zone to the Nares Inlet shear zone.

6) The temporal and kinematic evolution of late Grenvillian extensional shear zones in the Pointe-au-Baril area bears some resemblance to middle- and upper-crustal extensional fault systems that occur at sites of previously thickened crust. The Shawanaga and Nares Inlet shear zones may therefore represent lower crustal analogues to these structures.

CHAPTER 4

Metamorphic Assemblages And Thermobarometry

4.1 INTRODUCTION

Interactions between thermal and tectonic processes in orogenic belts are best evaluated by combined metamorphic and structural studies. In the high-grade core of deeply exhumed orogens such as the Grenville Province, an integrated structural-metamorphic approach is essential for accurate characterization of thermotectonic history because of the strong link that exists between high-temperature tectonic and metamorphic processes (*e.g.*, Brodie and Rutter 1985). Until recently, the metamorphic history of large tracts of amphibolite- to granulite-facies gneiss in the Grenville orogen was poorly understood, principally due to an absence of structural information required to place metamorphic data in a geological context, and because well-calibrated geothermometers and geobarometers appropriate for common mineral assemblages in these rocks were lacking (Anovitz and Essene 1990). However, recent study of high-grade Grenvillian terranes in conjunction with advances in thermobarometry has remedied this situation. Qualitative and quantitative metamorphic data for the Grenville Province have been presented by numerous authors (*e.g.*, Davidson et al. 1982; Rivers and Chown 1986; Owen et al. 1986; Schau et al. 1986; Grant 1989; Indares and Martignole 1989, 1990*a*, *b*; Anovitz and Essene 1990; Davidson et al. 1990; Nadeau 1990; Tuccillo et al. 1990, 1992; Davidson 1991; Jamieson et al. 1992, 1995; Bethune 1993; Connelly et al. 1993; Indares 1993; Wodicka 1994) and in conjunction with models

of crustal structure (*e.g.*, Davidson et al. 1982; Rivers and Chown 1986; Rivers et al. 1989; Culshaw et al. 1983, 1990, 1994) and seismic reflection data (*e.g.*, Green et al. 1988; White et al. 1994) have allowed metamorphic studies to be placed in a regional tectonic context.

In this chapter, metamorphic mineral assemblages and textures, mineral chemistry, thermobarometric estimates, and possible *P-T-t* paths are discussed for allochthonous and parautochthonous rocks in the Pointe-au-Baril area. As noted by Jamieson et al. (1992) and Ketchum et al. (1994), parautochthonous rocks in this area preserve both Grenvillian and pre-Grenvillian (*ca.* 1450-1430 Ma) assemblages, allowing the polymetamorphic history of the parautochthon to be directly characterized. This chapter also presents new data on a metamorphic isograd within the Shawanaga shear zone, and examines unusually strong chemical zonation in garnet porphyroblasts from this shear zone. Both can be linked to the *P-T* evolution of the study area during late orogenic extension, the principal focus of this chapter. As emphasized by other workers (*e.g.*, Corrigan et al. 1994; Wodicka 1994) and stressed in this study, insights on the tectonometamorphic history of the Grenville Province cannot advance without a clear understanding of the age and relationship between tectonic fabrics and metamorphic mineral assemblages.

4.2 METAMORPHIC SETTING

U-Pb metamorphic ages from the Ontario Central Gneiss Belt are reviewed in Chapter 5 and a brief summary of previous work on metamorphism in the Pointe-au-Baril

area is presented in Chapter 2. The discussion presented below places metamorphism in the Central Gneiss Belt in a tectonic context.

Metamorphic grade throughout the Central Gneiss Belt is mainly upper amphibolite facies (above the temperature of muscovite breakdown; Wynne-Edwards 1972) although granulite facies assemblages underlie a significant portion of the Belt in Ontario (Fig. 4.1; Davidson et al. 1982; Culshaw et al. 1983; Davidson 1991). It is not entirely clear whether amphibolite- to granulite-facies transitions in this area represent intact metamorphic gradients, tectonically distinct metamorphic terranes, partial re-equilibration of older assemblages, or are merely a function of variations in metamorphic fluid activity (*e.g.*, Davidson 1991). Based on work to date it appears that all of these explanations are plausible, although some (*e.g.*, variations in aH_2O, retrogression of older granulites) may be more applicable than others (Grant 1989; Davidson 1991; Ketchum et al. 1994).

Grenvillian metamorphism is considered by most workers to be a response to northwest-directed thrust thickening driven by continent-continent collision southeast of the present limit of exposure. An additional contribution of magmatic heat to the thermal regime is indicated by voluminous intrusion of anorthosite-mangerite- charnockite-granite (AMCG) suites at 1.16-1.12 Ga over much of the central and eastern Grenville Province (Martignole 1986; Emslie and Hunt 1990). It has been suggested that crustal weakening by AMCG magmatism (Emslie and Hunt 1990) or asthenospheric upwelling (Hoffman 1989) may have facilitated regional-scale, Grenvillian ductile deformation. However, plutonic rocks of Grenvillian age are sparse in the western Central Gneiss Belt, suggesting

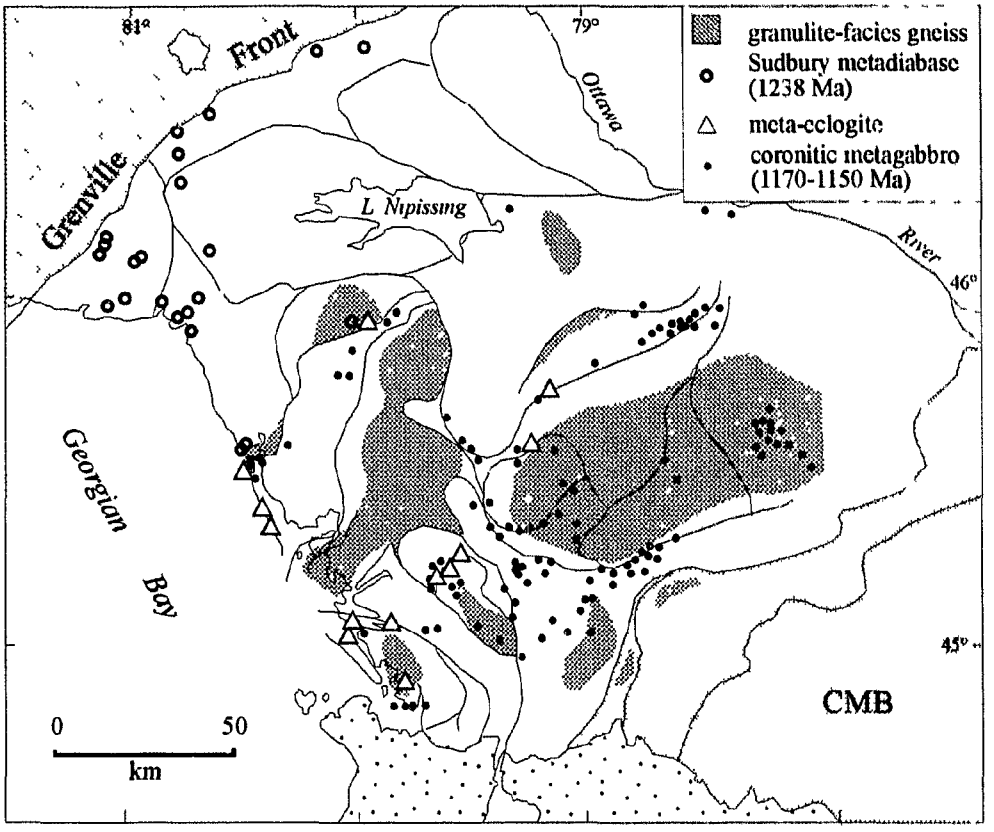

Fig. 4.1. Distribution of granulite facies gneiss, *ca.* 1238 Ma (Krogh et al. 1987) Sudbury metadiabase, and *ca* 1170-1150 Ma (Davidson and van Breemen 1988; van Breemen and Davidson 1990; Heaman and LeCheminant 1993) coronitic olivine metagabbro in the Central Gneiss Belt of Ontario (after Davidson 1991). CMB = Central Metasedimentary Belt. Note association of meta-eclogite bodies with shear zones except for southwesternmost body (in the Go Home domain) where this relationship is apparently absent. See text for further details

that metamorphism was principally due to thrust thickening.

The relationship between metamorphism and tectonism in the Central Gneiss Belt is partly revealed by abrupt variations in metamorphic grade and crystallization history noted across several regional-scale thrust zones (*e.g.*, Davidson et al. 1982). This suggests that crustal thickening in this part of the orogen was by tectonic assembly of metamorphically distinct crustal blocks, a view supported by work in the central and eastern Grenville Province (*e.g.*, Rivers and Chown 1986; Indares and Martignole 1989). Thermobarometric differences between thrust slices have not been distinguished, however (Anovitz and Essene 1990), most likely due to widespread re-equilibration following thrusting and peak metamorphism (Grant 1989; Davidson 1991; Nadeau and Hanmer 1992). Regional metamorphic re-equilibration is also suggested by isolated occurrences of meta-eclogite which, in conjunction with thermobarometric and petrologic evidence from metabasic rocks (Grant 1987; Needham 1992; Jamieson et al. 1995), indicate early, high-pressure metamorphism (~14-16 kbar). An early Grenvillian age for this event is suggested by paleopressures of up to 14 kbar for metamorphosed, 1238 Ma Sudbury diabase dykes in the Britt domain (Jamieson et al. 1995). However, these data may not provide a constraint on the age of high-pressure metamorphism as recorded in isolated meta-eclogite bodies to the southeast (Fig. 4.1) as the dykes and meta-eclogites may have contrasting tectonic histories (see Chapter 6). Grant (1989) suggested that meta-eclogite lenses, restricted to domain-bounding shear zones, were tectonically transported from depth and do not indicate an early episode of regional high-pressure metamorphism. However, the occurrence of meta-eclogite apparently unassociated with major structures

in the Go Home domain (Fig. 4.1) casts doubt on this hypothesis (Davidson 1991). If high-pressure metamorphism occurred within the Central Gneiss Belt, it must have taken place prior to widespread intrusion of *ca.* 1170 Ma olivine gabbro (Fig. 4.1; Grant 1987; Davidson 1990, 1991).

4.3 METAMORPHIC ASSEMBLAGES, TEXTURES, AND OVERPRINTING RELATIONSHIPS

As outlined in Chapter 3, the Pointe-au-Baril study area has been divided into a number of structural zones. Metamorphism is best examined within this framework as mineral assemblages of distinct age and/or grade are in some cases restricted to particular structural zones, and some zones are characterized by metamorphic textures or minerals that are not observed in other zones.

The identification and characterization of well-preserved, pre-Grenvillian metamorphic assemblages in the Pointe-au-Baril area is an important contribution of this study as it represents the first documentation of this type in the interior of the southwest Grenville orogen. At the outcrop scale, pre-Grenvillian metamorphic assemblages are distinguished from Grenvillian ones by their higher metamorphic grade (granulite versus amphibolite facies) in conjunction with an absence of Grenvillian tectonic fabrics. On the scale of the study area, pre-Grenvillian granulites are mainly restricted to structural zone 3, the only zone lacking a penetrative Grenvillian overprint, and to a few competent mafic bodies outside of this zone. In zone 3, metamorphic orthopyroxene is fresh in the interior of mafic supracrustal units but is absent at the margins where younger, amphibolite-facies

tectonic fabrics of presumed Grenvillian age occur. These observations and U-Pb data (Chapter 5) form a basis for the identification of pre-Grenvillian granulites.

Mafic dykes intruded after pre-Grenvillian high-grade metamorphism preserve rare metamorphic orthopyroxene that is visible only in thin section. These are the only rocks in which Grenvillian granulite-facies assemblages have been identified in the study area, suggesting that a low aH_2O in the dykes may have facilitated orthopyroxene growth during upper amphibolite-facies Grenvillian metamorphism. Alternatively, the previously unmetamorphosed dykes may preserve the only record of an early, short-lived, granulite facies metamorphism that was not preserved in older metamorphic rocks. There is no evidence to indicate that granulites identified as pre-Grenvillian are the product of this later high-grade event.

Parautochthon

Pre-Grenvillian (ca. 1450-1430 Ma) Mineral Assemblages

Within structural zone 3 (Fig. 3.2), pre-Grenvillian granulite-facies mineral assemblages are preserved in mafic supracrustal gneiss, amphibole-bearing calc-silicate gneiss, and megacrystic granite. Despite a low degree of Grenvillian strain (Chapter 3), it is likely that many pre-Grenvillian assemblages in this zone at least partly re-equilibrated during Grenvillian metamorphism, although textural data and *P-T* calculations (see below) indicate that older assemblages are wholly preserved in some areas.

The assemblage Pl-Hbl-Opx-Ilm±Qtz±Cpx±Grt±Ged±Mt±Spl±Hem (all abbreviations mainly after Kretz 1983; see Table 4.1) is locally preserved within mafic

Table 4.1. Mineral abbreviations (mainly after Kretz 1983)

Ab	albite	FePrg	Fe-pargasite	Phl	phlogophite
Aln	allanite	Fs	orthoferrosilite	Pl	plagioclase
Alm	almandine	Grt	garnet	Py	pyrite
Ann	annite	Ged	gedrite	Prp	pyrope
An	anorthite	Gr	graphite	Qtz	quartz
Ap	apatite	Grs	grossular	Rt	rutile
Bt	biotite	Hc	hercynite	Sil	sillimanite
Cal	calcite	Hbl	hornblende	St	staurolite
Ccp	chalcopyrite	Ilm	ilmenite	Ttn	titanite
Cpx	clinopyroxene	Kfs	K-feldspar	Tur	tourmaline
Crn	corundum	Ky	kyanite	Tr	tremolite
Di	diopside	Mt	magnetite	Ts	tschermakite
En	orthoenstatite	Ms	muscovite	Zrn	zircon
Ep	epidote	Mnz	monazite	Zo	zoisite
FeTs	Fe-tschermakite	Opx	orthopyroxene	W	water
FeTr	Fe-tremolite	Prg	pargasite		

Table 4.2. Selected equilibra used in TWQ calculations (see Figs. 4.9 to 4.11)

1. Alm + Phl = Prp + Ann
2. Grs + 2 Ky/Sil + Qz = 3 An
3. Alm + 3 Rt = 2 Qtz + Ky/Sil + 3 Ilm
4. Alm + Ms = Ann + 2 Ky/Sil + Qtz
5. Alm + 5 Crn = 3 Hc + 3 Ky
6. Prp + Ms = Phl + 2 Ky/Sil + Qtz
7. 3 Ky/Sil + Grs = 3 An + Crn
8. 3 Tr + 5 Alm = 3 FeTr + 5 Prp
9. 3 Prg + 4 Alm = 3 FePrg + 4 Prp
10. 3 FePrg + 2 Grs + Alm + 18 Qtz = 3 FeTr + 6 An + 3 Ab
11. 3 FeTs + 4 Grs + 2 Alm + 12 Qtz = 3 FeTr + 12 An
12. 3 Tr + 5 Prp + 10 Grs + 3 Ab = 12 An + 18 Di + 3 Prg
13. 3 Ann + 4 Grs + 5 Prp + 18 Qtz = 3 Tr + 3 Kfs + 6 An + 3 Alm
14. 3 Tr + Prp + 10 Grs + 4 Alm + 3 Ab = 12 An + 18 Di + 3 FePrg
15. 3 An + 3 En = 2 Prp + Grs + 3 Qtz
16. Prp + 2 Grs + 3 Qtz = 3 An + 3 Di
17. 3 En + 2 Alm = 3 Fs + 2 Prp
18. 3 En + Grs = 3 Di + Prp
19. 3 An + 3 Fs = Grs + 2 Alm + 3 Qtz

supracrustal gneiss where Grenvillian fabrics are absent. Zircon, apatite, and rutile are accessory minerals, and biotite occurs as a retrograde phase. Idioblastic to subidioblastic garnet porphyroblasts (Fig. 4.2*a*) contain plagioclase, ilmenite, and orthopyroxene inclusions; some grains also have abundant, wormy fluid inclusions. All other mineral species are subidioblastic to xenoblastic. Orthopyroxene is fresh and is intergrown with amphibole and garnet. Amphibole also locally forms narrow rims on orthopyroxene (Fig. 4.2*a*).

Plagioclase-rich segregations in mafic granulite cut a weak to moderate foliation and contain coarse-grained orthopyroxene porphyroblasts (*e.g.*, Fig. 5.3*a*). Partial recrystallization of orthopyroxene was accompanied by garnet growth as Opx-Grt intergrowths locally rim unrecrystallized porphyroblast cores (Fig. 4.2*b*). Orthopyroxene also occurs as inclusions in clinopyroxene porphyroblasts which themselves are rimmed by fine-grained orthopyroxene (Fig. 4.2*c*). These textures are consistent with U-Pb isotopic data from zone 3 (Ketchum et al. 1994; Chapter 5) indicating two episodes of granulite-facies metamorphism in the interval *ca.* 1450-1430 Ma.

Calc-silicate gneiss and megacrystic granite in zone 3 both locally contain the assemblage Pl-Kfs-Qtz-Grt-Cpx-Opx-Hbl-Bt-Mt±Ilm with accessory Ttn-Zrn±Ap. The presence of orthopyroxene in megacrystic granite is typically indicated in outcrop by a waxy greenish tinge. Garnet is embayed in calc-silicate gneiss but forms numerous subidioblastic grains in megacrystic granite. Sparse orthopyroxene ranges from subidioblastic prisms to highly embayed relicts in both rock types. Rarely, orthopyroxene also forms narrow overgrowths on clinopyroxene and magnetite in calc-silicate gneiss and

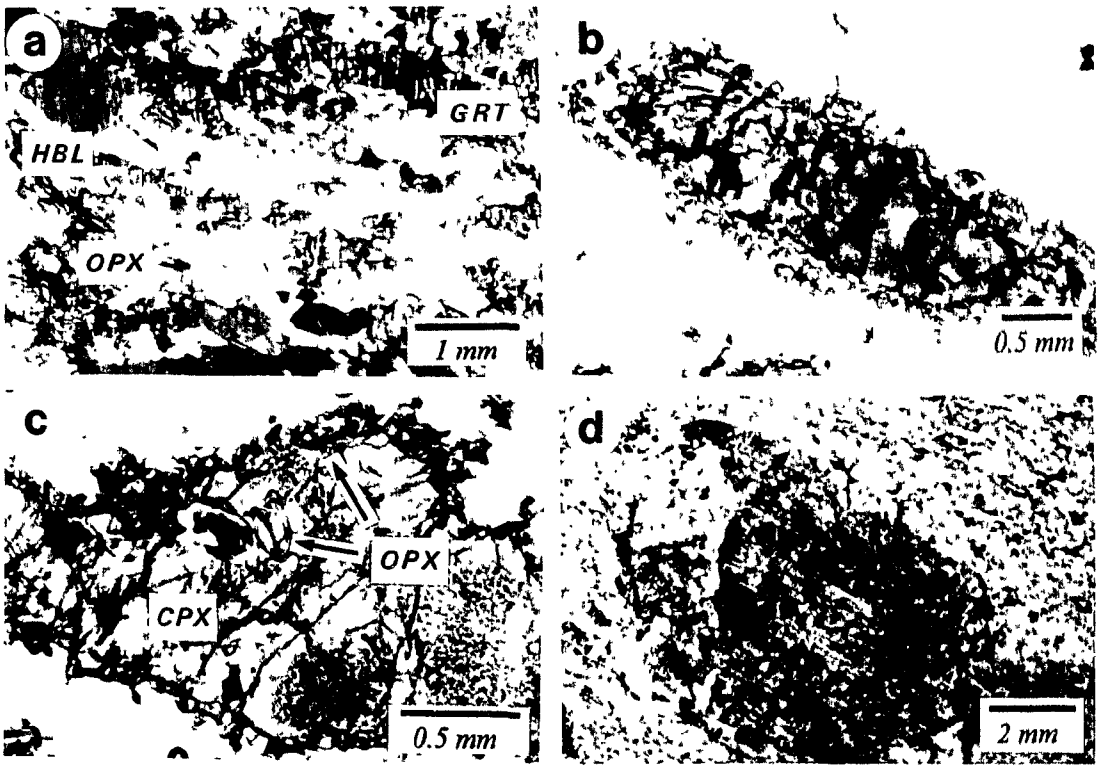

Fig. 4.2. Pre-Grenvillian (*ca.* 1450-1430 Ma) metamorphic textures in structural zone 3. Sample numbers in brackets. **a)** Orthopyroxene in garnet-bearing mafic supracrustal gneiss (89-73*a*). **b)** Orthopyroxene porphyroblast in mafic supracrustal gneiss leucosome rimmed by garnet and recrystallized orthopyroxene (91-266). **c)** Orthopyroxene inclusion in a clinopyroxene porphyroblast, itself rimmed by amphibole and fine-grained orthopyroxene (89-88*b*). **d)** Corundum porphyroblast in quartz-free paragneiss with inclusion trails of opaque oxide at high angle to external foliation (89-39*b*). See text for further details.

granite. This indicates that orthopyroxene in Pointe-au-Baril granite is a metamorphic rather than relict igneous phase.

Corundum porphyroblasts in quartz-free paragneiss of the Nadeau Island gneiss association overgrow a pre-*ca.* 1450 Ma migmatitic foliation but are replaced by kyanite-sillimanite aggregates in Grenvillian high-strain zones (Chapter 2), suggesting that corundum grew during *ca.* 1450-1430 Ma granulite-facies metamorphism. The close spatial association of corundum-bearing gneiss with mafic granulite and Pointe-au-Baril complex granite (Chapter 2) indicates that (*i*) corundum-bearing gneiss and mafic granulite may be preserved in the same low Grenvillian strain windows, and (*ii*) nucleation of corundum porphyroblasts may have been assisted by heat from crystallizing granite (emplaced in the interval 1460-1430 Ma).

Corundum-bearing rocks contain the polymetamorphic assemblage Kfs-Pl-Crn-Ky-Sil-Bt-Ilm±Grt±Spl±Mt. Corundum porphyroblasts contain inclusions of ilmenite, magnetite, K-feldspar, biotite, and rare kyanite, and are weakly to strongly embayed. Rare inclusion trails of opaque oxide in larger porphyroblasts mark an early foliation at high angles to the external foliation (Fig. 4.2*d*). Smaller corundum laths aligned within the foliation contain fewer inclusions and show only minor resorption features. Kyanite and sillimanite are texturally stable matrix phases although some larger kyanite grains are strongly embayed. Fine-grained, subidioblastic garnet contains inclusions of biotite, opaque oxides, and kyanite. Spinel occurs only as inclusions in opaque oxides. Biotite is a relatively abundant matrix phase.

Taken together, these relationships indicate that the assemblage Crn-Spl-Ky was

stable during pre-Grenvillian granulite-facies metamorphism and was replaced by the assemblage Ky-Sil-Grt-Bt during Grenvillian metamorphism. Small corundum laths may also have grown during the younger event. Inclusion trails in corundum may mark a pre-1450 Ma foliation, or a *ca.* 1450 Ma foliation that formed prior to corundum growth; it is not possible to distinguish between these possibilities. Pre-Grenvillian kyanite may be an early product of granulite-facies metamorphism prior to the onset of corundum growth, although the possibility that it is a relict phase from an even earlier metamorphic event cannot be ruled out.

Grenvillian Mineral Assemblages

Although upper amphibolite-facies assemblages of Grenvillian age are widespread in the Britt domain, complete overprinting of early metamorphic assemblages is often difficult to demonstrate given comparable grades of Grenvillian and pre-Grenvillian metamorphism (Jamieson et al. 1992). This creates difficulties for petrographic and thermobarometric studies in the Pointe-au-Baril area because (*i*) pre-Grenvillian assemblages are better preserved here than elsewhere in the Britt domain (Ketchum et al. 1994), (*ii*) the geometry of a tectonic fabric does not always provide a constraint on its age, (*iii*) structural overprinting relationships are commonly obscure, and (*iv*) metamorphic textures in many of these rocks are ambiguous. For these reasons, mineral assemblages are described below from rocks for which a Grenvillian age of mineral growth is unequivocal, *i.e.*, from pre-Grenvillian assemblages clearly overprinted during Grenvillian metamorphism, from Grenvillian high-strain zones, and from metabasic dykes

and pods emplaced after the youngest pre-Grenvillian metamorphism.

Where a Grenvillian structural overprint is evident, pre-Grenvillian granulite-facies assemblages in mafic supracrustal gneiss of zone 3 are replaced by the assemblage Pl-Qtz-Hbl-Gt-Ilm±Cpx±Qtz±Mt with accessory apatite. A granoblastic texture is characteristic, and alternating, millimetre-width bands rich in hornblende and plagioclase define the foliation. This assemblage is also typical of post-1450 Ma metamafic dyke suites, although as noted earlier, least deformed members of the youngest suite (correlated with Sudbury metadiabase; Chapter 2) preserve rare metamorphic orthopyroxene.

A striking feature of corundum-bearing gneiss reworked in Grenvillian high-strain zones is the presence of lensoid kyanite-sillimanite aggregates after corundum porphyroblasts. These aggregates typically comprise abundant fine-grained kyanite with minor interstitial biotite overgrown by prismatic to acicular sillimanite (Fig. 4.3*a*). Both Al_2SiO_5 polymorphs generally show intragranular strain features (*e.g.*, sweeping or patchy extinction) and the grains themselves may also be visibly deformed. A grain-shape preferred orientation parallel to the external foliation is common, although the grains may trace out a sigmoidal foliation within individual aggregates. The aluminosilicate lenses are up to ~10 cm long and are clearly the product of synkinematic breakdown of corundum porphyroblasts. Petrographic textures and mineral compositional data provide little evidence of the reaction(s) responsible for this transformation, but SiO_2 must have been externally introduced (in a fluid phase?) or liberated from another mineral (plagioclase?) for it to occur. Aluminosilicate zonation in several lenses (sillimanite rims a kyanite core) and replacement of kyanite by sillimanite indicates that deformation initiated in the stability

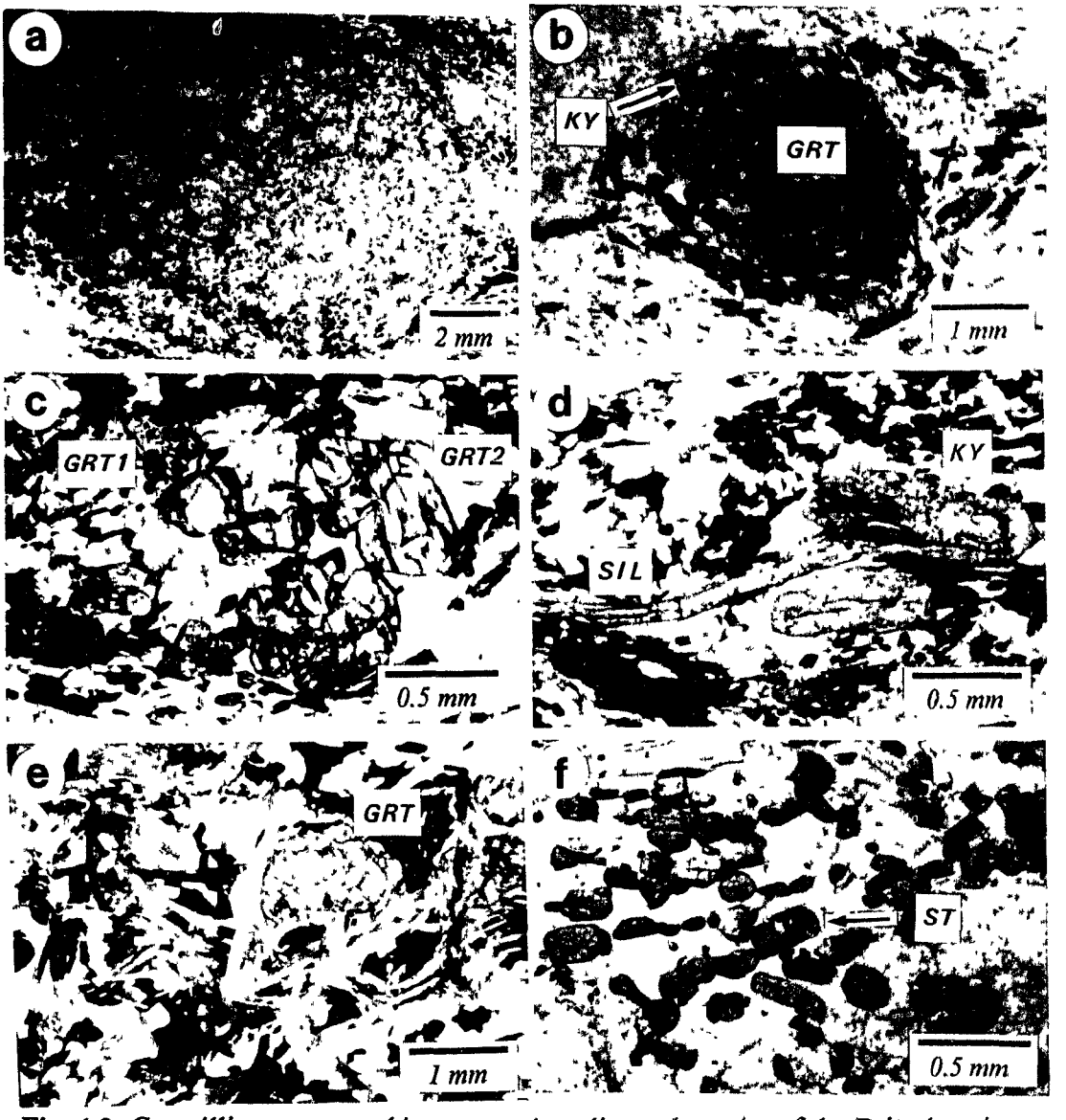

Fig. 4.3. Grenvillian metamorphic textures in pelite and granite of the Britt domain. Sample numbers in brackets. **a)** Kyanite-sillimanite intergrowth after corundum porphyroblast in deformed, quartz-free paragneiss (90-39*d*). **b)** Embayed garnet porphyroblast overgrown by biotite and kyanite. Note kyanite in matrix. (89-3). **c)** Embayed garnet with inclusions (Grt1) and idioblastic, relatively inclusion-free garnet (Grt2) in megacrystic granite, Shawanaga shear zone (89-116*c*). **d)** Embayed kyanite partly replaced by fresh (but deformed) sillimanite, Shawanaga shear zone (90-138*a*). **e)** Folded sillimanite overgrown by younger, axial planar sillimanite in hinge zone of outcrop-scale, northwest-trending fold, Shawanaga shear zone (89-67*c*). **f)** Rounded kyanite and idioblastic, retrograde staurolite in quartz-free paragneiss, Nares Inlet (90-155). See text for further details.

field of kyanite and was active after transition into the sillimanite field. This is consistent with a paragenetic sequence for aluminosilicate polymorphs in the Shawanaga shear zone (see below) and lends further credence to a Grenvillian age for new mineral growth in deformed corundum-bearing paragneiss.

Mineral assemblages in the Shawanaga shear zone consist of Pl-Qtz-Kfs-Bt-Grt±Ky±Sil±Ms±Ilm±Rt±Gr in pelitic gneiss and Pl-Qtz-Kfs-Bt-Grt-Hbl-Ilm±Mt in megacrystic granite. Muscovite is normally retrograde except at structurally higher levels where it may form part of the equilibrium assemblage. Pelitic rocks invariably contain strongly embayed garnet porphyroblasts (up to 2 cm in diameter) in a matrix of plagioclase, biotite, kyanite/sillimanite, and quartz (Fig. 4.3*b*), suggesting that pressure-sensitive reactions of the type:

$$\text{Grossular} + Al_2SiO_5 + \text{Quartz} = \text{Anorthite} \quad \text{(GASP)}$$

and:

$$\text{Almandine} + \text{Rutile} = \text{Ilmenite} + Al_2SiO_5 + \text{Quartz} \quad \text{(GRAIL)}$$

were responsible for garnet consumption. Operation of the latter reaction is also indicated by the typical occurrence of rutile as inclusions in garnet and ilmenite as a matrix phase. A number of metapelitic and granitic gneisses examined in thin section also contain small, subidioblastic to idioblastic garnet grains (Fig. 4.3*c*), indicating that local growth of new garnet followed garnet-consuming reactions. In pelitic gneiss, kyanite forms inclusions in all garnet morphologies, suggesting that both periods of garnet growth occurred in the stability field of kyanite. Scattered sillimanite needles <0.2 mm long were noted in garnet porphyroblasts in a few samples, although it could not be determined whether this

fine-grained sillimanite forms an included phase or overgrows garnet. Tuccillo et al. (1992) observed sillimanite inclusions in resorbed garnet porphyroblasts from the Shawanaga shear zone. Additional included minerals in both garnet populations are biotite, quartz, plagioclase, K-feldspar, Ti magnetite, zircon, monazite, pyrite, and apatite in metapelitic gneiss, and plagioclase, K-feldspar, biotite, and ilmenite in granitic gneiss.

Kyanite occurs in metapelitic gneiss throughout the Shawanaga shear zone whereas sillimanite is restricted to structurally higher levels of this zone. Kyanite is coarse- to fine-grained and ranges from idioblastic prisms to strongly embayed relics. The latter texture is commonly observed where kyanite and sillimanite coexist (*cf.* Davidson et al. 1982; Tuccillo et al. 1990, 1992). Sillimanite ranges from coarse-grained prisms to felted fibrolite masses but mainly occurs as bundles of acicular grains aligned within the mylonitic foliation (Fig. 4.3*d*). In the hinge zones of a few outcrop-scale, northwest-trending folds, axial planar sillimanite overgrows folded sillimanite bundles (Fig. 4.3*e*). Textural relationships throughout the Shawanaga shear zone clearly indicate that sillimanite crystallized after kyanite, with nucleation of sillimanite on biotite±muscovite apparently preferred over the kinetically more difficult polymorphic inversion (*e.g.*, Carmichael 1969; Foster 1991). Both polymorphs are deformed in many localities, consistent with growth of these phases during syn-metamorphic extensional shear. The geometric distribution of aluminosilicates in the Shawanaga shear zone is discussed below.

Textures and mineral assemblages outside of the Shawanaga shear zone in the Britt domain are generally similar to those described above. Kyanite is regularly overgrown by sillimanite in Nares Inlet, and both polymorphs are common in pelites of structural zone 3.

Staurolite is found in a number of quartz-poor or quartz-free supracrustal rocks in the Bayfield and Nadeau Island gneiss associations where it ranges from idioblastic grains (Fig. 4.3*f*) to embayed relicts with mantles of retrograde muscovite. Similar textures are observed in corundum-bearing lithologies although muscovite mantles on staurolite are rare. Staurolite inclusions in garnet are observed in some of these rocks, but staurolite mainly forms a matrix mineral that rims or is in contact with kyanite and garnet, suggesting that it represents a retrograde phase formed by a reaction such as:

$$\text{Garnet} + \text{Hercynite} + \text{Kyanite} + H_2O = \text{Staurolite}$$

or, in corundum-bearing rocks:

$$\text{Garnet} + \text{Corundum} + \text{Kyanite} + H_2O = \text{Staurolite}$$

However, the absence of staurolite from quartz-bearing pelites suggests that the lower-temperature retrograde reaction:

$$\text{Garnet} + Al_2SiO_5 + H_2O = \text{Staurolite} + \text{Quartz}$$

was not widespread. This interpretation contrasts with that of Tuccillo et al. (1992) who suggested that the presence of staurolite in pelitic gneiss was due to incomplete breakdown of this mineral during prograde metamorphism.

Allochthon

The allochthonous Sand Bay gneiss association, Ojibway gneiss association, and Shawanaga pluton preserve no evidence for pre-Grenvillian orogenesis (Culshaw et al. 1989; Jamieson et al. 1992) and therefore their mineral assemblages are considered to be entirely of Grenvillian age .

Granodiorite gneiss in the Shawanaga pluton typically contains the assemblage Pl-Kfs-Qtz-Hbl-Bt-Grt-Mt-Ttn with accessory allanite, apatite, and zircon. Garnet mainly occurs as highly resorbed porphyroblasts in a plagioclase-rich matrix (Fig. 4.4*a*). Other minerals in the pluton are subiodioblastic to xenoblastic with irregular to straight grain boundaries. Hornblende and biotite are aligned within the gneissic foliation.

The assemblage Pl-Kfs-Qtz-Hbl-Bt-Ttn±Grt±Ep is characteristic of granodiorite and tonalite orthogneiss of the Ojibway gneiss association. Apatite, allanite, and zircon are accessory. Embayed relict garnets were noted in only a few localities, suggesting that garnet-consuming reactions largely went to completion in these rocks. Titanite is relatively abundant (>5% by volume) and commonly forms idioblastic grains with rounded, optically distinct cores. A well-developed granoblastic texture with little evidence of intragranular strain is typical of Ojibway association rocks (Chapter 3).

Metamorphic assemblages in coronitic metagabbro in the Shaanaga pluton and Ojibway gneisss association record higher grade conditions than those indicated by their host rocks. Recrystallized domains lacking corona structure contain the assemblage Grt-Hbl-Pl-Cpx-Ilm-Bt±Opx (Fig. 4.4*b*). A similar mineral assemblage is found in an 8 m-wide tectonic enclave of fine-grained meta-eclogite in the Shawanaga shear zone on the east side of Shawanaga Island (Fig. 2.2). The core of this body, hosted by Ojibway association straight gneiss, consists of massive clinopyroxene-plagioclase symplectite which is reduced to foliated amphibolite near the margins. Orthopyroxene is a relict matrix phase in symplectite (Fig. 4.4*c*). This rock is texturally and mineralogically identical to meta-eclogite in the Shawanaga shear zone near Arnstein (compare Fig. 4.4*c* with Fig. 4*b*

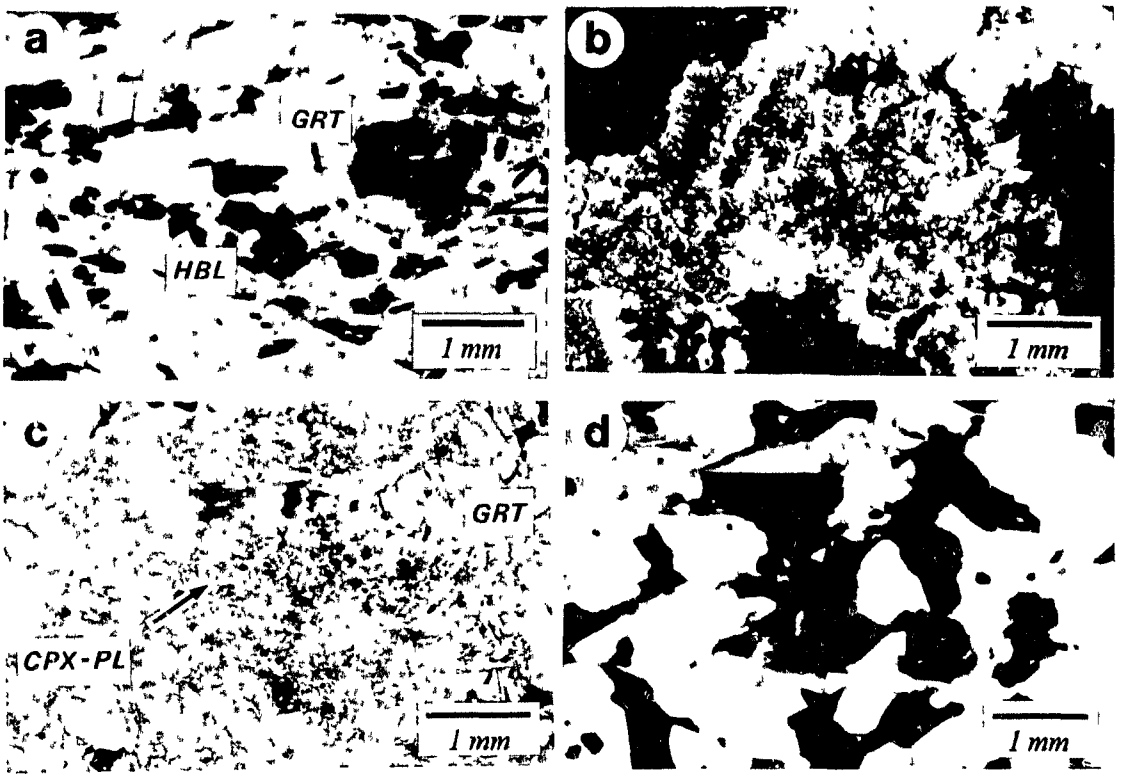

Fig. 4.4. Grenvillian metamorphic textures in the Shawanaga domain. Sample numbers in brackets. **a)** Strongly embayed garnet in plagioclase-rich domain, Shawanaga pluton (90-180). **b)** Recrystallized aggregate of orthopyroxene, clinopyroxene, amphibole and garnet in coronitic metagabbro (89-125). **c)** Clinopyroxene-plagioclase symplectite in core of tectonic enclave of meta-eclogite, Shawanaga shear zone (90-181*a*). **d)** Amphibole, biotite, and apatite in recrystallized, granoblastic Dillon schist of the Sand Bay gneiss association (90-185*a*). See text for further details.

of Grant 1989). Mineral assemblages in coronite and meta-eclogite collectively indicate high-pressure metamorphism prior to initial re-equilibration in the granulite facies and final equilibration in the amphibolite facies (see also Needham 1992). This metamorphic history can be confidently inferred only for the Ojibway gneiss association, as meta-eclogite has not been observed in the Shawanaga pluton, and coronite and meta-eclogite are both absent from the Sand Bay gneiss association. Metastable preservation of early, high-grade assemblages in metabasite is common as reaction kinetics are relatively sluggish in these anhydrous, competent rocks (*e.g.*, Brodie and Rutter 1985, Grant 1989; Indares 1993).

Paragneisses of the Sand Bay association contain the assemblage Qtz-Kfs-Pl-Bt-Ms-Ep-Ap-Mt±Hbl±Cal±Aln±Ttn±Chl±Rt±Ilm (*e.g.*, Fig. 4.4*d*). K-feldspar is common except in the Dillon schist where it was only observed in granitic segregations. Plagioclase ranges from fresh to strongly sericitized with overgrowths of muscovite, calcite, and epidote. Other overgrowth relationships include muscovite on biotite, epidote on allanite, and titanite on ilmenite. Allanite, titanite, apatite, and rutile individually form >2-3% of the matrix in some rocks. Biotite is variably chloritized. Although strongly deformed by extensional shear fabrics, all Sand Bay lithologies in the study area are granoblastic and equigranular and contain little evidence of intragranular strain. These textures suggest widespread recovery and post-kinematic grain growth (see also Chapter 3).

Metamorphic mineral assemblages and textures in Sand Bay gneiss are generally similar to those observed in the Ojibway association, but there are some important differences, namely (*i*) garnet occurs only as rare relict grains in amphibolite within the

Sand Bay association, and (*ii*) muscovite and chlorite are ubiquitous in the Sand Bay association but were not observed in Ojibway gneiss. Although these differences may be attributed to variations in bulk rock and/or metamorphic fluid composition, evidence for a structural boundary beneath the Sand Bay association (see above) indicates that they could also be due to tectonic juxtaposition of crustal slices with contrasting metamorphic histories.

Metamorphic Isograd in the Shawanaga Shear Zone

The geographic distribution of kyanite and sillimanite in pelitic gneiss within the Shawanaga shear zone is shown in Figure 4.5. Each symbol indicates the Al_2SiO_5 polymorph(s) observed in one or more thin sections from the locality shown without reference to the textural stability of these minerals. Pelitic gneiss is mainly confined to the parautochthonous segment of the shear zone, but pelites have also been documented southeast of the allochthon-parautochthon boundary as enclaves in metaplutonic rock (Tuccillo et al 1992; this study) and in the large exposure of supracrustal rock mapped as a tectonic window of Nadeau Island gneiss (Fig. 4.5; Culshaw et al. 1991*a*, 1994).

A transition from kyanite-bearing assemblages at low structural levels to sillimanite±kyanite-bearing assemblages at higher levels defines the position of an 'inverted' metamorphic isograd that roughly parallels the trace of the shear zone (Fig. 4.5). Inversion is suggested by the high temperature assemblage Sil+Kfs overlying the lower temperature assemblages Ky+Kfs. The position of this sillimanite-in isograd is well constrained in the central study area but is somewhat speculative in the east and southwest

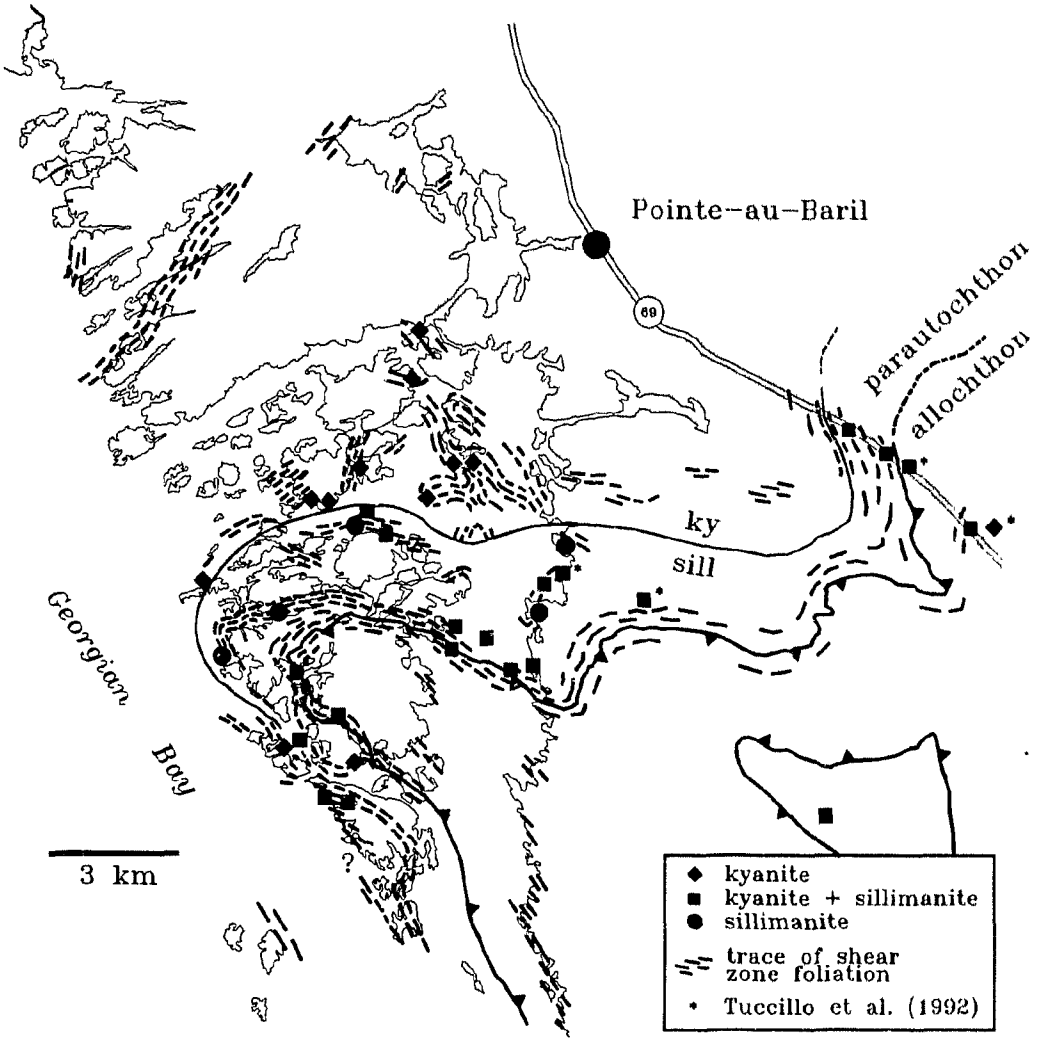

Fig. 4.5. Aluminosilicate polymorph distribution in parautochthonous rocks of the Shawanaga shear zone. The first appearance of sillimanite toward higher structural levels marks the location of an 'inverted' isograd. Kyanite is texturally stable in high-strain fabrics below the isograd but is a relict phase in sillimanite-bearing rocks. K-feldspar is stable throughout the shear zone. Note tectonic window of Nadeau Island paragneiss south of allochthon-parautochthon boundary. For further discussion see text.

due to limited exposure or to an absence of metapelite. A 'best-estimate' position is shown in these regions based on both the presence or absence of sillimanite and on its abundance in thin section. For instance, along Highway 69 the isograd is placed near the northwesternmost outcrop of metapelite in the Shawanaga shear zone as this rock contains only trace sillimanite. A progressive southeastward increase in sillimanite abundance suggests that this placement is reasonable. West of Shawanaga Island, the isograd is constrained on the sillimanite-absent side by a single sample which also dictates the broadly folded geometry of the isogradic surface. The presence of a folded isograd is also indicated by structural reasoning (see *Discussion*) but its confirmation awaits petrographic study south of the present study area.

Inverted metamorphic isograds have been documented in other orogenic belts such as the Himalayas where some workers suggest they record a temporary inversion of the thermal gradient during (*i*) thrusting of a 'hot,' upper plate onto a 'cold,' lower plate (*e.g.*, Le Fort 1975; Hubbard 1989), (*ii*) folding of isograds in the overthrust block (*e.g.*, Searle and Rex 1989), and (*iii*) shear heating (*e.g.*, England and Molnar 1993). However, 'inverted' isograds can also occur where the distribution of metamorphic mineral assemblages (*iv*) is an artifact of post-metamorphic tectonic juxtaposition (*e.g.*, Treloar et al. 1989), (*v*) is due to polymetamorphism (*e.g.*, Hodges and Silverberg 1988, (*vi*) is a function of pressure rather than of temperature, or (*vii*) is a function of kinetic and deformation controls on metamorphic reactions (*e.g.*, Grocott 1979). Given the extensional setting of the inverted isograd in the Shawanaga shear zone and its confinement to parautochthonous rocks, it appears that only the last two of these

mechanisms can account for the observed aluminosilicate distribution as the rest are specific to compressional structures or can be ruled out for the Pointe-au-Baril area. In order to evaluate these possibilities fully, it is necessary to first consider all available structural, petrographic, and thermobarometric data. The origin and significance of this isograd is considered further after thermobarometric results and *P-T* paths for allochthonous and parautochthonous rocks have been presented (see *Discussion*).

4.4 THERMOBAROMETRY AND *P-T* PATHS

Pressures and temperatures were calculated for allochthonous and parautochthonous rocks in the Pointe-au-Baril region in order to (*i*) determine the *P-T* conditions of pre-Grenvillian granulite facies metamorphism in the parautochthon, (*ii*) establish whether peak and post-peak *P-T* conditions are different in allochthonous and parautochthonous rocks, (*iii*) constrain possible *P-T* paths for allochthonous and parautochthonous domains, and (*iv*) investigate *P-T* differences, if any, across the 'inverted' isograd in the Shawanaga shear zone.

Approach

Twenty-one samples of mafic and felsic supracrustal gneiss, pelitic gneiss, granitic orthogneiss, and metabasite were selected for thermobarometry (sample locations indicated in Fig. 4.6). Of these, five contain granulite-facies mineral assemblages attributed to pre-Grenvillian metamorphism. Sampling was mainly confined to the parautochthon as appropriate mineral assemblages for thermobarometry are not widespread in the

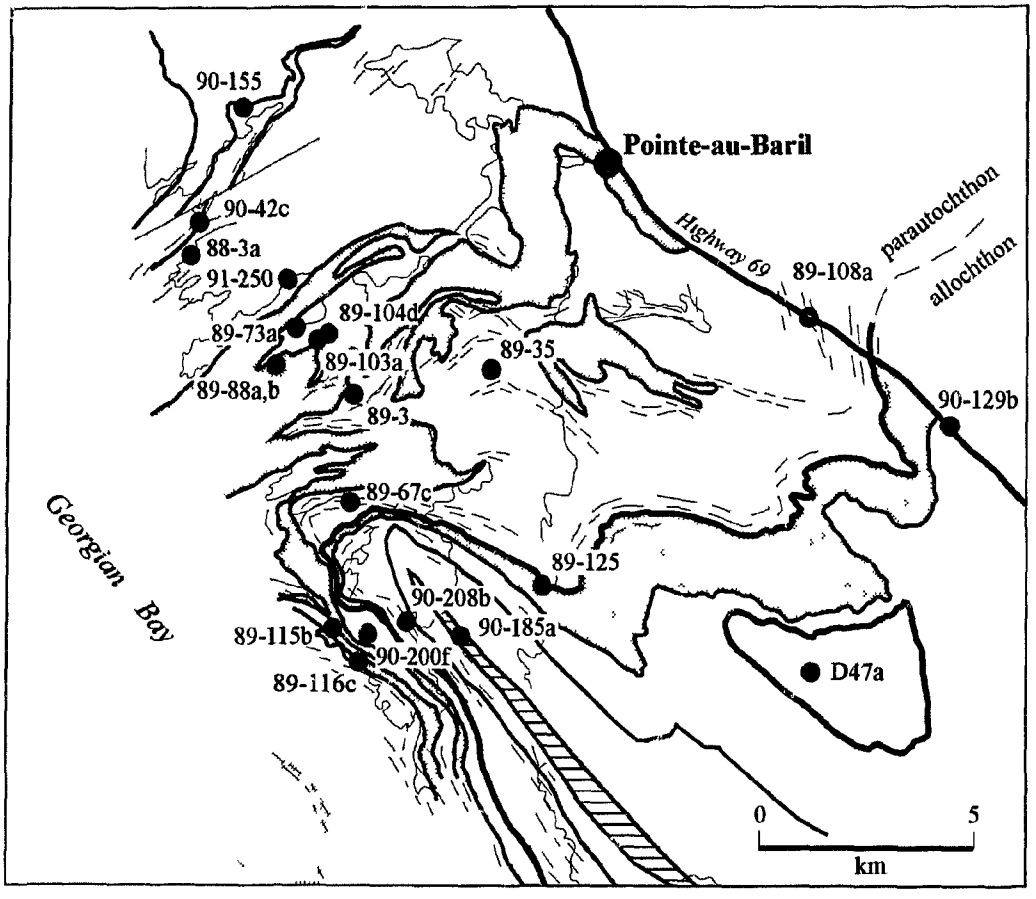

Fig. 4.6. Simplified geological map showing location of samples used in thermobarometry Shaded units are ca 1450 Ma granitoid plutons Horizontally ruled unit is Dillon Schist of the Sand Bay gneiss association

allochthon, principally due to an absence of garnet.

Mineral compositions were obtained by energy-dispersive analysis with the automated JEOL 733 Superprobe at Dalhousie University. Operating conditions were 15 kV accelerating voltage, 13 nA probe current, 1 μm beam diameter, and a counting time of 40 seconds. The beam was defocussed (10 μm diameter) for analysis of plagioclase in order to minimize Na loss. A ZAF matrix correction program was employed in the reduction of raw data. Compositional data were collected from three or more microdomains within each polished thin section to check for consistency of mineral compositions. Where consistency of a given mineral composition was indicated, the data were averaged to yield a representative analysis for use in thermobarometry. Where compositions varied within an individual grain or on the scale of the thin section, analyses were either treated separately or were used to calculate an average analysis for grains of similar composition. Analyses which showed evidence of late retrograde exchange (*e.g.*, high Fe in garnet adjacent to biotite) were excluded from the averaging calculation. Core and rim analyses were obtained for garnet and plagioclase, and large garnet grains with chemical zoning were also analysed at intermediate locations in order to characterize compositional gradients. In general, 20 to 60 analyses were obtained from each sample. Averaged and individual analyses used in thermobarometry are reported in Appendix A.

All *P-T* calculations were performed by the TWEEQU (Thermobarometry With Estimation of EQUilibrium state) method of Berman (1991). In this thermobarometric approach a computer program (TWQ) and an internally consistent set of thermodynamic

data (Berman 1988, 1990; McMullin et al. 1991) are used to calculate the position in *P-T* space of all stable and metastable equilibria for a given mineral assemblage. Provided that thermodynamic and compositional data are accurate, this approach allows a qualitative assessment of equilibrium state as univariant reactions involving phases that last equilibrated together should intersect at a single point in *P-T* space. Stated another way and given the same condition of thermodynamic and compositional accuracy, equilibria displaced from an intersection are likely to involve a phase or phases that did not last equilibrate with the rest of the mineral assemblage. In practice, it is generally not apparent whether displaced equilibria are due to poor thermodynamic data, poor compositional data, and/or disequilibrium within the assemblage. These equilibria are normally excluded from subsequent runs of TWQ by eliminating the phase(s) common to the displaced equilibria, thereby refining the precision of the *P-T* calculation.

In this study, a mineral assemblage was considered to yield an acceptable *P-T* estimate if the 1σ standard deviation of reaction intersections (calculated with the INTERSX program; Berman 1991) was less than 25°C and 0.5 kbar before application of an exclusion analysis to remove outlying equilibria. This is a more stringent requirement than that proposed by Berman (1991) but is reasonable here given that tight reaction intersections were obtained for most samples. Three samples do not satisfy this equilibrium assumption but their *P-T* results are considered acceptable for reasons discussed below. All calculations were performed using the solution models of Berman (1991) for garnet, Fuhrman and Lindsay (1988) for plagioclase, McMullin et al. (1991) for

biotite, Newton (1983) for pyroxene, and Mader (written communication 1993; modified from Mader and Berman 1992) for amphibole. Unless stated otherwise, all other minerals were treated as pure phases.

Table 4.3 gives the complete mineral assemblage for samples used in thermobarometry (with phases used in the thermobarometric calculation indicated). Equilibria *P-T* plots generated by TWQ are presented in Figures 4.9 to 4.11, and *P-T* are summarized in Fig. 4.12 and with respect to sample location in Fig. 4.13. Either three or four linearly independent equilibria were among the complete set of reactions calculated for each sample. However, *P-T* estimates based on three independent equilibria for five samples were calculated with water ($aH_2O = 1$) in the equilibrium assemblage (Fig. 4.10). Inclusion of water adds a greater degree of uncertainty to *P-T* estimates than for those based solely on solid species equilibria because fluid composition is unknown and aH_2O must be assumed (*e.g.*, Essene 1989). However, in each case, hydrous reactions were in close agreement with those involving only solid species, indicating that assigning $aH_2O \sim 1$ is reasonable for these rocks. This assumption is strengthened by TWQ calculations for two samples (90-129*b*, 90-155; Fig. 4.10) for which hydrous equilibria with unit water activity intersect at the same *P-T* point as anhydrous equilibria derived from three independent reactions (*i.e.*, a total of four independent reactions).

Approach to Textural and Compositional Variations

It is widely accepted that a number of textural and chemical criteria for equilibrium (*e.g.*, mutual grain contacts, lack of reaction textures, assemblage compatibility with the

Table 4.3. Mineral Assemblages of Thermobarometry Samples

Sample	Qtz	Kfs	Pl	Bt	Grt	Ky	Sil	Crn	St	Ms	Hbl	Cpx	Opx	Rt	Ilm	Ttn	Hc	Other
Paragneiss, Granitic Gneiss																		
89-03	●	✓	●	●	●	●				●							✓	Mt, Zrn
89-35	●	●	●	●	●	●								☑				Mnz,Py,Zrn,Ap,Gr
90-42c		✓	●	●	●	●		●	✓	☑				●	●		●	Zrn
D47a	●	✓	◔	●	●	✓	●							●	●			Zrn
89-67c	●	●	●	●	●		●			●					✓			Zrn, Mnz
89-103a	●	●	●	●	●						●	✓	✓					Mt, Ap
89-104d		✓	●	●	●	✓	●	●						●	●		☑	Mt, Ap
89-108a	●	●	●	●	●	●	✓			x				●	◔			Zrn, Py, Gr
89-115b	●	●	●	●	●	●				●				●	●			Zrn
89-116c	●	●	◔	●	●						●				✓			Zrn, Mt, Ap
89-129b	●	●	●	●	●	✓	◔			●				●	●			Zrn
90-155	●	●	●	●	●	✓	●		✓	●				☑	✓			Zrn
90-185a	●		●	●							●				●	●		Zrn,Ep,Mt,Ap,Aln
Metabasite																		
89-125			●	●	●						●	●	✓		✓			Ap
90-200f			●		●						●	●		☑	✓	✓		Zo
90-208b	●		●	●	●						●				✓			Ap
91-250			●	●	●						●	●	✓		✓		☑	Ap
Granulite-facies Gneiss																		
88-3a	●		●	✓	●						●	✓	◔		✓			Ap
89-73a			●		●						●		◔	◔	◔		☑	Ap, Ged
89-88a	●		●	✓	●						✓	●	◔	✓	✓			Ap
89-88b	●	✓	●	✓	●						✓	✓	◔		◔	◔		Ap,Zrn,Mt,Py,Ccp
89-103a	●	✓	●	✓	●						✓	●	◔					Mt, Ap

Key: ✓ = present in mineral assemblage; ● = present in mineral assemblage and used in TWQ; ☑ = included phase; x = retrograde phase

phase rule, chemical homogeneity of a given phase on the grain and thin section scale; *e.g.*, Vernon 1977) should be met by rocks used in geothermobarometry. Unfortunately, metamorphic mineral assemblages in high-grade gneiss terranes regularly exhibit ambiguous textures, overgrowth relationships, and preserve chemical zoning in phases important for thermobarometry such as garnet and plagioclase. Some of these characteristics are due to partial re-equilibration upon cooling, while others result from a lack of complete equilibration of prograde phases at peak metamorphic conditions. On the other hand, equilibrium is likely to be attained in high-grade mineral assemblages due to the effectiveness of volume and grain boundary diffusion at elevated temperatures.

Rocks in the study area commonly exhibit textural and chemical evidence of disequilibrium. The application of thermobarometry to these rocks demands that criteria used to determine 'equilibrium' assemblages and compositions are clearly stated. In the present study, the following approach has been applied:

1) where possible, *P-T* conditions were calculated using either core-inclusion suite compositions, or rim and/or 'typical' compositions (*i.e.*, a composition or narrow compositional range that was regularly obtained during multiple analyses of a solid solution phase).

2) mineral compositions in a single microdomain were used in the *P-T* calculation when compositions varied between domains (*e.g.*, Jamieson 1988).

3) where 1) and 2) failed to yield a TWQ intersection suggesting equilibrium, the most 'evolved' phase compositions (*e.g.*, garnet with highest Fe/Mg; plagioclase with lowest

An for normally zoned grains) were selected for the calculation. These compositions were not necessarily from the same microdomain.

4) where combinations of 1) through 3) failed to give a reasonable equilibria intersection, a 'trial-and-error' matching of compositions was attempted.

These criteria necessarily rely heavily on compositional data because mineral compositions vary on the thin section-scale in a number of samples, and textural evidence of equilibrium compositions is lacking. However, textural evidence was used in most cases to determine which phases should be included in the *P-T* calculation. For nearly all samples, reaction intersections suggesting equilibrium were obtained by applying one or both of the first two criteria. As will be seen, the consistency of *P-T* results amongst samples from the same tectonic domain suggests that these criteria effectively discriminate between equilibrium and disequilibrium assemblages.

Garnet Zoning in Pelitic Gneiss

In the Britt domain, embayed garnet porphyroblasts in pelitic gneiss samples analysed for thermobarometry exhibit an increase in X_{Fe} (almandine) and a decrease in X_{Mg} (pyrope) from core to rim, or are unzoned in these components. The porphyroblasts generally show no appreciable zoning in X_{Mn} (spessartine) and X_{Ca} (grossular), but many samples contain at least one analysed garnet with a significantly higher grossular content in the core than in the rim. Compositional maps for two garnets with unusually strong zoning in X_{Fe} and X_{Ca} are considered here in order to investigate possible causes of zonation.

These garnet porphyroblasts are from two highly-strained, migmatitic pelitic gneiss samples from the kyanite zone of the Shawanaga shear zone. Complete mineral assemblages for these samples (89-35, 89-115*b*) are given in Table 4.3. Both rocks also contain unzoned garnet of similar morphology and size to the strongly zoned grains. The unzoned garnets have a similar composition to the rims of the zoned grains.

The garnet porphyroblast mapped in sample 89-35 is a xenoblastic grain with resorbed edges and minor embayments (Fig. 4.7). X_{Ca} decreases by up to 10 mol % from core to rim and is mainly compensated by an increase in X_{Fe}. X_{Mg} increases by 2-3 mol % from the core toward rim segments in contact with plagioclase and quartz but decreases by an equal amount toward rim segments touching biotite. This variable zoning trend is also reflected in the Mg-number (Mg/(Mg+Fe)) which decreases in the direction of abutting biotite grains but remains relatively constant throughout the rest of the grain. Zoning of grossular and almandine components is markedly concentric in this porphyroblast except where almandine isopleths are 'truncated' at grain boundaries adjacent to biotite.

Sample 89-115*b* contains a larger and more strongly embayed garnet porphyroblast with compositional trends similar to those described above (Fig. 4.8). Grossular content varies by up to 14 mol % and almandine content by up to 17 mol % from core to rim, with smaller but substantial variations in pyrope (9 mol %) and Mg-number (11). Zoning of X_{Ca} and X_{Fe} is complementary and regular whereas zoning profiles for X_{Mg} and Mg-number are irregular due to weaker compositional gradients. Variations in X_{Mg} and Mg-number near matrix biotite and plagioclase are similar to those

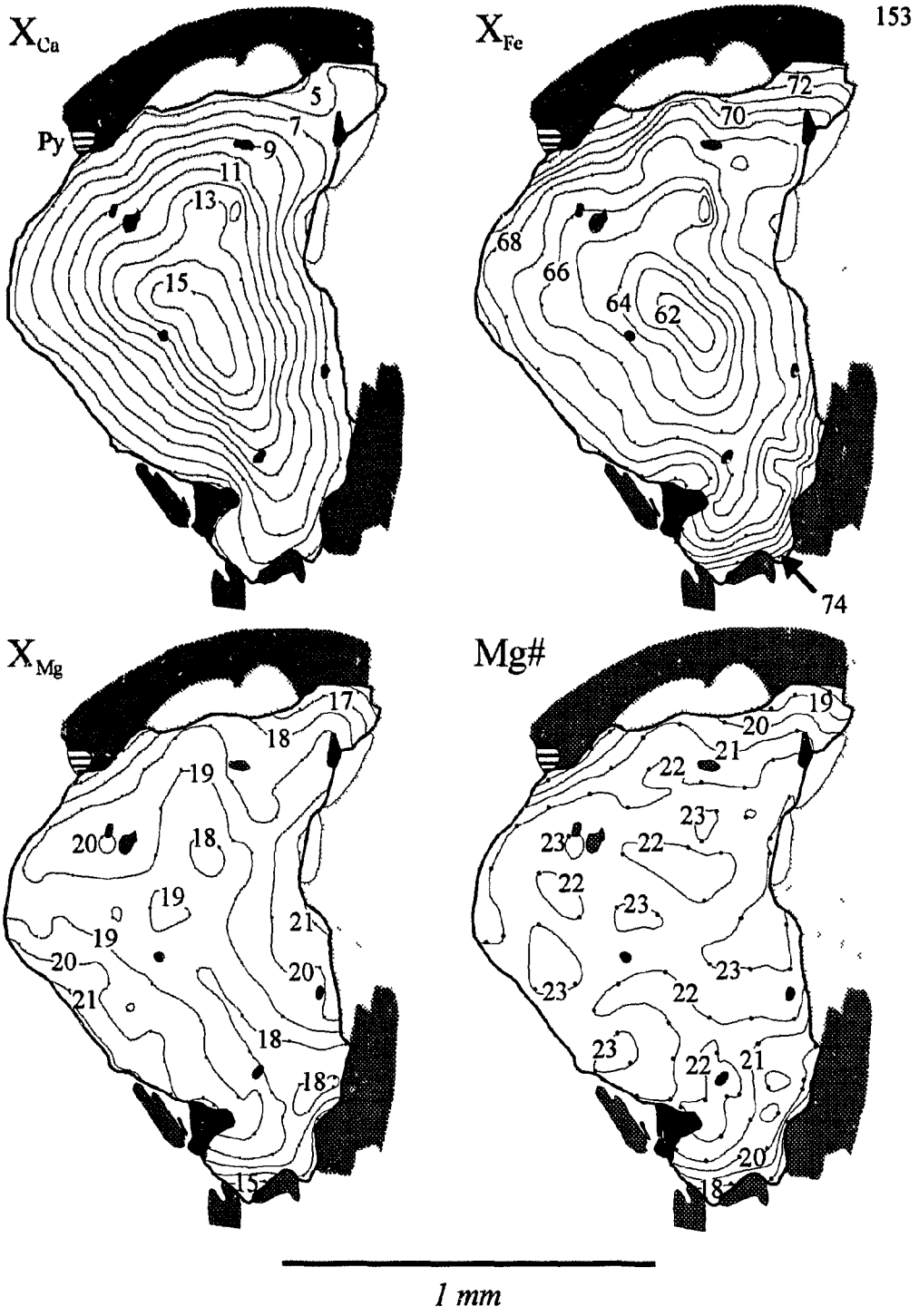

Fig. 4.7. Contoured compositional maps for garnet porphyroblast in pelitic gneiss sample 89-35. Dots represent location of probe analyses. X_{Ca} = Ca/(Fe + Mg + Ca + Mn), etc., Mg# = Mg/(Mg + Fe). Shading as in Fig 4.8

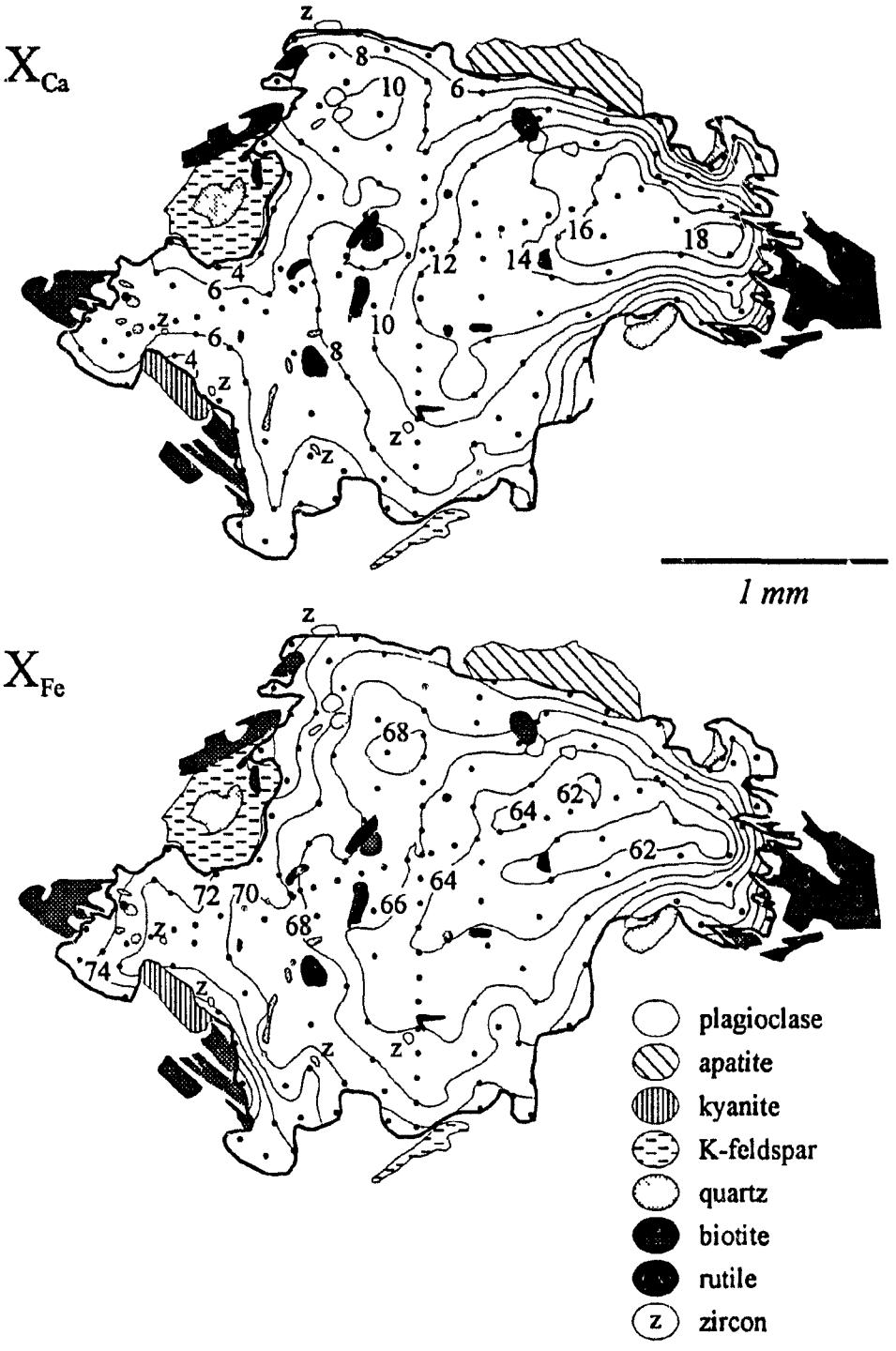

Fig. 4.8. Contoured compositional maps for garnet porphyroblast in pelitic gneiss sample 89-115*b*. Dots represent location of microprobe analyses X_{Ca} = Ca/ (Fe + Mg + Ca + Mn), X_{Fe} = Fe/(Fe + Mg + Ca + Mn).

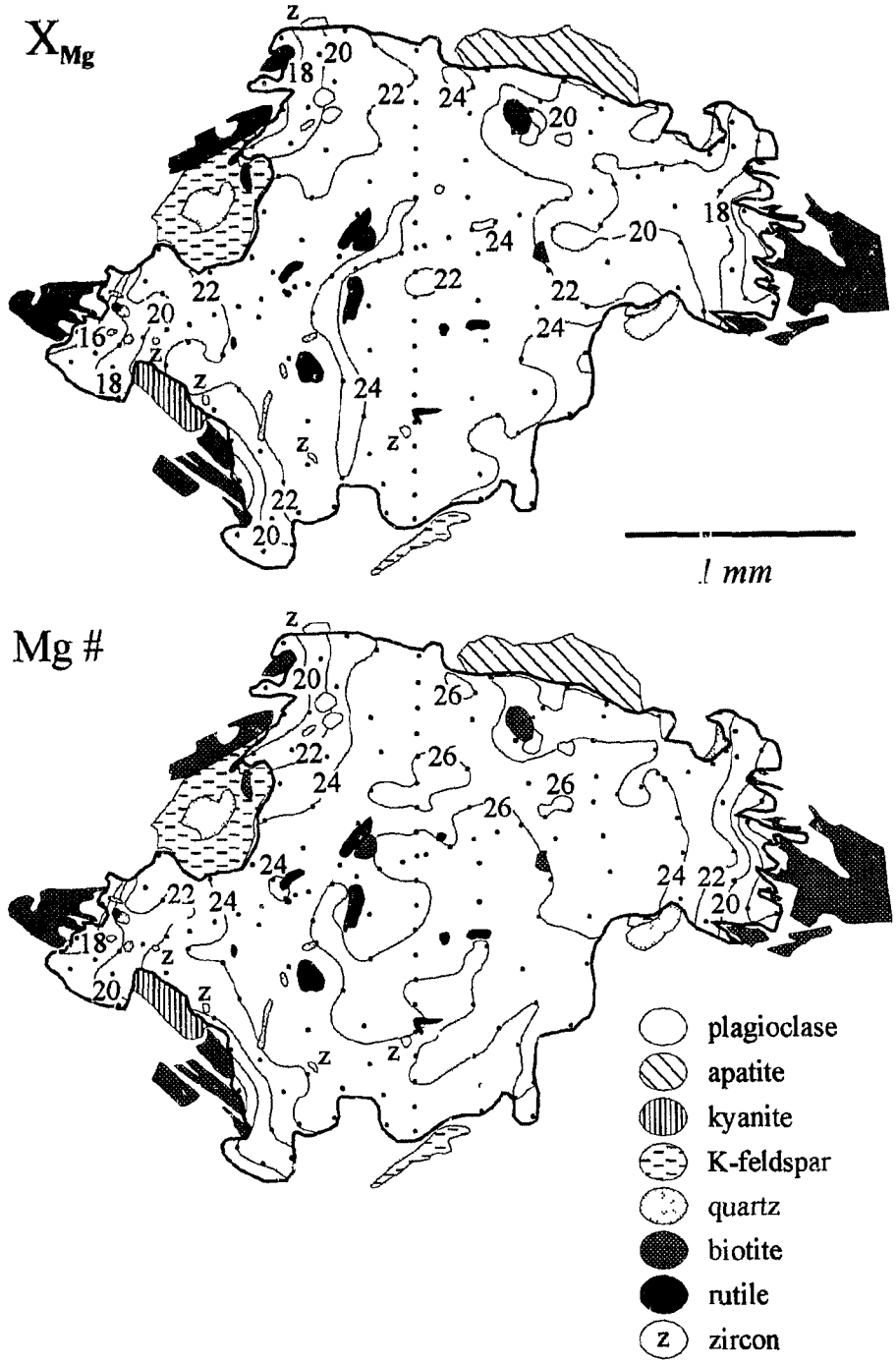

Fig. 4.8. (*continued*) X_{Mg} = Mg/(Mg + Fe + Ca + Mn) and Mg# = Mg/(Mg + Fe).

described above. However, a narrow, irregular rim of plagioclase commonly occurs between biotite and garnet in this sample. 'Core' X_{Ca} and X_{Fe} contours are markedly offset from the geometric grain centre, but despite this offset, X_{Ca} displays a remarkable uniformity along the rim (7-4 mol %) except where embayments cut a steep gradient (Fig. 4.8). No major element zoning in garnet near biotite and plagioclase inclusions was detected in either garnet.

Several features are apparent from zoning patterns observed in both grains:

1) Fe and Mg zoning profiles near garnet-biotite contacts indicate late Fe-Mg exchange between these phases (*e.g.*, Tracy et al. 1976; Tracy 1982; Selverstone and Chamberlain 1990; Pattison and Bégin 1994). Garnet rims are enriched in Fe and depleted in Mg relative to where garnet is in contact with a non-ferromagnesian phase (*e.g.*, plagioclase). The exchange reaction has steepened gradients of X_{Fe}, X_{Mg}, and Mg-number in garnet and is responsible for the apparent truncation of these gradients at garnet rims.

2) away from areas of obvious Fe-Mg exchange, grossular zoning is compensated by systematic changes in both almandine and pyrope content. For example, an 8-9 mol % decrease in X_{Ca} from core to rim in sample 89-35 is offset by a 6-7 mol % increase in X_{Fe} and a 1-3 mol % increase in X_{Mg}. A similar pattern is observed in the garnet from sample 89-115*b*. These patterns suggest linkage of Ca, Fe, and Mg distribution and thus a common zoning mechanism for these elements. In areas of late Fe-Mg exchange, only the sum (Fe+Mg) varies systematically to compensate for grossular variations (as required by stoichiometry, *e.g.*, Chakraborty and Ganguly 1991).

3) reactions involving garnet consumption in sample 89-115*b* continued beyond the time when element zoning patterns were 'locked-in' as embayments cut the compositional gradients. Continuous reactions of the type:

$$\text{Garnet} + \text{K-feldspar} + H_2O = \text{Biotite} + \text{Kyanite} + \text{Quartz}$$

(*e.g.*, Tracy et al 1976), or:

$$\text{Garnet} + \text{Muscovite} = \text{Quartz} + \text{Kyanite} + \text{Biotite},$$

both which consume garnet upon cooling, are suggested by biotite and kyanite rims on garnet in both samples (visible mainly for grains other than those depicted). Operation of this reaction before or during ductile extensional shear is indicated by the presence of deformed kyanite grains along garnet margins.

Although the distribution of Ca, Mg, and Fe in these garnets could be attributed to growth zoning, a number of factors suggest that this is not the case. Homogenization of garnet by volume diffusion normally occurs at temperatures above 650°C (Tracy 1982 and references therein). In the Pointe-au-Baril area, peak Grenvillian temperatures in the parautochthon were >100°C above this temperature (see below), indicating that preservation of growth zoning is unlikely (see, however, Tuccillo et al. 1990). Growth of zoned grains after the metamorphic peak ('retrograde growth zoning;' Cygan and Lasaga 1982) is also considered unlikely as garnet-consuming reactions are indicated by resorbed grains rimmed by biotite, kyanite, and plagioclase in both samples. In addition, Ca growth zoning, which typically mirrors the form of the new garnet, should show no uniformity along resorbed garnet rims unless this zoning was modified by post-growth volume

diffusion.

The above arguments suggest that diffusion zoning (Tracy 1982) rather than growth zoning is responsible for the observed distribution of major elements in the mapped garnets. Given the high temperatures of regional metamorphism indicated by thermobarometry (*e.g.*, Anovitz and Essene 1990; this chapter), it is likely that these garnets grew during prograde metamorphism but were completely homogenized at peak temperatures (~770°C; see below). In order for strong zoning to develop subsequently, post-peak volume diffusion must have redistributed major elements in the homogenized grains. It is suggested here that relict compositions closest to the stable composition during high-temperature homogenization are preserved in areas of highest Ca and lowest Fe but were progressively reset elsewhere in the grains. A continuous net-transfer reaction of the type:

$$\text{Grossular} + \text{Kyanite} + \text{Quartz} = \text{Anorthite} \quad \text{(GASP)}$$

is likely to have controlled Ca redistribution in garnet as plagioclase is the only other Ca-bearing mineral now in the matrix. Although matrix plagioclase is normally zoned in both samples, reversely-zoned plagioclase (An_{32-35}) in the leucosome of sample 89-35 is consistent with the operation of this reaction and furthermore suggests that leucosomes and garnet zoning profiles may have developed synchronously. Depletion of grossular from garnet rims by the above reaction may have established a compositional gradient that drove volume diffusion of Ca in the relict grains (*e.g.*, Martignole and Pouget 1993). Grossular is consumed by reaction GASP with decreasing P, suggesting that the observed Ca zoning developed in response to decompression. This is consistent with the extensional

tectonic setting of the pelitic gneiss samples. Decompression is also indicated for these garnets by compositional isopleth diagrams (*e.g.*, Fig. 7 of Spear et al. 1990) for garnets that have acquired their zoning by volume diffusion. For the mineral assemblages and garnet zoning profiles in the rocks considered here, these diagrams constrain possible *P-T* paths to those involving near-isothermal decompression.

Diffusion-controlled garnet zoning has also been proposed by Petrakakis (1986) for rocks in the Moldanubian Zone of the Bohemian Massif, Austria, and by Martignole and Pouget (1993) for garnet zoning in the Réservoir Cabonga area, Grenville Province, Quebec. Both studies document paleotemperatures in the range 700-800°C, a strong core-to-rim decrease of X_{Ca} in garnet, and *P-T* and structural data indicating exhumation at high metamorphic grade. In contrast to this study, however, these authors suggest that the high Ca garnet cores represent older grains contained within lower Ca overgrowths, with later modification of this zoning by volume diffusion. Tuccillo et al. (1990, 1992) have also suggested that Ca zoning patterns documented in garnets from the Shawanaga shear zone indicate multiple growth events. These garnets contain two or more X_{Ca} maxima in individual porphyroblasts suggesting coalescence of smaller grains (Tuccillo et al. 1990, 1992). However, there are no zoning irregularities in the garnets studied here to indicate a polyphase growth history. It is curious that maximum X_{Ca} values for the garnet in sample 89-115*b* and in porphyroblasts mapped by Tuccillo et al. (1990, 1992) occur adjacent to the grain boundary. Perhaps an alternative mechanism, such as one that considers the influence of intragrain stress gradients on cation diffusivity (*cf.* Mueller 1967), is required to account for these unusual Ca zoning profiles.

P-T Results

Pre-Grenvillian Metamorphism

Four orthopyroxene-bearing samples from structural zone 3 (the 'low-strain area' of Ketchum et al. 1994) and one from structural zone 2 immediately above the Nares Inlet shear zone were used to quantify *P-T* conditions of granulite facies metamorphism at *ca.* 1450-1430 Ma. These rocks lack textural evidence of Grenvillian mineral growth and are not overprinted by Grenvillian fabrics, suggesting that they preserve pre-Grenvillian mineral compositions. However, orthopyroxene is texturally unstable in two samples (89-88*b*, 89-103*a*), most likely due to retrogression following peak metamorphism or to partial Grenvillian re-equilibration. A granulite-facies mafic supracrustal gneiss (89-73*a*) with texturally stable orthopyroxene was employed in both thermobarometry and U-Pb geochronology. This sample shows no isotopic evidence of Grenvillian resetting (Chapter 5), providing further support for the pre-Grenvillian age of these mineral assemblages.

Four *P-T* estimates from three rocks (88-3*a*, 89-73*a*, 89-88*a*) with texturally stable orthopyroxene indicate that pre-Grenvillian granulite facies mineral assemblages equilibrated in the range 625-700°C and 7.2-8.4 kbar (Fig. 4.9). The highest pressure estimate was obtained from sample 89-88*a*, a mafic supracrustal gneiss enclave in the Pointe-au-Baril complex, using core compositions of weakly zoned garnet and plagioclase. Zoning profiles in garnet (core-to-rim increase in Fe/Mg) suggest minor retrograde diffusion, indicating that peak granulite-facies conditions may have been closest to the high-pressure limit of the *P-T* range. This range overlaps the *P-T* conditions of melting in

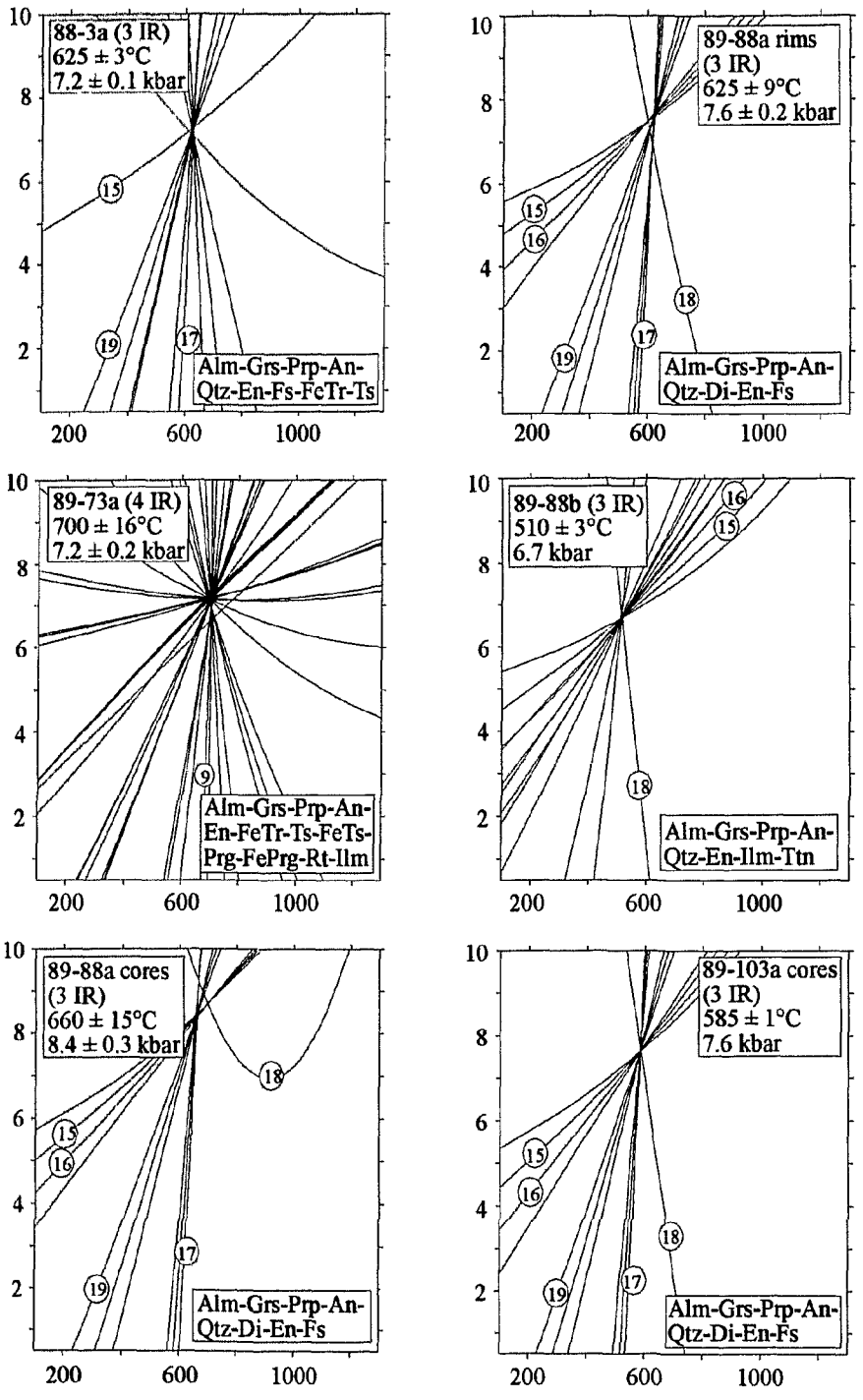

Fig. 4.9. TWQ equilibria plots for granulites in zone 3 of the Britt domain, Pointe-au-Baril area. Mineral abbreviations and numbered reactions given in Tables 4.1 and 4.2, respectively. 3 IR, 4 IR indicates 3 or 4 independent reactions in the set of reactions used to calculate P and T.

hydrous amphibolites (Yoder and Tilley 1962; see Fig. 4.12*a*) which is consistent with the presence of leucosomes in mafic supracrustal gneiss.

Sample 88-3*a* was collected from the recrystallized but undeformed interior of the Nares Inlet metagabbro pluton (Fig. 4.6; Chapter 2). Although this body lies outside of zone 3, granulite facies assemblages and an absence of Grenvillian fabrics at the sample site suggest an analogous setting to zone 3 granulites. A *P-T* estimate of 625°C and 7.2 kbar for this sample lies within the range determined from the other granulites (Fig. 4.12). From this evidence, it is suggested that metamorphic assemblages in the interior of the Nares Inlet metagabbro are pre-Grenvillian.

Thermobarometry was attempted on two granulite-facies samples (89-88*b*, 89-103*a*) with textural evidence of orthopyroxene instability. In both cases, good TWQ intersections (Fig. 4.9) could only be obtained using 'end-member' compositions of zoned minerals (see [3] under *Approach to Textural and Compositional Variations*, above). High-Fe, low-Ca garnet analyses from both samples in conjunction with low-An plagioclase and most Mg-rich orthopyroxene in 89-103*a*, and high-An plagioclase and least Mg-rich orthopyroxene in 89-88*b* gave the best intersections. However, temperatures of 510°C (89-88*b*) and 585°C (89-103*a*) obtained from these rocks are considered too low for orthopyroxene stability. This indicates that the thermobarometric results are incorrect or that orthopyroxene is metastable.

Grenvillian Metamorphism

Parautochthon. Conditions of metamorphic equilibration in the parautochthon

were determined from thermobarometric calculations on thirteen samples. All of the structural zones defined in the parautochthon (Chapter 3) are represented in this sample suite.

Supracrustal and granitic rocks yield a wide range of *P-T* results (Fig. 4.10); many fall in the interval 10.3-5.1 kbar and 680-555°C (Fig. 4.12). Highest pressures and temperatures in this range (10.3-8.6 kbar, 680-645°C) were obtained from core and inclusion compositions in two kyanite-bearing pelites (89-35, 89-115*b*) and a Pointe-au-Baril complex granitic gneiss (89-116*c*) from the Shawanaga shear zone. Compositional data from strongly zoned garnet porphyroblasts and their inclusions in 89-35 and 89-115*b* (Figs. 4.7, 4.8) were used in the *P-T* calculations.

Most *P-T* estimates for pelitic and granitic gneiss fall in the range 6.0-5.1 kbar and 615-555°C (Fig. 4.12). Sample 90-155, a pelitic gneiss collected north of the Nares Inlet shear zone, plots slightly outside of this range (4.3 kbar, 560°C). In all cases, typical and/or rim compositions of zoned phases were used in these calculations. The estimates span the Ky-Sil transition, consistent with the presence of both polymorphs in the parautochthon. Individual *P-T* estimates for all samples plot within the appropriate aluminosilicate stability field or coincide with the Ky-Sil boundary Rocks from the kyanite zone of the Shawanaga shear zone plot, with one exception, at higher pressures than those from the sillimanite zone. An average *P-T* of 5.7 kbar, 580°C is obtained for the kyanite zone whereas this average is 5.2 kbar, 588°C for the sillimanite zone. Despite these differences, the results plot with remarkable consistency over a narrow interval suggesting that the assemblages last equilibrated at the same time.

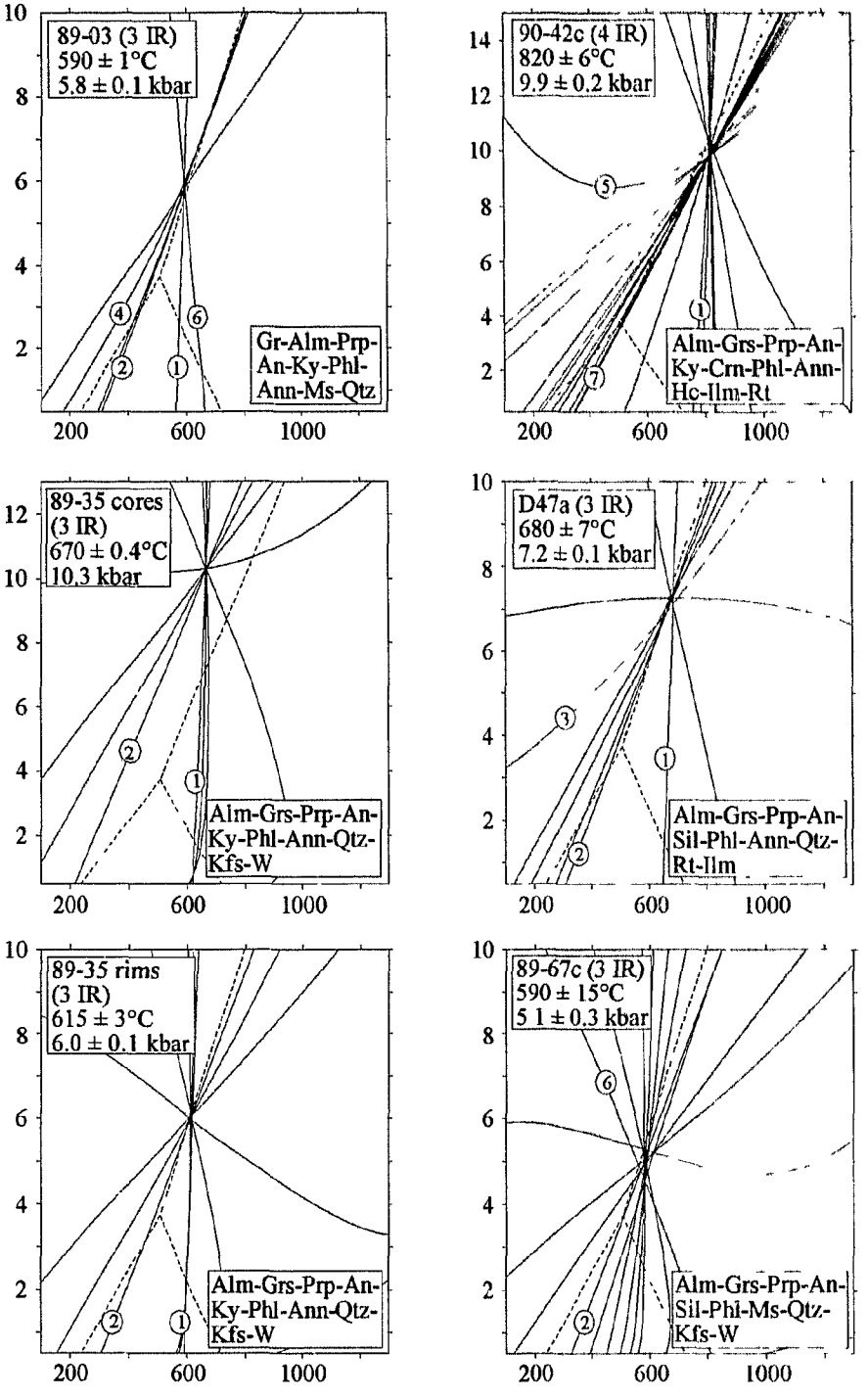

Fig. 4.10. TWQ equilibria plots for paragneiss and granitic orthogneiss in the Britt and Shawanaga domains, Pointe-au-Baril area. Mineral abbreviations and numbered reactions given in Tables 4.1 and 4.2, respectively. 3 IR, 4 IR indicates 3 or 4 independent reactions in the set of reactions used to calculate P and T.

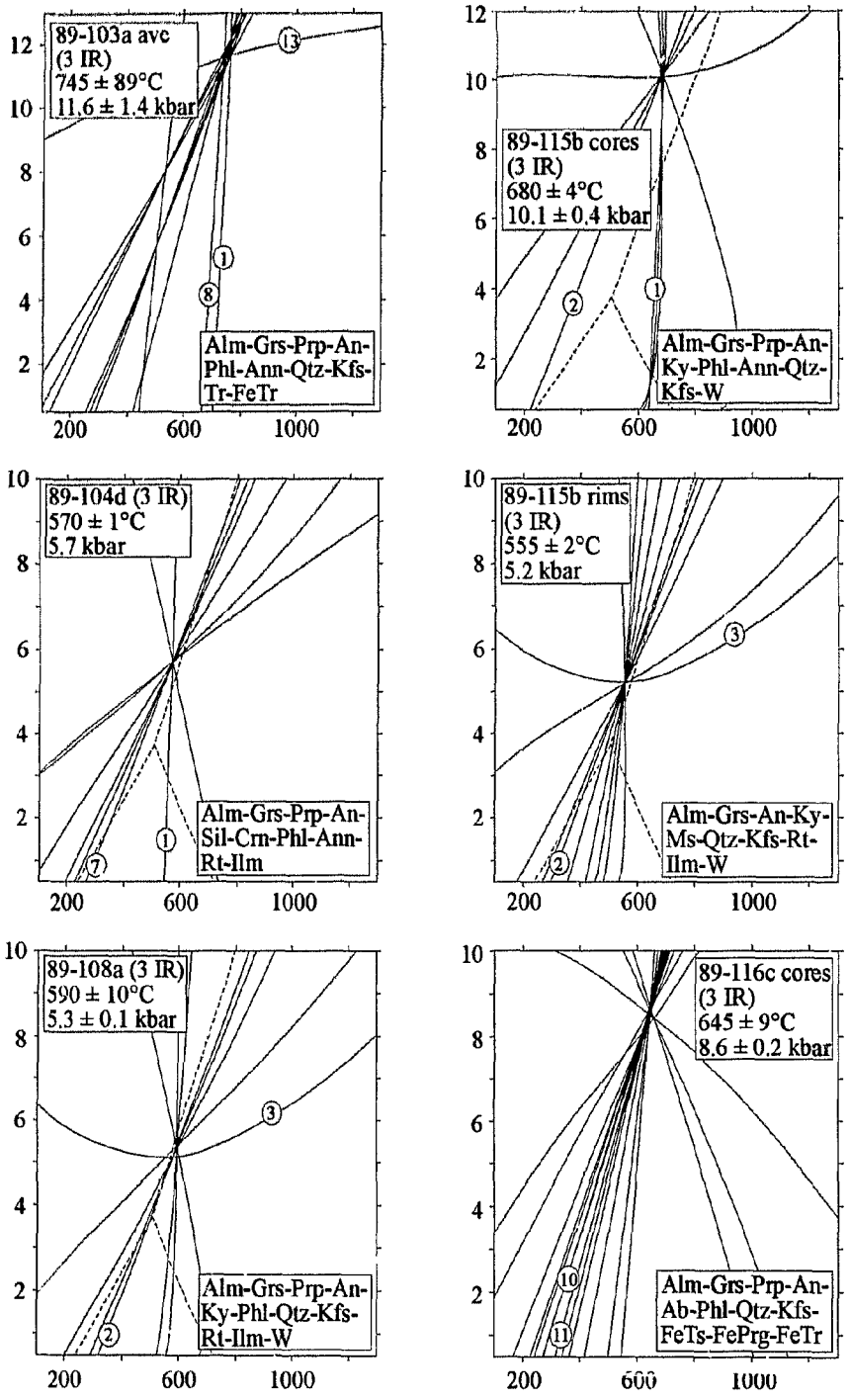

Fig. 4.10 (*continued*).

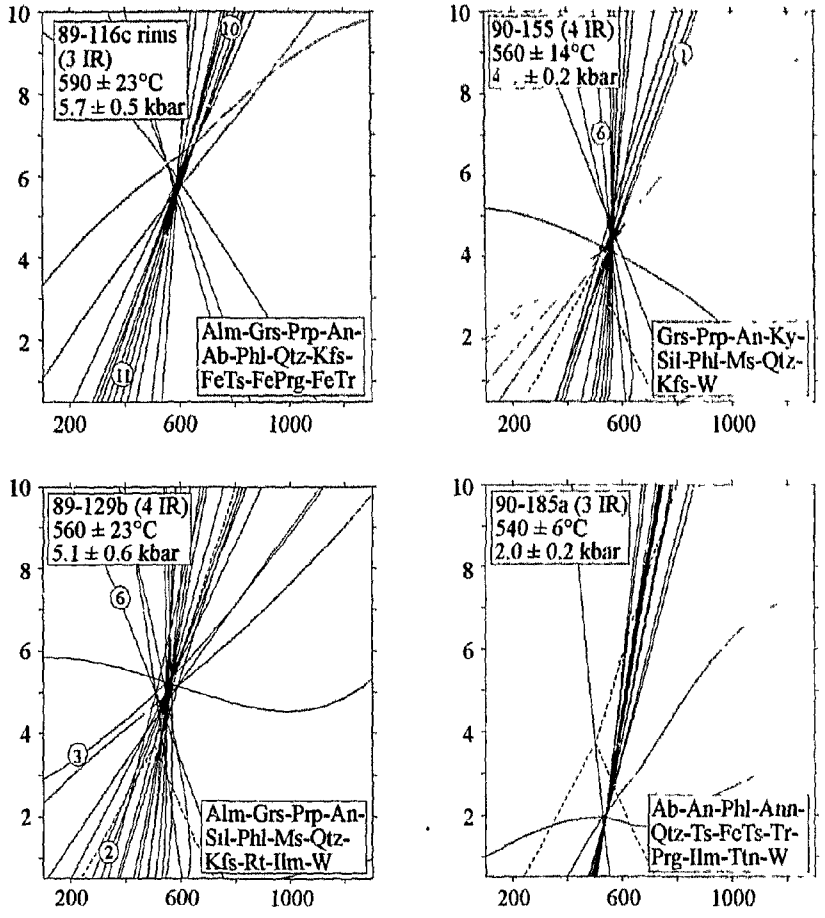

Fig. 4.10 (*continued*)

Three samples of metabasic and calcareous rock record higher pressures and temperatures than pelitic and granitic gneisses (Fig. 4.11), consistent with their lower degree of structural reworking and hence greater resistance to fluid influx and retrograde reaction (*e.g.*, Brodie and Rutter 1985; Grant 1989; Indares 1993). Texturally re-equilibrated, plagioclase-amphibole-bearing meta-eclogite from the Frederic Inlet metagabbro (90-200*f*) and a boudined metadiabase dyke from the northern margin of zone 3 (91-250) yield similar results (10.8 kbar, 755°C and 10.6 kbar, 770°C, respectively). The metadiabase (depicted in Fig. 2.8*b*) is a member of the youngest dyke suite in the parautochthon and has been tentatively correlated with the *ca.* 1238 Ma Sudbury swarm (A. Davidson, written communication 1993; Culshaw et al. 1994; Chapter 2). Assuming that this correlation is valid, *P-T* conditions recorded by the metadiabase can only be attributed to Grenvillian metamorphism.

The highest Grenvillian pressure estimate was obtained from calc-silicate gneiss (89-103*a*) with relict, pre-Grenvillian orthopyroxene. A *P-T* estimate of 585°C and 7.6 kbar reported above for this sample was suggested to be erroneous or to indicate orthopyroxene metastability (see *Pre-Grenvillian Metamorphism*). However, a second TWQ calculation employing average mineral compositions in a pyroxene-absent sub-assemblage yielded an estimate of 11.6 kbar and 745°C with a large 1σ error (±1.4 kbar, ±89°C). Despite the large error, this result is within 1 kbar and 25°C of metabasite *P-T* estimates, suggesting that (*i*) the *P-T* estimate for calc-silicate gneiss is reasonable, (*ii*) the high pressure recorded by this rock reflects Grenvillian rather than pre-Grenvillian

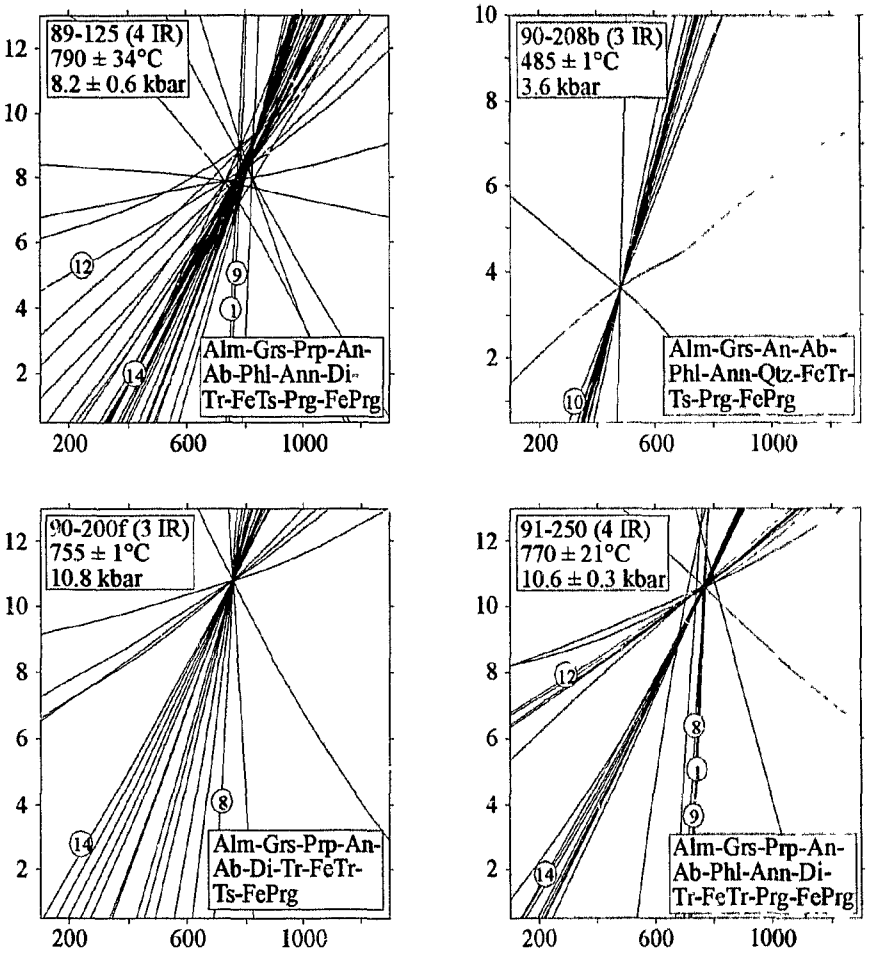

Fig. 4.11. TWQ equilibria plots for metabasites in the Britt and Shawanaga domains, Pointe-au-Baril area. Mineral abbreviations and numbered reactions given in Tables 4.1 and 4.2, respectively. 3 IR, 4 IR indicates 3 or 4 independent reactions in the set of reactions used to calculate *P* and *T*.

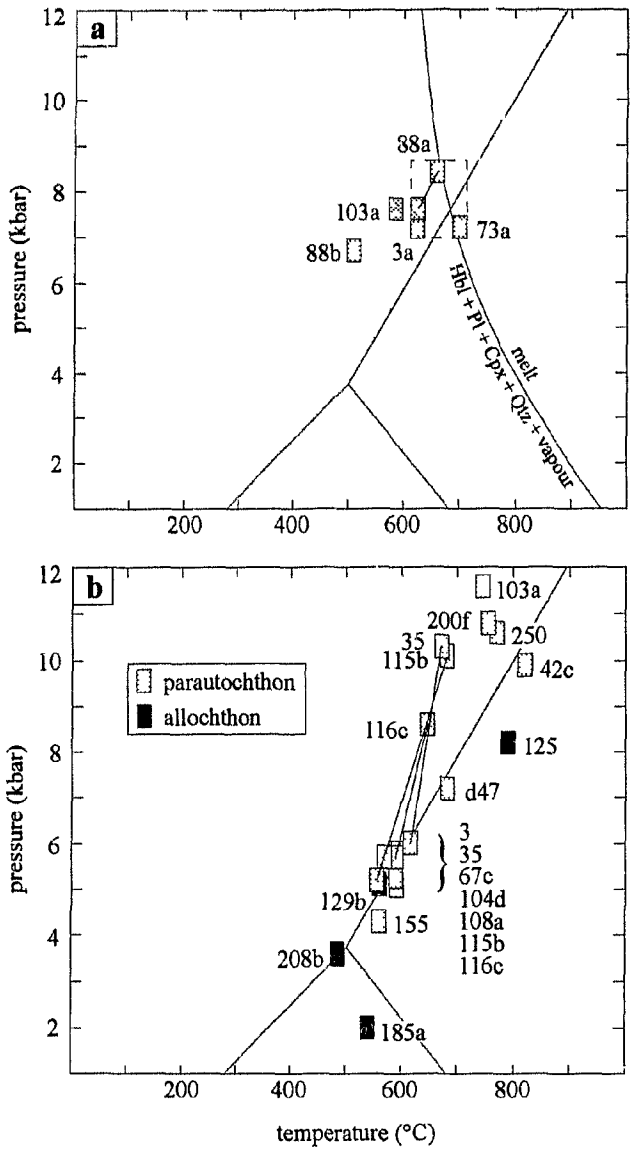

Fig. 4.12. *P-T* data for allochthonous and parautochthonous rocks (see Fig. 4 6 for sample locations) Error boxes are shown at ±12 5°C and ±0 25 kbar for clarity Actual errors are likely ±50°C and ±1 kbar (*e.g.*, Essene 1989) Sample numbers are abbreviated. Aluminosilicate stability field shown in both figures. **a)** Pre-Grenvillian metamorphism (dashed box shows *P-T* estimates from unretrogressed granulites) Minimum melt reaction after Yoder and Tilley (1962). **b)** Grenvillian metamorphism. Tie lines join *P-T* estimates from core-inclusion and rim-'typical' compositions in the same sample.

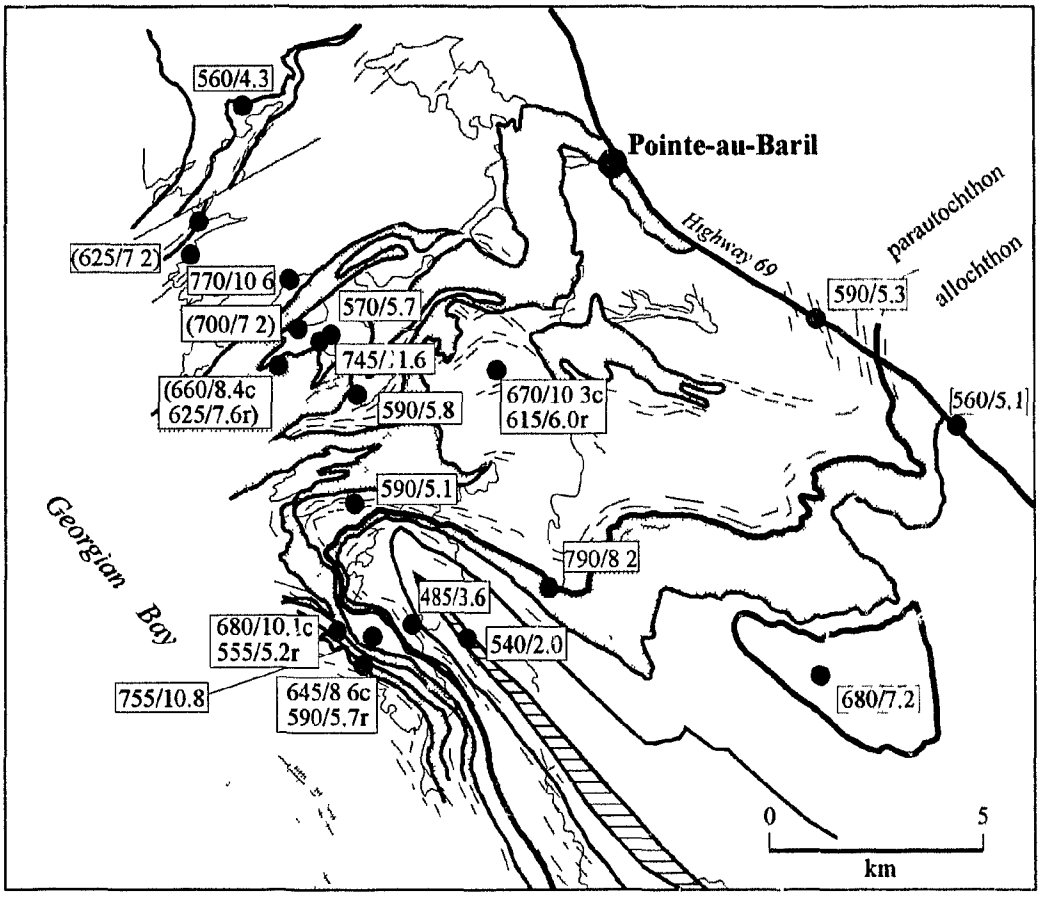

Fig. 4.13. *P-T* results for the study area Temperature estimate (°C) is followed by pressure estimate (kbar). Estimates shown in brackets are for pre-Grenvillian granulite facies assemblages Letter indicates that *P-T* estimate was obtained from core and inclusion suite compositions (c) or rim and 'typical' compositions (r). No *P-T* estimate is presented for sample 90-42*c* (Nares Inlet) as the result is considered erroneous. Shaded units are *ca.* 1450 Ma granitoid plutons

metamorphism, and (*iii*) metabasites and calcareous gneiss record an earlier point on the *P-T* path for the Britt domain and may have last equilibrated at approximately the same time.

P-T estimates for two pelite samples fall outside the ranges reported thus far. Sample D47*a* was collected from the tectonic window of Nadeau Island gneiss association within the Ojibway gneiss association (Fig. 4.6). An estimate of 7.2 kbar and 680°C for rim/typical compositions falls in the sillimanite stability field, consistent with sillimanite overgrowths on embayed kyanite in this sample, but lies distinctly outside the *P-T* field for parautochthonous rocks (Fig. 4.12). Sample 90-42*c* was collected from a moderately strained outcrop of migmatitic aluminous paragneiss in the Nares Inlet shear zone. Relict staurolite is present in a quartz-free assemblage that includes garnet, corundum, kyanite, and spinel (hercynite-gahnite solid solution). A *P-T* estimate of 9.9 kbar and 820°C was obtained for this sample using rim compositions. However, GeO-Calc modelling (Brown et al. 1988) of the staurolite breakdown reaction:

$$\text{Staurolite} = \text{Kyanite} + \text{Corundum} + \text{Almandine} + H_2O$$

indicates staurolite decomposition in this rock at a temperature slightly above 700°C which is inconsistent with the presence of staurolite in this sample. However, the assemblage used in the *P-T* calculation lies ~1.5 cm from an anhydrous, garnet-bearing leucosome, suggesting that excess heat from this coarse-grained vein (>10 cm wide) may have driven locallized, rapid chemical re-equilibration before staurolite decomposition reactions had gone to completion. Despite this possibility, the *P-T* estimate for this sample is not considered further.

Allochthon. Quantitative *P-T* conditions were calculated for four samples from the Shawanaga domain. The highest *P-T* estimate (8.2 kbar, 790°C; Fig. 4.11) was obtained from recrystallized coronitic metagabbro in the Shawanaga pluton (sample 89-125). This result is considered to be in error for reasons outlined below (see *P-T Paths*).

An enclave of pelitic gneiss in the Ojibway gneiss association (90-129*b*) gave an estimate of 5.1 kbar and 560°C (Fig. 4.10), similar to those obtained from several parautochthonous rocks (Fig. 4.12). This result falls on the Ky-Sil univariant curve, consistent with the presence of embayed kyanite and fresh sillimanite in the gneiss. A 1σ error of ±0.6 kbar is considered slightly high but stems largely from a calculation involving four independent equilibria. Elimination of ilmenite (in low modal abundance) from the TWQ assemblage results in a 0.2 kbar decrease in pressure with no temperature change; the statistical error in pressure is reduced to 0.4 kbar. The *P-T* estimate for the ilmenite-bearing assemblage is preferred because this calculation considers more components.

Final equilibration near the aluminosilicate triple point (Figs. 4.11, 4.12) is indicated for an amphibolite sample (90-208*b*) from the Ojibway gneiss association. Garnet occurs as rare, embayed relicts in a plagioclase-rich matrix, suggesting that garnet-consuming decompression reactions largely went to completion. Garnet rim compositions nevertheless appear to be in equilibrium with matrix minerals as a tight intersection at 3.6 kbar and 485°C was obtained for this sample.

The only *P-T* constraint for the Sand Bay gneiss association was obtained from the Dillon schist (Figs. 2.1, 2.2; sample 89-185*a*). A estimate of 2.0 kbar and 540°C for this biotite-amphibole quartzofeldspathic gneiss is based mainly on biotite-amphibole thermometry and amphibole-plagioclase-quartz±biotite barometry (Fig. 4.10). These reactions are poorly calibrated (*e.g.*, Mader and Berman 1992) which may account for the unusually low and probably inaccurate pressure estimate. Until further compositional data are obtained from mineral assemblages better suited to thermobarometry, *P-T* conditions for the Sand Bay gneiss association cannot be quantitatively assessed.

P-T Paths

A *P-T* path consistent with thermobarometric data and the tectonic setting of parautochthonous rocks in the southern Britt domain is shown in Figure 4.14. This path shows decompression from ~11.0 to 5.5 kbar accompanied by cooling from 755 to 585°C. However, two path segments are indicated by the data (Fig. 4.12). A short, post-metamorphic peak segment is not tightly constrained as *P-T* estimates for metabasite and calcareous paragneiss span a 1 kbar interval. The high pressure end of this segment is placed at the average *P* and *T* for these rocks. However, a longer, steep *P-T* path segment for the southern Britt domain is tightly constrained by the consistency of core (high pressure) and rim (lower pressure) thermobarometric estimates, and by individual *P-T* paths determined for samples 89-35, 89-115*b*, and 89-116*c* (Fig. 4.12*b*). Construction of a path that links all these data is justified as the samples were collected from structural zones that comprise a single tectonic unit.

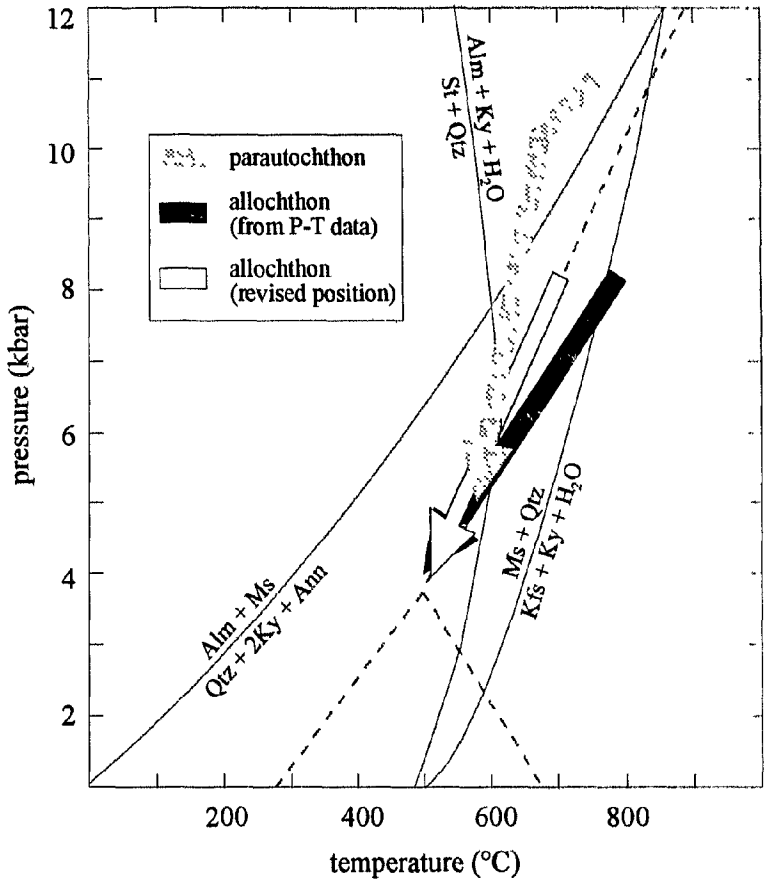

Fig. 4.14. *P-T* paths for the Pointe-au-Baril area. Unfilled path is the revised position of the allochthon *P-T* path based on petrographic data (see text). All reactions modeled using GeO-Calc (Brown et al. 1988). Muscovite breakdown in the presence of quartz shown for $aH_2C = 1$ (reaction shifts to lower *T* with decreased activity). Staurolite breakdown in the presence of quartz modeled for sample 89-155 ($aH_2O = 1$). The general absence of muscovite in parautochthonous pelites is attributed to a reaction of the type garnet + muscovite = quartz + kyanite + biotite, modeled for sample 89-03 Aluminosilicate stability fields shown by dashed lines.

There are fewer data from allochthonous rocks to constrain a *P-T* path for the Shawanaga domain, but results from three samples suggest decompression accompanied by steady cooling (Fig. 4.12*b*). This path (Fig. 4.14), which was constructed ignoring thermobarometric data from the Sand Bay gneiss association (sample 90-185a), has a shallower slope than for parautochthonous rocks and crosses from the sillimanite field to the kyanite field. However, this is inconsistent with mineral textures in sample 90-129*b* which clearly indicate sillimanite growth after kyanite. The slope of the allochthon path is largely controlled by the *P-T* estimate for sample 89-125, a coronitic metagabbro in the Shawanaga pluton. If this rock and sample 89-129*b* equilibrated on the same *P-T* path (as suggested by their structural position), then the aluminosilicate textures suggest that the temperature estimate for coronitic metagabbro is too high and that the allochthon *P-T* path has a steeper slope. A reduction in the metagabbro temperature estimate to ~700°C yields a revised path (Fig. 4.14, unshaded) consistent with the petrographic data and places the new *P-T* estimate well within a range reported for coronitic metagabbro in the Central Gneiss Belt (Grant 1987). The revised path is also consistent with thermobarometric data reported for the northern Shawanaga domain by other workers (*e.g.*, <10.2 kbar, 700-710°C for coronitic metagabbro, Anovitz and Essene 1990; ~7-9 kbar at 700°C for garnet metagabbro and pelite, Tuccillo et al. 1992).

4.5 DISCUSSION

The Kyanite-Sillimanite Transition in the Shawanaga Shear Zone

An inverted metamorphic isograd is indicated within the Shawanaga shear zone by

the stability of Ky+Kfs at low structural levels and Sil+Kfs at high structural levels. Inverted metamorphic sequences have been documented in a number of thrust belts worldwide but have not previously been described in extensional shear zones. However, normal metamorphic sequences are reported from extensional shear settings. An example relevant to the present study is the work of Buick and Holland (1989) who investigated the *P-T-t* evolution of migmatitic, kyanite±sillimanite-bearing pelites within a metamorphic core complex on the island of Naxos, Greece. Amphibolite-facies mineral assemblages in these rocks are stable in the extensional shear fabrics, and kyanite porphyroblasts are overgrown by sillimanite, similar to relationships observed in the Pointe-au-Baril area. However, kyanite-bearing rocks *overlie* kyanite±sillimanite-bearing rocks, in direct contrast to the pattern observed in the Shawanaga shear zone. A similar lower- over higher-grade transition is commonly noted in Cordilleran metamorphic core complexes in western North America where a narrowing and upward migration of the kinematically active detachment zone during extensional unroofing is suggested from structural and metamorphic evidence (*e.g.*, Coney 1980; Lister and Davis 1989). The upper levels of these detachment zones are progressively overprinted by lower temperature structures as the core complex is exhumed, providing a continuous record of the exhumation history. Given that normal metamorphic sequence are documented in these and other extensional shear settings, it is evident that metamorphic assemblages in the Shawanaga shear zone record an unusual paragenetic sequence .

Insights into the observed distribution of aluminosilicate polymorphs in the Shawanaga shear zone can be gained by considering structural, petrographic, and

thermobarometric data. In Chapter 3 it was noted that extensional shear fabrics at lower structural levels are pervasively folded on the metre- to kilometre-scale whereas at higher levels, open, map-scale folds predominate. It was also noted that tectonic fabrics and sinistral kinematic indicators pre-dating extensional shear are preserved within a structurally distinct region near the base of the shear zone (zone 4*a*, Fig. 3.2) and locally throughout zone 4 in low-strain windows. Comparison of Figures 3.2 and 4.5 reveals that strongly folded segments of the shear zone mainly lie beneath the kyanite-sillimanite isograd, as does all of zone 4*a* and a majority of lower-strain windows preserving older tectonic fabrics (Fig. 2.2). Given that these structural variations must be linked to differences in tectonic history, it is reasonable to suggest that variations in metamorphic assemblage may also be linked to a contrasting tectonic history. However, with the exception of pre-extensional shear structures, all structural and metamorphic characteristics of the Shawanaga shear zone must be accounted for within a framework of southeast-directed, syn-metamorphic extensional shear.

The proposed linkage of metamorphic assemblage with deformation history is supported by a re-evaluation of finite stretching lineation data from the Shawanaga shear zone. Markedly different stereonet patterns for zone 4 and zone 5 lineations (Chapter 3) were interpreted to reflect differences in the structural history of allochthonous and parautochthonous rocks. To test the hypothesis that structural variations may also exist within the parautochthon across the isograd, lineation data from zone 4 of the Shawanaga shear zone were replotted according to position with respect to this isograd (Fig. 4.15). It is apparent from Figure 4.15 that finite stretching lineations above the isograd mainly lie

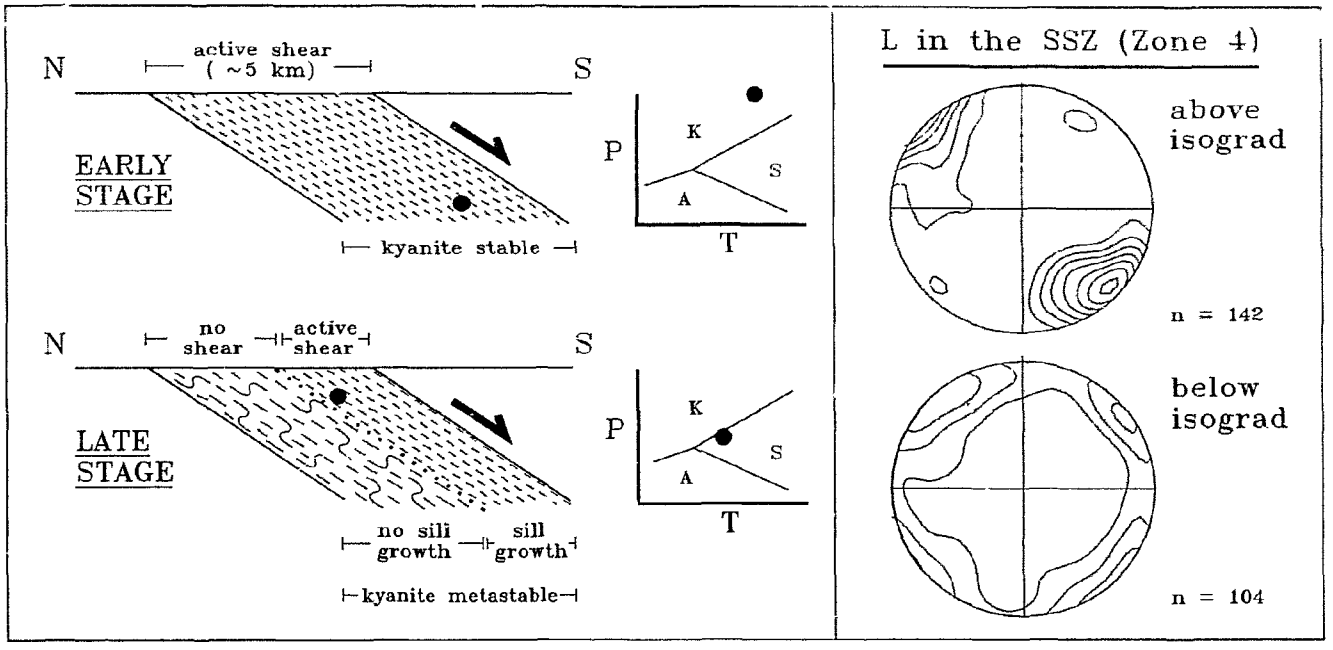

Fig. 4.15. Schematic model of Al_2SiO_5 isograd development in the Shawanaga shear zone. Point in shear zone and schematic *P-T* diagram tracks hypothesized crustal evolution of rock at base of sillimanite zone during extensional shear. Initial extensional shearing took place in the stability field of kyanite, resulting in growth of syn-kinematic, kyanite-bearing assemblages in pelite across the width of the shear zone. At a later stage, isolation of active shear at higher levels of the zone, combined with decompression into the stability field of sillimanite, resulted in kinetically favoured sillimanite growth at higher structural levels but no sillimanite growth at kinematically inactive lower levels. Contoured lineation data from zone 4 of the Shawanaga shear zone show strong maxima in the tectonic transport direction above the isograd and more random orientations below the isograd. This is taken to reflect a more protracted period of extensional shear at higher structural levels.

within the tectonic transport direction whereas more widely dispersed orientations are found below this isograd. This is taken as evidence that sillimanite-zone rocks experienced a higher degree of extensional shear, with stronger re-orientation of pre-extension lineations and more widespread development of new lineations in this zone than in the kyanite zone. These lineation data suggest contrasting structural and metamorphic histories for rocks below and above the isograd.

Textural observations in parautochthonous and allochthonous rocks suggest that decompression reactions may have controlled the paragenetic sequence observed in the Shawanaga shear zone. This is supported by *P-T* estimates suggesting equilibration at a higher pressure in the kyanite zone than in the sillimanite zone, and by thermobarometric data indicating near-isothermal decompression in parautochthonous rocks. A pressure dependence for contrasting mineral assemblages in the Shawanaga shear zone is also indicated by application of the bathozonal scheme of Carmichael (1978). The assemblage Ky-Kfs in migmatitic pelites is diagnostic of bathozone 6 whereas sillimanite-bearing rocks with additional equilibrium phases Ms-Pl-Qtz are constrained to bathozone 5 or lower. The diagnostic bathozone 5 assemblage Ky-Sil-Grt-Bt-Ms-Pl-Qtz can be inferred for rocks above the isograd even though kyanite is typically a relict phase and muscovite is sparse. It is therefore suggested that the kyanite-sillimanite transition in the Shawanaga shear zone marks the approximate position of the bathozone 5-6 bathograd (it will actually lie at a slightly higher structural level where muscovite first appears).

Evidence discussed above suggests that the inverted isograd in the Shawanaga shear zone is unlikely to record a thermal inversion during extensional shear, although the

requirement of rapid cooling and exhumation necessary to preserve such a gradient (*e.g.*, England and Richardson 1977; Thompson and Ridley 1987) may have been met in the tectonically exhumed parautochthon. Preservation of an inverted isograd from earlier thrusting is also ruled out as mineral assemblages are syn-metamorphic with respect to extensional shear. The metamorphic data instead indicate that the isograd is a function of pressure rather than of temperature, and that contrasting structural histories for rocks above and below the isograd may have led to the observed aluminosilicate distribution. This requires a fundamental link between deformation and metamorphism and suggests that metamorphic reactions in the Shawanaga shear zone were controlled in part by the temporal and spatial distribution of extensional shear strains.

Based on arguments outlined above, the following model for the tectonometamorphic evolution of the Shawanaga shear zone is proposed:

1) at the onset of southeast-directed extensional shear (and during earlier sinistral shear), metamorphic conditions in the parautochthon were in the stability field of kyanite. Extensional shear was active across the width of the zone, and synkinematic mineral assemblages in migmatitic pelites contained kyanite and K-feldspar (Fig. 4.15).

2) Metamorphic reactions which consumed (among other phases) garnet and rutile and produced plagioclase and ilmenite (*e.g.*, GRAIL, GASP) occurred during tectonic unroofing of the parautochthon. Syn-extension folding of shear zone fabrics at this time, particularly at lower structural levels, may have led to a 'hardening' of shear fabrics and localization of shear at higher levels of the zone. This style of structural migration is

widely inferred in metamorphic core complexes (Coney 1980; Davis 1983; Lister and Davis 1989; Andersen and Jamtveit 1990).

3) With continued extensional shear, *P-T* conditions in the parautochthon entered the sillimanite stability field along a steep *P-T* path compatible with tectonic exhumation. Sillimanite-forming reactions occurred in pelitic rocks throughout the kinematically active upper portion of the zone, but did not occur at kinematically inactive lower levels (Fig. 4 15). This suggests that strain energy was necessary to drive metamorphic reactions, which is commonly inferred for cooling metamorphic terranes (Grocott 1979; Brodie and Rutter 1985; Bell et al 1986, Jamieson 1988) Metamorphic fluid flow may also have been enhanced in the kinematically active zone (Beach 1976; Reynolds and Lister 1987), allowing these mylonites to thoroughly re-equilibrate to ambient *P-T* conditions. The abundance of syn- and post-kinematic muscovite at upper levels and its relative absence at lower levels suggests that rock-fluid interaction may have been greater toward the structural top of the Shawanaga shear zone.

4) The kyanite-sillimanite 'isograd' was quenched in when extensional shear ended as strain energy was no longer available to drive metamorphic reactions in the cooling parautochthon.

This mechanistic model is consistent with data presented above and can reasonably account for the apparently inverted metamorphic isograd in the Shawanaga shear zone. This isograd appears to mark a limit of deformation-enhanced metamorphic reaction in a volume of rock undergoing decompression and cooling, rather than a mineral stability

boundary within a thermal gradient. A familiar but temperature-dependent analogue is provided by metamorphic boundaries that coincide with the edges of post metamorphic-peak shear zones (*e.g.*, Grocott 1979). Given that the position of the isograd is structurally controlled and that the Shawanaga shear zone is broadly folded, it is reasonable to assume that the isograd is folded in the manner depicted in Figure 4.5.

P-T Paths

Parautochthon

The proposed *P-T* path for the southern Britt domain (Fig. 4.14) is consistent with a major episode of tectonic exhumation independently indicated by kinematic evidence of southeast-directed extensional shear within the 3 km-wide Shawanaga shear zone. A substantial portion of the retrograde *P-T* history of the parautochthon can be obtained because thermobarometry was applied to relatively undeformed rocks as well as to strongly recrystallized rocks within the Shawanaga shear zone. Final equilibration occurred early in the retrograde history for little-deformed rocks and at a later time in strongly deformed rocks (*cf.* Hodges and Royden 1984; Jamieson 1988; Frost and Tracy 1991).

The proposed *P-T* path is generally consistent with mineral parageneses in rocks of the southern Britt domain. Petrographic traits that are compatible with decompression from the kyanite field to the sillimanite field (Fig. 4.14) include kyanite inclusions in garnet, and replacement of matrix kyanite by sillimanite. However, muscovite is absent from the equilibrium assemblage of most Britt domain pelites in the study area,

inconsistent with the position of the reaction:

$$\text{Muscovite} + \text{Quartz} = \text{K-feldspar} + Al_2SiO_5 + H_2O$$

which lies at higher temperatures than the trace of the *P-T* path (Fig. 4.14). Reasons for this discrepancy are not immediately apparent, but explanations could include inaccurate thermobarometric results, a reduced water activity for the above reaction, kinetically unfavourable muscovite-producing reactions, muscovite-consuming reactions, or some combination of the above. Underestimated core-inclusion temperatures for samples 89-35, 89-115*b*, and 89-116*c*, combined with a low aH_2O (probably < 0.5) for the muscovite decomposition reaction (resulting in a shift of this reaction to lower temperatures), provides a possible explanation, but one that is inconsistent with TWQ modelling of hydrous reactions in samples 89-35 and 89-115*b* ($aH_2O = 1$). The close agreement of the *P-T* path for sample 89-116*c*, determined using an H_2O-absent assemblage, with those for 89-35 and 89-115*b* suggests that temperature estimates for the latter two samples are unlikely to be grossly underestimated.

A number of parautochthonous pelite samples contain sparse evidence of muscovite-consuming reactions that produced biotite and kyanite (*e.g.*, rare relict muscovite in garnet pressure shadows; muscovite inclusions in kyanite formed during garnet consumption) although textural relationships between biotite and rare muscovite in these rocks are typically ambiguous. This suggest that a muscovite-consuming reaction such as:

$$\text{Garnet} + \text{Muscovite} = \text{Kyanite} + \text{Biotite} + \text{Quartz}$$

(modelled with GeO-Calc for sample 89-03 in Fig. 4.14) may be responsible for the general

absence of muscovite in syn-kinematic equilibrium assemblages.

The southern Britt domain path shows more decompression with cooling than do most *P-T* paths for the Central Gneiss Belt and Grenville Front Tectonic zone (*e.g.*, Grant 1989, Nadeau 1990, Bethune 1993) but resembles one proposed for the northern Britt domain by Jamieson et al. (1995). The northern and southern Britt domain paths differ significantly only in that maximum recorded pressures are 14 kbar in the north and ~11 kbar in the south, and isothermal decompression (or possibly decompression with slight heating) is indicated for pressures <10 kbar in the north whereas rocks in south cooled by ~90°C during this interval. A striking feature of both *P-T* paths is the presence of a 'bend' at ~9-10 kbar and ~650-700°C resulting in a steeper d*P*/d*T* slope at lower pressures. Jamieson et al. (1995) concluded from structural and petrographic evidence that the higher-*P* segment of the northern Britt domain path records exhumation and cooling during thrusting whereas the lower-*P* segment marks tectonic exhumation associated with extension. Although there is little evidence in the Pointe-au-Baril area to link early decompression and cooling to thrusting, there is plentiful evidence to suggest that extensional exhumation influenced the late *P-T* history. Syn-orogenic extension may therefore have played a significant role in the post-peak Grenvillian metamorphic history of the entire Britt domain (*cf.* Jamieson et al. 1995).

Allochthon

The *P-T* path for the allochthon is less tightly constrained by thermobarometric data but also shows significant decompression. There are few useful reaction textures to

indicate whether this path is reasonable on petrographic grounds, but the presence of lower grade mineral assemblages in the Shawanaga domain is consistent with final equilibration at a lower P and T than in parautochthonous rocks.

The P-T result for sample D47*a* (Fig. 4.12), a metapelite from the tectonic window of Nadeau Island gneiss, falls on the revised path for the allochthon (Fig. 4.14), hinting at the possibility that this 'window' may actually represent a lithologic unit of the Ojibway gneiss association. This hypothesis provides one explanation for the absence of a margin of Shawanaga orthogneiss around the paragneiss unit (required by structural reasoning if the paragneiss is part of the Nadeau Island association; Fig. 2.2). Pelitic rocks occur in the Shawanaga domain at an inland location near the contact with the Parry Sound domain (A. Davidson, personal communication 1994), indicating that pelites could also be present in the western Shawanaga domain. However, without additional structural and metamorphic data, this hypothesis must be regarded as tentative.

Comparison with Previous Thermobarometry

Thermobarometric results for this study are generally in accord with the results of other workers. Peak Grenvillian pressures and temperatures obtained in this study for parautochthonous rocks (10.6-11.6 kbar, 745-770°C) are in agreement with the peak estimates of Anovitz and Essene (1990) and Corrigan (1990) for the northern Britt domain, and fall on the P-T path of Jamieson et al. (1995) for the Key Habour area (Fig. 1.2). Core-inclusion suite P-T results of 10.1-10.3 kbar and 670-680°C for metapelite with zoned garnet porphyroblasts (89-35, 89-115*b*) are similar to the estimated conditions of

post-thrusting, pre-extension equilibration in the northern Britt domain (Jamieson et al. 1995). Rim thermobarometric estimates indicate that these rocks underwent 4-5 kbar of near-isothermal decompression, consistent with the magnitude of decompression documented by Tuccillo et al. (1990) in the same lithologic package. The *P-T* conditions of final equilibration in parautochthonous rocks (5.1-6.0 kbar, 555-615°C) are marginally lower in both pressure and temperature than a range proposed by Needham (1992) for the same area. Needham (1992) also reported thermobarometric data for charnockitic granites in the Pointe-au-Baril complex that are in general agreement with estimates from pre-Grenvillian granulites in zone 3 (7.2-8.4 kbar, 625-700°C). Needham (1992) assigned his *P-T* estimates for charnockitic granite to a Grenvillian *P-T* path, but the results of the present study indicate that these data may instead record pre-Grenvillian metamorphism.

The results of this study are at odds with the work of Tuccillo et al. (1992) who attributed pressure estimates of 9-13 kbar for the Pointe-au-Baril area to pre-Grenvillian (*ca.* 1450 Ma) metamorphism and estimates of 5-8 kbar to Grenvillian metamorphism. These authors based their conclusions in part on a U-Pb age of 1396 Ma for strongly zoned metapelite garnet which was suggested to represent a mixed growth age (pre-Grenvillian cores and Grenvillian overgrowths). Zoned garnets were attributed to incomplete Grenvillian homogenization of these polymetamorphic grains. Tuccillo et al. (1992) also proposed that embayed kyanite relicts in pelite grew during the early metamorphism whereas sillimanite formed during Grenvillian metamorphism.

In contrast, this study has shown that (*i*) pressures of at least 10-11 kbar are recorded in pelite and metabasite, including a metadiabase dyke for which field,

geochemical and petrographic evidence indicate emplacement after the latest pre-Grenvillian metamorphism, (*ii*) quantitative *P-T* estimates from pre-Grenvillian granulites suggest that this metamorphism occurred at lower pressures (~7-8 kbar) than proposed by Tuccillo et al. (1992), and (*iii*) kyanite was undoubtedly the stable Al_2SiO_5 polymorph during Grenvillian strike-slip and early extensional displacement on the Shawanaga shear zone. These observations and results suggest that the high-pressure estimates of Tuccillo et al. (1992) reflect Grenvillian rather than pre-Grenvillian metamorphism, and that garnets from which their high-pressure results were derived acquired their major element zoning through early Grenvillian homogenization followed by a partial re-homogenization during near-isothermal decompression. A U-Pb age of 1396 Ma for strongly zoned garnet (Tuccillo et al. 1992) does not rule out this hypothesis as major element zoning in garnet is homogenized above ~650°C (Tracy 1982 and references therein) whereas isotopic closure of the U-Pb system in garnet occurs at a much higher temperature (>800°C; Mezger et al. 1989*a*). This demonstrates that geochronological evidence for polymetamorphic garnets (Tuccillo et al. 1992) need not be taken to indicate that pre-Grenvillian garnet compositions are preserved in the cores of these grains.

4.6 SUMMARY

1) Pre-Grenvillian (*ca.* 1450-1430 Ma) granulite-facies mineral assemblages are locally preserved in structural zone 3 (Fig. 3.2) of the study area. Orthopyroxene is preserved in migmatitic mafic supracrustal gneiss, metagabbro, and *ca.* 1460 Ma megacrystic granite, and corundum is preserved in quartz-free aluminous paragneiss. *P-T* estimates of 7.2-8.4

kbar and 625-700°C obtained for this metamorphism are interpreted as recording peak, or more likely near-peak, pre-Grenvillian conditions. The allochthonous Shawanaga domain lacks evidence of pre-Grenvillian metamorphism.

2) Grenvillian orogenesis resulted in localized overprinting of pre-Grenvillian assemblages in zone 3, and pervasive metamorphic recrystallization throughout the rest of the study area. Rocks in the Britt domain contain widespread upper amphibolite-facies mineral assemblages, but rare orthopyroxene in the youngest suite of metabasic dykes (correlated with the 1238 Ma Sudbury swarm) indicates that granulite facies conditions were briefly attained, and/or that orthopyroxene was stable in the dykes during upper amphibolite facies metamorphism because of a low aH_2O. In allochthonous rocks, meta-eclogitic mineral assemblages (of unknown age) are preserved in several mafic bodies, and granulite-facies assemblages (younger than *ca.* 1170-1150 Ma) are preserved in coronitic metagabbro, indicating a high-grade Grenvillian metamorphic history prior to widespread amphibolite facies re-equilibration.

3) Grenvillian metamorphism in the Britt domain was marked by early growth of kyanite and later growth of sillimanite in pelitic gneiss. Many pelites in the study area contain both polymorphs although kyanite is typically a relict phase. Staurolite crystallized after the metamorphic peak in quartz-free pelitic assemblages but is absent from quartz-bearing assemblages. Metamorphic textures in rare pelitic enclaves within Shawanaga domain orthogneiss suggest a similar aluminosilicate growth history during Grenvillian metamorphism.

4) *P-T* estimates of 10.6-11.6 kbar and 745-770°C for metabasite and calc-silicate

gneiss are interpreted as marking the peak of Grenvillian metamorphism in the southern Britt domain. Peak metamorphic conditions in the allochthonous Shawanaga domain are poorly constrained by thermobarometric data obtained in this study, but may have reached at least ~8 kbar and ~700°C. This estimate is consistent with *P-T* results for the Shawanaga domain obtained by other workers.

5) Allochthonous and parautochthonous rocks were variably re-equilibrated during high-temperature extensional exhumation and decompression following the Grenvillian metamorphic peak. Final metamorphic equilibration occurred at 5.1-6.0 kbar and 555-615°C in the parautochthon and at a lower *P* and *T* in the allochthon (perhaps at 3.6 kbar and 485°C).

6) Thermobarometric data obtained in this and other studies have been used to construct *P-T* paths for allochthonous and parautochthonous rocks. Both paths show significant decompression with limited cooling. The Britt domain *P-T* path shows a 'bend' at 10.2 kbar and 675°C, which may mark the beginning of extensional unroofing of this domain by the Shawanaga shear zone.

7) Pelitic rocks in the parautochthonous segment of the Shawanaga shear zone contain garnets with strong major element zoning and suggest the presence of an inverted metamorphic isograd. Garnet zoning is interpreted as a product of diffusion-controlled zoning that formed during near-isothermal decompression of the Britt domain. The inverted isograd is marked by the first appearance of sillimanite toward higher structural levels in kyanite-bearing rocks. A model of progressive shear localization toward higher levels of the Shawanaga shear zone during extensional unroofing, in conjunction with

metamorphic equilibration only in kinematically active rocks, is proposed to account for the observed aluminosilicate distribution.

CHAPTER 5

U-Pb Geochronology

5.1 INTRODUCTION

In the middle to lower levels of orogenic belts, U-Pb dating of accessory minerals has proven an effective tool in evaluating the timing of tectonic, metamorphic and plutonic events linked to orogenic evolution. Knowledge of the temperature range over which these minerals become closed to Pb diffusion permits post-orogenic cooling histories to be characterized. The ability of some mineral chronometers (*e.g.*, zircon) to at least partly retain radiogenic Pb during later high-grade metamorphism (Heaman and Parrish 1991) allows pre-orogenic geological events to be dated. These characteristics make U-Pb geochronology an invaluable tool in determining crustal evolution history in the high-grade metamorphic terranes of the Grenville orogen.

This chapter reports the results of precise U-Pb isotopic dating of 21 rocks collected from the Britt and Shawanaga domains in the Pointe-au-Baril area. The new data constrain the timing of metamorphism, tectonism, pegmatite dyke emplacement, and post-metamorphic cooling, and are discussed with reference to three problems addressed by U-Pb geochronology, namely: (*i*) what is the age of granulite facies assemblages preserved in mafic rocks north of the Shawanaga shear zone? (*ii*) when was the Shawanaga shear zone active as an extensional shear zone? (*iii*) what influence, if any, did extension have on metamorphism and cooling within and adjacent to the Shawanaga shear zone?

5.2 PREVIOUS GEOCHRONOLOGICAL WORK

Isotopic dating has been carried out in the Central Gneiss Belt and Grenville Front Tectonic Zone of Ontario (Fig. 5.1) over the past few decades, and databases of published ages have been compiled (*e.g.*, Stockwell 1982; Easton 1986). As noted by Easton (1986), however, some of the isotopic systems used (*e.g.*, K-Ar, Rb-Sr) lack the precision necessary to resolve the ages of closely-spaced geologic events, and many of the studies have been undertaken without an adequate knowledge of local geology. In addition, for systems easily disturbed following initial isotopic closure (*e.g.*, K-Ar), it is not always clear if a reported age represents a protolith age, a metamorphic age, or is the product of partial metamorphic resetting. For these reasons the summary of Grenvillian and pre-Grenvillian crustal events given below is based primarily on U-Pb data. The U-Pb isotopic system provides a relatively high degree of accuracy and precision (errors of less than ±10 Ma are now routinely reported), and allows both Grenvillian and pre-Grenvillian crustal events to be confidently dated. U-Pb geochronological studies in Ontario post-dating Easton's (1986) compilation (*e.g.*, van Breemen et al. 1986; Krogh et al. 1987; van Breemen and Davidson 1988, 1990; Davidson and van Breemen 1988; Krogh 1989; Corrigan 1990; Nadeau 1990; Haggart 1991; Tuccillo et al. 1992; Haggart et al. 1993; Bethune 1993; Mezger et al. 1993; Wodicka 1994; Corrigan et al. 1994; Ketchum et al. 1994; Culshaw et al. in prep.), many of which were carried out in conjunction with detailed field work, provide a wealth of new data on the timing of Grenvillian and pre-Grenvillian events.

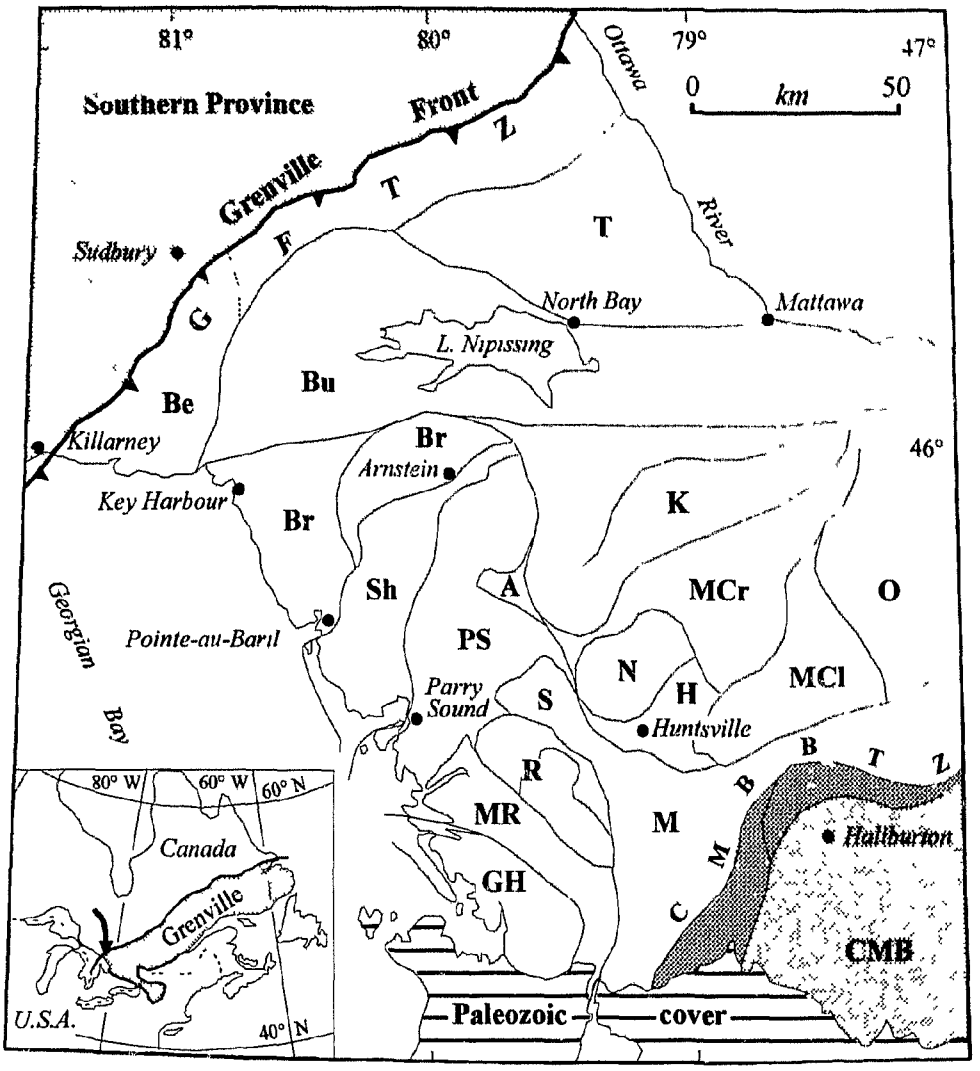

Fig. 5.1. Lithotectonic domains in the Central Gneiss Belt of Ontario, after Davidson and van Breemen (1988), Culshaw et al (1990), and Anovitz and Essene (1990). A simplified subdivision of the northern Central Gneiss Belt is used here as the location of U-Pb data (Table 5.1) in this region is in many cases not specified. **GFTZ**, Grenville Front Tectonic Zone, **CMB**, Central Metasedimentary Belt; **CMBBTZ**, Central Metasedimentary Belt boundary thrust zone; **Be**, Beaverstone domain; **Br**, Britt domain; **T**, Tomiko domain; **Bu**, Burwell domain; **A**, Ahmic domain; **K**, Kiosk domain; **N**, Novar subdomain; **H**, Huntsville subdomain; **MCr**, McCraney subdomain; **MCl**, McClintock subdomain; **O**, Opeongo subdomain; **R**, Rosseau subdomain; **GH**, Go Home subdomain; **S**, Seguin subdomain; **M**, Muskoka domain; **MR**, Moon River subdomain; **PS**, Parry Sound domain; **Sh**, Shawanaga domain.

A compilation of U-Pb ages reported from the Central Gneiss Belt and Grenville Front Tectonic Zone is given in Table 5.1. All ages have been calculated (or recalculated) using the decay constants recommended by Steiger and Jäger (1977). Ages reported in Table 5.1 are those suggested by the authors to date a particular geologic event and comprise both discordia line intercept ages and $^{207}Pb/^{206}Pb$ ages of individual fractions. Some ages are excluded where lacking precision or deemed here to be inaccurate based on additional U-Pb data from the same area. Imprecise ages are retained where they represent the only available information for a particular time interval in a given region. Ages based on a single analysis are also excluded where it can be determined that the analysis is strongly discordant and therefore of uncertain reliability. The significance of the data reported in Table 5.1 is that suggested by the authors or, in a few cases where this interpretation is unclear, the most probable significance.

Table 5.1 shows that ages of plutonism, tectonic activity, metamorphism and deposition of supracrustal rocks in the Central Gneiss Belt and Grenville Front Tectonic Zone can be broadly divided into four periods.

Late Archean Events (*ca.* 2740-2560 Ma)

Rocks with oldest U-Pb ages of primary crystallization, metamorphism, and/or deformation are found entirely within a poorly delimited region of Archean rock underlying portions of the Grenville Front Tectonic Zone and the Burwell domain (Fig. 5.1). This Archean belt, as currently defined by U-Pb data, extends north and northwest from Lake Nipissing to the Grenville Front. Easton (1992, Fig. 19.2) has depicted this belt

TABLE 5.1. U-Pb Ages from the Central Gneiss Belt and Grenville Front Tectonic Zone

Abbreviations

Domain		
A - Ahmic	R - Rosseau	Oga - Ojibway gneiss association
Br - Britt	S - Seguin	PBC - Pointe-au-Baril complex
Bu - Burwell	Sh - Shawanaga	SBga - Sand Bay gneiss association
GFTZ - Grenville Front	T - Tominko	SP - Shawanaga pluton
Tectonic Zone	Unit	Mineral
GH - Go Home	amph. - amphibolite	a - allanite
H - Huntsville	anorth. - anorthosite	b - baddeleyite
K - Kiosk	mig. - migmatite	g - garnet
MCl - McClintock	ogn - orthogneiss	m - monazite
MCr - McCraney	peg - pegmatite, pegmatitic	t - titanite
MR - Moon River	pgn - paragneiss	ur - uraninite
N - Novar	porph. - porphyry	wr - whole rock (Pb-Pb age)
O - Opeongo	Bga - Bayfield gneiss association	z - zircon
PS - Parry Sound	NIga - Nadeau Island gneiss association	

1.) Late Archean Ages

Locality	Domain	Unit	Age (Ma), Mineral	Significance	Reference
Hagar	Bu	pgn	ca. 2737 (z,t)	metamorphism	Krogh (1989)
W/NW of L. Nipissing	Bu	grey ogn	2680 ± 3 (t)	metamorphism	Chen et al. (1993)
N of L. Nipissing	Bu	grey ogn	2680 ± 2 (z)	plutonism	Krogh et al. (1992)
N of L. Nipissing	Bu	grey ogn	2672 ± 3 (z)	plutonism	Krogh et al. (1992)
W/NW of L. Nipissing	Bu	grey ogn	2672 ± 3 (t)	metamorphism	Chen et al. (1993)
N of L. Nipissing	Bu	grey ogn	2671 ± 3 (z)	plutonism	Krogh et al. (1992)
N of North Bay	GFTZ	peg in ogn	ca. 2660 (z)	min. meta. /deform.	Krogh & Davis (1970b)
N of North Bay	GFTZ	dyke	2650 ± 5 (z,m)	min. meta. age	Krogh (1991)
N of North Bay	GFTZ	ogn	2647 ± 12 (z)	plutonism	Steiger & Wasserburg (1969)
N of North Bay	GFTZ	peg	ca. 2600 (z)	min. meta. age	Krogh & Davis (1974)
N of North Bay	GFTZ	peg in gneiss	ca. 2600 (z)	min. deform./meta.	Krogh & Wardle (1984)
River Valley	GFTZ	River Valley anorth.	2560 ± 155 (wr)	plutonism	Ashwal & Wooden (1989)

Locality	Domain	Unit	Age (Ma), Mineral	Significance	Reference

2.) Late Paleoproterozoic Ages

Locality	Domain	Unit	Age (Ma), Mineral	Significance	Reference
Coniston	GFTZ	Wanapitei ogn	1747 + 6/-5 (z)	plutonism	Prevec (1992)
French River	Bu	gneiss	1744 ± 11 (z)	max. deposition age?	Krogh (1989)
Killarney	GFTZ	Killarney ogn	1742 ± 1 (z)	plutonism	van Breemen & Davidson (1988)
Killarney	GFTZ	ogn	ca. 1740 (z)	plutonism	Krogh & Wardle (1984)
Pointe-au-Baril	Br	ogn (Bga)	1739 ± 34 (z)	plutonism	Krogh et al. (1993a)
Colins Inlet	GFTZ	Killarney porph.	1732 + 7/-6 (z)	plutonism	van Breemen & Davidson (1988)
Beaverstone Bay	GFTZ	Grodine ogn	1715 + 6/-5 (z)	plutonism	Davidson et al. (1992)
Huntsville	H	ogn	1714 + 123/-71 (z)	plutonism	Nadeau (1990)
Beaverstone Bay	GFTZ	Grodine ogn	1711 + 10/-8 (z)	plutonism	Davidson et al. (1992)
Collins Inlet	GFTZ	Fox Is. granite	ca 1703 (z)	plutonism	Davidson et al. (1992)
S of Bell Lake	GFTZ	ogn	ca. 1700 (z)	plutonism	Krogh et al. (1971)
Key Harbour	Br	Key Harbour ogn	1694 ± 3 (z)	plutonism	Corrigan et al. (1994)
NW of Mattawa	T	quartzite	1686 + 19/-16 (z)	max. deposition age	Krogh (1989)
SE of Sudbury	GFTZ	Chief Lake ogn	ca. 1626 (z)	plutonism	Krogh & Davis (1969)
Honey Harbour	GH	ogn	ca. 1608	plutonism	Krogh (1991)
Pointe-au-Baril	Br	ogn (NIga)	1606 ± 2 (z)	plutonism	Culshaw et al. (in prep.)

3.) Early Mesoproterozoic Ages

Locality	Domain	Unit	Age (Ma), Mineral	Significance	Reference
Tyson L.	GFTZ	Bell L. granite	ca. 1523 (z)	plutonism	Krogh et al. (1971)
Tyson L.	GFTZ	Bell L. granite	1471 ± 3 (z)	plutonism	van Breemen & Davidson (1988)
Pointe-au-Baril	Sh	ogn (Oga)	1466 ± 11 (z)	plutonism	Culshaw et al. (in prep.)
Huntsville	H	ogn	1460 ± 60 (z)	plutonism	van Breemen et al. (1986)
Pointe-au-Baril	Br/Sh	ogn (PBC, SP)	1460 + 12/-8 (z)	plutonism	Culshaw et al. (in prep.)
Go Home River	GH	mig. ogn	1460 ± 5 (z)	plutonism or meta.	Krogh et al. (1993a)
Go Home River	GH	ogn	1458 ± 9 (z)	plutonism	Krogh et al. (1993a)
Britt	Br	Britt ogn	1457 + 9/-6 (z)	plutonism	van Breemen et al. (1986)
Key Harbour	Br	leucosome in ogn	1456 + 12/-11 (z)	plutonism	Corrigan (1990)
Killarney	GFTZ	ogn, amph dykes	1454 ± 8 (t,z)	metamorphism	Haggart et al. (1993)

Locality	Domain	Unit	Age (Ma), Mineral	Significance	Reference
Huntsville	S	ogn	1453 ± 6 (z)	plutonism	Nadeau (1990)
Killarney	GFTZ	pgn	1453 ± 7 (z)	metamorphism	Krogh (1989)
Collins Inlet	GFTZ	peg dyke	1450 ± 50 (z)	min. deform. age	van Breemen & Davidson (1988)
Pointe-au-Baril	Br	pgn (NIga)	1450 ± 1 (a)	metamorphism	Tuccillo et al. (1992)
Pointe-au-Baril	Br	ogn (Bga)	1450 - 1420 (z,t)	metamorphism	Krogh et al. (1992)
Tyson L.	GFTZ	pgn	ca. 1445 (m)	metamorphism	Bethune et al. (1990)
Huntsville	N	ogn	1444 + 12/-8 (z)	plutonism	Nadeau (1990)
Huntsville	H	ogn	1442 + 9/-8 (z)	plutonism	Nadeau (1990)
Key Harbour	Br	ogn	1442 + 7/-6 (z)	plutonism	Corrigan (1990)
Key Harbour	Br	ogn dyke	ca. 1442 (z)	dyke emplacement	Corrigan (1990)
Parry Sound	PS	quartzite	1438 - 1120 (z)	deposition interval	Wodicka (1994)
Huntsville	H	ogn	1432 + 54/-98 (z)	metamorphism	Nadeau (1990)
Pointe-au-Baril	Br	ogn (Bga)	1430 ± 23 (t)	metamorphism	Krogh et al. (1993a)
Pointe-au-Baril	Br	ogn (PBC)	1430 ± 17 (z)	plutonism	Krogh et al. (1993a)
Huntsville	S	ogn	1427 + 16/-13 (z)	plutonism	Nadeau (1990)
Parry Sound	PS	McKellar ogn	1425 ± 75 (z)	plutonism	van Breemen et al. (1986)
Pointe-au-Baril	Br	ogn (PBC)	ca. 1420 (z)	plutonism	Krogh et al. (1992)
Pointe-au-Baril	Sh	pgn (SBga)	<1417 ± 5 (z)	sedimentation	Culshaw et al. (in prep.)
L. Muskoka	R	Muskoka ogn	ca. 1414 (z)	plutonism	Krogh & Davis (1969)
W of L. Nipissing	Bu	Cosby ogn	ca. 1400 (z)	plutonism	Silver in Lumbers (1975)
Pointe-au-Baril	Sh	pgn (SBga)	<1390 - 1360 (z)	sedimentation	Culshaw et al. (in prep.)
L. Nipissing	?	Powassan ogn	ca. 1380 (z)	plutonism	Kamo et al. (1989)
Whitney	O	ogn	1375 + 13/-12 (z)	plutonism	van Breemen & Davidson (1990)
Parry Sound	PS	ogn	1360 - 1312 (z)	plutonism	Wodicka (1994)
Parry Sound	PS	Whitestone anorth.	1350 ± 50 (z)	plutonism	van Breemen et al. (1986)
Parry Sound	PS	Isabella Is. ogn	1350 - 1286 (z)	plutonism	Wodicka (1994)
Parry Sound	Sh	Marginal ogn	1346 + 69/-39 (z)	plutonism	van Breemen et al. (1986)
Pointe-au-Baril	Sh	pgn (SBga)	1333 + 32/-27 (z)	volcanism?	Culshaw et al. (in prep.)
Parry Sound	PS	ogn	1315 -1288 (z)	plutonism	Wodicka (1994)
Parry Sound	PS	ogn	ca. 1313 (z)	plutonism	Macfie et al. (1992)
Twelve Mile Bay	PS	ogn	1280 ± 7 (z)	plutonism	Wodicka (1994)

Locality	Domain	Unit	Age (Ma), Mineral	Significance	Reference

4.) Late Mesopoterozoic (Grenvillian) Ages

Locality	Domain	Unit	Age (Ma), Mineral	Significance	Reference
NE of L. Nipissing	T	Mulock ogn	1244 + 4/-3 (z)	plutonism	Lumbers et al. (1991)
Espanola	-	Sudbury diabase	1238 ± 4 (b)	dyke emplacement	Krogh et al. (1987)
SW of L. Nipissing	Bu	Mercer anorth.	1222 ± 2 (z)	plutonism	Prevec (1992)
NW of L. Nipissing	Bu	St. Charles anorth.	1206 ± 18 (z)	plutonism	Prevec (1992)
SW Central Gneiss Belt	-	coronitic gabbro	1170 ± 30 (b)	plutonism	Davidson & van Breemen (1988)
Parry Sound	PS	Parry Is. anorth.	1163 ± 3 (z)	plutonism	Wodicka (1994)
Parry Sound	PS	pgn	1161 ± 3 (z)	metamorphism	van Breemen et al. (1986)
Parry Sound	PS	pgn	1159 ± 1 (m)	max. cooling age	Wodicka (1994)
Parry Sound	PS	peg	1159 + 5/-4 (z)	thrusting	van Breemen et al. (1986)
Parry Sound	PS	peg dyke	1157 ± 3 (z)	syn-thrusting	Wodicka (1994)
Parry Sound	PS	pgn	1157 ± 1 (m)	metamorphism	Tuccillo et al. (1992)
Parry Sound	PS	aplite veins	1156 - 1146 (m)	reset and/or cooling	Wodicka (1994)
Parry Sound	PS	pgn	1153 ± 2 (m)	cooling age	Wodicka (1994)
Parry Sound	PS	mafic dyke	1152 ± 2 (z)	min. meta. age	Wodicka (1994)
Pointe-au-Baril	Sh	coronitic gabbro	1152 ± 2 (z)	plutonism	Heaman & LeCheminant (1994)
Wahnapitae	GFTZ	peg leucosomes	ca. 1150 (z)	metamorphism	Krogh & Wardle (1984)
Parry Sound	PS	amphibolite	1148 ± 6 (z)	min. meta. age	Wodicka (1994)
Parry Sound	PS	peg dyke	1146 - 1140 (m)	reset and/or cooling	Wodicka (1994)
Parry Sound	PS	pgn	1123 ± 3 (g)	metamorphism	Tuccillo et al. (1992)
Parry Sound	PS	peg	1121 ± 5 (z)	late thrusting	van Breemen et al. (1986)
Twelve Mile Bay	PS	quartzite	1121 - 1025 (z)	deposition interval	Wodicka (1994)
Parry Sound	PS	mafic dykes	1120 - 1114 (z)	metamorphism	Bussy et al. (1993)
Parry Sound	PS	leucogabbro	1119 - 1104 (t)	isotopic resetting	Wodicka (1994)
Parry Sound	PS	amphibolite	1117 - 1077 (t)	isotopic resetting	Wodicka (1994)
Parry Sound	PS	peg in boudin	1117 - 1116 (z)	deformation	Krogh et al. (1993a)
Parry Sound	PS	pgn	1116 + 16/-10 (m)	metamorphism	Wodicka (1994)
Parry Sound	PS	amph. dyke	1111 - 1089 (t)	isotopic resetting	Wodicka (1994)
Parry Sound	PS	Parry Is. anorth.	1109 ± 1 (t)	isotopic resetting	Wodicka (1994)
Parry Sound	MR/PS	peg	1103 + 6/-4 (z)	late thrusting	van Breemen & Davidson (1990)

Locality	Domain	Unit	Age (Ma), Mineral	Significance	Reference
Madawaska	O	pgn	1100 ± 1 (m)	meta. or cooling	Mezger et al. (1993)
Huntsville	S	peg	1097 ± 3 (z)	syn-thrust/min. meta.	Nadeau (1990)
Twelve Mile Bay	PS	ogn	1086 - 1049 (a)	reset or cooling	Wodicka (1994)
Parry Sound	PS	Isabella Is. ogn	1080 ± 2 (t)	metamorphism	Wodicka (1994)
Huntsville	S	coronitic gabbro	1080 ± 4 (z)	metamorphism	van Breemen & Davidson (1990)
Huntsville	H	peg	1080 ± 1 (z)	late syn-thrusting	Nadeau (1990)
Magnetawan	A	mafic dyke, mig	1080 - 1079 (z)	meta., deformation	Bussy et al. (1993)
W of Parry Sound	Sh	peg	1080 - 1078 (z)	deformation	Krogh et al. (1993a)
Parry Sound	PS	quartz vein	1078 ± 4 (t)	late thrusting	Tuccillo et al. (1992)
Algonquin Park	MCI/O	pgn	1074 ± 2 (m)	meta. or cooling	Mezger et al. (1993)
Huntsville	H	ogn	1068 + 51/-12 (m)	cooling age	Nadeau (1990)
W of Parry Sound	Sh	anorthosite	ca. 1068 (z)	deformation	Krogh et al. (1993a)
Huntsville	H	peg	1063 ± 3 (m)	cooling age	Nadeau (1990)
S of Parry Sound	MR	mafic dyke	1063 ± 2 (z)	metamorphism	Bussy et al. (1993)
French River	Bu	gneiss	1062 ± 15 (z)	metamorphism	Krogh (1989)
Pointe-au-Baril	Br	ogn (Bga)	1062 - 1050 (z)	mylonitization	Krogh et al. (1992)
Pointe-au-Baril	Br	ogn (Bga)	ca. 1062 (z)	new zircon growth	Krogh et al. (1993a)
Pointe-au-Baril	Br	pgn (NIga)	1062 ± 2 (m)	reset or cooling	Tuccillo et al. (1992)
SW Central Gneiss Belt	-	coronitic gabbro	1060 - 1030 (z)	metamorphism	van Breemen & Davidson (1990)
Bracebridge	S/R	ogn dyke	1058 + 8/-4 (z)	min. meta./thrusting	van Breemen & Davidson (1990)
Dorset	S	granite	1056 ± 3 (t)	cooling age	Mezger et al. (1993)
Pointe-au-Baril	Sh	pgn (SBga)	1053 ± 2 (z)	metamorphism	Culshaw et al. (in prep.)
Pointe-au-Baril	Br	pgn (NIga)	1053 ± 2 (m)	reset or cooling	Tuccillo et al. (1992)
S of Parry Sound	MR	mafic dyke	1051 ± 2 (z)	metamorphism	Bussy et al. (1993)
Pointe-au-Baril	Sh	ogn (Oga)	1050 ± 12 (z)	metamorphism	Culshaw et al. (in prep.)
Pointe-au-Baril	Sh	coronitic gabbro	ca. 1050 (z)	metamorphism	Heaman and LeCheminant (1993)
Dwight	H	ogn dyke	ca. 1050 (z)	dyke emplacement	van Breemen & Davidson (1990)
Huntsville	H	peg	1049 ± 2 (m)	late syn-thrusting	Nadeau (1990)
Honey Harbour (?)	GH	mafic dyke	1047 ± 1 (z)	metamorphism	Bussy et al. (1993)
SW Central Gneiss Belt	-	coronitic gabbro	1047 ± 5 (z)	metamorphism	Davidson & van Breemen (1988)
Honey Harbour (?)	GH	peg	ca. 1047 (z)	post-folding	Bussy et al. (1993)
Pointe-au-Baril	Br	ogn (Bga)	ca. 1047 (z)	new zircon growth	Krogh et al. (1993a)
Huntsville	H	peg	1046 ± 2 (z)	late syn-thrusting	Nadeau (1990)

Locality	Domain	Unit	Age (Ma), Mineral	Significance	Reference
Whitney	O	ogn	1043 + 22/-23 (z)	metamorphism	van Breemen & Davidson (1990)
Britt	Br	peg	1043 (ur)	peg emplacement	Wanless & Lowdon (1961)
Huntsville	H	peg	1039 + 4/-2 (z)	extensional shear	Nadeau (1990)
Novar	N	amphibolite	1039 ± 2 (t)	cooling age	Mezger et al. (1993)
Key Harbour	Br	pgn	1037 ± 1 (m)	cooling age	Corrigan (1990)
Key Harbour	Br	pgn	1035 ± 1 (m)	cooling age	Corrigan (1990)
Twelve Mile Bay	PS	ogn	1034 - 1024 (t)	reset or cooling	Wodicka (1994)
Tyson L.	GFTZ	coronitic dykes	ca. 1032 - 985 (z)	metamorphism	Bethune (1993)
Huntsville	H	ogn	1030 + 50/-20 (z)	metamorphism	van Breemen et al. (1986)
Huntsville	MCl	peg	1027 ± 2 (z)	late syn-thrusting	Nadeau (1990)
Dorset	S	amphibolite	1024 ± 2 (t)	cooling age	Mezger et al (1993)
Huntsville	H	ogn	1018 ± 45 (z)	metamorphism	Nadeau (1990)
Blackstone Lake	MR	peg	1017 (ur)	peg emplacement	Nier et al. (1941)
Key Harbour	Br	leucosome in ogn	1015 + 16/-17 (z)	metamorphism	Corrigan (1990)
Blackstone Lake	MR	peg	1014 (ur)	peg emplacement	Tilton et al. (1960)
Butt Lake	K	peg	1012 (ur)	peg emplacement	Shillibeer & Cumming (1956)
Honey Harbour	GH	peg	1008 + 9/-5 (z)	late tectonic	Krogh (1991)
NW of Mattawa	T	quartzite	1007 ± 43 (z)	metamorphism	Krogh (1989)
Pointe-au-Baril	Sh	peg (SBga)	ca. 1006 (z)	new zircon growth	Krogh et al. (1993a)
Key Harbour	Br	leucosome in ogn	ca. 1004 - 1001 (t)	cooling ages	Corrigan (1990)
Hagar	GFTZ	pgn	1000 ± 2 (m)	meta. or cooling	Mezger et al. (1993)
Tyson Lake	GFTZ	coronitic dykes	ca. 1000 (z)	metamorphism	Bethune et al. (1990)
Pointe-au-Baril	Br	ogn (Bga)	998 ± 15 (t)	metamorphism	Krogh et al. (1993a)
W/NW of L. Nipissing	Bu	grey ogn	ca. 995 (t)	metamorphism	Chen et al. (1993)
Hagar	Bu	pgn	ca. 992 (z,t)	metamorphism	Krogh (1989)
French River	Bu	peg in pgn	ca. 991 (z)	syn-tectonic/meta.	Krogh & Davis (1974)
N of North Bay	GFTZ	leucosome	ca. 991 (t)	metamorphism	Krogh et al. (1993b)
Key Harbour	Br	peg	990 + 2/-1 (z)	dyke emplacement	Corrigan (1990)
Pointe-au-Baril	Sh	pgn (SBga)	ca. 990 (z)	metamorphism	Culshaw et al. (in prep.)
N of North Bay	GFTZ	dyke	988 ± 10 (m)	mylonitization	Krogh (1991)
N of North Bay	GFTZ	leucosome	988 ± 5 (m)	deformation	Krogh (1991)
S of Sudbury	GFTZ	peg	988 (m)	meta., deformation	Krogh et al. (1993b)
N of North Bay	GFTZ	leucosome	987 - 986 (z)	meta., deformation	Krogh et al. (1993b)

Locality	Domain	Unit	Age (Ma), Mineral	Significance	Reference
Tyson Lake	GFTZ	coronitic dykes	ca. 985 (z)	metamorphism	Bethune (1991)
Blackstone Lake	MR	peg	984 (ur)	peg emplacement	Wanless in Stockwell (1982)
Killarney	GFTZ	ogn	982 ± 27 (t)	metamorphism	Krogh (1989)
Key Harbour	GFTZ	ogn dyke	ca. 980 - 963 (t)	cooling ages	Corrigan (1990)
Killarney	GFTZ	ogn, amph. dykes	978 ± 13 (t,z)	metamorphism	Haggart et al. (1993)
Blackstone Lake	MR	peg	976 (ur)	peg emplacement	Wasserburg & Hayden (1955)

as comprising the Nepewassi and Tilden Lake domains and the Grenville Front Tectonic Zone northeast of the Beaverstone domain (Fig. 1.2) and reported ages of 2.7-2.3 Ga for it. Krogh and Davis (1969) first documented the presence of Archean orthogneiss in this region using Rb-Sr methods; concurrent and more recent U-Pb zircon and titanite ages (Steiger and Wasserburg 1969; Krogh and Davis 1970*b*, 1974; Krogh and Wardle 1984; Krogh 1991; Krogh et al. 1992; Chen et al. 1993) indicate primary crystallization of orthogneiss and high-grade metamorphism in the interval 2680-2600 Ma. Metamorphism and deformation before 2700 Ma is also locally indicated (Krogh 1989). The River Valley anorthosite complex, located 50 km east of Sudbury near the Grenville Front, was emplaced at *ca.* 2560 Ma (Ashwal and Wooden 1989) and is the oldest anorthosite body known in the Grenville Province. Minimal Proterozoic disturbance of isotopic systems in this complex and other rocks suggests that Grenvillian metamorphism was not strong near the Grenville Front (Krogh and Davis 1970; Ashwal and Wooden 1989). The data from Ontario are broadly consistent with Archean Rb-Sr and U-Pb ages south of the Grenville Front in western Quebec (Doig 1977; Krogh and Wardle 1984).

Late Paleoproterozoic Events (*ca.* 1750-1600 Ma)

A second age group is mainly defined by plutonic rocks of the Parautochthonous Belt that were intruded between 1750-1600 Ma. A granitic orthogneiss in the French River area has a Rb-Sr age of *ca.* 1845 Ma (Krogh and Davis 1973) and represents the oldest orthogneiss known in the Central Gneiss Belt outside of the Archean gneiss region described above; this age remains to be confirmed by U-Pb dating. Within and immediately

northwest of the Grenville Front Tectonic Zone, primary crystallization of felsic to ultramafic igneous rocks, including felsic hypabyssal and volcanic units near Killarney (Killarney Magmatic Belt; Easton 1992), took place at *ca.* 1747-1700 Ma (Krogh et al. 1971; Krogh and Wardle 1984; van Breemen and Davidson 1988; Krogh 1989; Davidson et al. 1992; Prevec 1992). The Chief Lake granite appears to be a younger intrusion (*ca.* 1626 Ma; Krogh and Davis 1969). Similar plutonic ages have been obtained from orthogneiss near Huntsville, Key Harbour and Pointe-au-Baril (Nadeau 1990; Krogh et al. 1993*a*; Corrigan et al. 1994), indicating that this plutonism extended to the southeast. The youngest plutonic rocks in this age group are *ca.* 1608 Ma orthogneisses in the Go Home domain (Krogh 1991) and a 1606 ± 2 Ma granodiorite member of the Nadeau Island gneiss association in the Pointe-au-Baril area (Culshaw et al. in prep.).

The *ca.* 1750-1600 Ma plutons appear to have intruded subordinate supracrustal units for which few isotopic constraints on deposition age currently exist. Northwest of Mattawa in the Tomiko domain (Fig. 5.1), Krogh (1989) documented a *ca.* 1686 Ma maximum deposition age for quartzite. At Key Harbour, Corrigan et al. (1994) showed that deposition and high-grade metamorphism of paragneiss occurred before emplacement of the Key Harbour orthogneiss at 1694 Ma. The timing of early metamorphism is not precisely known, but Krogh and Davis (1971) suggest a *ca.* 1800 Ma age based on Rb-Sr data.

Early Mesoproterozoic Events (*ca.* 1520-1280 Ma)

The third age group encompasses plutonic, metamorphic and depositional events

documented in the western Central Gneiss Belt mainly at 1470-1280 Ma, including late intrusion of anorthositic and granitic-tonalitic masses. A *ca.* 1523 Ma primary crystallization age reported for granite near Killarney (Krogh et al. 1971) represents an anomalously old age in this group.

Voluminous felsic to intermediate plutons were emplaced into allochthonous and parautochthonous domains between 1471 Ma and 1375 Ma (Lumbers 1975; Krogh and Davis 1969; van Breemen et al. 1986; van Breemen and Davidson 1988, 1990; Corrigan 1990; Nadeau 1990; Krogh et al. 1992, 1993*a*; Corrigan et al. 1994; Culshaw et al. in prep.). High-grade metamorphism in the parautochthon at *ca.* 1454-1420 Ma accompanied magmatism (Krogh 1989; Bethune et al. 1990; Nadeau 1990; Tuccillo et al. 1992; Haggart et al. 1993; Krogh et al. 1992, 1993*a*; Ketchum et al. 1994). Plutonism, volcanism and clastic sedimentation in the interval 1360-1280 Ma contributed new crust in at least two allochthonous domains. The Whitestone anorthosite and Marginal orthogneiss were emplaced in the Parry Sound and Shawanaga domains, respectively, at about 1350 Ma (van Breemen et al. 1986). Granitic to tonalitic plutons that intruded the Parry Sound domain between 1360 Ma and 1280 Ma (Macfie et al. 1992; Wodicka 1994) form a significant component of this domain. Detrital zircon data for two quartzite units in the Parry Sound domain imply deposition after 1438 ± 23 Ma and 1121 ± 4 Ma; the former maximum deposition age can likely be reduced to 1385 ± 4 Ma, the $^{207}Pb/^{206}Pb$ age of a weakly discordant single grain from this unit (Wodicka 1994). Sedimentation in the Shawanaga domain occurred after 1417 ± 5 Ma, with deposition of volcanogenic sediments in the interval 1390-1360 Ma and further volcanism(?) at ca. 1333 Ma (Culshaw

et al. in prep.).

Late Mesoproterozoic (Grenvillian) Events (*ca.* 1240-960 Ma)

The fourth age group comprises geologic events after intrusion of the 1244 Ma, A-type Mulock Batholith (Lumbers et al. 1991) and 1238 Ma Sudbury diabase dyke swarm (Krogh et al. 1987). Many, if not all, of the events after 1238 Ma are considered here to be manifestations of Grenvillian orogenesis.

Small anorthositic plutons were emplaced west of Lake Nipissing in the interval *ca.* 1222-1206 Ma (Prevec 1992), followed by widespread but volumetrically minor intrusion of olivine-bearing metagabbro at *ca.* 1170-1150 Ma (Davidson and van Breemen 1988; van Breemen and Davidson 1990; Heaman and LeCheminant 1994). Thrust movement on the Parry Sound shear zone at *ca.* 1159-1157 Ma (van Breemen et al. 1986; Wodicka 1994) represents the oldest-known Grenvillian tectonic event in the Central Gneiss Belt; granulite facies metamorphism, intrusion of anorthosite and rapid cooling from granulite facies at high structural levels within the Parry Sound domain accompanied thrusting (van Breemen et al. 1986; Tuccillo et al. 1992; Wodicka 1994). Between 1160 Ma and 1080 Ma, movement on bounding shear zones and metamorphism continued in the Parry Sound domain (van Breemen et al. 1986; van Breemen and Davidson 1990; Jamieson et al. 1992; Krogh et al. 1993*a*; Bussy et al. 1993; Wodicka 1994). Final northwest-directed thrust emplacement of this domain likely occurred at *ca.* 1120-1080 Ma (Wodicka 1994). In contrast, van Breemen et al. (1986) suggested ca. 1160 Ma emplacement of the Parry Sound domain onto the Shawanaga domain. The 1160 Ma

result has recently been interpreted to date intra- rather than inter-domain thrusting (*i.e.*, Parry Sound thrust sheet over the Parry Island thrust sheet; Jamieson et al. 1992; Wodicka 1994).

Grenvillian events in the interval 1080-960 Ma were characterized by relative quiescence in the Parry Sound domain and extensive tectonic and metamorphic activity throughout the rest of the western Central Gneiss Belt. In allochthonous and parautochthonous domains east of the Parry Sound domain, late syn-thrusting pegmatites were intruded between 1097 and 1027 Ma (Nadeau 1990). High-grade tectonometamorphic events before 1097 Ma (Nadeau 1990; Mezger et al. 1993) were followed by further high-grade thermal and tectonic activity south and east of the Parry Sound domain until at least *ca.* 1020 Ma (van Breemen et al. 1986; Davidson and van Breemen 1988; van Breemen and Davidson 1990; Nadeau 1990; Mezger et al. 1993; Bussy et al. 1993). Pegmatite ages of 1080-1078 Ma and 1068 Ma in boudined anorthosite from the Shawanaga shear zone (Krogh et al. 1993*a*) may record an early deformation phase on this zone (northwest-directed thrusting?). Zircon, titanite and monazite ages in the Britt and Shawanaga domains record metamorphism in the interval *ca.* 1060-1020 Ma (Corrigan 1990; Tuccillo et al. 1992; Krogh et al. 1993*a*; Culshaw et al. in prep.); a northward younging of metamorphic ages is consistent with advance of the orogen toward the northwest during this period (Jamieson et al. 1992; Culshaw et al. in prep.).

The waning stages of Grenvillian orogenesis in Ontario are recorded mainly in parautochthonous rocks near the Grenville Front. Ages of *ca.* 1020-960 Ma for

deformation, metamorphism, pegmatite emplacement, and cooling are reported from the Grenville Front Tectonic Zone and the northern Britt domain (Krogh and Davis 1974; Krogh 1989; Corrigan 1990; Krogh 1991; Haggart 1991; Bethune 1991; Haggart et al. 1993; Mezger et al. 1993; Chen et al. 1993; Krogh et al. 1993*b*; Corrigan et al. 1994). U-Pb ages between 1020 Ma and 960 Ma from the orogenic interior include a late tectonic pegmatite dyke emplaced in the Go Home domain at 1008 Ma (Krogh 1991), *ca.* 1006 Ma and *ca.* 990 Ma growth of new zircon at a high structural level in the Shawanaga shear zone near Pointe-au-Baril (Krogh et al. 1993*a*; Culshaw et al. in prep.), a 998 ± 15 Ma titanite lower intercept in Britt domain orthogneiss west of Pointe-au-Baril (Krogh et al. 1993*a*), and uraninite ages of 1017-976 Ma for pegmatite emplacement in the Moon River and Kiosk domains (Nier et al. 1941; Wasserburg and Hayden 1955; Shillibeer and Cummings 1956; Tilton et al. 1960; Stockwell 1982). New data presented below extend the number of ages in the 1020-960 Ma interval for the Pointe-au-Baril area.

5.3 SAMPLE SELECTION AND ANALYTICAL PROCEDURE

Twenty one samples were collected in the Pointe-au-Baril area for U-Pb dating. The results presented herein represent a portion of the data obtained from these samples; the remaining analyses are reported by Krogh et al. (1992, 1993*a*) and Culshaw et al. (in prep.) and are summarized in this chapter where relevant.

Fresh samples weighing up to 25 kg were collected from the locations shown in Figure 5.2 and reported in Appendix B (UTM coordinates). Collection strategy was based on a number of criteria, including (*i*) geographic location (to obtain adequate coverage

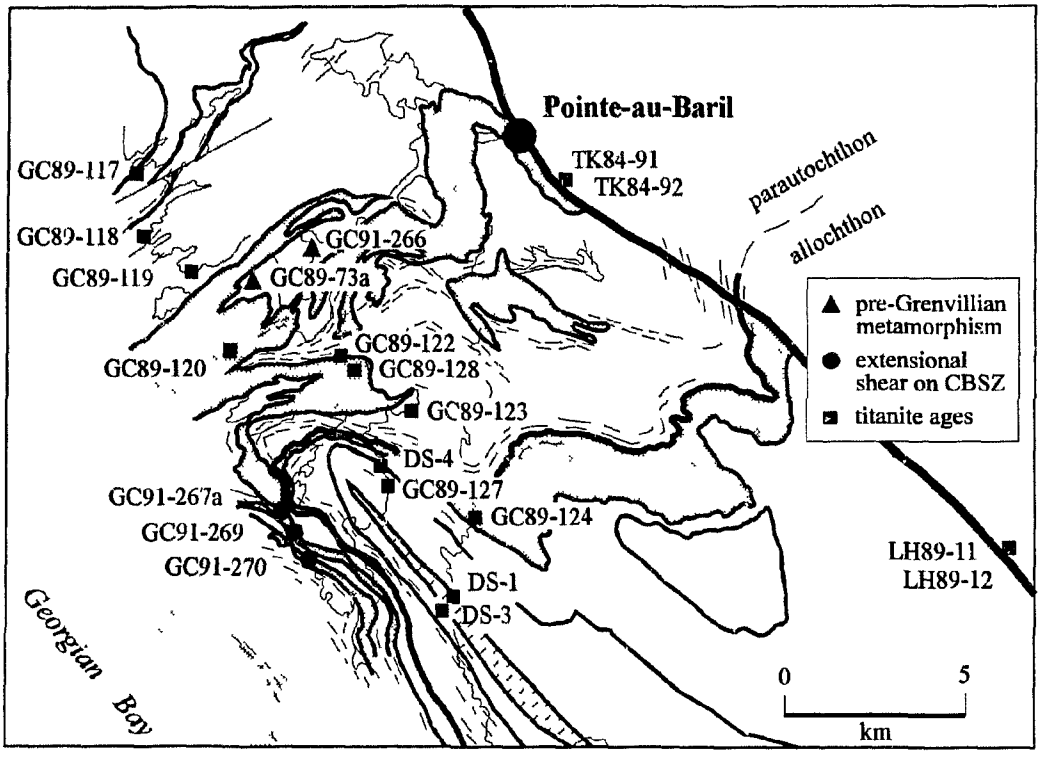

Fig. 5.2. Location of samples collected in the Pointe-au-Baril area for U-Pb dating. Solid lines = geological boundaries (Fig. 2.2); dashes = trend of shear fabrics; shading = ca. 1.45 Ga granitoid plutons; diagonal line pattern = Dillon schist (Sand Bay gneiss association). See Appendix B for UTM sample coordinates.

forthermal history studies), (*ii*) lithology (to determine protolith ages), (*iii*) deformation state (to determine the influence of high-grade deformation on U-Pb systematics, and to bracket the timing of deformation), and (*iv*) metamorphic characteristics (to obtain ages of metamorphism and leucosome formation). A description of the full analytical procedure is provided in Appendix C. Fraction descriptions, U-Pb concentrations, isotopic ratios and ages are reported in Tables 5.2-5.4 and concordia diagrams are presented in Figures 5.5, 5.8, 5.9, and 5.11. Errors in the Pb/U and $^{207}Pb/^{206}Pb$ ratios, shown as ellipses on the concordia diagrams, represent 2-sigma uncertainties calculated using a software program written at the Royal Ontario Museum by L. Heaman (now at the University of Alberta) that propagates all known sources of error. Discordia lines were calculated following the two-error regression treatment of Davis (1982).

5.4 RESULTS

Age of Pre-Grenvillian Granulite Facies Metamorphism

As described in Chapters 2 and 3, granulite facies mineral assemblages pre-dating Grenvillian orogenesis are located in a low-strain window between the Nares Inlet and Shawanaga shear zones. These high-grade assemblages are preserved in mafic supracrustal (volcanic?) gneiss interlayered with other gneisses of supracrustal origin. Grenvillian amphibolite facies fabrics locally overprint the early assemblages. The supracrustal package is intruded by megacrystic granite and tonalite of the Pointe-au-Baril complex. Extensive dating of Pointe-au-Baril complex rocks and the granodioritic Shawanaga pluton indicates igneous crystallization of both bodies at 1460 +12/-8 Ma (Culshaw et al.

in prep.). Krogh et al. (1993*a*) obtained a *ca.* 1430 Ma crystallization age for the volumetrically less abundant tonalite member of the Pointe-au-Baril complex. Although further geochronometric work is required, the data imply a *ca.* 30 M.y. emplacement interval for the Pointe-au-Baril complex. These ages are consistent with U-Pb data from other felsic to intermediate plutons throughout the western Central Gneiss Belt and Grenville Front Tectonic Zone indicating extensive *ca.* 1470-1375 Ma magmatic activity.

Sample and Fraction Descriptions

Three fresh, orthopyroxene-bearing samples were collected from little-deformed mafic supracrustal gneiss with plagioclase-rich leucosomes in order to constrain the timing of pre-Grenvillian granulite facies metamorphism. Sample GC89-73*a* is a migmatitic mafic gneiss with the assemblage plagioclase + amphibole + garnet + orthopyroxene + ilmenite-hematite, with accessory quartz, apatite and rutile. A *P-T* estimate of 7.2 kbar and 700°C has been obtained for this sample (Chapter 4). Plagioclase, orthopyroxene and garnet are abundant in medium-grained leucosomes which locally cut a weak foliation (Fig. 5.3*a*). The dominant zircon population consists of small, equant, colourless, multifaceted grains without fractures or inclusions (Fig. 5.4*a*). This morphology is typical of zircon growth in a high-grade metamorphic environment (van Breemen et al. 1987). Larger, rounded grains with apparent resorption features are less abundant and range from irregular and roughly equant (Fig. 5.4*b*) to irregular with highly concave grain surfaces (Fig. 5.4*a*). The former morphology suggests resorption of low aspect ratio prisms whereas the latter may represent zircon overgrowths that have broken away from their

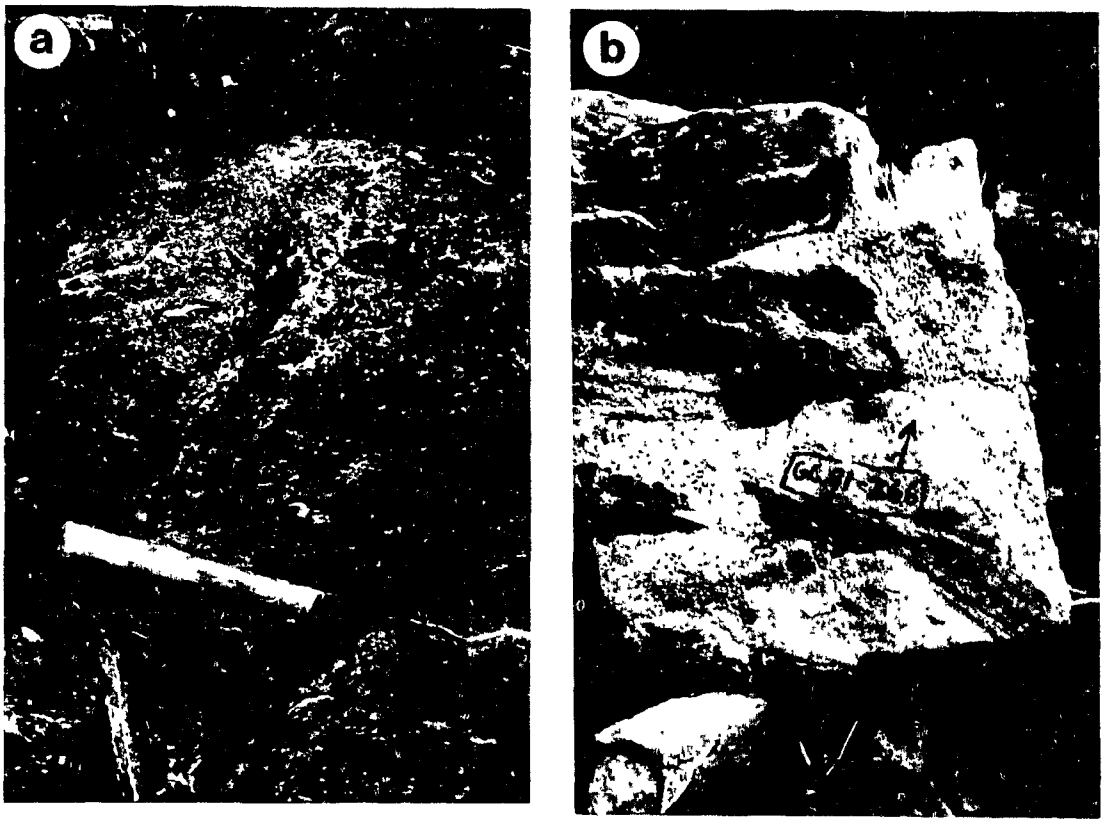

Fig. 5.3. Pre-Grenvillian granulite facies rocks dated by U-Pb geochronology. Sample locations given in Figure 5.2 and Appendix B. **a)** Mafic supracrustal gneiss with orthopyroxene-bearing, plagioclase-rich leucosomes cutting a weak foliation (GC89-73a). **b)** Abundant leucocratic veins identical to those in a) containing enclaves of mafic supracrustal gneiss (GC91-266).

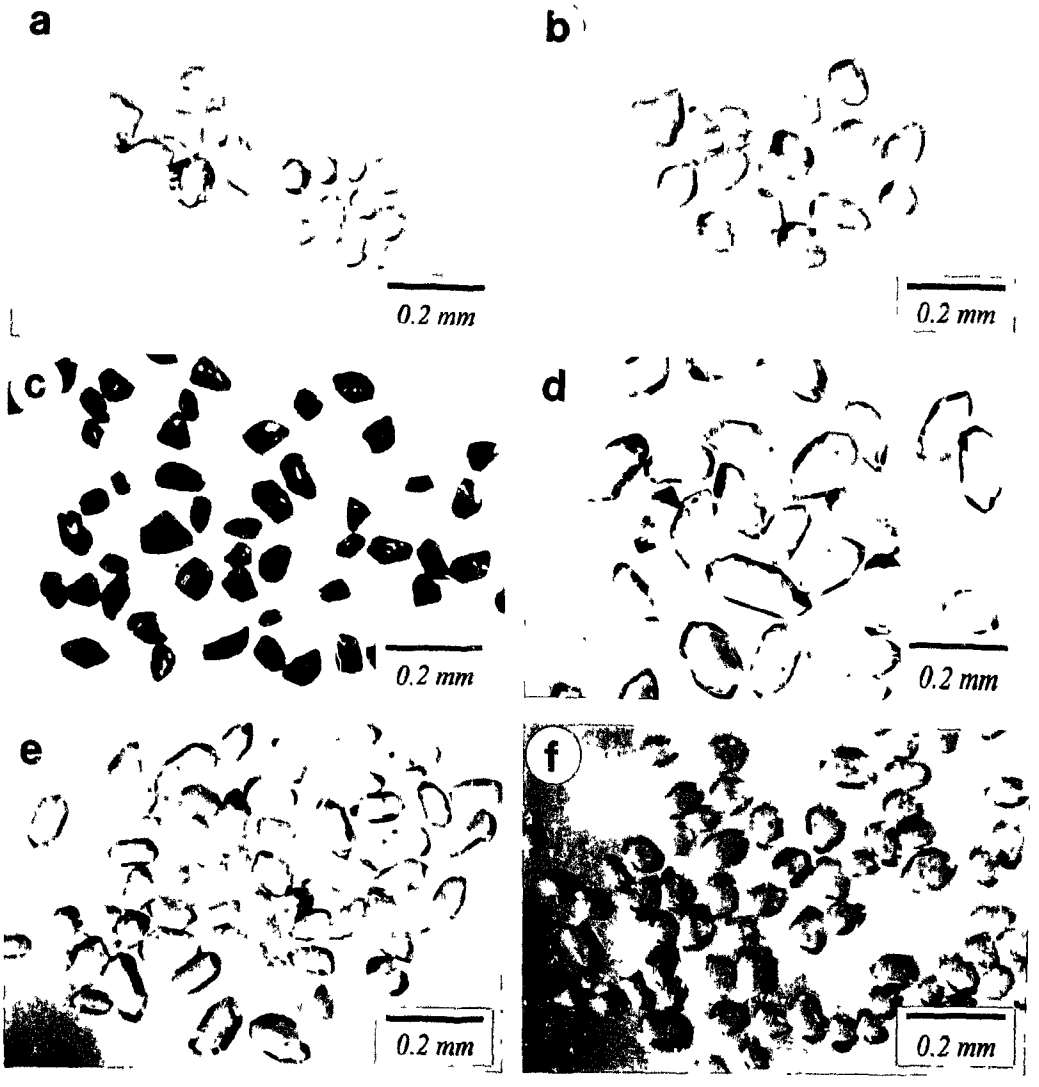

Fig. 5.4. Zircon and rutile fractions from granulite facies gneiss. Fraction numbers in parentheses. **a)** Equant, multifaceted zircon (73a-1, right) and irregular grains with concave surfaces suggesting an overgrowth phase broken away from cores. **b)** Rounded, irregular zircon (73a-2). **c)** Multifaceted, euhedral rutile (73-3). **d)** Euhedral, 3:1 aspect ratio, prismatic zircon (266-3). **e)** 2:1, euhedral zircon prisms (266-1). **f)** Prismatic, stubby zircon (266-2).

cores during sample crushing. A fraction of small multifaceted grains (Fig. 5.4*a*) and one of irregular, 2:1 aspect ratio grains without concave surfaces (Fig. 5.4*b*) were selected for analysis.

Abundant rutile in sample GC89-73*a* is yellow to dark brownish red and gem-like with strong variations in transparency and abundance of fractures. Strong colour zonation is common within individual grains. A fraction of dark red rutile grains without fractures and a minimum of intra-grain colour variation was isolated for analysis (Fig. 5.4*c*).

Samples GC91-266*a* and GC91-266*b* consist almost entirely of leucosome material from the mafic gneiss and were collected from a locality where this component is abundant (Fig. 5.3*b*). The sampled veins are compositionally identical to smaller segregations which fill the necks of boudined gneiss layers (*e.g.*, Fig. 5.3*a*). Plagioclase and orthopyroxene dominate the mineral asemblage; amphibole, biotite, garnet, hematite-ilmenite and magnetite are also present. The samples are identical except in the amount of mafic host material present (~5-6% in GC91-266*a* versus ~3% in GC91-266*b*) and were combined to form a single sample (GC91-266). Fragments of host rock were removed during coarse crushing to further enrich the leococratic component. Three zircon fractions were isolated from this sample for analysis. Each consisted of high-quality, colourless grains with numerous crystal facets, a hexagonal to octagonal cross-section, and rare inclusions. Fractions of large, 3:1 aspect ratio prisms (Fig. 5.4*d*) and smaller 2:1 prisms (Fig. 5.4*e*), and a fraction of roughly equant grains (Fig. 5.4*f*) were chosen. The bipyramidal prismatic form of these grains is characteristic of unimpeded growth in a liquid (*e.g.*, Silver 1969), suggesting growth in the crystallizing leucosome during

high-grade metamorphism. Dissimilarities in mineralogy and zircon morphology preclude the possibility that the sampled material represents veins of Pointe-au-Baril complex granite.

U-Pb Results

U-Pb results for the granulite facies samples are given in Table 5.2 and Figure 5.5. The low (<300 ppm) U contents of all analysed zircon fractions lends support to a metamorphic origin for these grains (Heaman and Parrish 1991).

Small multifaceted grains from the weakly migmatitic mafic gneiss (GC89-73a) are concordant at 1452 ± 2 Ma, whereas rounded, irregular grains from this sample yield a $^{207}Pb/^{206}Pb$ age of 1433 ± 1 Ma with slight negative discordance. Incomplete dissolution of this very low U (15 ppm) fraction may account for the slight negative discordance (*e.g.*, Krogh 1973). Rutile from the mafic gneiss sample is 3.3 % discordant with a $^{207}Pb/^{206}Pb$ age of 917 Ma. If this discordance is a function of recent isotopic disturbance, the $^{207}Pb/^{206}Pb$ ratio provides the most accurate estimate of age, presumed to reflect cooling through the rutile closure temperature (~400°C; Mezger et al. 1989*b*).

Three fractions of prismatic zircon from sample GC89-266 are from 0.4 to 1.7 % discordant and define a discordia line with an upper intercept of 1448 ± 1 Ma (95% probability of fit). A lower intercept of -14 Ma indicates that discordance may be due to recent Pb-loss during weathering or high-level, low-temperature fluid interaction (*e.g.*, Heaman and Parrish 1991).

These data provide conclusive evidence for new zircon growth associated with

TABLE 5.2. U/Pb Zircon and Rutile Data for Granulites

Description	Weight	Concentrations			Atomic Ratios[c]				Apparent Age (Ma)		
fraction number and properties[a]	(mg)	U (ppm)	Pb^{rad} (ppm)	common Pb (pg)	$\frac{^{206}Pb}{^{204}Pb}$[b]	$\frac{^{206}Pb}{^{238}U}$	$\frac{^{207}Pb}{^{235}U}$	$\frac{^{207}Pb}{^{206}Pb}$	$\frac{^{206}Pb}{^{238}U}$	$\frac{^{207}Pb}{^{235}U}$	$\frac{^{207}Pb}{^{206}Pb}$
GC89-73a mafic granulite											
1. s, eu, mf, eq, (42)	0.121	14	4	27	1608	0.25229	3.1752	0.09128	1450	1451	1452
2. m, an, rsb, 2:1, (15)	0.082	15	4	7	10903	0.24957	3.1086	0.09034	1436	1435	1433
3. rutile, s, eu, mf, eq, (150)	0.372	5	1	30	1573	0.14772	1.4176	0.06960	888	896	917
GC91-266 leucosome											
1. m, eu, pr, 2:1, (53)	0.181	255	67	5	>100000	0.25094	3.1514	0.09108	1443	1445	1448
2. m, eu, pr, eq, (86)	0.246	249	65	16	88077	0.24987	3.1318	0.09109	1438	1442	1448
3. l, eu, pr, 3:1, (12)	0.156	250	64	13	53497	0.2476	3.1096	0.09109	1426	1435	1448

[a] All fractions are zircon except where indicated. Zircon selected from non-magnetic fractions at 1.6 A, 1° forward slope and 0° side tilt on a Frantz isodynamic separator. All fractions (except rutile) were abraded using the technique of Krogh (1982). Properties: s = small (<80 μm), m = medium (>80 and <150 μm), l = large (>150 μm), eu = euhedral, an = anhedral, mf = multifaceted, pr = prismatic, rsb = resorbed, eq = equant, 2: 1, 3:1 = length:width ratio. Parentheses enclose number of grains analysed.

[b] Corrected for blank (0.5-2 pg U and 2-10 pg Pb) and spike Pb, and for mass fractionation (+0.1%/amu for U and Pb).

[c] Corrected for blank and spike Pb, fractionation, and initial common Pb calculated after Stacey and Kramers (1975).

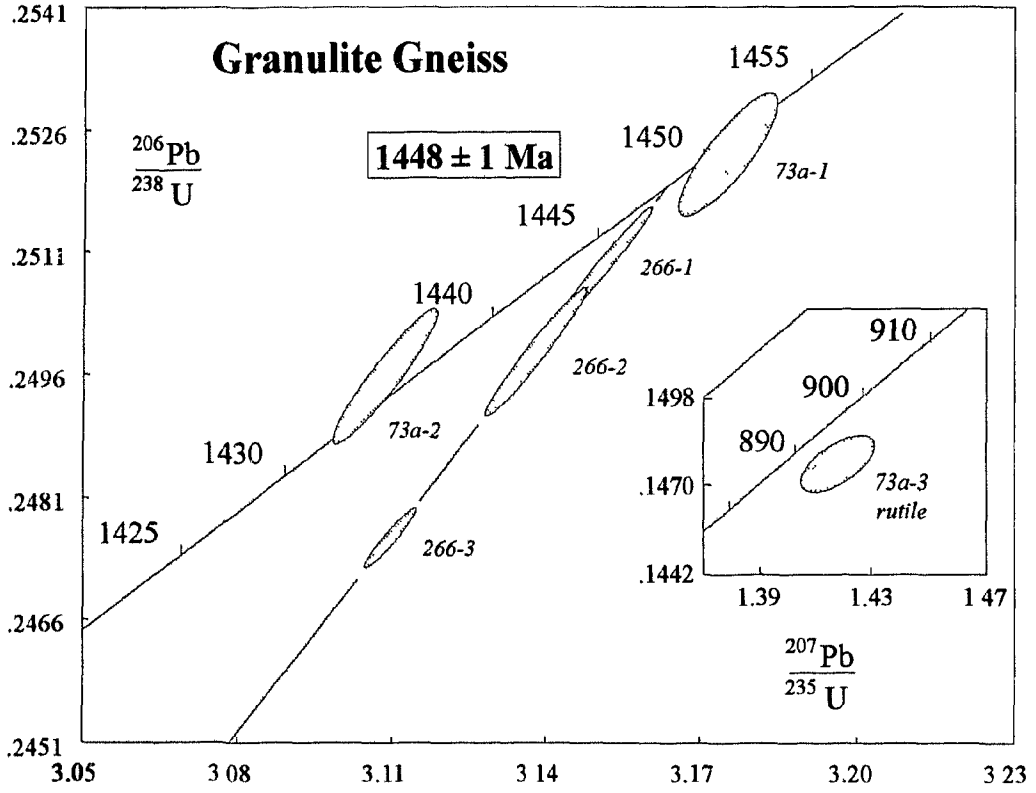

Fig. 5.5. U-Pb concordia diagram for migmatitic mafic granulite (sample GC89-73a) and orthopyroxene-bearing leucosome from mafic granulite (sample GC91-266). Inset shows rutile analysis from migmatitic mafic granulite. Sample locations shown in Fig. 5.2.

granulite-facies metamorphism and anatexis at *ca.* 1450 Ma. A clustering of ages between 1452-1448 Ma suggests that leucosome development and metamorphic zircon growth mainly occurred at this time. The 1433 Ma age of irregular grains from the mafic gneiss sample is less readily interpreted. If the irregular form of these grains indicates high-grade resorption of prismatic grains at or shortly after 1433 Ma, why is there no morphological or isotopic evidence of this event in older multifaceted zircons from the same sample?

At least four possibilities can account for the younger zircon age: (*i*) corrections for common and blank Pb yield an incorrect age as the magnitude of these corrections is greatest for low total Pb concentrations (344 pg for this fraction), (*ii*) prismatic grains crystallized in, and were subsequently resorbed by, a second melt fraction formed at 1433 Ma, (*iii*) prismatic and multifaceted grains crystallized at *ca.* 1450 Ma, but only prismatic zircon underwent resorption and isotopic resetting at 1433 Ma, or (*iv*) the irregular shape represents an original morphology of zircon that crystallized at *ca.* 1433 Ma.

Of these possibilities, the first and second are difficult to evaluate without further data (*e.g.*, common Pb isotopic data from feldspars, and field evidence for cross-cutting leucosomes), and the third relies on the assumption that isotopic resetting is a function of grain resorption, a premise neither supported nor refuted by the data. Evidence that the irregular grain shape represents an original morphology is also lacking. However, Poldervaart (1956) and Spotts (1962) describe irregular zircon morphologies in mafic igneous rocks which they interpreted to reflect impeded late-stage growth in a crystal-rich magmatic environment. Zircon from a meta-quartz gabbro in the Parry Sound domain has a rounded, irregular form, taken to indicate an original igneous morphology that is

preserved beneath narrow metamorphic overgrowths (van Breemen et al. 1986). Based on these descriptions, it appears plausible that zircon growth morphologies in mafic gneiss at anatectic conditions could resemble those of late-crystallizing zircon in mafic igneous rocks. This would indicate high-grade metamorphic zircon growth in the mafic gneiss at 1433 ± 1 Ma, and is consistent morphological evidence (*e.g.*, Fig. 5.3*a*) for two episodes of zircon growth. A second high-grade thermal event at 1433 Ma would be consistent with the observed temporal relationship of early Mesoproterozoic plutonism and metamorphism in the Central Gneiss Belt (*e.g.*, Schau et al. 1986; Nadeau 1990; Tuccillo et al. 1992) as intrusion of megacrystic tonalite in the Pointe-au-Baril complex is indicated at 1430 ± 17 Ma (Krogh et al. 1993*a*).

Timing of Extension Reactivation of the Shawanaga Shear Zone

The Shawanaga shear zone is a ~3 km thick succession of highly deformed, folded gneissic tectonite interleaved with lower strain panels preserving older fabrics. Although it closely resembles thrust-sense tectonite zones in the Central Gneiss Belt (*e.g.*, Davidson 1984*a*), numerous shear-sense indicators in the Shawanaga shear zone near Pointe-au-Baril indicate syn-metamorphic, southeast-directed extensional displacement. Evidence for earlier northwest-directed thrusting is preserved 60 km along strike to the northeast where extensional shear fabrics are less penetrative (Ketchum et al. 1992). Clearly, knowledge of the timing of both thrusting and extension on the Shawanaga shear zone has important implications for the local and regional orogenic evolution if this structure marks the Allochthon Boundary Thrust in the western Grenville orogen (*e.g.*,

Culshaw et al. 1994; Chapter 2).

In the absence of stratigraphic controls and biotic markers, workers have increasingly relied on quantitative geochronology to constrain the timing of deep-level tectonic activity in collisional orogens. A popular method of determining shear zone movement age is by obtaining the crystallization age of synkinematic igneous veins within these zones. The veins are considered synkinematic where they cut ductile shear fabrics but themselves contain similarly-oriented fabrics that are interpreted to have formed during continued shearing (*e.g.*, Nadeau and Hanmer 1992; Hanmer and McEachern 1992; McEachern and van Breemen 1993; Scott et al. 1993). In the Grenville Province, U-Pb dating of synkinematic veins has been used to constrain the timing of both Grenvillian and pre-Grenvillian tectonic events (*e.g.*, Krogh and Davis 1974; van Breemen and Hanmer 1986; van Breemen et al. 1986; Nadeau 1990; van Breemen and Davidson 1990; Krogh 1991; Hanmer and McEachern 1992; McEachern and van Breemen 1993; Connelly and Heaman 1993; Scott et al. 1993; Wodicka 1994). An example of the use of this method comes from the Central Gneiss Belt where U-Pb zircon ages of synkinematic pegmatites and granitic veins have been suggested to indicate a southeastward migration of latest thrusting, inferring thrust stacking in an out-of-sequence or 'break-back' fashion (Nadeau 1990; Nadeau and Hanmer 1992).

Syntectonic versus Synkinematic

Several authors (*e.g.*, van Breemen et al. 1986; van Breemen and Hanmer 1986; Hanmer and Passchier 1991; Hanmer and McEachern 1992; Scott et al.1993) have

described veins emplaced during progressive shear as 'syntectonic'. Although this term refers to "...a geologic process or event occurring during any kind of tectonic activity..." (Glossary of Geology, American Geological Institute) and is therefore scale-independent, tectonic activity is most commonly described on a regional to orogen-wide scale. Given this common usage, geochronologic data from a vein interpreted as syntectonic may be presumed to yield information on large-scale tectonic events when in fact this relationship is often difficult to prove However, the data always contribute to a local kinematic analysis of a shear zone regardless of the contribution of this zone to the regional tectonic evolution. For this reason, the term *synkinematic* is preferred here in describing these veins. In order to demonstrate the large-scale tectonic significance of shear zone activity, additional information on related orogenic events such as the timing of metamorphism and cooling is often required.

Potential Problems in Dating Synkinematic Veins

Although a potentially powerful tool for dating deformation, several pitfalls can hamper U-Pb dating of synkinematic veins. Some of these potential problems are described below (*cf* Gower 1993).

1) A common (and sometimes erroneous) conclusion reached in employing this technique is that the crystallization age of a synkinematic vein directly represents the age of significant tectonic activity, such as thrusting within an orogenic belt. These veins, and hence their crystallization ages, are more precisely interpreted as *late* synkinematic (*e.g.*,

van Breemen and Hanmer 1986; Nadeau 1990; Hanmer and McEachern 1992) as veins emplaced prior to the waning stages of deformation will become highly deformed and sub-concordant, making a synkinematic interpretation difficult. In fault zones which remain active over a lengthy time interval, late synkinematic veins may only provide a minimum age for the bulk of tectonic transport.

2) At most crustal levels, reactivation of older fault zones is often kinematically favoured over propagation of new faults during tectonism. For the construction of accurate tectonic models, it must first be established whether reactivation has taken place, and if so, which phase of movement is being dated by synkinematic veins. Independent evidence may be required to determine if veins are synkinematic with respect to a period of tectonically significant fault movement. In orogenic belts, metamorphic and cooling ages in footwall and hanging wall lithologies can provide additional constraints on the timing of major fault displacements.

3) Periods of tectonic activity may alternate with tectonically quiescent intervals, with net displacement along a fault zone equalling the sum of several increments. If the displacement vector remains relatively constant over successive shearing episodes, finite strain fabrics in a shear zone may represent a composite of temporally distinct incremental strain fabrics. This raises the possibility that a cross-cutting 'synkinematic' vein can yield an emplacement age that is significantly older than its actual deformation age (Gower 1993). Where this possibility cannot be convincingly ruled out, independent evidence for the timing of displacement is required. This problem can be overcome to some degree by dating variably deformed veins (*e.g.*, pre-, syn-, and post-kinematic) in a single high-strain

zone. Multi-vein geochronologic data may potentially highlight a false synkinematic relationship and can provide constraints on the initiation and cessation of fault movement.

4) In ductile shear zones, synkinematic dykes of granitic composition are regularly selected for U-Pb dating. However, granitic magmas are typically enriched in Zr which reduces their ability to dissolve inherited zircon (Watson and Harrison 1983). Complex zircon populations in granitic veins may therefore indicate a strong component of inheritance and require several analyses of both single and multi-grain fractions in order to obtain an accurate vein emplacement age. Knowledge of the host rock age may assist in the recognition of an inherited zircon population in a granitic vein if the inherited component is locally derived.

Pegmatite Dykes in the Shawanaga shear zone

Variably deformed, granitic pegmatite dykes are present throughout the Shawanaga shear zone but are most abundant within megacrystic granite of the *ca.* 1460 Ma Pointe-au-Baril complex. The dykes range from little-recrystallized dykes that cut shear fabrics and contain sheared host rock enclaves to highly tectonized and recrystallized concordant sheets (some of which are reduced to narrow trains of feldspar aggregates).

Three pegmatite dykes with variable degrees of finite strain were dated by U-Pb geochronology in order to constrain the timing of extensional displacement on the Shawanaga shear zone. The dykes are pre-kinematic to early synkinematic, late synkinematic, and post-kinematic with respect to extensional shear (Fig. 5.6). All are hosted by strongly sheared megacrystic granite gneiss of the Pointe-au-Baril complex. The

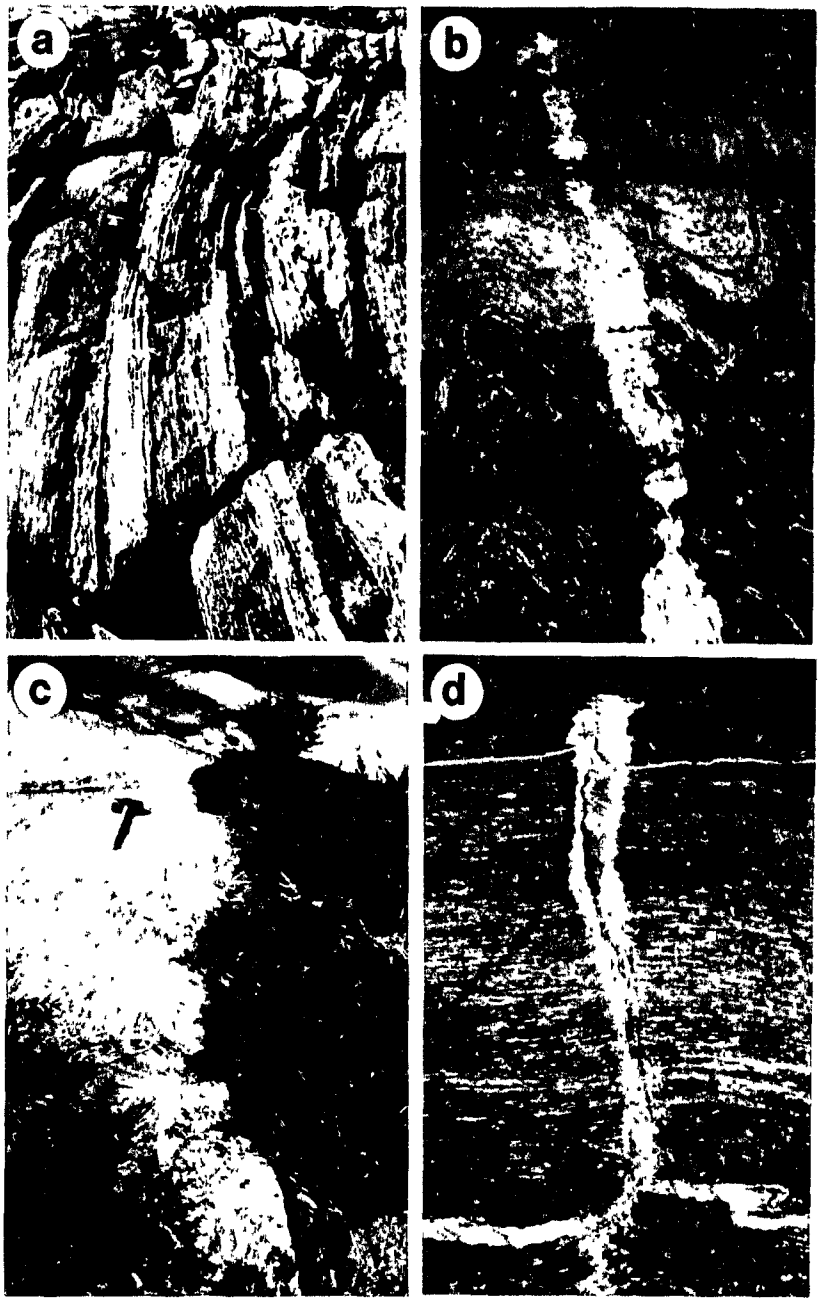

Fig. 5.6. Pegmatite dykes hosted by Pointe-au-Baril complex granite in the Shawanaga shear zone. Sample locations given in Fig. 5.2. **a)** Transposed, strongly sheared, pre-kinematic to early synkinematic dykes (GC91-270). **b)** Late synkinematic dyke with pinch-and-swell structure in the interaxial region of a "Z" fold of porphyroclastic gneiss. **c)** Boudined, partly recrystallized, weakly foliated member of the late synkinematic dyke suite cutting shear fabrics (GC91-267a). **d)** Unrecrystallized, post-kinematic dyke cutting shear fabrics. Note enclaves of sheared host rock in dyke (GC91-269).

samples were collected west of Shawanaga Island within a 400 m across-strike interval over a strike length of less than 1.5 km (Fig. 5.2). Numerous kinematic indicators within this area attest to dextral (extensional) shear.

Pre-Kinematic to Early Synkinematic Dyke. Sample GC91-270 was collected from a highly tectonized, concordant pegmatite sheet (Fig. 5.6*a*). This dyke contains coarse feldspar grains, some with asymmetric tails indicating dextral shear, in a strongly recrystallized quartzofeldspathic matrix containing accessory titanite, allanite, amphibole, biotite and zircon. Isolated amphibole-rich aggregates within the dyke attest to tectonic incorporation of host rock. A strong internal foliation parallel to dyke margins is defined by quartz and feldspar ribbons, by alignment of large (up to 1 cm long) titanite crystals, and locally, by cm-scale feldspar- and amphibole-rich bands. Emplacement of this dyke predates the bulk of extensional shear but whether it was intruded prior to, or during, the early stages of deformation is not known.

A number of zircon morphologies are present in sample GC91-270. Resorbed colourless prisms with fluid inclusions predominate over smaller, clear to light yellow, gem-quality prisms and rounded, multifaceted forms. Rare brown zircon fragments with numerous cracks, possibly derived from crushing of larger prismatic grains, are also observed. A number of anhedral colourless grains are enclosed by thick zircon overgrowths of probable metamorphic origin. Brown zircon overgrowths on colourless rounded cores are rarely observed (Fig. 5.7*b*). To evaluate this complex zircon population, two fractions of resorbed, colorless prisms (Fig. 5.7*a*), two single grain fractions of brown zircon (Fig. 5.7*b*), and a fraction of clear metamorphic overgrowths removed from their

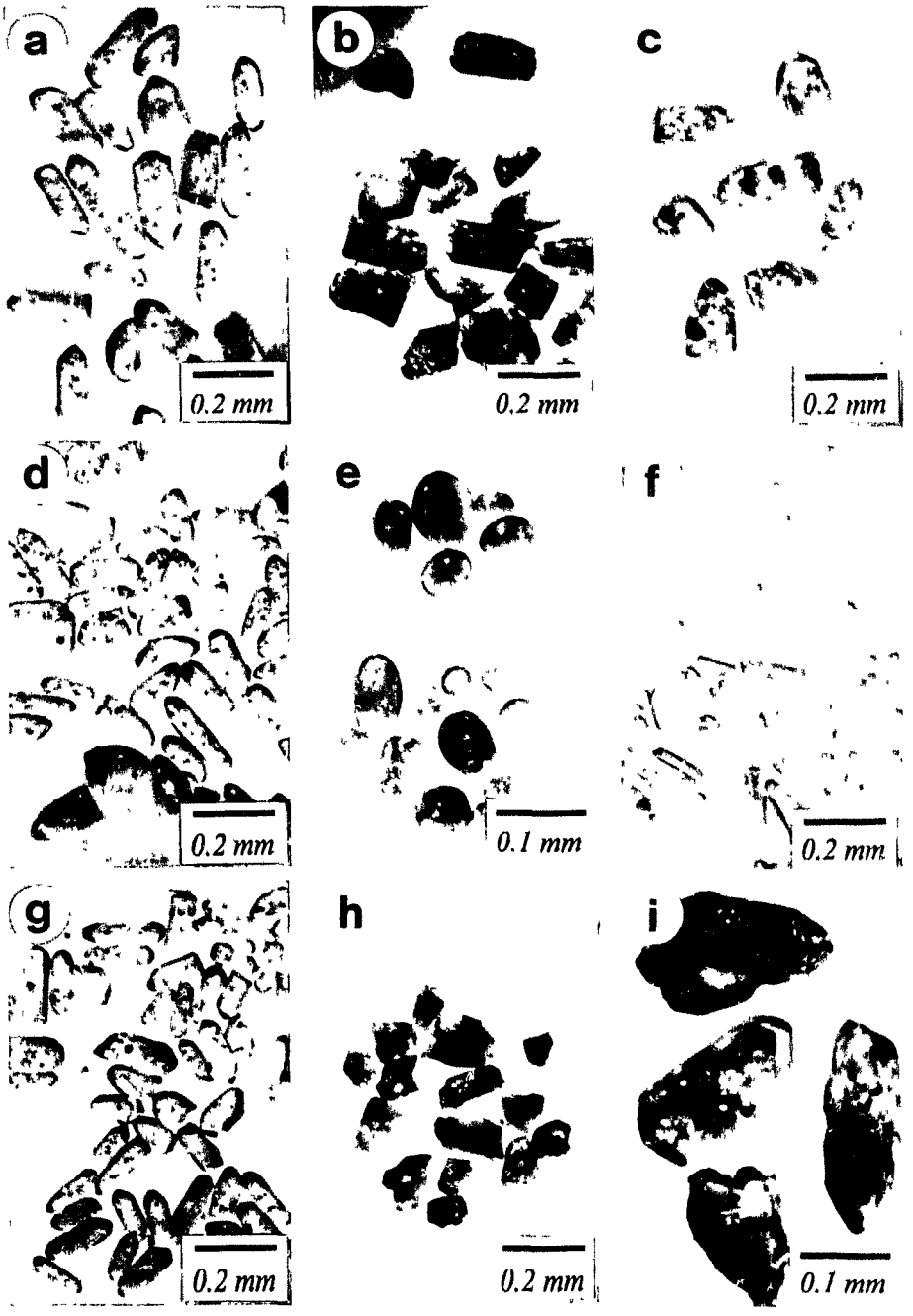

Fig. 5.7. Zircon from pegmatite dykes in the Central Britt shear zone. Brown zircon is a primary crystallizing phase; all other zircon is inherited. Fraction numbers in parentheses. **a)** Prismatic, weakly resorbed grains (270-1,2). **b)** Brown, cracked fragments (270-4,5) and two grains (top) with extensive brown overgrowths. **c)** Clear overgrowths (270-3) on clear, rounded cores. **d)** Moderately resorbed prisms (267a-1,2). **e)** Best (top) and second-best abraded brown fragments (267a-4,5,6, selected from best grains). **f)** Weakly resorbed, needle-shaped grains (267a-3). **g)** Weakly resorbed prisms (269-1). **h)** Brown fragments (269-2,3). **i)** Clear rounded grains with clear prismatic overgrowths; both appear to be overgrown by brown zircon.

cores (Fig. 5.7*c*) were selected for analysis.

Late Synkinematic Dyke. W- to WNW-striking pegmatite dykes, generally less than 1 m wide, cut NW-striking fabrics in the Shawanaga shear zone but are partly recrystallized and contain a weak to moderate tectonic foliation. These dykes typically occupy the interaxial region of minor, asymmetric 'Z' folds (Fig. 5.6*b*), attesting to clockwise rotation of both dykes and adjacent host rocks during extensional shear. Some of these dykes have undergone heterogeneous extension during the latter stages of rotation to form oblique boudin trains (Hanmer and Passchier 1991, p. 62). All of these features suggest emplacement of this dyke suite during late extensional shear.

Sample GC91-267*a* was collected from a 0.4 m wide, boudined member of the late synkinematic suite (Fig. 5.6*c*). Quartz veins typically fill the neck regions between boudins, and ductile flow of adjacent host rocks into these regions is evident from the presence of flow-folded mylonitic foliations. The dyke has a heterogeneous grain size and contains accessory biotite, amphibole, apatite, garnet, titanite, zircon, and late muscovite.

The zircon population in this sample is similar to that described for the pre-kinematic to early synkinematic dyke (GC91-270). Two fractions of resorbed, colourless prisms with fluid inclusions (Fig. 5.7*d*) and three single fragments of brown zircon (Fig. 5.7*e*) were selected for analysis. A single fraction of needle-shaped, 5:1 prisms with rounded terminations, a morphology not present in the older dyke, was also selected (Fig. 5.7*f*).

Post-Kinematic Dyke. Sample GC91-269 was collected from a little-recrystallized, 0.5 m wide pegmatite dyke that cuts shear zone fabrics at a high angle (Fig. 5.6*d*). Granite

enclaves within the dyke have high-strain fabrics identical to those in the host rocks. This pegmatite cuts and offsets granitic veins of the late synkinematic dyke suite (Fig. 5.6*d*), confirming the field chronology indicated for these suites by their deformation states. The presence of chlorite in the sampled dyke is consistent with post-deformation emplacement in a cooling metamorphic terrane.

The zircon population in the post-kinematic dyke is similar to that described for the pre-kinematic to early synkinematic dyke (GC91-270). Colourless prismatic overgrowths on resorbed cores are in some instances overgrown by brown zircon (Fig. 5.7*i*), suggesting two periods of metamorphic zircon growth. A fraction of weakly resorbed, mostly 3:1 colourless prisms with fluid inclusions (Fig. 5.7*g*), and two single grain fractions of brown zircon (Fig. 5.7*h*) were selected for analysis.

U-Pb Results

U-Pb data from the pegmatite dykes (Table 5.3) indicate a wide variety of zircon ages in each sample. As will be demonstrated, this variety can be attributed to the presence of both primary and inherited zircon in the pegmatites. Data for single- and multi-grain fractions interpreted as primary or inherited are presented separately below.

Inherited Zircon Results. Seven fractions of colourless, mainly prismatic zircon were analysed from the three pegmatite dykes. As can be seen in Figure 5.8, all the analyses plot on or near a single discordia line with an upper intercept age of 1457 +10/-11 Ma and a lower intercept age of 1021 ± 23 Ma (47% probability of fit). Fractions 267a-2 (prismatic grains) and 270-3 (colourless metamorphic overgrowths) fall slightly off

TABLE 5.3. U/Pb Zircon Data for Pegmatite Dykes

Description	Weight	Concentrations			Atomic Ratios[c]				Apparent Age (Ma)		
fraction number and properties[a]	(mg)	U (ppm)	Pb^{rad} (ppm)	common Pb (pg)	$^{206}Pb/^{204}Pb$[b]	$^{206}Pb/^{238}U$	$^{207}Pb/^{235}U$	$^{207}Pb/^{206}Pb$	$^{206}Pb/^{238}U$	$^{207}Pb/^{235}U$	$^{207}Pb/^{206}Pb$
GC91-269 post-kinematic dyke											
1. c, pr, wrsb, fl, (13)	0.069	185	36	7	66449	0.19600	2.1751	0.08042	1155	1173	1207
2. b, fr, (1)	0.001	5175	791	8	9503	0.16576	1.6473	0.07208	989	989	988
3. b, fr, (1)	0.001	5593	860	2	>100000	0.16632	1.6576	0.07228	992	992	994
GC91-267a syn-kinematic dyke											
1. c, pr, wrsb, fl, (25)	0.084	96	24	10	22120	0.23347	2.8382	0.08817	1353	1366	1386
2. c, pr, wrsb, fl, (38)	0.161	87	23	28	9126	0.23651	2.9093	0.08921	1369	1384	1409
3. c, n, wrsb, 5:1, (177)	0.120	183	48	11	38106	0.23557	2.8776	0.08860	1364	1376	1395
4. b, fr, (1)	0.001	2229	323	3	20940	0.15673	1.5780	0.07302	939	962	1015
5. b, fr, (1)	0.001	3941	572	3	33384	0.15711	1.5816	0.07301	941	963	1014
6. b, fr, (1)	0.002	3252	496	3	53570	0.16511	1.6642	0.07311	985	995	1017
GC91-270 pre- to early syn-kinematic dyke											
1. c, pr, wrsb, fl, (12)	0.060	90	20	5	>100000	0.20809	2.3880	0.08323	1219	1239	1275
2. c, pr, wrsb, fl, (28)	0.260	92	19	13	39596	0.20310	2.2928	0.08187	1192	1210	1242
3. c, ovgr, (19)	0.036	200	33	13	10195	0.17733	1.8285	0.07478	1052	1056	1063
4. b, fr, (1)	0.010	2849	463	5	>100000	0.17310	1.7657	0.07398	1029	1033	1041
5. b, fr, (1)	0.002	4838	772	5	36510	0.17104	1.7434	0.07393	1018	1025	1039

[a] All zircon grains selected from non-magnetic fractions at 1.6 A, 1° forward slope and 0° side tilt on a Frantz isodynamic separator. Fractions were abraded using the technique of Krogh (1982). Properties: c = colourless, b = brown, fr = fragments, pr = prismatic, wrsb = weakly resorbed, fl = fluid inclusions, ovgr = overgrowths, 5:1 = length:width ratio. Parentheses enclose number of grains analysed.

[b] Corrected for blank (0.5-2 pg U and 2-10 pg Pb) and spike Pb, and for mass fractionation (+0.1%/amu for U and Pb).

[c] Corrected for blank and spike Pb, fractionation, and initial common Pb calculated after Stacey and Kramers (1975).

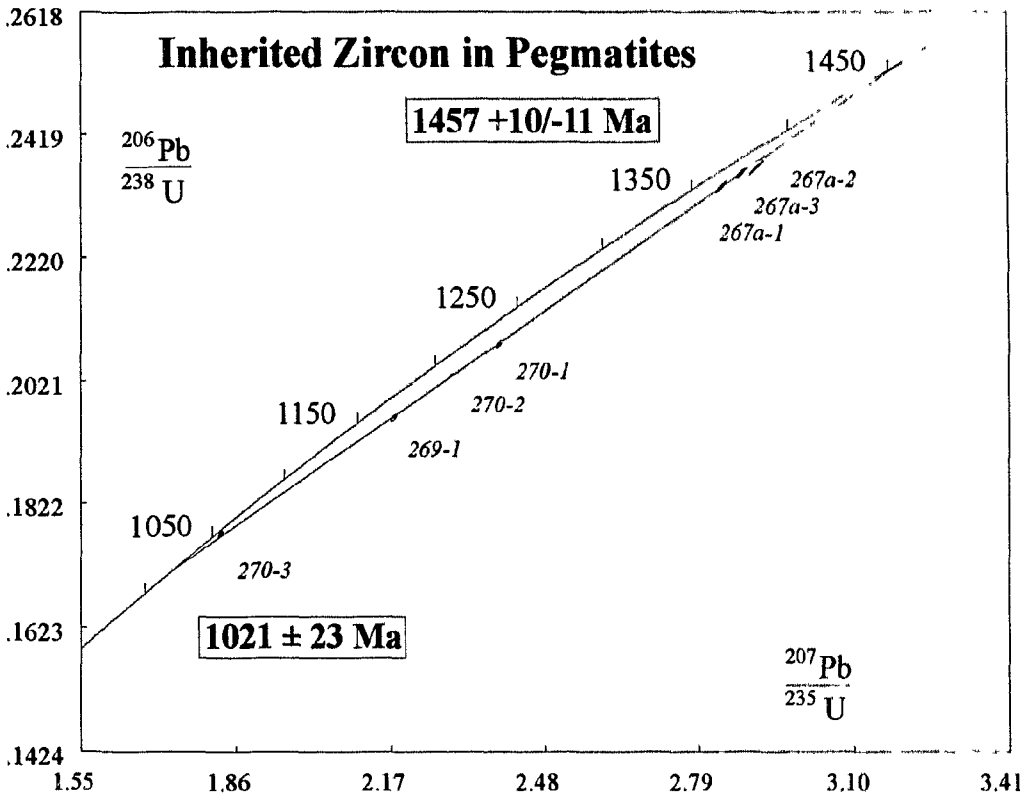

Fig. 5.8. U-Pb concordia diagram for inherited zircon fractions from pre-kinematic (GC91-270), late synkinematic (GC91-267a) and post-kinematic (GC91-269) pegmatite dykes from the Shawanaga shear zone. Discordia line calculated using all analyses except 267a-2 and 270-3. Sample locations shown in Fig. 5.2.

the discordia line and were excluded from the regression analysis. The close fit of all analyses to a single discordia line is surprising given that field relationships show the dykes to be structurally, and therefore temporally, distinct.

At least two interpretations of these data are possible: (*i*) the dykes are pre-, syn-, and post-kinematic with respect to *ca.* 1457 Ma extensional shearing and underwent partial isotopic resetting during Grenvillian metamorphism and deformation at *ca.* 1021 Ma, or (*ii*) the dykes are of Grenvillian age and the colinearity of analyses is due to inheritance from a single-aged source.

Given that Shawanaga shear zone fabrics deform *ca.* 1460 Ma granitic plutons and younger mafic bodies cutting these plutons, and overprint *ca.* 1452 Ma granulite facies assemblages in the footwall (see above), it is unlikely that the first option represents a tenable hypothesis. The second interpretation is therefore considered the more plausible. No evidence for a mixed zircon population was observed in any of the fractions to account for the moderate to strong discordance (22-70%) of the analyses. It is therefore suggested that the 1457 +10/-11 Ma upper intercept represents the age of inherited grains whereas the 1021 ± 23 Ma lower intercept represents a time of partial isotopic resetting. A likely source of inheritance is the Pointe-au-Baril complex granite (1460 +12/-8 Ma; Culshaw et al. in prep.), a premise supported by morphological similarity of the analysed grains to zircon from the granite. The moderate to strong discordance of the analyses is likely the result of *ca.* 1021 Ma Pb-loss during syn-metamorphic extensional shear (see below).

Information on the timing of metamorphism is provided by the analysis of colourless overgrowths on inherited zircon from the pre- to early synkinematic dyke (Fig.

5.7*c*; Fig. 5.8, analysis 270-3). This fraction is 1% discordant with a $^{207}Pb/^{206}Pb$ age of 1063 Ma which dates the metamorphic crystallization of overgrowths if the slight discordance is due to recent Pb-loss. Another possibility is that the discordance is due to a small component of *ca.* 1457 Ma core material in the zircon separate. A regression line forced through 1457 Ma and this analysis yields a lower intercept age of 1035 Ma which provides a second age estimate for the colourless overgrowths. Although both options can account for the slight discordance of analysis 270-3, the presence of brown zircon rims (correlated with dyke emplacement at 1042 Ma; see below) on colourless overgrowths suggests that the latter formed prior to entrainment of inherited zircon in the pegmatitic fluid. This constraint suggests that the colourless overgrowths most likely formed during *ca.* 1063 Ma metamorphism in the Britt domain. High-grade metamorphism in the Britt domain at this time is also reported by Tuccillo et al. (1992), and by other workers for the Huntsville, Moon River, and Burwell domains (see Table 5.1 for ages and references). This metamorphism is unlikely to be responsible for the significant Grenvillian Pb-loss experienced by inherited zircon as the overgrowth analysis lies above the 1457-1021 Ma discordia line (Fig. 5.8).

Primary Zircon Results. A total of seven single-grain fractions of brown zircon were analysed from the three pegmatite dykes. Two fractions from the pre- to early synkinematic dyke are 1.2 % and 2.3% discordant and define a discordia line projecting to concordia at 1042 Ma (Fig. 5.9). Three grains from the late synkinematic dyke are 3.4%, 7.8% and 8.1% discordant and lie on a discordia line with an upper intercept age of 1019 ± 4 Ma (83% probability of fit). Two single brown grains from the post-kinematic dyke

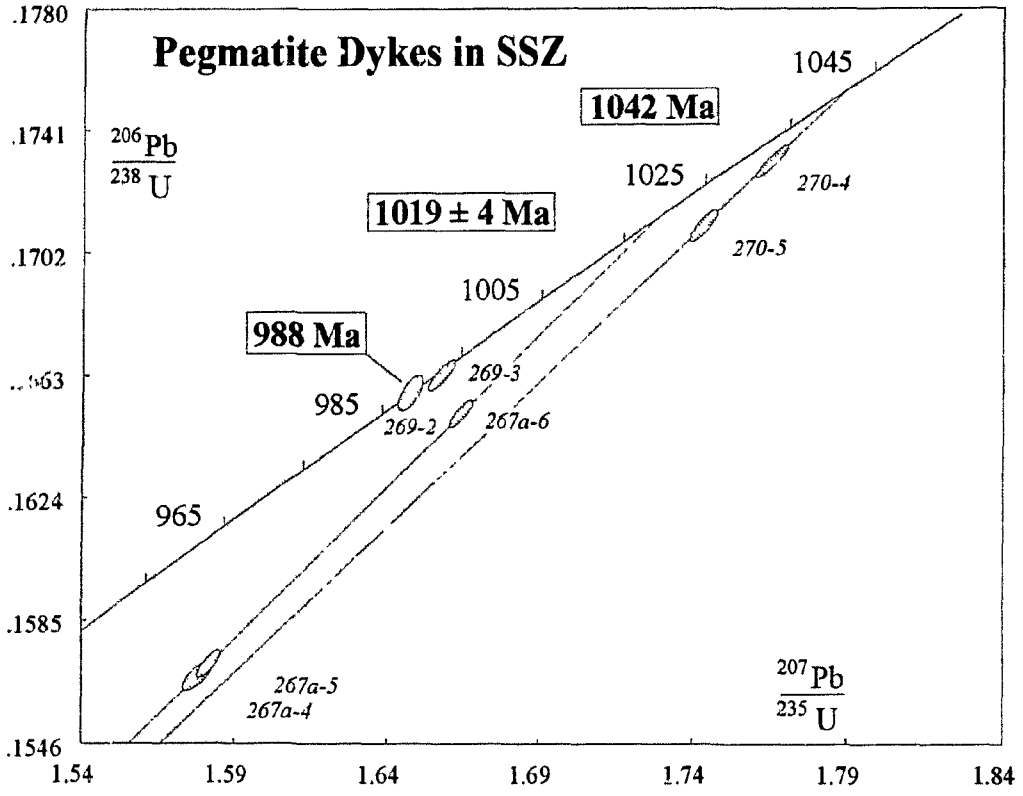

Fig. 5.9. U-Pb concordia diagram for single-grain zircon fractions from pre-kinematic (GC91-270), late synkinematic (GC91-267a) and post-kinematic (GC91-269) pegmatite dykes from the Shawanaga shear zone. Upper intercept ages and fraction 269-2 are interpreted as igneous crystallization ages of the dykes. Sample locations shown in Fig. 5.2.

are concordant at 994 Ma and 988 Ma and do not overlap within error. A small component of older zircon in the 994 Ma single brown grain may account for the age discrepancy, in which case the 988 Ma result represents a more accurate age estimate.

The correlation of progressively younger ages with decreasing deformation state of the pegmatite dykes strongly suggests that the brown zircon analyses yield ages of primary crystallization. This conclusion is supported by the high U content (2200-5600 ppm) of brown zircon in these dykes, a property typical of zircons formed in pegmatitic fluids (Heaman and Parrish 1991). It is therefore concluded that the pegmatite dykes were emplaced in the Shawanaga shear zone at *ca.* 1042 Ma, 1019 Ma, and 988 Ma. These data constrain a major episode of Grenvillian extensional deformation on the Shawanaga shear zone and are discussed further later in this chapter.

Titanite Ages in the Pointe-au-Baril Area

In high-grade metamorphic terranes, the significance of a U-Pb age for a mineral chronometer can vary. Depending on variables such as peak temperature, heating and cooling rates, and deformation state, an analysis may provide (*i*) the age of mineral growth, (*ii*) the age of complete isotopic resetting, (*iii*) a partly reset age, (*iv*) the average of a mixed age population, or (*v*) the time of cooling through the mineral closure temperature (T_c). Uranium-bearing minerals that completely retain radiogenic daughter products following isotopic closure ideally have concordant analyses for ages of mineral growth, complete resetting, and cooling through T_c. Analyses are apt to be discordant for

partly reset and mixing ages, but discordance may not be observed if mixing lines are short (and therefore sub-parallel to concordia). For any given analysis, the geochronologist is faced with determining which of these possibilities is most likely to apply. This can prove difficult in terranes where peak metamorphic temperatures approximated T_c or where metamorphism was episodic over a short time interval.

In the Pointe-au-Baril area, titanite ages are expected to record the time of cooling through the titanite closure temperature (~500-600°C; Tucker et al. 1987; Mezger et al. 1991*a*; Heaman and Parrish 1991) as peak temperatures exceeded T_c. However, multiple Grenvillian thermal and deformational events in this region indicated by previous geochronological data (*e.g.*, Tuccillo et al. 1992; Krogh et al. 1993*a*; Culshaw et al. in prep.; this study) suggest that titanite ages may reflect a complex orogenic history.

Samples for titanite dating were collected along two NW-SE transects (Fig. 5.2) across the Shawanaga shear zone in order to characterize the Grenvillian tectonothermal evolution of rocks in the Pointe-au-Baril area. The titanite data are expected to yield information on the effect, if any, of extension on the thermal development of rocks within and to either side of the Shawanaga shear zone. Titanite was separated from 14 samples of diverse lithology (rock types indicated in Table 5.5). Ten samples were collected along the Georgian Bay coast and four were obtained from roadcuts along Highway 69. Sample locations are given in Figure 5.2 and Appendix B, and data from 19 titanite analyses are presented in Table 5.4 and Figures 5.11 and 5.12. This large number of analyses over a 20 x 15 km area makes this one of the most detailed U-Pb titanite studies to be carried out.

Previous Titanite Dating in the Britt domain

U-Pb titanite data have been reported from three regions of the Britt domain. Corrigan (1990) and Corrigan et al. (1994) presented titanite ages from the Key Harbour area of the northern Britt domain (Fig. 5.1). Single fractions of multifaceted, euhedral grains from two samples closely overlap on concordia at *ca.* 1004 Ma and are suggested to date regional cooling through ~600°C. Four additional fractions of xenomorphic grains and titanite fragments from two samples yield roughly concordant ages between 980 Ma and 963 Ma. These grains are thought to be derived from overgrowths on Fe-Ti oxides, and the ages may date the growth of this phase (Corrigan et al. 1994).

Titanite U-Pb data from a sample of migmatitic granodiorite orthogneiss collected north of the Nares Inlet shear zone in the Bayfield gneiss association (GC89-117; Fig. 5.2) are reported by Krogh et al. (1993*a*) and Culshaw et al. (in prep.). Three fractions of brown to dark brown titanite from this sample are 27%, 53% and 61% discordant along a discordia line (91% probability of fit) with intercepts at 1430 ± 23 Ma and 998 ± 15 Ma, clearly indicating the presence of pre-Grenvillian titanite. Discordance is due either to a mixture of 1430 Ma and 998 Ma titanite or to partial diffusive Pb-loss in 1430 Ma titanite. Preservation of an older isotopic signature is remarkable considering that Grenvillian metamorphic temperatures of up to 770°C, well above the closure temperature of titanite, are recorded in the parautochthon (Chapter 4).

Tuccillo et al. (1992) report titanite data from the Ojibway gneiss association in the Shawanaga domain. A single fraction of 2-5 mm diameter grains from a sample collected ~8 km northwest of the town of Parry Sound yielded a discordant $^{207}Pb/^{206}Pb$ age of 1058

± 2 Ma. No other details were given for this analysis.

Fraction Descriptions

Five titanite morphologies in samples collected for dating were commonly observed in mineral separates: (*i*) euhedral, multifaceted disk- to egg-shaped grains and elongate crystals, colourless to light brown or yellow (Fig. 5.10*a*), (*ii*) fragments of similar colour derived from larger grains of unknown morphology, (*iii*) subhedral to rounded, brown and yellow grains (Fig. 5.10*b*), (*iv*) brown anhedral grains and fragments (Fig. 5.10*c*), and (*v*) grains with visible core and rim components (Fig. 5.10*d*). The majority of samples contain two or more of these morphologies and several samples contain grains with core-rim relationships; both suggest multiple titanite growth events. An assumption made during fraction selection was that grains of similar morphology, size, and colour were likely to have formed at the same time and therefore should be isotopically similar. Every attempt was made during fraction selection to isolate grains of a single morphology so that the possibility of obtaining a mixing age was minimized.

Maximum grain dimensions in the analysed fractions range from 0.03 to 0.2 mm but typically fall between 0.06-0.1 mm. The original grain size of fragmented titanite could not be determined from mineral separates but, where visible in thin section, maximum titanite dimensions are 0.2-0.5 mm except in samples LH89-11 and LH89-12 (1.0 mm).

U-Pb Results

Titanite data obtained in this study are presented in Table 5.4 and Fig. 5.11;

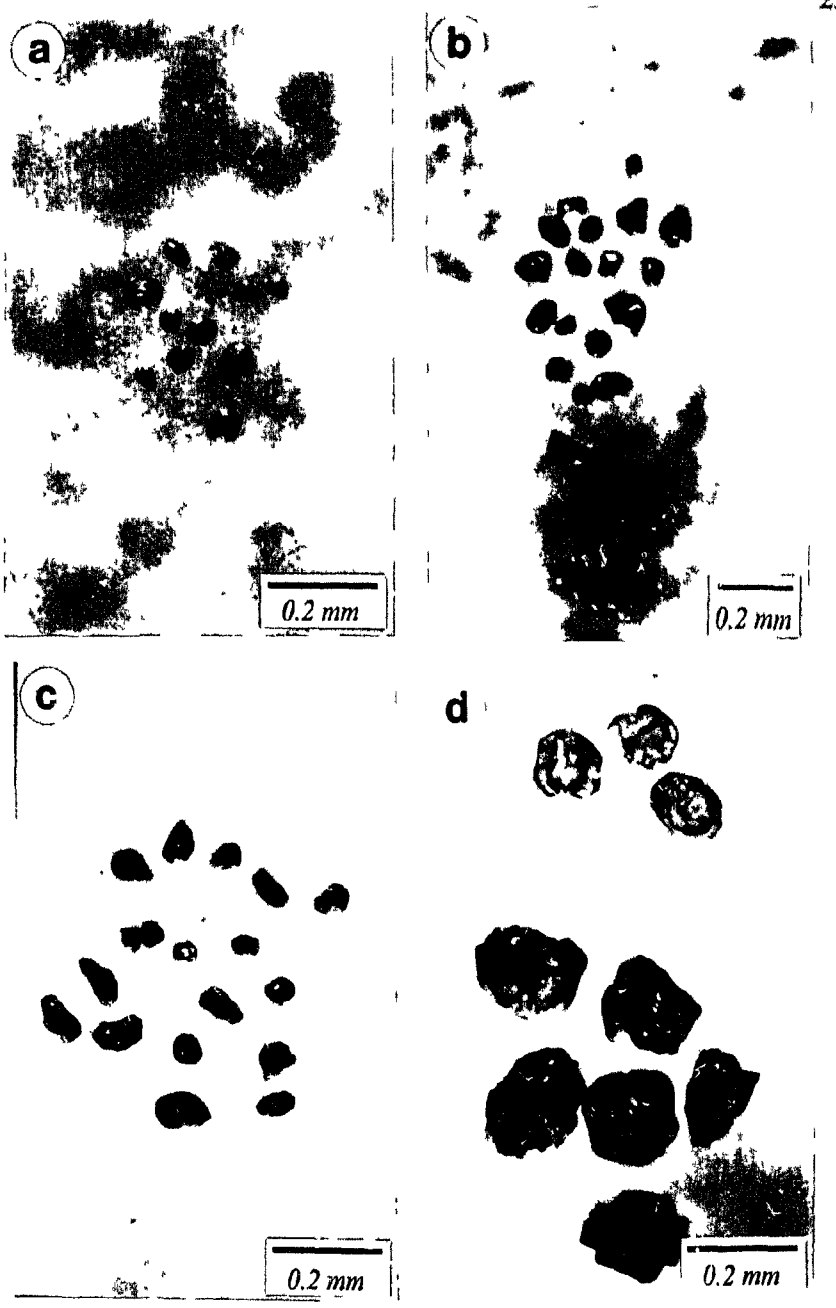

Fig. 5.10. Typical titanite morphologies Fraction numbers enclosed in parentheses. **a)** Euhedral, multifaceted, disk- to egg-shaped yellow grains (119-2). **b)** Subhedral, rounded, brown grains (124-1). **c)** Anhedral brown grains (119-1) **d)** Clear euhedral rims on clear rounded cores, and brown euhedral to subhedral rims on clear rounded cores (sample LH89-12; components not separately dated).

$^{207}Pb/^{206}Pb$ ages are also presented with respect to sample location in Figure 5.12. The 19 analyses are concordant to near-concordant and have $^{207}Pb/^{206}Pb$ ages ranging from 956 Ma to 1049 Ma. Five analyses have slight negative discordance while the remaining 14 analyses are from 0.1% to 1.9% discordant. Only four analyses do not overlap concordia within error. Negatively discordant fractions (Table 5.4) generally have low $^{206}Pb/^{204}Pb$ ratios and therefore are most sensitive to corrections for common Pb. This correction can generate negative discordance if a common Pb isotopic composition that is too radiogenic is assumed. Fraction TK84-91-1 is the only analysis that lies significantly above concordia (-2.8%). If this discordance is due to an incorrect estimate of common Pb composition, the true $^{207}Pb/^{206}Pb$ age of this fraction may be as much as 20 to 30 M.y. older (L.M. Heaman, written communication 1990). Three analyses (GC89-119-1, GC89-119-2, and GC89-128-1) lie below concordia and may reflect incomplete isotopic resetting, mixing of different age populations, or episodic Pb-loss. The discordant analysis of Tuccillo et al. (1992) is also shown in Figure 5.11.

Several correlations are notable amongst data presented in Table 5.4. Uranium content and $^{206}Pb/^{204}Pb$ ratio generally correlate with titanite colour, a characteristic noted in other studies (*e.g.*, Cumming and Krstic 1991). Brown and dark brown grains generally have a higher average U concentration (291 ppm) and $^{206}Pb/^{204}Pb$ ratio (2238) than light brown, light yellow, and yellow grains (126 ppm and 1010, respectively). Uranium concentrations, although variable, are generally lowest for the five youngest fractions (94 ppm average) compared with all other fractions (218 ppm average). Four of five analyses of euhedral to subhedral titanite yield ages between 1026 Ma and 1018 Ma, indicating that

TABLE 5.4. U/Pb Titanite Data

Description	Weight	Concentrations			Atomic Ratios[c]				Apparent Age (Ma)			
fraction number and properties[a]	(mg)	U (ppm)	Pb^{rad} (ppm)	common Pb (pg)	$^{206}Pb/^{204}Pb$[b]	$^{206}Pb/^{238}U$	$^{207}Pb/^{235}U$	$^{207}Pb/^{206}Pb$	$^{206}Pb/^{238}U$	$^{207}Pb/^{235}U$	$^{207}Pb/^{206}Pb$	discord. (%)[d]
Parautochthon												
GC89-118-1, br, an	0.426	231	41	1063	1041	0.16808	1.6835	0.07264	1001	1002	1004	0.3
GC89-118-2, yel, eu	0.246	230	41	598	1097	0.16713	1.6703	0.07248	996	997	1000	0.4
GC89-119-1, br, an	0.070	439	75	208	2045	0.16714	1.6749	0.07268	996	999	1005	0.9
GC89-119-2, lyel, an-sb	0.035	299	52	72	4919	0.16923	1.7120	0.07337	1008	1013	1024	1.7
GC89-122-1, lbr, an	0.565	115	18	1180	622	0.16854	1.6851	0.07251	1004	1003	1000	-0.4
GC89-123-1, lbr, an	0.334	56	9	536	404	0.16062	1.5728	0.07102	960	959	958	-0.3
GC89-128-1, dbr, an	0.452	189	31	862	1133	0.16947	1.7176	0.07351	1009	1015	1028	1.9
TK84-91-1, lbr, an	0.340	23	4	744	129	0.16534	1.6217	0.07114	986	978	961	-2.8
TK84-91-2, lyel, an, a	0.510	26	5	1105	142	0.16565	1.6440	0.07198	988	987	985	-0.3
TK84-92-1, yel, an, a	0.220	43	8	535	258	0.17545	1.7965	0.07426	1042	1044	1049	0.7
Allochthon												
GC89-124-1, lbr, eu-sb	0.621	124	21	1798	489	0.17108	1.7291	0.07330	1018	1019	1022	0.4
GC89-127-1, lbr, an	0.352	87	18	265	1457	0.16209	1.5937	0.07131	968	968	966	-0.2
LH89-11-1, lyel, eu	0.213	192	31	476	966	0.17240	1.7460	0.07345	1025	1026	1026	0.1
LH89-11-2, dbr, an	0.362	435	72	770	2286	0.17465	1.7848	0.07412	1038	1040	1045	0.7
LH89-12-1, lbr, an	0.457	198	33	892	1132	0.17195	1.7406	0.07341	1023	1024	1025	0.3
DS-1-1, lyel, an, a	0.293	62	9	237	826	0.15921	1.5575	0.07095	952	953	956	0.4
DS-1-2, br, an, a	0.162	242	36	164	2625	0.16129	1.5866	0.07134	964	965	967	0.3
DS-3-1, lbr, eu, a	0.405	77	16	1512	241	0.16981	1.7127	0.07315	1011	1013	1018	0.7
DS-4-1, br, ?	0.279	167	26	102	5353	0.16833	1.6892	0.07278	1003	1004	1008	0.5

Table 5.4. (continued)

[a] All titanite selected from magnetic fractions at 1.0-1.7 A, 1° forward slope and 2°side tilt on a Frantz isodynamic separator. A number of fractions were abraded using the technique of Krogh (1982). Properties: br = brown, lbr = light brown, dbr = dark brown, yel = yellow, lyel = light yellow, eu = euhedral, sb = subhedral, an = anhedral, ? = morphology and colour unknown, a = abraded (all other fractions unabraded).

[b] Corrected for blank (0.5-2.0 pg U and 2-10 pg Pg) and spike Pb, and for mass fractionation (+0.1%/amu for U and Pb).

[c] Corrected for blank and spike Pb, fractionation, and initial common Pb calculated after Stacey and Kramers (1975).

[d] Discordance in $^{207}Pb/^{206}Pb$ age

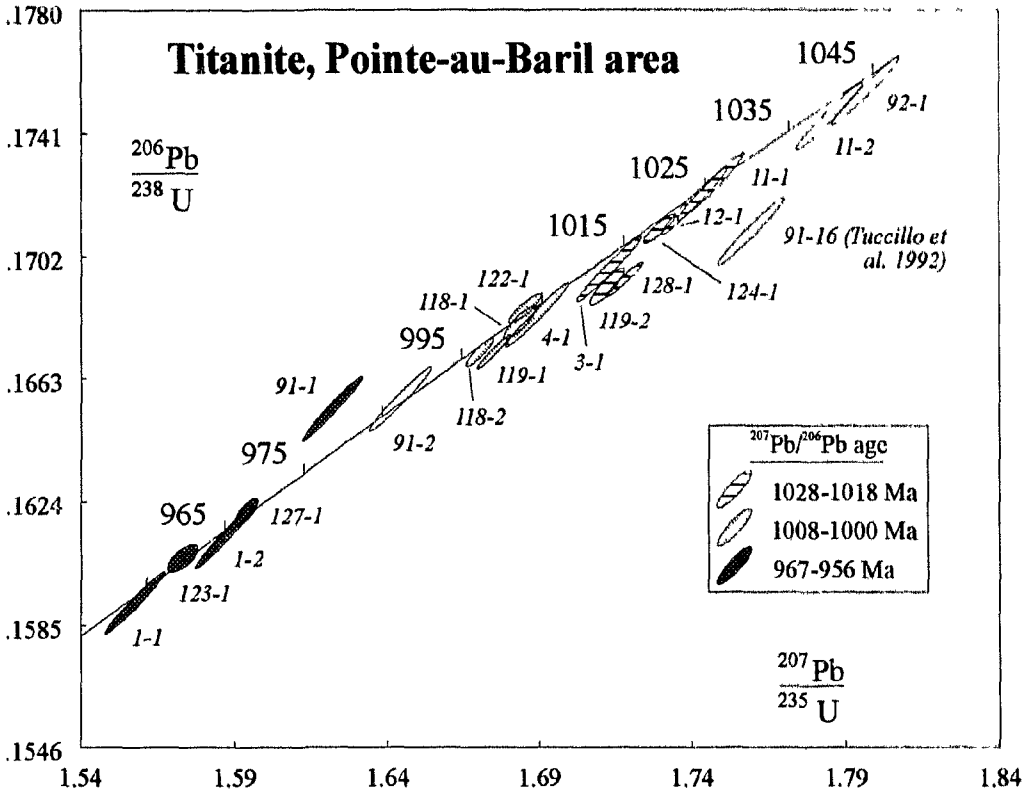

Fig. 5.11. U-Pb concordia diagram of titanite analyses from the Pointe-au-Baril area. Fraction numbers are abbreviated from Table 5.4 and in text. Analysis of Tuccillo et al. (1992) from sample collected 8 km NW of Parry Sound in Shawanaga domain also shown (error ellipse assumed) Sample locations indicated in Fig. 5.2.

this morphology is characteristic of a narrow time interval. These grains are light brown to light yellow unlike anhedral grains and fragments which exhibit the full range of colour. Another correlation is noted in samples where two ages of titanite were obtained. Younger fractions are generally less discordant than older fractions and contain paler titanite.

The distribution of analyses along a 93 M.y. segment of concordia suggests a complex Grenvillian history for the Pointe-au-Baril area. Similar titanite age distributions noted in other studies (*e.g.*, Corfu 1988; Mezger et al. 1991*b*; Cumming and Krstic 1991) are attributed to factors such as grain size-related differences in T_c, metamorphic growth over an extended period, prolonged post-orogenic thermal and fluid activity, thermal discontinuities across tectonic boundaries, and mixing of igneous, metamorphic, and syn-deformational growth ages. Few of these studies, however, have attempted to characterize titanite age distribution with reference to titanite and host rock characteristics and local structural and metamorphic features. In the Pointe-au-Baril area, evaluation of titanite ages in this manner provides insights on both the timing of metamorphism and deformation in this region, and on the isotopic behaviour of titanite in high-grade metamorphic terranes.

^{207}Pb/^{206}Pb Age Groups and Correlation with Titanite and Host Rock Properties

The titanite ^{207}Pb/^{206}Pb age data group into three intervals of 11 M.y. duration or less (Fig. 5.11). Six fractions define a 1028-1018 Ma group while five others plot between 1008 Ma and 1000 Ma. An additional five fractions make up the youngest group with ages

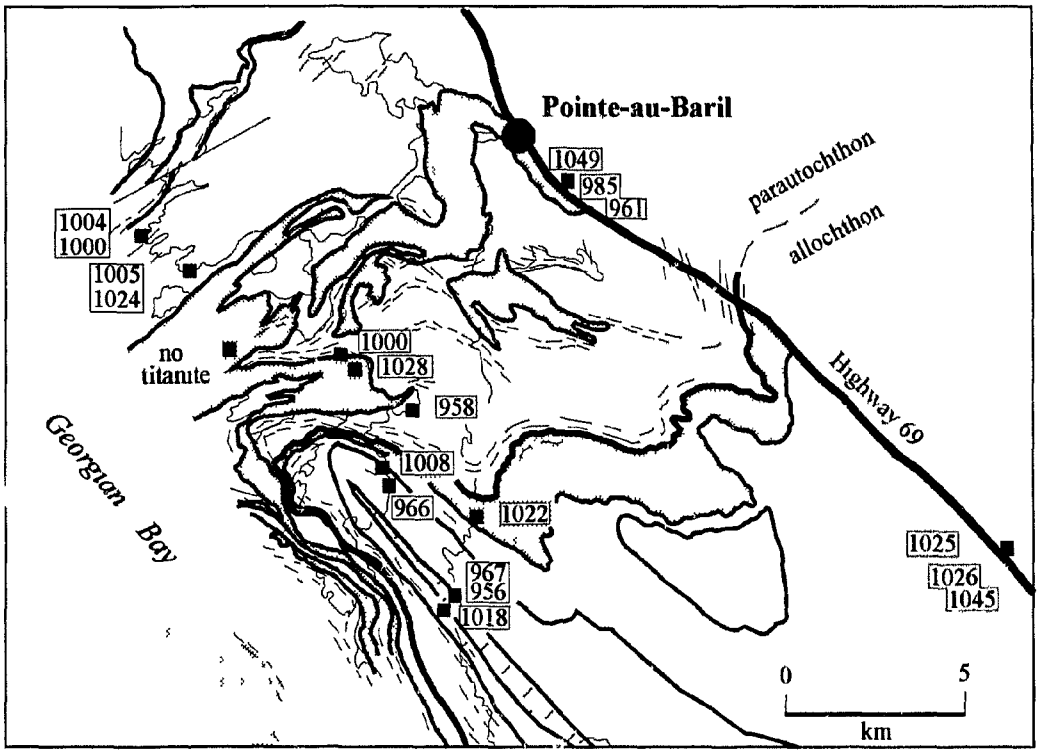

Fig. 5.12. Sample locations and $^{207}Pb/^{206}Pb$ ages of titanite from the Pointe-au-Baril area. Solid lines = geological boundaries (Fig 2 2); dashes = trend of shear fabrics, shading = ca. 1 45 Ga granitoid plutons, diagonal line pattern = Dillon schist (Sand Bay gneiss association)

of 956 Ma to 967 Ma. Only three fractions do not fall within these groups.

Examination of titanite morphology, petrographic characteristics, deformation state, and structural position of the dated samples reveals that each age group has a characteristic combination of titanite and host rock properties. These properties are described below and summarized in Table 5.5.

1028-1018 Ma Group. The six samples with titanite in this age group were collected from both allochthonous and parautochthonous units. Those collected from the Shawanaga shear zone are from lower-strain segments of this zone. In thin section, four samples have a non-uniform grain size and undulatory extinction in quartz whereas two samples, both from the allochthon, show signs of recovery and post-deformation grain growth (*e.g.*, grain-boundary pinning). Titanite fractions mainly consist of euhedral to subhedral, light brown and yellow grains. These grains have an idioblastic crystal form similar to that exhibited by overgrowths on rounded titanite cores in some samples.

1008-1000 Ma Group. Apart from sample DS-4, a moderately-strained paragneiss from the Shawanaga shear zone, samples with titanite in this age group consist of mylonitic and porphyroclastic gneiss from the Shawanaga and Nares Inlet shear zones and straight gneiss from structural zone 2 (southeast of the Nares Inlet shear zone). All samples except DS-4 are from parautochthonous lithologies. Overall grain size and shape in these rocks is irregular, and quartz displays undulatory extinction and deformation bands. Analysed fractions mainly consist of brown to light brown fragments and anhedral grains.

967-956 Ma Group. Four samples with titanite of this age were collected from

TABLE 5.5. Correlation of Titanite Properties with Host Rock Characteristics

Sample	Rock Characteristics			Titanite Fraction Properties			
	lithology	microtexture	titanite properties in thin section	fraction	colour[a]	morph.[a]	$^{207}Pb/^{206}Pb$ age
1028-1018 Ma Age Group							
GC89-128	megacrystic tonalite ogn	irregular gr. size, strained quartz	anhedral grains	-1	dbr	an	1028
LH89-11	migmatitic tonalite ogn	irregular gr. size, strained quartz	euhedral rims, anhedral cores	-1	lyel	eu	1026
LH89-12	tonalite ogn	irregular gr. size, strain recovery	euhedral rims, anhedral cores	-1	lbr	an	1025
GC89-119	straight granodiorite ogn	irregular gr. size, strained quartz	not observed	-2	lyel	eu-sb	1024
GC89-124	migmatitic granodiorite ogn	irregular gr. size, strained quartz	resorbed anhedral grains	-1	lbr	eu-sb	1022
DS-3	migmatitic amphibolite gn	large gr. size, strain recovery	euhedral grains; recryst'd rims	-1	lbr	eu	1018
1008-1000 Ma Age Group							
DS-4	impure metaquartzite	uniform gr. size, strain recovery	not observed	-1	br	-	1008
GC89-119	straight granodiorite ogn	irregular gr.size, strained quartz	not observed	-1	br	an	1005
GC89-118	migmatitic mylonite gn	irregular gr. size, strained quartz	anhedral grains; rims on	-1	br	an	1004
GC89-118	as above	as above	as above	-2	yel	eu	1000
GC89-122	mylonitic granite ogn	irregular gr. size, strain recovery	anhedral grains (recryst'd?)	-1	lbr	an	1000
967-956 Ma Age Group							
DS-1	schistose pgn	uniform gr. size, strain recovery	rims on biotite, oxides	-1	lyel	an	956
DS-1	as above	as above	as above	-2	br	an	967
GC89-127	leucocratic pgn	uniform gr. size, strain recovery	recryst'd grs; rims on oxides	-1	lbr	an	966
TK84-91	megacrystic tonalite ogn	irregular gr. size, strain recovery	recryst'd grs; rims on oxides	-1	lbr	an	961
GC89-123	migmatitic tonalite ogn	irregular gr. size, strain recovery	anhedral grains; rims on	-1	lbr	an	958

[a] Abbreviations are those listed in Table 5.4.

allochthonous and parautochthonous units. All but one (TK84-91) were collected within the Shawanaga shear zone. Although macroscopic strain-state varies considerably in these rocks, partly- to completely-annealed textures and a relatively uniform grain size are characteristic in thin section. Quartz microstructures are absent or are less evident than in the other age groups, most likely due to recovery and post-kinematic grain growth. Sample TK84-91 is not strongly annealed but contains polycrystalline titanite aggregates derived from recrystallization of larger grains. Titanite is also observed rimming Fe-Ti oxides in all samples. The five fractions in this age group are composed of light brown to light yellow fragments.

Other Ages. Fractions TK84-92 and LH89-11-2, along with the analysis of Tuccillo et al. (1992), suggest the presence of a 1058-1045 Ma group although this requires confirmation by additional titanite dating. These ages are obtained from both sides of the Shawanaga shear zone and appear to be limited to rocks lacking strong extensional shear fabrics. No description of titanite morphology and colour is given for the fraction analysed by Tuccillo et al. (1992), but light yellow and dark brown fragments make up the other two fractions. Intragranular strain features in quartz and a heterogeneous grain size/shape characterize the host rocks.

Fraction TK84-91-2 (light yellow fragments) is concordant at 985 Ma. A second fraction from this sample (TK84-91-1) may have a similar $^{207}Pb/^{206}Pb$ age if the common Pb correction for this fraction is in error (see above). A granoblastic texture and strain-free quartz are observed in this sample.

Significance of Titanite Ages

The spread of essentially concordant titanite ages over a 93 M.y. range indicates that factors other than regional cooling through T_c are responsible for the observed distribution of ages. As outlined above, the bulk of the analyses fall into three distinct $^{207}Pb/^{206}Pb$ age groups, each bearing a distinctive combination of titanite and host rock characteristics. These characteristics provide evidence for the geological significance of the titanite ages.

The euhedral to subhedral form of titanite in the 1028-1018 Ma group, and the distribution of samples with this age, strongly suggest that titanite crystallized during a period of metamorphic growth that affected allochthonous and parautochthonous rocks alike. This period may correspond to the time of titanite growth or (as favoured below) to the time of cooling through T_c. It is unlikely that these titanites date a period of isotopic resetting as a sample from this age group (LH89-11) also contains an older titanite fraction (*ca.* 1045 Ma) which presumably would not have survived the resetting event.

Pegmatite crystallization ages in the Shawanaga shear zone (see above) indicate that extensional displacement likely occurred during the 1028-1018 Ma period of titanite growth. This raises the possibility that the titanite ages are linked in some manner to syn-metamorphic deformation, marking either growth and/or cooling through T_c during this event. Titanite in this age group appears to have been unaffected by subsequent events responsible for younger titanite ages.

Titanite ages of 1008-1000 Ma, mainly limited to highly-strained rocks in the Shawanaga and Nares Inlet shear zones, indicate that shear zones represent an isotopically

unique environment for titanite. This is not surprising given that processes such as dynamic recrystallization and enhanced fluid flow (*e.g.*, Tucker et al. 1987; Gromet 1991), all capable of influencing U-Pb systematics, are prominent in shear zones. Correlation of 1008-1000 Ma titanite with strongly deformed gneiss indicates that growth of new titanite and/or isotopic resetting of older grains in a (fluid-rich?) high-strain environment may best account for this age group. Evidence for late, possibly renewed extensional deformation on the Shawanaga shear zone at 1006 Ma (Krogh et al. 1993*a*) supports this hypothesis. This interpretation contrasts with that proposed for *ca.* 1004 Ma titanites in the Key Harbour area (Corrigan 1990; Corrigan et al. 1994) which were suggested to date cooling of the northern Britt domain through ~600°C. However, the Key Harbour titanites may record exhumation and cooling of the northern Britt domain following exhumation by extensional displacement on the structurally higher Shawanaga shear zone (Jamieson et al. 1995).

Evidence for recrystallization and post-kinematic grain growth in all samples, and recrystallized titanite observed in several thin sections, suggests that titanite ages of 967-956 Ma are best attributed to a period of recrystallization in deformed rocks. Gromet (1991) has suggested that migration of dislocation surfaces or grain boundaries through a crystal lattice create high-diffusivity pathways that can liberate radiogenic daughter products. Grain boundary migration recrystallization 'sweeps out' a large volume of a crystal lattice and can isotopically reset minerals below their T_c. Evidence for grain boundary migration recrystallization including grain boundary pinning, strain-free grains, an exaggerated grain size, and annealed textures in all samples with 967-956 Ma titanite

indicates that this process may have influenced U-Pb systematics in titanite. The distribution of samples with these textures and titanite ages suggests that recrystallization occurred mainly within allochthononous rocks and locally within the parautochthon. Sericitization of feldspar and growth of late muscovite and chlorite in several samples suggest the presence of a late fluid phase which may have enhanced recrystallization.

Of the titanite ages that do not fall within one of the defined age groups, the 985 Ma fraction from TK84-91 may also reflect a recrystallization event based on titanite and host rock textures observed in this sample. The 1049 Ma and 1045 Ma fractions from TK84-92 and LH89-11 most likely contain titanite that grew during *ca.* 1050 Ma metamorphism (Tuccillo et al. 1992; Culshaw et al. in prep.) and was not reset by later thermal or deformational events.

5.5 DISCUSSION

Pre-Grenvillian Granulite-Facies Metamorphism

U-Pb zircon ages of *ca.* 1450-1430 Ma reported above and in Ketchum et al. (1994) represent the first isotopic data to be obtained from fresh, pre-Grenvillian metamorphic assemblages in the interior of the western Grenville Province. This granulite-facies metamorphism is contemporaneous with igneous crystallization of the Pointe-au-Baril complex and Shawanaga pluton (*ca.* 1460-1430 Ma; Krogh et al. 1993*a*; Culshaw et al. in prep.) and the Britt pluton, located 20 km north of the study area (1457 Ma; van Breemen et al. 1986), indicating a magmatic heat contribution to the thermal regime.

Other workers have presented isotopic evidence for early Mesoproterozoic high-grade metamorphism in the western Grenville Province. Within the present study area, $^{207}Pb/^{206}Pb$ ages of 1450 ± 1 Ma and 1435 ± 2 Ma from a centimetre-size metamorphic allanite crystal were reported by Tuccillo et al. (1992), and Krogh et al. (1992, 1993*a*) and Culshaw et al. (in prep.) presented zircon and titanite data indicating metamorphism and isotopic resetting at *ca.* 1450-1420 Ma. One hundred kilometres to the east, Nadeau (1990) obtained an imprecise zircon lower intercept age of 1432 +54/-98 Ma from orthogneiss in the Huntsville thrust zone which was suggested to date metamorphic zircon growth. Southeast of Sudbury in the Grenville Front Tectonic Zone, Bethune et al. (1990) and Bethune (1993) reported a *ca.* 1445 Ma monazite age in metapelite, and Haggart et al. (1993) showed that high-grade assemblages near the Grenville Front crystallized at 1454 ± 8 Ma. Combined with widespread field evidence in the parautochthon for pre-Grenvillian granulite facies metamorphism (*e.g.*, Davidson et al. 1982; Schau et al. 1986; Culshaw et al. 1988; Corrigan 1990; Jamieson et al. 1992; Corrigan et al. 1994), these data suggest that early Mesoproterozoic metamorphism affected a significant volume of crust in the western Grenville Province. The tectonic setting of this metamorphism is discussed in Chapter 6.

Bethune (1993) presented evidence for high-grade metamorphic and tectonic activity in the Grenville Front Tectonic Zone southwest of Sudbury at 1470-1450 Ma. Curiously, this event did not influence the U-Pb systematics of zircon, monazite and titanite along the Grenville Front Tectonic Zone to the northeast, nor was it isotopically recorded in rocks of Archean age in the Lake Nipissing area (*e.g.*, Krogh 1991; Krogh et

al. 1992; Chen et al. 1993). Archean and Labradorian-aged orogenic rocks south of the Grenville Front in Quebec and Labrador were also reworked for the first time late in the Grenvillian orogeny (*e.g.*, Krogh and Davis 1974; Krogh and Wardle 1984; Schärer et al. 1986; Connelly and Heaman 1993) with no evidence of an early Mesoproterozoic overprint. This suggests that *ca.* 1450 Ma metamorphism and thrusting within the Grenville Front Tectonic Zone may have been confined to the northwestern margin of the Beaverstone domain (Fig. 5.1), supporting the terrane status assigned by Rivers et al. (1989) for this aeromagnetically distinct region.

Timing of Extension on the Shawanaga Shear Zone

U-Pb data presented for variably deformed pegmatite dykes in the Shawanaga shear zone indicate that southeast-directed extensional displacement occurred during the period 1042-988 Ma. The structural state of individual dykes further indicates that extension was likely in the waning stages at 1019 ± 4 Ma and had ceased by 988 Ma. It is not clear if the strongly deformed, 1042 Ma pegmatite was intruded prior to extensional shear or during an early stage of this activity. However, the steep decompression path indicated by *P-T* data from the parautochthon (Chapter 4) suggests that extensional shearing resulted in rapid tectonic unroofing of the footwall. Based on this information, it is likely that extensional shear occurred within a short time interval immediately preceeding emplacement of the late synkinematic dyke at *ca.* 1020 Ma. This would suggest that the 1042 Ma dyke is pre-kinematic with respect to extensional shear.

Further evidence for *ca.* 1020 Ma extensional shear is provided by the analyses of

inherited zircon in the pegmatite dykes. The discordia line calculated for inherited grain analyses indicates isotopic resetting at 1021 ± 23 Ma, an event that affected inherited zircon already incorporated in the pre-kinematic pegmatite as well as grains that were later scavenged by the post-kinematic dyke. As outlined above, metamorphism is unlikely to have been solely responsible for *ca.* 1020 Ma Pb-loss in these grains. Given the high strain state of the granite and the pre-kinematic dyke, the best mechanism to account for substantial Pb-loss at *ca.* 1021 Ma is deformation in a high-temperature ductile shear environment. Pb-loss by this mechanism has also been proposed for mylonites studied by Wayne and Sinha (1988) and Connelly and Heaman (1993) who interpreted discordia lower intercepts for highly discordant analyses as dating the time of ductile shearing. In the present study area, additional evidence of deformation-induced Pb-loss in inherited grains is indicated by the relative discordance of these analyses (Fig. 5.8). Three fractions from the late syn-kinematic (GC89-267*a*) dyke plot near the upper intercept of the discordia line, in contrast to analyses from the other dykes which are much more discordant. This may indicate that Pb-loss was less significant in inherited zircon hosted by the 'soft,' crystallizing, syn-kinematic pegmatite.

The data presented above indicate that the Shawanaga shear zone accommodated a major episode of extensional deformation at *ca.* 1020 Ma. This represents the first evidence for large-scale tectonic activity at this time in the Central Gneiss Belt of Ontario.

Titanite Ages in the Pointe-au-Baril Area

The *ca.* 90 M.y. spread of U-Pb titanite ages in the Pointe-au-Baril area

demonstrates the necessity of dating a variety of titanite morphologies from rocks of contrasting strain state and microtexture in order to adequately characterize the range and probable significance of titanite ages in high-grade orogenic belts.

A P-T path for parautochthonous rocks in the Pointe-au-Baril area (Fig. 4.14), and U-Pb data from pegmatite dykes in the Shawanaga shear zone, collectively indicate that cooling through the titanite closure temperature (~600°C) likely occurred during *ca.* 1020 Ma extensional exhumation of the parautochthon. Titanite ages of 1028-1018 Ma may therefore mark cooling (at least in the parautochthon) through T_c. This interpretation is supported by a temperature-time (*T-t*) plot (Fig. 5.13) constructed for the southern Britt domain employing the monazite age data of Tuccillo et al. (1992), $^{40}Ar/^{39}Ar$ hornblende and muscovite data of Culshaw et al. (1991*b*), and a rutile age obtained in this study (sample 89-73a, Table 5.2). The 1028-1018 Ma age group appears to best fit a *T-t* path defined by the other mineral chronometers. A simplistic *T-t* path incorporating all these data indicates initial cooling of the southern Britt domain at ~3.5°C/Ma and later cooling at ~2.5°C/Ma (Fig. 5.13). The shape of this path is similar to that proposed for the Britt domain by Culshaw et al. (1991*b*), although the southern Britt domain data indicate cooling through 600°C at an earlier time. However, a simplistic *T-t* path like that shown in Figure 5.13 may not be appropriate for the southern Britt domain thermochronologic data. An alternative *T-t* path that is more consistent with the extensional tectonic setting of the study area is presented in Chapter 6.

By analogy with parautochthonous rocks, allochthonous rocks likely also cooled through ~600°C at 1028-1018 Ma as four samples from the Shawanaga domain contain

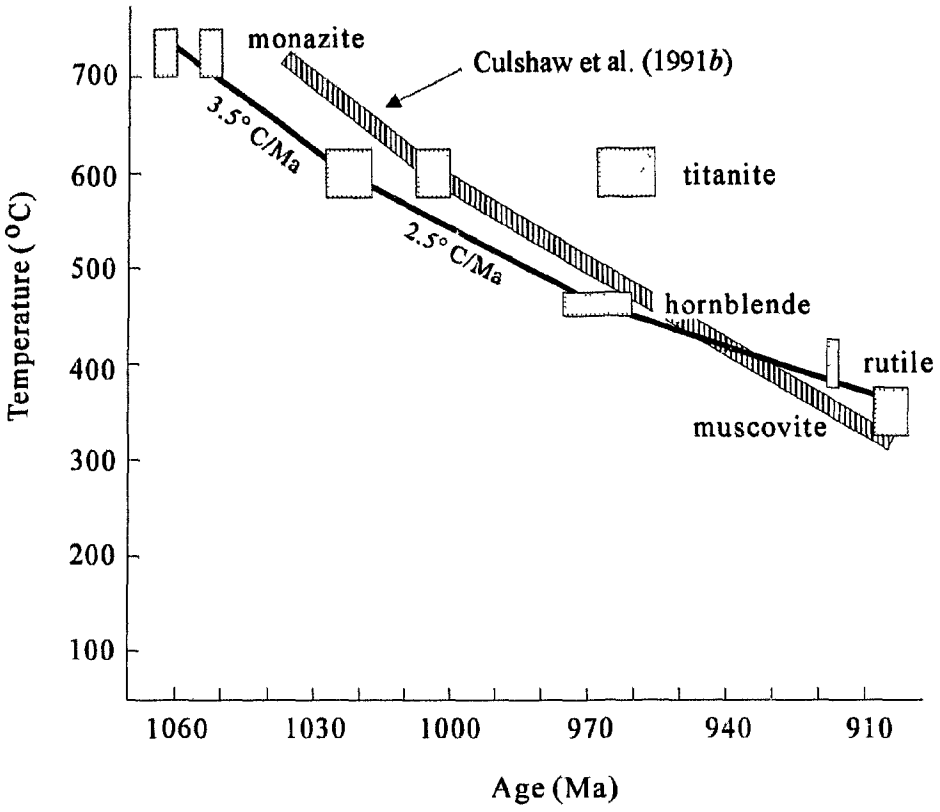

Fig. 5.13. Preliminary time-temperature (*T-t*) diagram for parautochthonous rocks in the study area (see, however, Fig. 6.2 for an alternative, preferred path). The three titanite age groups obtained in the study area are shown; the oldest is suggested to yield titanite cooling ages whereas the younger groups reflect recrystallization and/or late titanite growth. The *T-t* path of Culshaw et al. (1991*b*), constructed with monazite and titanite data from the northern Britt domain (Corrigan 1990), is shown for comparison. Closure temperatures and isotopic systems are: 725 ± 25°C for monazite (U-Pb; Parrish 1990); 600 ± 25°C for titanite (U-Pb; Heaman and Parrish 1991); 450-475°C for hornblende ($^{40}Ar/^{39}Ar$; McDougall and Harrison 1988 (used by Culshaw et al. 1991*b*); 400 ± 25°C for rutile (U-Pb; Mezger et al. 1989*b*); and 350 ± 25°C for muscovite ($^{40}Ar/^{39}Ar$; Jäger 1979). Sources: monazite - Tuccillo et al. (1992); titanite, rutile - this study; hornblende, muscovite - Culshaw et al. (1991*b*).

titanite of this age.

The remaining titanite age groups appear to reflect local- to broad-scale episodes of recrystallization and fluid influx. The 1008-1000 Ma titanites are mainly confined to extensional shear zones and likely reflect a recrystallization event, perhaps due to continued shearing after 1020 Ma, or alternatively, due to enhanced fluid mobility within the shear zones. The 967-956 Ma age group also marks a recrystallization event that likely occurred in the presence of a fluid phase. Both of these periods represent episodes of titanite growth and/or isotopic resetting that took place below the titanite blocking temperature. This is particularly evident for 967-956 Ma titanites which overlap with hornblende $^{40}Ar/^{39}Ar$ cooling ages (Culshaw et al. 1991*b*; Fig. 5.13). Because these mineral chronometers do not overlap in T_c (600°C for titanite versus *ca.* 500°C for hornblende), and because hornblende cooling ages are consistent throughout the Britt domain (Culshaw et al. 1991*b*), it seems likely that the youngest titanite age group must reflect either local growth of new grains below T_c, or recrystallization-controlled isotopic resetting.

5.6 SUMMARY

1) A compilation of U-Pb age data from the Central Gneiss Belt and Grenville Front Tectonic Zone of Ontario delineates major crust-forming or crust-modifying events in the late Archean, late Paleoproterozoic, early Mesoproterozoic, and late Mesoproterozoic. Pre-Grenvillian (pre-late Mesoproterozoic) crustal events were primarily marked by voluminous plutonism, but sedimentation, metamorphism, and/or deformation are also

indicated during each period. Grenvillian orogenesis did not contribute to significant crustal growth (*i.e.*, plutonism and sedimentation) but instead was characterized by widespread tectonism and high-grade metamorphism.

2) In the Pointe-au-Baril area, metamorphic zircon from migmatitic, pre-Grenvillian granulite (preserved in structural zone 3 of the Britt domain) yields concordant to weakly discordant ages of 1452-1433 Ma, interpreted as marking a period of anatexis and crystallization of granulite-facies assemblages. Coeval granitoid plutonism in the Pointe-au-Baril area and throughout the Central Gneiss Belt suggests that the thermal budget of metamorphism was enhanced by magmatic heat.

3) Granitic pegmatite dykes that are pre- to early syn-kinematic, late syn-kinematic, and post-kinematic in extensional shear fabrics of the Shawanaga shear zone crystallized at 1042 Ma, 1019 Ma, and *ca.* 990 Ma, respectively. These data indicate that extensional displacement on this zone was largely complete by *ca.* 1020 Ma and had ceased by *ca.* 990 Ma. The relationship of the oldest, strongly deformed pegmatite dyke to extensional shear fabrics is equivocal, but *P-T* data (Chapter 4) indirectly suggest that emplacement of this dyke may have pre-dated extensional shear.

4) Nineteen U-Pb analyses of titanite from the Pointe-au-Baril area are concordant to weakly discordant between 1049 and 956 Ma. Sixteen analyses are assigned to three $^{207}Pb/^{206}Pb$ age groups (each spanning ≤11 M.y.) which are distinctive in titanite morphology and colour, and in structural position and microtexture of the host rock. A 1028-1018 Ma age group consists of euhedral and subhedral, light brown and yellow titanite from

parautochthonous and allochthonous gneisses lacking a strong Grenvillian foliation. This group best satisfies a preliminary *T-t* curve for parautochthonous rocks and is suggested to mark regional cooling through the titanite closure temperature (~600°C) during or immediately following extensional shearing and exhumation. A 1008-1000 Ma age group comprising brown and light brown titanite fragments and anhedral grains is from highly-strained rocks mainly from the Shawanaga and Nares Inlet shear zones. This age group is interpreted to reflect isotopic resetting and/or new titanite growth during (fluid-assisted?) recrystallization, and indicates that the extensional shear zones represent an isotopically unique environment for titanite. The youngest age group (967-956 Ma) is characterized by light brown and light yellow titanite fragments obtained from allochthonous and parautochthonous rocks with a well-developed granoblastic texture, strain-free grains, and a uniform, relatively large grain size. This age group likely marks a period of recovery and grain boundary migration recrystallization that reset the U-Pb isotopic system in titanite. Titanite overgrowths on biotite and Fe-Ti oxide may have also formed at this time. The wide range of titanite ages in this 20 x 20 km study area cautions against the interpretation in high-grade terranes of titanite age solely in terms of blocking temperature, and emphasizes the importance of dating all titanite morphologies in a given sample.

CHAPTER 6

Regional Tectonic Implications And Conclusions

6.1 INTRODUCTION

This study indicates that late orogenic extension at deep crustal levels is likely to have a marked influence on metamorphic mineral assemblages, isotopic systematics, *P-T-t* history, and crustal architecture. It also shows that evidence of earlier tectonic and metamorphic events can survive late orogenic overprinting if this overprint is structurally heterogeneous and if intensive variables of metamorphism are favourable (*e.g.*, low aH_2O, sluggish reaction kinetics).

The purpose of this chapter is not to provide a comprehensive model of Grenvillian orogenesis in the Central Gneiss Belt, but rather to document the local tectonic evolution of the Pointe-au-Baril area and to suggest how these findings may be incorporated into regional-scale tectonic models. This chapter will demonstrate that structural, metamorphic, and geochronologic data from the present study area can be linked into a coherent picture of pre-Grenvillian and Grenvillian orogenic events with implications for regional crustal evolution.

6.2. CRUSTAL EVOLUTION IN THE POINTE-AU-BARIL AREA AND COMPARISON WITH REGIONAL DATA

Pre-Grenvillian Events

In the Pointe-au-Baril area, evidence of pre-Grenvillian crustal events prior to *ca.*

1460 Ma is restricted to parautochthonous rocks of the southern Britt domain. The oldest plutonic rocks in the study area are granodiorite orthogneisses of the Bayfield gneiss association for which U-Pb data indicate igneous crystallization at *ca.* 1739 Ma (Krogh et al. 1993*a*). A younger igneous crystallization age of 1606 ± 2 Ma is indicated for granodiorite orthogneiss of the Nadeau Island gneiss association (Culshaw et al. in prep.). The maximum deposition age of supracrustal rocks in both associations is less tightly constrained. Rb-Sr ages of *ca.* 1800 Ma for paragneiss near Pointe-au-Baril and in the northern Britt domain are interpreted as metamorphic ages (Krogh and Davis 1969, 1970*a*, 1971) and provide a minimum time constraint for supracrustal deposition. That the supracrustal rocks were gneissic prior to intrusion of granodiorite is indicated by rare paragneiss enclaves that are discordant to the host rock foliation. Few constraints exist for the age of earliest high-grade deformation and metamorphism of the orthogneisses. A minimum age for these events is provided by *ca.* 1460 Ma granites of the Pointe-au-Baril complex which cut migmatitic fabrics in Nadeau Island orthogneiss.

The *ca.* 1740-1605 Ma ages of granitoid plutonism in the study area span the range of late Paleoproterozoic plutonism reported in the Central Gneiss Belt and Grenville Front Tectonic Zone (see Table 5.1). Plutonism was widespread throughout Laurentia in the interval 1.8-1.6 Ga (*e.g.*, in the Yavapai-Mazatzal and Central Plains orogens of the United States (Hoffman 1989) and in the Labrador orogen of eastern Canada (Gower 1990)), and it is reasonable to suggest (*e.g.*, van Breemen and Davidson 1988) that rocks now exposed in the Grenville Front Tectonic Zone and parautochthonous Central Gneiss Belt can be linked to one or more of these flanking orogens. Older plutonic components of

Archean age identified in the Lake Nipissing area (*e.g.*, Krogh 1989; Chen et al. 1993) may have formed a basement to late Paleoproterozoic plutonic and supracrustal rocks (Easton 1992). Sm-Nd data for the parautochthonous Central Gneiss Belt (Dickin and McNutt 1989) suggest that al least some of these early crustal components were juvenile.

This interpretation of early geological history in the Pointe-au-Baril area is fully compatible with the pre-Grenvillian crustal evolution of the northern Britt domain as outlined by Corrigan et al. (1994). The early Britt domain history is remarkably similar to that documented for the eastern Grenville Province where juvenile Labradorian granitoid plutons (1710-1620 Ma) intruded extensive tracts of older metasedimentary rock (Gower 1990).

A second period of tectonic, metamorphic, and plutonic activity occurred in the Pointe-au-Baril area at *ca.* 1470-1430 Ma. The oldest-known rocks of the allochthonous Shawanaga domain formed during this interval. The Shawanaga pluton, Ojibway gneiss association, and granitic members of the Pointe-au-Baril complex were emplaced between *ca.* 1466 Ma and 1460 Ma (Culshaw et al. in prep.), and a megacrystic tonalite member of the Pointe-au-Baril complex was intruded at *ca.* 1430 Ma (Krogh et al. 1993*a*). Anatexis and granulite-facies zircon growth in mafic gneiss of the Nadeau Island gneiss association occurred at *ca.* 1450 Ma, with renewed high-grade metamorphism at *ca.* 1433 Ma (Chapter 5). The *P-T* conditions of final equilibration of granulite-facies assemblages are estimated at 7.2-8.4 kbar and 625-700°C (Ketchum et al. 1994; Chapter 4). Metamorphism evidently had a temporal relationship with early Mesoproterozoic plutonism (see also Tuccillo et al. 1992; Krogh et al. 1993*a*). There is no comparable

evidence for *ca.* 1450-1430 Ma high-grade metamorphism in the allochthonous Shawanaga domain.

The tectonic setting of *ca.* 1450-1430 Ma granulite-facies metamorphism is poorly constrained. Orthopyroxene is syn-kinematic in a number of strongly deformed mafic gneiss exposures in the study area, but most granulite-facies rocks are only weakly deformed. Granulite-facies deformation must have mainly preceded *ca.* 1460 Ma emplacement of the Pointe-au-Baril complex as this body is relatively undeformed where Grenvillian strain is low.

Other workers in the Central Gneiss Belt and Grenville Front Tectonic Zone have reported field and U-Pb evidence for high-grade metamorphism at *ca.* 1455-1430 Ma (*e.g.*, Grenville Front Tectonic Zone - Bethune et al. 1990; Haggart 1991; Bethune 1993; Haggart et al. 1993: northern Britt domain - Corrigan 1990; Corrigan et al. 1994: Huntsville domain - Nadeau 1990: Go Home domain - Krogh et al. 1993*a*) although the present study area represents the only location where field, thermobarometric and U-Pb data obtained from fresh granulites of this age have been reported. Information on the regional extent of metamorphism is limited due to extensive Grenvillian overprinting of early fabrics and mineral assemblages, but the wide distribution of areas where it has been documented indicates that it must have been a regional event. The only evidence for the tectonic setting of *ca.* 1450 Ma metamorphism is from the Grenville Front Tectonic Zone where southwest-dipping, high-grade thrust fabrics formed at this time (Haggart 1991; Bethune 1993). This suggests that thrusting was driven by tectonism in the southeast, perhaps in response to crustal thickening (Bethune 1993). Evidence in Quebec for

subduction-related tectonic and plutonic activity along the Laurentian margin (Dickin and Higgins 1992; Nadeau and van Breeman 1993) lends some tentative support to a compressional tectonic setting for metamorphism. Although widespread felsic to intermediate plutonism in the Central Gneiss Belt at *ca.* 1470-1430 Ma has been interpreted as anorogenic by comparison with coeval plutonism elsewhere in the Laurentian craton (*e.g.*, Bickford et al. 1986; Windley 1989), recent work in the United States (van Schmus et al. 1993; Nyman et al. 1994) suggests that *ca.* 1.5-1.4 Ga plutons may have been emplaced within a convergent tectonic setting, consistent with evidence outlined above from the Grenville Province in Ontario and Quebec.

Deposition of supracrustal rocks took place in the Shawanaga domain after *ca.* 1460 granitoid plutonism but before the Grenvillian orogeny. Quartzite of the Sand Bay gneiss association was deposited after *ca.* 1420 Ma, with deposition of the protolith to the Dillon schist in the interval 1390-1360 Ma (Culshaw et al. in prep.). Detrital zircons in the latter unit are mainly of a single age, indicating (along with field and petrographic characteristics) that the Dillon schist may represent an immature volcanogenic sediment. The structural position of these crustal components and similarity of deposition and provenance age to supracrustal rocks in the Parry Island thrust sheet (Wodicka 1994) suggests that both may belong to a rifted continental margin sequence (Culshaw et al. in prep.).

Grenvillian Events

A suite of metabasic dykes in the southern Britt domain (the 'youngest dyke suite;'

Chapter 2) may represent metamorphosed diabase dykes of the *ca.* 1238 Ma (Krogh et al. 1987) Sudbury swarm. Tectonized remnants of the Sudbury swarm have been identified near Key Harbour in the northern Britt domain (*e.g.*, Corrigan 1990) but their presence in the study area, although implied by field, petrographic and geochemical data (Culshaw et al. 1994; A Davidson, unpublished data), awaits confirmation. Geochemical data from the Arnstein area (Fig. 1.2) strongly suggest that Sudbury dykes extend to the southern edge of the Britt domain in this region (A. Davidson, written communication 1993), strengthening the possibility that they occur along strike in the Pointe-au-Baril area. These dykes, which only record Grenvillian deformation and metamorphism, have not been recognized southeast of the Shawanaga shear zone (Davidson 1991).

In the Pointe-au-Baril area, the youngest (Sudbury?) dykes underwent high-grade metamorphism and were transposed within sub-vertical, northeast-striking straight gneiss with low-rake stretching lineations. These events, of unknown absolute age but termed here 'early' Grenvillian, can be documented in structural zone 2 (Fig. 3.2). Here, least deformed youngest dykes preserve sparse metamorphic orthopyroxene, indicating that early Grenvillian metamorphic conditions briefly attained the granulite facies, or that orthopyroxene was stable during upper amphibolite-facies metamorphism because of a low a_{H_2O} in the dykes. In structural zone 3, this event was responsible for metamorphic orthopyroxene growth in the youngest dykes (some of which preserve relict igneous minerals) and heterogeneous overprinting of pre-Grenvillian assemblages. Metamorphic textures and Grenvillian strain gradients indicate, however, that granulite facies assemblages throughout zone 3 are largely pre-Grenvillian This interpretation is

supported by an absence of Grenvillian U-Pb isotopic resetting in *ca.* 1450 Ma metamorphic zircon (Chapter 5).

Granulite facies assemblages in youngest dykes were overprinted during amphibolite facies straight gneiss development in zone 2. The extent to which this tectonic event affected rocks of the Pointe-au-Baril area is unknown, but weaker fabrics of similar orientation in zone 3 suggest that it was not limited to zone 2. A component of dextral shear is indicated by rare kinematic indicators in zone 2 straight gneiss but the tectonic significance of this event is uncertain. Other Central Gneiss Belt occurrences of northeast-striking straight gneiss with a low rake stretching lineation have been variably attributed to local deviations in extension direction during northwest-directed thrusting (Nadeau and Hanmer 1992), to regional crustal extension during northwest-southeast convergence (Wodicka 1994), or to northeast-directed thrusting (Gower 1992).

Northwest-directed overthrusting of allochthonous domains along a basal detachment within the Shawanaga shear zone (Culshaw et al. 1990, 1994) is considered an early Grenvillian event, but the relationship of this event to straight gneiss development is unclear because of later extensional reworking of the thrust fabrics. Thrusting may have occurred at *ca.* 1080 Ma based on the data of Krogh et al. (1993*a*), but the absolute age of this event is unknown. A *ca.* 1080 Ma thrusting event is broadly consistent, however, with metamorphism in the southern Britt domain at *ca.* 1060-1050 Ma (Tuccillo et al. 1992; Krogh et al. 1993*a*; Culshaw et al. in prep). If overthrusting of allochthonous domains was responsible for granulite-facies mineral growth in the youngest dyke suite in the parautochthon, then overprinting of these assemblages during northeast-striking

straight gneiss development indicates that these fabrics formed *after* thrusting. The northeast-striking straight gneisses may therefore record an intermediate (transitional?) tectonic event between northwest-directed thrusting and southeast-directed extensional shear.

Allochthonous rocks in the Shawanaga domain contain early Grenvillian folds and high-strain fabrics that are suggested to record the thrust emplacement of this domain (Culshaw et al. 1994). The Shawanaga pluton and Ojibway gneiss association contain bodies of coronitic olivine metagabbro that are correlated with a regionally extensive but volumetrically minor, *ca.* 1170-1150 Ma mafic plutonic suite (Davidson and van Breemen 1988; Heaman and LeCheminant 1993). This suite yields isotopic evidence for a regional metamorphic event in the Central Gneiss Belt at *ca.* 1060-1030 Ma (Davidson and van Breemen 1988; van Breemen and Davidson 1990; Heaman and LeCheminant 1993). In the study area, coronitic metagabbro is absent from the Sand Bay gneiss association and has not been identified northwest of the Shawanaga shear zone (Davidson et al. 1990; Davidson 1991; Culshaw et al. 1991*a*). The metagabbros were recrystallized in the granulite facies and show no evidence of the high-pressure metamorphism indicated by scattered occurrences of meta-eclogite in the Shawanaga domain.

Late Grenvillian events in the study area include amphibolite-facies extensional shearing on the Shawanaga and Nares Inlet shear zones, folding about axes parallel to the extensional transport direction, pegmatite dyke intrusion, and exhumation of allochthonous and parautochthonous domains. A late syn-kinematic, *ca.* 1020 Ma pegmatite records the waning stages of extension at an intermediate structural level of the

Shawanaga shear zone (Chapter 5). U-Pb data from a higher structural level (Krogh et al. 1993*a*) suggest that extensional shear may have persisted until, or been renewed at, 1006 Ma. Top-side-southeast transport had ceased at this level of the shear zone by 990 Ma, the age of a straight-walled pegmatite dyke cutting extensional shear fabrics. The Shawanaga shear zone was folded about northwest-trending axes during its extensional shear history, but these folds do not deform the Nares Inlet shear zone, suggesting that it may be a younger structure. This is consistent with the hypothesis (Chapter 3) that extensional displacement was transferred to the Nares Inlet shear zone after the Shawanaga zone was folded and was no longer able to accommodate extension.

Petrographic, mineral chemical, and thermobarometric data from the Pointe-au-Baril area indicate that latest metamorphism was syn-kinematic with late orogenic folding and extensional shearing. Peak Grenvillian *P-T* conditions throughout the Britt domain prior to extension were ~10-14 kbar and ~700-850°C (Corrigan 1990; Anovitz and Essene 1990; Tuccillo et al. 1990; Jamieson et al. 1995; this study); similar peak conditions are tentatively indicated for the allochthonous Shawanaga domain (Anovitz and Essene 1990). U-Pb geochronologic data (Tuccillo et al. 1992; Krogh et al. 1993a; Culshaw et al. in prep.; Chapter 4) suggest that peak metamorphism was approximately coeval in allochthonous and parautochthonous rocks (1060-1050 Ma). This late Grenvillian period saw significant decompression with limited cooling of both footwall and hanging wall rocks to the Shawanaga shear zone. Final equilibration occurred at 5-6 kbar and 555-615°C in the parautochthon, and at a lower *P* and *T*, perhaps near the aluminosilicate triple point, in the allochthon. Decompression of parautochthonous rocks

is attributed to extensional unroofing by the Shawanaga shear zone, and the tectonic setting of decompression recorded by allochthonous rocks is discussed below.

P-T-t Paths

U-Pb data obtained in this study and by other workers from the Pointe-au-Baril area allow time constraints to be placed on *P-T* paths for the southern Britt and northern Shawanaga domains (paths 1 and 2, respectively; Fig. 6.1).

Parautochthon. Peak Grenvillian *P-T* conditions in the parautochthon (~11 kbar, 750°C) are correlated here with *ca.* 1060 Ma metamorphism in the Parryfield and Nadeau Island gneiss associations (U-Pb monazite and zircon ages; Tuccillo et al. 1992; Krogh et al. 1993*a*). This event may have been responsible for orthopyroxene growth in the youngest metadiabase dykes (see above). Path 1*a* (Fig. 6.1) indicates that the southern Britt domain underwent limited cooling and decompression after peak metamorphism, perhaps in response to erosionally controlled exhumation, or alternatively due to thrusting (as suggested for early cooling and decompression in the northern Britt domain; Jamieson et al. 1995).

Path 1*b* (Fig. 6.1) is interpreted to record extensional exhumation of the parautochthon in response to top-side-southeast displacement on the Shawanaga shear zone. The onset of extensional shearing (top of path 1*b*) is not rigorously constrained by the geochronological data but it must have occurred after 1060 Ma but before 1020 Ma, the age of a late syn-kinematic pegmatite dyke in the Shawanaga shear zone (Chapter 5). The latter age is assigned to the low *P* end of the path 1*b* which marks a period of

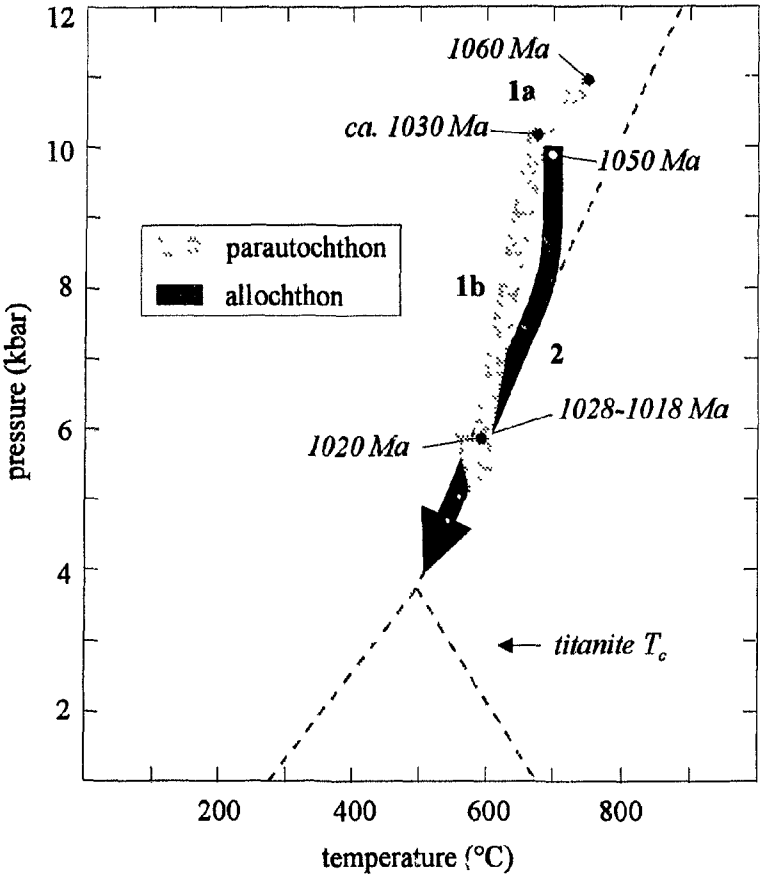

Fig. 6.1. *P-T-t* paths for the southern Britt (parautochthonous) and northern Shawanaga (allochthonous) domains. Aluminosilicate stability fields shown by dashed lines, and titanite closure temperature to diffusion of Pb indicated Path labels 1a, 1b, and 2 correspond to terminology used in text See text for further details.

widespread, late- to post-extension metamorphic equilibration.

Cooling through 680-670°C (the inferred temperature at the beginning of extensional shear) is suggested at ~1043 Ma on a preliminary *T-t* diagram for the southern Britt domain (Fig. 5.13). However, a *ca.* 23 M.y. period of tectonic exhumation (*i.e.*, between 1043 and 1020 Ma) is inconsistent with the preservation of strongly zoned garnets and a metamorphic isograd in parautochthonous rocks of the Shawanaga shear zone (Chapter 4). These indicators of incomplete metamorphic equilibration instead suggest that rapid cooling accompanied and/or immediately followed extensional exhumation, which in turn suggests that unroofing of the parautochthon occurred over a relatively short time interval.

Based on the above evidence, it is suggested that extensional displacement on the Shawanaga shear zone occurred over a period of <23 M.y (perhaps ~10 M.y.?). An age of *ca.* 1030 Ma is tentatively assigned to the beginning of this event (Fig. 6.1). This age is slightly older than titanite ages of 1028-1018 Ma which are interpreted to mark cooling through ~600°C during the decompression event (Chapter 5) and which provide a lower time constraint for the onset of extensional displacement. A ~10 Ma duration of extensional shearing appears reasonable as it allows for rapid rates of both footwall exhumation and cooling, and is comparable to the time span of extensional unroofing in other terranes with a similar fault dip and magnitude of near-isothermal decompression (*e.g.*, Reinhardt and Kleemann 1994). Movement on the Shawanaga shear zone after *ca.* 1020 Ma (implied by U-Pb zircon data; Krogh et al. 1993*a*) is considered here to have contributed little to the tectonic unroofing of the Britt domain.

This interpretation indicates that a revised *T-t* diagram is required for the southern Britt domain. A new *T-t* path incorporating the tentative constraint for the beginning of extensional unroofing (*ca.* 1030 Ma, 670-680°C) is presented in Figure 6.2. This path shows a period of relatively slow post-metamorphic peak cooling, followed by rapid syn- and post-extensional cooling, followed by a return to the pre-extension cooling rate. The path is divided into three segments in Figure 6.2. The form of *segment A*, between 725-600°C, is largely controlled by the proposed constraint for the beginning of extensional shear. *Segment B* (600°C to 475°C) represents the simplest interpretation inferred by the data but is dashed to indicate that alternative paths can be proposed. For instance, fast cooling is shown to persist for a short time after 1020 Ma as the southern Britt domain was rapidly transported ~15 km closer to the surface and most likely continued to cool rapidly following extension. However, the duration of this postulated fast cooling could be shorter or longer than indicated in Figure 6.2. Segment B cooling could also have been delayed by the development of overlying extensional sedimentary basins (*e.g.*, Jamieson et al. 1995), or influenced by *ca.* 1000-980 Ma tectonic activity within the Grenville Front Tectonic Zone (Haggart et al. 1993; Bethune 1993). Titanite ages of 1008-1000 Ma (Fig. 6.2) from shear zone rocks (Chapter 5) may indicate tectonic activity in the Pointe-au-Baril area which potentially had (presently undetected) thermal consequences for the southern Britt domain. Clearly, more data are needed to better constrain this cooling interval. Below 475°C (*segment C*), the *T-t* history of the parautochthon most likely reflects post-orogenic, isostatically-controlled unroofing.

The concave-convex form of the revised *T-t* path for the southern Britt domain is

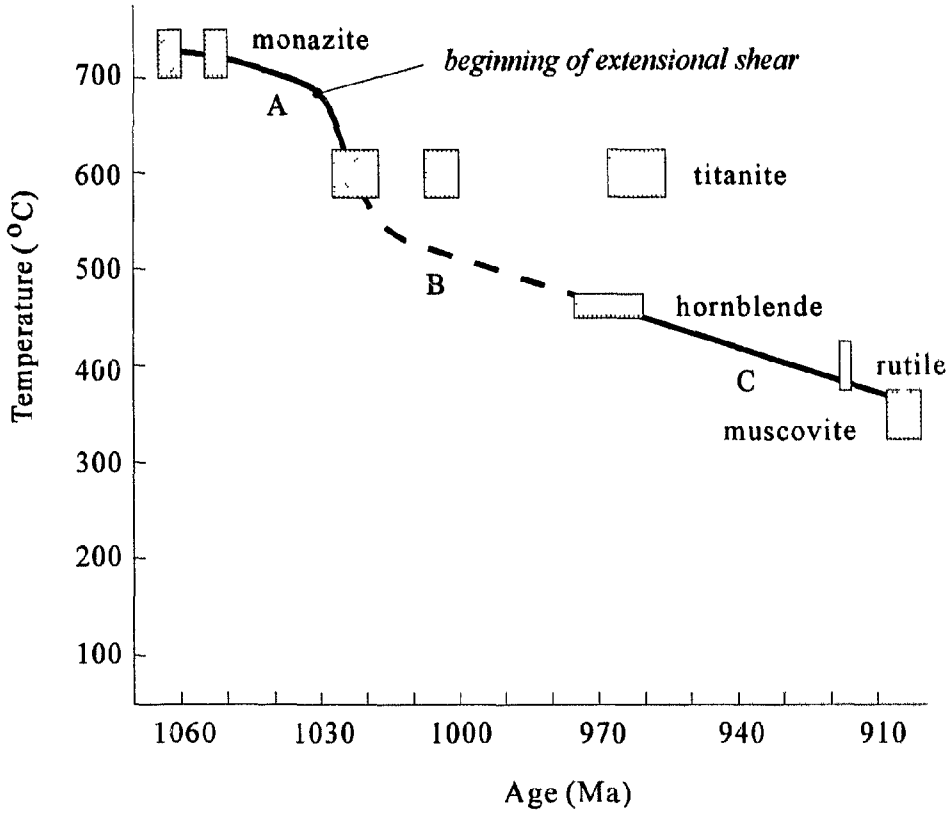

Fig. 6.2. Revised time-temperature (*T-t*) diagram for parautochthonous rocks in the Pointe-au-Baril area. Revised path incorporates estimate of *T-t* conditions at the beginning of extensional displacement on the Shawanaga shear zone. For significance of various titanite age groups, see Fig. 5.13. Path is divided into three segments (A,B,C) for purposes of discussion in text. Segment B dashed as *T-t* history is poorly constrained in this interval. Closure temperatures and isotopic systems are: 725 ± 25°C for monazite (U-Pb; Parrish 1990); 600 ± 25°C for titanite (U-Pb; Heaman and Parrish 1991); 450-475°C for hornblende ($^{40}Ar/^{39}Ar$; McDougall and Harrison 1988 (used by Culshaw et al. 1991); 400 ± 25°C for rutile (U-Pb; Mezger et al. 1989); and 350 ± 25°C for muscovite ($^{40}Ar/^{39}Ar$; Jäger 1979). Sources: monazite - Tuccillo et al. (1992); titanite, rutile - this study; hornblende, muscovite - Culshaw et al (1991*b*).

similar to that proposed by Grasemann and Mancktelow (1993) for footwall rocks to the Simplon normal fault in the Swiss Alps. Thermal models of the Simplon *T-t* paths suggest that the concave-convex form indicates an initial period of rapid extensional displacement on the Simplon fault, consistent with the conclusions of the present study. A thermal model for the Britt domain based largely on data from the Key Harbour area (Culshaw et al. 1991*b*) also predicts a short period of extensional exhumation preceeding erosionally-controlled exhumation and cooling.

Allochthon. The *P-T* path for the northern Shawanaga domain (path 2, Fig. 6.1) is not tightly constrained by thermobarometric data obtained in this study, but additional *P-T* estimates for this region are available. Anovitz and Essene (1990) report a temperature of ~700°C at a maximum pressure of 10.2 kbar for coronitic metagabbro on Highway 69 that underwent metamorphic recrystallization at *ca.* 1050 Ma (Heaman and LeCheminant 1993). Assuming that ~10 kbar is a reasonable equilibrium pressure estimate (as suggested by *P-T* data from other coronites; Grant 1987), an early *P-T-t* point on path 2 can be proposed (Fig. 6.1). The shape of path 2 immediately following *ca.* 1050 Ma metamorphism is poorly constrained by the available thermobarometric data, but if sample D47a is allochthonous rather than parautochthonous (see Chapter 4, *Discussion/P-T Paths*), then its thermobarometric result (Fig. 4.12*b*) suggests a period of isothermal decompression in the Shawanaga domain. Petrographic observations for this sample indicate that sillimanite grew after kyanite but that both polymorphs are texturally stable, suggesting that decompression was to the kyanite-sillimanite transition but not into the sillimanite stability field. The *P-T* data of Tuccillo et al. (1992) for the Shawanaga domain

are consistent with the proposed isothermal decompression history but do not provide rigorous constraints as temperature estimates were not uniquely determined.

Following isothermal decompression, thermobarometric data (Fig. 4.12*b*) indicate further decompression with cooling, most likely along a path that overlapped with the kyanite-sillimanite univariant curve (Fig. 6.1). Cooling of the allochthon through 600°C at 1028-1018 Ma, suggested by U-Pb titanite data (Chapter 5), provides a second *P-T-t* constraint for path 2. The overlap of *P-T* estimates for allochthonous and parautochthonous rocks at *ca.* 1020 Ma suggests that they shared a common metamorphic history after this time.

Alternative Model. An alternative hypothesis for the *P-T-t* evolution of the Pointe-au-Baril area that satisfies the thermochronometric data can be proposed. This model involves (*i*) initiation of extensional shear at the peak of *ca.* 1060 Ma metamorphism in the parautochthon, (*ii*) heating of allochthonous rocks in response to uplift of the hotter footwall rocks, with peak metamorphism in the Shawanaga domain at 1050 Ma, and (*iii*) cooling of both footwall and hanging wall rocks through 600°C at 1028-1018 Ma near the end of extensional shear. This model would require a mechanism such as a change in the extensional displacement rate to account for the bend in path 1 (Fig. 6.1).

This interpretation is not favoured for two reasons. First, the *T-t* history of the parautochthon would involve a *ca.* 40 M.y. period at temperatures between 770-600°C which is inconsistent with evidence for disequilibrium and rapid cooling in these rocks. Second, metamorphic ages of *ca.* 1050 ± 10 Ma are widespread throughout the Central

Gneiss Belt (see Table 5.1). It therefore seems unnecessary to appeal to a local heating phenomenon to account for 1050 Ma metamorphism in the Shawanaga domain.

Tectonic Implications of the P-T-t Data

For simplistic models of extensional unroofing by a single fault (*i.e.*, ignoring the effects of erosion and sedimentation), a pressure drop is predicted for footwall rocks but is not expected in hanging wall rocks (Ridley 1989). An important conclusion reached above for the Pointe-au-Baril area is that both allochthonous and parautochthonous rocks underwent significant decompression at 1050-1020 Ma. The correlation in the southern Britt domain of decompression and cooling with extensional exhumation suggests that this mode of unroofing may also apply to the Shawanaga domain, and perhaps to a larger region of the Central Gneiss Belt. If normal faulting/shearing was an important process in the exhumation of the Central Gneiss Belt, it must have taken place during or after 1060-1030 Ma, the age of regional amphibolite to granulite facies metamorphism, but before cooling to 500°C, below which cooling rates suggest uniform uplift and erosion (Cosca et al. 1991). Extensional displacement ages for the Shawanaga shear zone (1030-1020 Ma), a metre-wide ductile shear zone in the Huntsville area (*ca.* 1039 Ma; Nadeau 1990), and the Bancroft shear zone in the northern Central Metasedimentary Belt (1045-1030 Ma; Mezger et al. 1991*b*) are all consistent with the hypothesis of a regional extensional event during or immediately following regional metamorphism.

As emphasized by Wheeler and Butler (1994), a number of structural, metamorphic, and geochronologic criteria should be considered before designating a

normal fault as an *extensional* fault (*i.e.*, a structure that has contributed to crustal extension). A metamorphic criterion for extensional faulting presented by these workers is that *P-t* histories across an extensional fault should indicate a faster exhumation rate in the footwall than in the hanging wall during the period of normal fault movement. *P-T-t* data obtained in this study suggest that the rate of decompression during *ca.* 1030-1020 Ma normal displacement on the Shawanaga shear zone was greater in the parautochthon than in the allochthon, indicating that this shear zone contributed to crustal extension. There is little geochronological evidence to suggest that this extension drove thrusting at the margin of the orogen (*i.e.*, in the Grenville Front Tectonic Zone) or was contemporaneous with compression in the interior of the orogen. It is possible, however, that an episode of ~1035 Ma thrusting in the northern Britt domain (Jamieson et al. 1995) may have been dynamically linked to extensional shearing in the southern Britt domain. If a linkage exists, then estimates of displacement on the contractional and extensional structures are required to determine if there was net crustal shortening or extension at this time. In the absence of offset marker horizons and knowlege of original shear zone orientations, this task would be difficult to accomplish in the Britt domain.

Apart from the Shawanaga shear zone, only a few large-scale structures that could have contributed to regional extensional exhumation have been identified in the Central Gneiss Belt (*e.g.*, two shear zones within the Parry Sound domain, Culshaw et al. 1989, Wodicka 1994; Parry Sound-Moon River domain boundary, Klemens and Schwerdtner 1991; Ahmic subdomain-Kiosk domain boundary, Schau et al. 1986) and northern Central Metasedimentary Belt (*e.g.*, Bancroft shear zone, van der Pluijm and Carlson 1989,

Carlson et al. 1990; Cosca et al. 1992). Smaller-scale extensional structures are also known in these regions (*e.g.*, metre-wide ductile shear zones in Huntsville area, Nadeau 1990; discrete extensional mylonite zones in the Central Metasedimentary Belt boundary thrust zone, Culshaw 1987) but it is unclear what their contribution, if any, may have been to regional exhumation.

The only other well-studied extensional structure in the Central Gneiss Belt is a southeast-dipping, tens of metres thick, amphibolite-facies shear zone within the western Parry Sound domain along Georgian Bay (Wodicka 1994). This >20 km-long structure lies less than a kilometre above the thrust detachment separating the Parry Sound and Shawanaga domains and parallels this boundary. A marked offset in hornblende $^{40}Ar/^{39}Ar$ cooling ages across this shear zone suggests that southeast-directed extensional movement occurred between *ca.* 1020 and 970 Ma (Wodicka 1994).

At the base of the Parry Sound domain east of Arnstein (Fig. 2.1), roadcut exposures of porphyroclastic tectonite located 4 km east of Milton Lake on Highway 522 contain plentiful kinematic evidence of ductile, top-side southeast displacement (Ketchum, unpublished data). The identification of extensional shear fabrics at this location and 60 km to the southwest near Parry Sound tentatively suggests that late, southeast-directed extensional displacement may represent an important tectonic event for the Parry Sound domain. Southeastward transport of this domain at *ca.* 1020 Ma (the upper age limit for this event; Wodicka 1994) provides a speculative but obvious mechanism for isothermal decompression and unroofing of the Shawanaga domain. If extensional displacement was of a large magnitude, this also provides a possible explanation for the absence of a *ca.*

1060-1030 Ma metamorphic overprint in the Parry Sound domain which is recorded in both structurally underlying and overlying domains. The bulk of the Parry Sound domain may have escaped *ca.* 1060-1030 Ma regional metamorphism by being located at a higher crustal level during this event, with later extensional displacement juxtaposing it (with its older hornblende cooling ages; Wodicka 1994) against rocks residing at a deeper crustal level. Wodicka (1994) noted the probable importance of the extensional shear zone along Georgian Bay in exhuming structurally deeper rocks, but she did not discuss the possibility of significant tectonic transport during this event.

The hypothesis of large-magnitude extensional displacement along the western margin of the Parry Sound domain could be tested by further kinematic and geochronological study of this tectonic boundary. Additional study of all extensional structures identified in the Central Gneiss Belt is required to fully assess their importance in the exhumation and cooling history of the Belt.

A Deep Crustal Equivalent of a Metamorphic Core Complex?

Many recent studies have focused on the role of extension in the tectonic evolution of orogenic belts (see, for example, Dewey 1988 and references therein). A number of these studies describe regions of thickened or formerly thickened crust where metamorphic rocks of moderate to high grade underlie low grade or even unmetamorphosed rocks along an extensional tectonic contact (*e.g.*, Coney 1980; Davis 1983; Davis et al. 1986; Brown and Journeay 1987; Malavieille 1987; Lister and Davis 1989; Anderson and Jamtveit 1990; Fossen and Rykkelid 1992; Hill and Baldwin 1993;

Mancktelow and Pavlis 1994). The metamorphic rocks of the lower plate and the extensional mylonites that cap them have been termed 'metamorphic core complexes' (Coney 1973) and are mainly found in Phanerozoic orogens These complexes commonly exhibit (*i*) a discrete, brittle, extensional detachment fault underlying brittlely deformed upper plate rocks, (*ii*) an underlying zone of ductile extensional mylonite with evidence of reworking ' progressively lower temperature structures, and (*iii*) a higher-grade, variably deformed gneissic core zone beneath the mylonitic carapace. This sequence of lower- over high-grade structures is attributed to the progressive localization of extensional displacement towards the top of the detachment zone (*i.e.*, brittle detachment and mylonitic carapace) as the footwall is tectonically exhumed (Davis 1983). Some metamorphic core complexes are also broadly 'folded' about axes parallel to the extensional transport direction. These structures have been variably interpreted as true folds formed during extensional exhumation (*e.g.*, Malavieille 1987; Mancktelow and Pavlis 1994), and as corrugations of the detachment zone that reflect the geometry of pre-extensional structures (*e.g.*, John 1987; Davis and Lister 1988).

Although the Shawanaga shear zone represents a middle to deep crustal structure that cannot be directly compared to metamorphic core complexes, there are a number of striking similarities that invite a general comparison. The Shawanaga shear zone does not display a brittle detachment surface, but it does contain structural and metamorphic evidence for a progressive migration of shearing toward higher structural levels during extension. This migration is identified by lower pressure metamorphic assemblages and a stronger preferred orientation of stretching lineations toward higher structural levels

(Chapter 4). The Shawanaga shear zone and adjacent rocks were folded about axes parallel to the displacement vector during extensional shear (Culshaw et al. 1994), and etamorphic and geochronologic data suggest rapid exhumation and cooling of the footwall during extensional shear, characteristics that are documented in many metamorphic core complexes (*e.g.*, Davis and Lister 1988; Andersen and Jamtveit 1990).

These similarities suggest that well-documented tectonic and metamorphic processes marking core complex development at structurally higher levels in thickened crust may also have operated at deeper crustal levels. Both the Shawanaga shear zone and related extensional structures (*e.g.*, transverse (northwest-trending) folds in the western Central Gneiss Belt; Culshaw et al. 1994) potentially provide important information on the nature of extension in the lower crust during core-complex style deformation at higher levels. This subject has been the focus of considerable debate, with the middle/lower crustal root zone to core complexes alternatively characterized as a region of distributed pure shear (*e.g.*, Miller et al. 1983) or as a region of simple shear on broad but discrete ductile shear zones (*e.g.*, Wernicke 1985).

6.3 REGIONAL IMPLICATIONS

Position of the Allochthon Boundary Thrust in Ontario

The Allochthon Boundary Thrust is a first-order Grenvillian structure separating reworked parautochthonous rocks of the Laurentian foreland from overlying allochthonous thrust sheets (Rivers et al. 1989). This boundary extends along the length of the Grenville orogen and in many places juxtaposes high-grade over lower-grade rocks. Its

position is well constrained by geological and aeromagnetic data in the eastern Grenville Province but is more speculative in the western part of the Province. In Ontario, the Allochthon Boundary Thrust was suggested to underlie the Parry Sound and Seguin domains (Rivers et al. 1989; Fig. 6.3). Rivers et al. (1989) indicated that their positioning of the Allochthon Boundary Thrust in Ontario and western Quebec was based on limited data and therefore subject to revision.

Detailed mapping along Georgian Bay by Culshaw et al. (1988, 1989) led to the suggestion that the basal detachment to allochthonous thrust sheets (*i.e.*, the Allochthon Boundary Thrust) coincided with the Shawanaga shear zone rather than with the Parry Sound shear zone (Culshaw et al. 1990). This interpretation accords well with the inference (Davidson et al. 1990; Davidson 1991) that the Shawanaga shear zone may be a fundamental crustal structure as 1238 Ma Sudbury dykes do not occur southeast of it and *ca.* 1170-1150 Ma coronites have not been identified northwest of it. The Shawanaga shear zone also marks the northwest limit of scattered occurrences of meta-eclogite (Culshaw et al. 1991*a*), providing further support of a first-order status for this tectonic boundary.

The distribution of distinctive metabasite suites across the Shawanaga shear zone indicates that (*i*) allochthonous domains southeast of this structure may not have been contiguous with the parautochthon at 1238 Ma or at 1170-1150 Ma, and (*ii*) Grenvillian tectonism (most likely northwest-directed thrusting) was responsible for the juxtaposition of domains with contrasting histories of mafic plutonism.

If the Shawanaga shear zone marks the position of the Allochthon Boundary

Option (*i*)

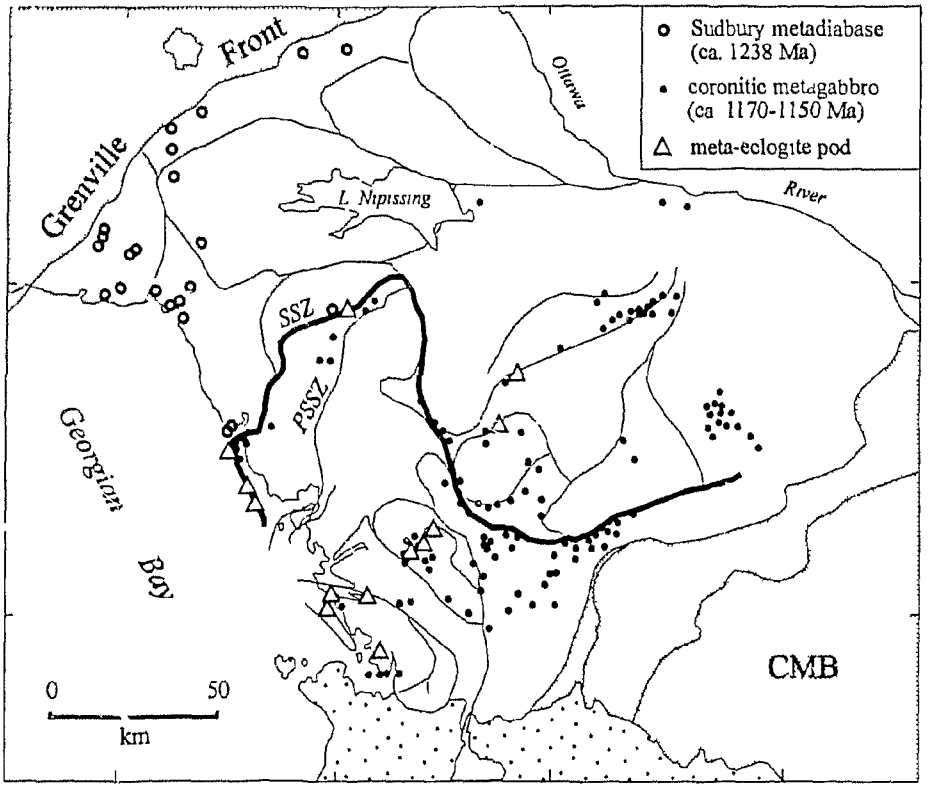

Fig. 6.3. Position of the Allochthon Boundary Thrust (thick line) in option (*i*) model of the Central Gneiss Belt (see text) The boundary follows a route proposed by Rivers et al. (1989) except in the west where it corresponds to the Shawanaga shear zone (SSZ) instead of the Parry Sound shear zone (PSSZ). Boundary does not subdivide mafic plutonic suites in the east as it does along the Shawanaga shear zone. See Fig. 1.2 for names of lithotectonic domains.

Thrust in the western Central Gneiss Belt, where then does this boundary lie to the east? The Shawanaga shear zone has been traced from Georgian Bay northeastward to the village of Arnstein (Fig. 1.2; Davidson et al. 1982), beyond which its position and lateral extent are uncertain. Based on reconnaissance-scale maps of the Central Gneiss Belt (*e.g.*, Davidson 1984*a*), the Allochthon Boundary Thrust may either (*i*) turn to the south and follow the eastern margin of the Parry Sound domain (Fig. 6.3), as originally proposed by Rivers et al. (1989), or (*ii*) it may continue along an unknown course following a generally eastward or northeastward trend. These scenarios are termed here option (*i*) and option (*ii*), respectively.

Option (*i*) was suggested for the Central Gneiss Belt by Rivers et al. (1989) because the Algonquin and Kiosk domains are temporally and lithologically similar to the Britt domain and are thought to share a similar polyorogenic history. Linkage of these domains was earlier proposed on structural grounds by Culshaw et al. (1983) who considered them as a common footwall to higher level thrust sheets emplaced during the Grenvillian orogeny. However, if the distribution of metabasic rocks noted across the Shawanaga shear zone is employed as a (presently speculative) criterion to delineate the position of the Allochthon Boundary Thrust elsewhere in the Central Gneiss Belt, option (*i*) is clearly not favoured as meta-eclogites and 1170-1150 Ma coronites occur on both sides of this boundary southeast of the Parry Sound domain (Fig. 6.3).

Option (*ii*) can satisfy the metabasite distribution criterion if the Allochthon Boundary Thrust lies north of occurrences of *ca.* 1170-1150 Ma coronitic metagabbro located east of the Parry Sound domain. Two tentative positions for this boundary are

shown in Figure 6.4; both separate regions where Sudbury dykes (in the north and west) and coronitic metagabbros (in the south) have been confidently or tentatively identified (Davidson 1991). A body of coronitic metagabbro east of Lake Nipissing lies north of the southern proposed boundary (SPB, Fig. 6.4), but its identification as a member of the *ca.* 1170-1150 Ma suite remains to be rigorously established (A. Davidson, personal communication 1993).

The northern proposed boundary (NPB, Fig. 6.4) follows lithotectonic domain boundaries shown by Easton (1992) and separates Archean rocks and younger lithologies identified north and west of Lake Nipissing (*e.g.*, Krogh 1989; Krogh et al. 1992; Chen et. al. 1993) from rocks for which Archean protolith ages have not been documented. Easton (1992) suggested that the mainly supracrustal Tomiko domain in the northern Central Gneiss Belt (Fig. 6.4) may be allochthonous. For this reason, the proposed northern boundary follows the western and northern margins of the Tomiko domain.

The position of the southern proposed boundary (Fig. 6.4) is based on the speculation of Davidson and Grant (1986) that straight gneisses in the Kiosk domain may form part of a regionally continuous high-strain belt linking with the Shawanaga shear zone to the northwest. The northern limit of straight gneisses in the Kiosk domain is marked by a southeast-dipping mylonite zone across which a marked variation in lineation trend occurs (Davidson and Grant 1986). The southern proposed boundary is placed along this mylonite zone and follows it eastward to a region where a northwest structural trend tentatively allows this boundary to be linked with the western edge of the Tomiko terrane (Fig. 6.4).

Option (*ii*)

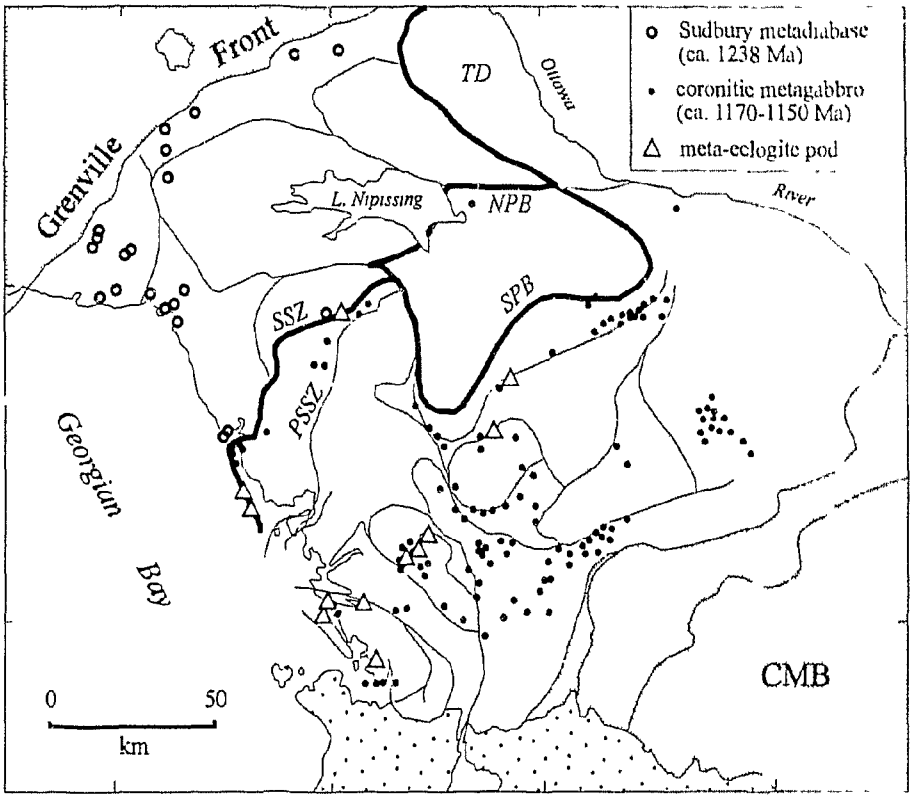

Fig. 6.4. Two tentative positions for the Allochthon Boundary Thrust proposed in option (*ii*) model of the Central Gneiss Belt (see text). Both the northern proposed boundary (NPB) and southern proposed boundary (SPB) separate known bodies of Sudbury metadiabase from coronitic metagabbro and meta-eclogite. Mafic body east of Lake Nipissing has not been rigorously identified as a member of the *ca.* 1170-1150 Ma coronite suite (A. Davidson, personal communication 1993). Both boundaries link with the western edge of the Tomiko domain (TD), suggested by Easton (1992) to be allochthonous. See Fig. 6.3 for further details.

There are several lines of evidence apart from the distribution of metabasic rocks suggesting that option (*ii*) or a similar model may be more tenable than option (*i*). White et al. (1994) correlated a deep crustal reflector imaged in seismic reflection lines 30 and 31 of the Lithoprobe Abitibi-Grenville Transect with the Shawanaga shear zone. If this correlation is correct, and if the Shawanaga shear zone contains the Allochthon Boundary Thrust, then this first-order boundary cannot coincide with the Parry Sound-Ahmic domain boundary (option *i*) as it passes well beneath the Ahmic domain and extends to an even greater depth toward the southeast.

Additional evidence that the Allochthon Boundary Thrust follows a different course than suggested in option (*i*) comes from western Quebec where several workers (*e.g.*, Indares and Martignole 1990*a*; Ciesielski and Parent 1992) have interpreted a convoluted tectonic boundary (Fig. 6.5) as the Allochthon Boundary Thrust. This interpretation places the Allochthon Boundary Thrust near the Grenville Front in western Quebec and makes difficult a linkage with shear zones in the southern Central Gneiss Belt of Ontario. This boundary may instead extend westward into the northern boundary of the Tomiko terrane as suggested in Figure 6.5, although current maps for the area (Easton 1992; Ciesielski and Parent 1992) show these boundaries to be offset by about 40 km along the Ontario-Quebec border. Further mapping should be undertaken to test this hypothesis.

A major implication of option (*ii*) is that not all crust lying structurally above the Allochthon Boundary Thrust in Ontario need be younger than *ca.* 1470 Ma, the age of the oldest allochthonous crust (as currently defined) in Ontario. Option (*ii*) suggests that

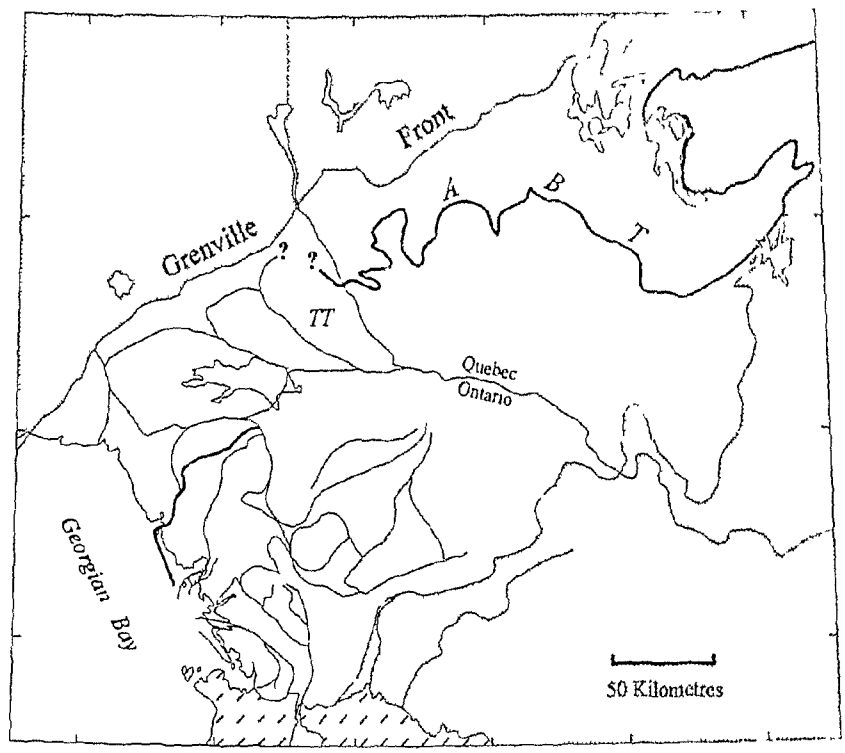

Fig. 6.5. Position of the Allochthon Boundary Thrust (ABT) in western Quebec as recently proposed by several workers (*e.g.*, Indares and Martignole 1990*a*, Ciesielski and Parent 1992) This boundary may link with the northern margin of the Tomiko terrane (TT), providing support for the option (*ii*) model of the Central Gneiss Belt (Fig. 6 4)

segments of older crust, including the Go Home and Rosseau subdomains (Fig. 1.2), were incorporated into the base of the allochthonous thrust wedge during Grenvillian crustal imbrication. This is not unlike the orogenic history for some allochthonous rocks in the eastern Grenville Province which were thrust over lithologically correlative units in the parautochthon (Rivers et al. 1989). In Ontario, many of the allochthonous thrust sheets (domains) depicted in Figure 6.4 contain evidence for an early, high-pressure metamorphism (in the form of meta-eclogite pods), and all allochthonous thrust sheets except for the Parry Sound domain contain *ca.* 1170-1150 Ma coronitic metagabbro. These elements suggest that the allochthonous thrust stack had a common metamorphic and plutonic history that was distinct from parautochthonous rocks during early Grenvillian orogenesis.

Nadeau (1990) postulated that peak metamorphism in the Algonquin thrust stack (Huntsville, Novar, McClintock, McCraney subdomains; Fig. 1.2) occurred before *ca.* 1100 Ma and perhaps as early as *ca.* 1170 Ma, with cooling below the monazite blocking temperature (~725°C; Parrish 1990) at *ca.* 1067 Ma. In contrast, U-Pb data for the Britt domain (Corrigan 1990; Tuccillo et al. 1992; Jamieson et al. 1992; Krogh et al. 1993a; Corrigan et al. 1994; Culshaw et al. in prep.; Chapter 5) provide no evidence of Grenvillian high-grade metamorphism prior to *ca.* 1060 Ma. These data, along with other geological and geochronological evidence, have been used to construct tectonic models for the Central Gneiss Belt in which the tectonic setting of metamorphism involved either normal sequence (Culshaw et al. 1990; Jamieson et al. 1992; Culshaw et al. 1994) or break-back (Nadeau 1990; Nadeau and Hanmer 1992) thrusting. Without addressing

either of these models in detail, option (*ii*) provides a means of accounting for discrepancies in metamorphic age data and thrusting sequence between the Algonquin thrust stack and the Britt domain. The Algonquin thrust stack may have been part of a metamorphic pile that did not include the Britt domain during its peak thermal history. Later overthrusting of this pile onto the parautochthon was likely responsible for burial and younger metamorphism in the Britt domain.

Delineation of candidate structures that link with previously identified segments of the Allochthon Boundary Thrust, across which distinctive variations in metamorphic age, structural style, and mafic plutonic history can be documented, provides a test of option (*ii*). Because of a current paucity of detailed data of this type, the presently speculative nature of this model must be emphasized.

Extensional Reactivation of the Allochthon Boundary Thrust

This study has established that the Allochthon Boundary Thrust along Georgian Bay was reactivated as an extensional shear zone at ~1030-1020 Ma, but so far has not suggested a cause for this reactivation. That extension can be considered a late orogenic (as opposed to a post-orogenic) event is indicated by evidence of northwest-directed thrusting in the Grenville Front Tectonic Zone as late as *ca.* 980 Ma (Haggart et al. 1993). Given this generally convergent tectonic setting, why then did the Central Gneiss Belt experience a major episode of northwest-southeast extension at *ca.* 1030-1020 Ma?

There are a number of reasons why thickened orogenic crust may undergo extension during convergence, including (*i*) the presence of a thermally weakened lower

crust which can no longer support the orogen (*e.g.*, Houseman and England 1986; Ridley 1989; Willett et al. 1993), (*ii*) a decrease in the rate of convergence (*e.g.*, Willett et al. 1993), (*iii*) detachment of a thickened mantle lithosphere (*e.g.*, England and Houseman 1988; Dewey 1988; Platt and Vissers 1989), and (*iv*) gravitational collapse of overthickened crust (*e.g.*, Burchfiel and Royden 1985; Dewey 1988). Some of these options were considered by Culshaw et al. (1994) for the Pointe-au-Baril area and it was concluded that thermal relaxation following overthrusting may have led to a gravity-assisted shape adjustment of the orogen. This was expressed in the western Central Gneiss Belt by the development of extensional shear zones and large-scale transverse folds.

The results of this study indicate that extensional reactivation of the Shawanaga shear zone post-dated peak metamorphism in the southern Britt domain by a minimum of 20 M.y. A similar temporal relationship of extensional exhumation to peak metamorphism has been described in the northern Britt domain (Jamieson et al. 1995). In the Huntsville area (Fig. 1.2), Nadeau (1990) also observed that metre-scale ductile extensional shear zones (one dated at *ca.* 1040 Ma) formed after the peak of metamorphism (>1100 Ma in this region). These observations from a wide region of the Central Gneiss Belt suggest that extension did not accompany peak metamorphism, but rather post-dated it by several tens of millions of years (however, see below).

The 1040-1020 Ma period of extension in the Central Gneiss Belt was contemporaneous with the waning stages of northwest-directed thrusting along the Central Metasedimentary Belt boundary zone (van Breemen and Hanmer 1986). Thrusting

may have slowed or stopped at this time due to a decrease in the northwest-southeast convergence rate. For a thick orogen with a thermally weakened base, such a change in boundary conditions would have caused the orogen to enter a state of extension (*cf.* Willett et al. 1993) and represents one possible reason for the initiation of late orogenic extension in the southwest Grenville Province. Another possibility, favoured by Nadeau (1990), is that late-stage break-back thrusting caused renewed crustal thickening that triggered extensional collapse. This scenario is difficult to postulate for the study area as there is no evidence for break-back thrusting in this region of the Central Gneiss Belt, and a thrust of 'correct' age (1030-1020 Ma) that thickened the crust prior to extension without renewed heating has not been identified.

England and Richardson (1977) noted that peak metamorphic conditions are reached at a progressively later time with increased depth in thrust-thickened crust. This observation leads to the alternative suggestion that extensional deformation in the Central Gneiss Belt occurred in response to thermal weakening at a deeper crustal level than is represented by the present-day erosion surface. A deep structure such as the Shawanaga shear zone may have been reactivated after the local metamorphic peak by peak-metamorphic extensional deformation at an even deeper crustal level.

Thermobarometric data presented by Anovitz and Essene (1990) suggest that highest Grenvillian pressures and temperatures in Ontario were reached in the western half of the Central Gneiss Belt (see their Figs. 3 and 6). It is tempting to speculate that extensional reactivation of the Shawanaga shear zone was linked to the presence of a thicker and warmer crust in this region. Deep burial by northwest-directed stacking of

thrust sheets, perhaps with a component of convergent movement into the bend in the Grenville Front (Fig. 1.2) that enhanced crustal thickening in the western Central Gneiss Belt, may have led to some combination of thermal weakening, gravity-driven collapse, and/or decreased convergence rate which allowed the orogen to enter a state of extension.

6.4 CONCLUSIONS

1) In the Central Gneiss Belt near Pointe-au-Baril, Ontario, the parautochthonous, polycyclic Britt domain is overlain by the allochthonous, monocyclic *Shawanaga domain* (new name) along a ~3 km-thick, southeast- to northeast-dipping ductile shear zone. This structure is termed the *Shawanaga shear zone* (new name),and has been proposed in this and other studies (*e.g.*, Culshaw et al. 1990, 1994; Jamieson et al. 1992) to coincide with the Allochthon Boundary Thrust (Rivers et al. 1989) in the western Grenville Province. The Shawanaga shear zone accommodated northwest-directed thrusting of the Shawanaga domain and overlying domains onto the parautochthon during the Grenvillian orogeny, but was reactivated as a top-side-southeast extensional shear zone during late Grenvillian, northwest-southeast ductile extensional flow. Extensional reactivation occurred in the upper amphibolite facies and was accompanied by metre- to kilometre-scale folding about axes parallel to the extensional transport direction. Kinematic evidence for early thrusting on the Shawanaga shear zone is absent near Pointe-au-Baril but has been observed ~65 km along strike to the northeast where the late extensional overprint is less intense. A smaller extensional mylonite zone (the Nares Inlet shear zone) lies structurally beneath the

Shawanaga shear zone and also accommodated late orogenic, top-side southeast normal displacement.

2) Structural data from a 20 x 20 km study area near Pointe-au-Baril are used to delineate six structural zones, each bearing a unique combination of planar and linear fabric orientations. A structural zone lying between the Shawanaga and Nares Inlet shear zones locally preserves pre-Grenvillian granulite-facies mineral assemblages. Northwest-trending folds found within and south of the Shawanaga shear zone and to the north of the Nares Inlet shear zone are absent from this structural zone and an adjacent zone, suggesting that the shear zones decoupled the intervening region from late Grenvillian reworking. Although the shear zones are contemporaneous structures, the Nares Inlet shear zone is not folded and may therefore have been kinematically active after movement on the Shawanaga shear zone had ceased. It is proposed that syn-extensional folding resulted in 'locking' of the Shawanaga shear zone and a transfer of extensional displacement to the underlying Nares Inlet shear zone.

3) Thermobarometric estimates from the study area indicate peak or near-peak *P-T* conditions of 625-700°C and 7.2 to 8.4 kbar for pre-Grenvillian granulite-facies metamorphism. Peak Grenvillian *P-T* conditions in the parautochthonous Britt domain were 745-770°C and 10.6-11.6 kbar. The post-peak metamorphic history of this domain was marked by an initial period of cooling and decompression, followed by a period of near-isothermal decompression in response to extensional unroofing by the Shawanaga shear zone. Final metamorphic equilibration in the Britt domain at the end of extensional shearing was at 555-615°C and 5.1-6.0 kbar. The allochthonous Shawanaga domain

underwent a similar decompression event at this time. Peak *P-T* conditions of 700°C and ~10 kbar are suggested for this domain by the data of Anovitz and Essene (1990), with final equilibration perhaps at 485°C and 3.6 kbar (this study). This *P-T* path is not tightly constrained by thermobarometric data but nevertheless suggests that the Shawanaga domain may have been unroofed by a structurally higher extensional fault. A candidate structure for this exhumation is a narrow extensional shear zone near the base of the Parry Sound domain.

4) Britt domain pelitic gneisses in the Shawanaga shear zone preserve garnet porphyroblasts with strong major element zoning and an inverted isograd marked by the first appearance of sillimanite at higher structural levels in kyanite + K-feldspar assemblages. The garnet zoning is interpreted as a product of incomplete homogenization of high-pressure (~10 kbar) garnet compositions during decompression and rapid cooling that accompanied extensional shear. The inverted isograd is proposed to indicate (*i*) migration and narrowing of the kinematically active shear belt toward the top of the Shawanaga shear zone during extension, combined with (*ii*) a dependence of mineral reaction kinetics on strain energy. Shear zone rocks at higher levels equilibrated to the ambient *P* and *T* while kinematically active whereas rocks at kinematically inactive lower levels of the shear zone did not continue to equilibrate. Given the steep *P-T* trajectory of extensional unroofing, the 'inverted' isograd represents a bathograd between higher-pressure (Ky-bearing) and lower-pressure (Sil-bearing) assemblages.

5) U-Pb zircon data from fresh, pre-Grenvillian granulite gneiss indicate that this metamorphism occurred at *ca.* 1450-1430 Ma. Grenvillian metamorphism did not

influence the U-Pb isotopic systems of pre-Grenvillian metamorphic zircon in the analysed samples. The pre-Grenvillian metamorphism was coeval with early Mesoproterozoic granitoid plutonism in the Pointe-au-Baril area and throughout the Central Gneiss Belt and Grenville Front Tectonic Zone

6) Granitic pegmatite dykes that are pre-kinematic to early syn-kinematic, late syn-kinematic, and post-kinematic in the Shawanaga shear zone were emplaced at *ca.* 1042 Ma, 1019 ± 4 Ma, and *ca.* 990 Ma. These data demonstrate that extensional shearing was in the waning stage at *ca.* 1020 Ma and had ceased by *ca.* 990 Ma. The *ca.* 1042 Ma pegmatite is suggested to pre-date extensional shear based on metamorphic and thermochronologic evidence for a short-lived extensional displacement event

7) U-Pb titanite ages from the study area span a 93 M y. interval and are concordant to near-concordant The titanite data fall into three $^{207}Pb/^{206}Pb$ age groups that are characterized by particular combinations of titanite morphology and colour, and host rock structural setting and metamorphic texture. The oldest age group (1028-1018 Ma) is interpreted to mark the time of cooling through 600°C in allochthonous and parautochthonous rocks. The intermediate age group (1008-1000 Ma) was obtained from strongly sheared rocks and indicates titanite recrystallization and/or growth at <600°C at this time in the extensional shear zones. The youngest age group (967-956 Ma) dates a final recrystallization/growth event that probably occurred in the presence of metamorphic fluids in the cooling crust. These data collectively demonstrate the numerous difficulties that can be encountered in interpreting U-Pb titanite ages from the Grenville Province, and caution against oversimplistic interpretations of titanite age data in high-grade terranes

8) A *T-t* curve for the southern Britt domain shows relatively slow cooling rates (*i*) between the peak of Grenvillian metamorphism at *ca.* 1060 Ma and the beginning of extension at *ca.* 1030 Ma, and (*ii*) beginning a short time after the end of extensional shearing. An intermediate period of more rapid cooling occurred during and immediately following extensional exhumation of the southern Britt domain.

9) An evaluation of Lithoprobe seismic reflection data, geological data from western Quebec, and the distribution of distinctive mafic rock suites across the Shawanaga shear zone suggests that the Allochthon Boundary Thrust may follow a different course than is currently proposed for the Central Gneiss Belt. Two revised positions for the Allochthon Boundary Thrust proposed in this study both require that lithotectonic domains with characteristics of parautochthonous crust were incorporated into the base of the allochthonous thrust stack during Grenvillian orogenesis.

10) A variety of structural, metamorphic and geochronologic data from the Pointe-au-Baril area indicate that extensional tectonism played an important role in the late orogenic history of this region. The extent to which this tectonometamorphic event affected a wider region of the Central Gneiss Belt is currently uncertain. This mode of Grenvillian crustal thinning was likely a consequence of orogenic thickening and thermal weakening of the lower crust, and may have been triggered by a slowing in the rate of northwest-southeast convergence.

APPENDIX A

Mineral Compositions Used In Thermobarometry

Analyses presented in the following tables represent averaged mineral compositions or, for cases where N = 1 (see below), a single analysis.

Symbols used in Table Headings:

Analysis	--	number refers to probe spot(s) where analyses were obtained
Location	--	matrix = matrix phase
		int/bt = intergrown with biotite
		inc/gt = included phase in garnet
		inc/pl = included phase in plagioclase
		rim = rim analyses of zoned phase
		core = core analyses of zone phase
		mid = analyses from midway between core and rim
		ave = analyses from core, mid, and rim
N	--	number of analyses used in averaging calculation

Table A1. Garnet compositions used in thermobarometry. Formulae calculated on the basis of 12 oxygens.

Sample	88-3a	89-3	89-35	89-35	89-42c	D47a	89-67c	89-73a
Analysis	3	3	1,3	3	1,2	1,2	1,2,3	1,2,3,4
Location	rim	rim	rim	core	rim	rim	rim	ave
n	4	2	4	1	5	6	7	11
SiO2	37.64	37.14	37.95	38.33	36.77	37.25	37.16	39.12
Al2O3	21.61	20.70	20.93	20.93	20.27	20.75	20.62	22.23
FeO	25.98	30.92	32.85	28.74	38.07	35.23	30.53	22.50
MnO	1.67	6.47	1.63	1.30	0.81	1.83	7.34	1.42
MgO	5.77	3.30	4.45	4.86	2.10	2.88	2.59	10.13
CaO	7.21	0.88	2.16	5.44	1.88	1.71	1.53	3.85
Na2O	0.06	0.00	0.27	0.17	0.13	0.21	0.14	0.00
Total	99.94	99.41	100.24	99.77	100.03	99.86	99.91	99.25
Si	2.952	3.010	3.016	3.025	2.998	3.009	3.010	2.994
Al	1.996	1.975	1.959	1.945	1.946	1.974	1.967	2.004
Fe	1.704	2.095	2.184	1.897	2.596	2.380	2.068	1.440
Mn	0.111	0.444	0.110	0.087	0.056	0.125	0.504	0.092
Mg	0.675	0.399	0.527	0.572	0.255	0.347	0.313	1.156
Ca	0.606	0.076	0.184	0.460	0.164	0.148	0.133	0.316
Na	0.009	0.000	0.042	0.026	0.021	0.033	0.022	0.000
Sum	8.053	7.999	8.022	8.012	8.036	8.016	8.017	8.002
Mg/(Mg+Fe)	0.284	0.160	0.194	0.232	0.089	0.127	0.131	0.445
Alm	0.550	0.695	0.727	0.629	0.845	0.793	0.685	0.479
Grs	0.196	0.025	0.061	0.153	0.053	0.049	0.044	0.105
Prp	0.218	0.132	0.175	0.190	0.083	0.116	0.104	0.385
Sps	0.036	0.147	0.037	0.029	0.018	0.042	0.167	0.031
Fe3+	0.051	0.020	0.083	0.075	0.088	0.061	0.056	0.000
Fe2+	1.619	2.079	2.097	1.827	2.488	2.315	2.008	1.438

Table A1.

Sample	89-88a	89-88a	89-88b	89-103a	89-103a	89-104d	89-108a	89-115b
Analysis	1	1	1	2,3	3	1,3	1,2,3	1,2,3
Location	core	rim	mid	ave	core	ave	rim	rim
n	3	3	1	8	1	5	3	6
SiO2	38.96	38.92	38.30	38.57	38.38	37.90	37.36	38.41
Al2O3	21.64	21.55	21.08	20.74	20.15	21.64	20.77	20.91
FeO	24.96	25.50	26.23	27.32	28.27	29.98	32 40	32.61
MnO	1.44	1.52	1.77	1.87	1.93	1.67	2.87	0.65
MgO	7.37	6.65	5.56	4.88	5.14	7.13	3.48	5.27
CaO	5.91	6.04	6.10	6.34	5.27	1.01	2.36	1.60
Na2O	0.18	0.07	0.22	0.18	0.18	0.00	0.24	0.29
Total	100.46	100.25	99.26	99.90	99.32	99.33	99.48	99.74
Si	3.001	3.013	3.017	3.035	3.047	2.987	3.010	3.043
Al	1.963	1.965	1.955	1.922	1.884	2.008	1.971	1.951
Fe	1.608	1.651	1.728	1.798	1.877	1.976	2.183	2.161
Mn	0.094	0.100	0.118	0.125	0.130	0.111	0.196	0.044
Mg	0.846	0.767	0.653	0.573	0.608	0.838	0.418	0.622
Ca	0.488	0.501	0.515	0 535	0.448	0.085	0.204	0.136
Na	0.027	0.011	0.034	0.027	0.028	0.000	0.037	0.045
Sum	8.027	8.008	8.020	8.015	8.022	8.005	8.019	8.002
Mg/(Mg+Fe)	0.345	0.317	0.274	0.242	0.245	0.298	0.161	0.223
Alm	0.530	0.547	0.573	0.593	0.613	0.656	0.727	0.729
Grs	0.161	0.166	0.171	0.177	0.146	0.028	0.068	0.046
Prp	0.279	0.254	0.217	0.189	0.198	0.278	0.139	0.210
Sps	0.031	0.033	0.039	0.041	0.042	0.037	0.065	0.015
Fe3+	0.073	0.043	0.078	0.096	0.133	0.000	0.069	0.076
Fe2+	1.526	1.610	1.648	1.708	1.752	1.968	2.109	2.102

Table A1.

Sample	89-115b	89-116c	89-116c	89-125	89-129b	89-155	89-200f	89-208b
Analysis	3	1,2	3	1	1,2,4	1,3,4	3	2
Location	core	rim	core	rim	ave	ave	rim	rim
n	2	4	1	1	11	8	4	2
SiO2	38.55	37.52	37.82	37.89	36.71	36.41	38 86	38.01
Al2O3	21.22	20.33	20.90	21.05	20.97	20.06	20.98	21.23
FeO	29.74	30.08	28.54	27.79	32.85	35.40	25.11	24.93
MnO	0.49	1.76	1.16	1.56	5.47	4.94	0.39	3.60
MgO	6.32	2.54	2.91	3.79	2.65	1.65	6.15	4.30
CaO	3.88	7.49	8.90	7.91	1.39	1.25	8.60	7.96
Na2O	0.21	0.17	0.17	0.00	0.00	0.12	0.09	0.00
Total	100.41	99.89	100.40	99.99	100.04	99.83	100.18	100.03
Si	3.010	3.009	2.996	2.997	2.976	2.993	3.016	2.993
Al	1.951	1.920	1.950	1.961	2.002	1.942	1.918	1.969
Fe	1.942	2.018	1.891	1.839	2.227	2.433	1.630	1.642
Mn	0.032	0.120	0.078	0.105	0.376	0.344	0.026	0.240
Mg	0.736	0.304	0.344	0.447	0.320	0.202	0.712	0.505
Ca	0.325	0.644	0.755	0.670	0.121	0.110	0.715	0.672
Na	0.032	0.026	0.026	0.000	0.000	0.019	0.014	0.000
Sum	8.028	8.041	8.040	8.019	8.022	8.043	8.031	8.021
Mg/(Mg+Fe)	0.275	0.131	0.154	0.196	0.126	0.077	0.304	0.235
Alm	0.640	0.654	0.616	0.601	0.732	0.788	0.529	0.537
Grs	0.107	0.209	0.246	0.219	0.040	0.036	0.232	0.220
Prp	0.243	0.099	0.112	0.146	0.105	0.065	0.231	0.165
Sps	0.011	0.039	0.025	0.034	0.124	0.111	0.008	0.078
Fe3+	0.086	0.117	0.092	0.046	0.015	0.096	0.100	0.041
Fe2+	1.848	1.888	1.782	1.784	2.191	2.313	1.525	1.592

Table A1.

Sample	89-250
Analysis	2,3
Location	rim
n	6
SiO2	38.56
Al2O3	20.85
FeO	28.42
MnO	0.77
MgO	5.94
CaO	5.81
Na2O	0.18
Total	100.53
Si	3.011
Al	1.918
Fe	1.856
Mn	0.051
Mg	0.692
Ca	0.486
Na	0.027
Sum	8.041
Mg/(Mg+Fe)	0.272
Alm	0.602
Grs	0.158
Prp	0.224
Sps	0.017
Fe3+	0.120
Fe2+	1.725

Table A2. Biotite compositions used in thermobarometry. Formulae calculated on the basis of 22 oxygens.

Sample	89-3	89-35	89-35	90-42c	D47a	89-67c	89-103a	89-104d
Analysis	1	1,2,3	3	1	1,2,4	1,2,3	1,3	1
Location	matrix	matrix	inc/gt	matrix	matrix	matrix	matrix	matrix
n	1	8	1	2	7	9	8	3
SiO2	35.79	36.21	36.63	33.98	35.06	35.05	38.01	36.87
TiO2	2.06	4.59	4.67	5.47	3.97	3.91	5.41	3.77
Al2O3	18.49	16.89	18.01	17.62	18.11	18.20	15.44	16.52
FeO	17.58	16.07	13.66	25.12	20.98	19.91	13.39	11.79
MnO	0.19	0.00	0.00	0.00	0.00	0.16	0.00	0.03
MgO	10.36	11.68	12.75	4.75	7.73	7.83	12.89	15.77
CaO	0.00	0.00	0.00	0.00	0.00	0.00	0.04	0.00
Na2O	0 45	0.27	0.26	0.00	0.29	0.23	0.29	0.10
K2O	9.37	9.60	9.32	9.81	9.69	9.27	9.28	9.37
Total	94.29	95.31	95.30	96.75	95.83	94.56	94.75	94.22
Si	5.464	5.440	5.417	5.276	5.370	5.401	5.646	5.477
AlIV	2.536	2.560	2.583	2.724	2.630	2.599	2.354	2.523
AlVI	0.789	0.428	0.554	0.498	0.636	0.704	0.347	0.367
Ti	0.237	0.519	0.519	0.639	0.457	0.453	0.604	0.421
Fe	2.245	2.019	1.689	3.262	2.687	2.566	1.663	1.465
Mn	0.025	0.000	0.000	0.000	0.000	0.021	0.000	0.004
Mg	2.358	2.616	2.811	1.099	1.765	1.799	2.854	3.492
Ca	0.000	0.000	0.000	0.000	0.000	0.000	0 006	0.000
Na	0.133	0.079	0.075	0.000	0.086	0.069	0.084	0.029
K	1.825	1.840	1.758	1.943	1.893	1.822	1.758	1.776
Sum	15.612	15.501	15.406	15.441	15.524	15.434	15.316	15.554
Mg/(Fe+Mg)	0.512	0.564	0.625	0.252	0.396	0.412	0.632	0.704

Table A2.

Sample	89-108a	89-115b	89-115b	89-116c	89-116c	89-125	90-129b	90-155
Analysis	1,2	1,2,3	3	1,2,3	4	1	1,2,4	1,4
Location	matrix	matrix	inc/gt	matrix	inc/pl	matrix	matrix	matrix
n	4	6	2	4	1	1	7	2
SiO2	35.74	36.17	36.46	35.50	33.91	34.93	35.42	33.55
TiO2	4.00	4.17	5.58	5.18	5.18	4.14	3.86	3.08
Al2O3	18.25	17.61	16.55	13.51	16.99	13.94	18.44	17.12
FeO	18.09	16.95	13.00	23.86	21.44	19.32	19.34	26.22
MnO	0.00	0.00	0.00	0.03	0.00	0.00	0.14	0.00
MgO	9.56	10.85	13.55	8.34	7.94	11.62	8.69	5.43
CaO	0.00	0.00	0.00	0.00	0.00	0.19	0.00	0.00
Na2O	0.19	0.32	0.54	0.27	0.20	0 33	0.04	0.18
K2O	9.55	9.41	8.16	9.40	9.50	8.76	9.78	8.83
Total	95.38	95.48	93.84	96.09	95.16	93.23	95.71	94.41
Si	5.407	5.435	5.443	5.525	5.266	5.476	5.382	5.355
AlIV	2.593	2.565	2.557	2.475	2.734	2.524	2.618	2.645
AlVI	0.658	0.551	0.352	0.001	0.373	0.050	0.682	0.573
Ti	0.455	0.471	0.627	0.606	0.605	0.488	0.441	0.370
Fe	2.289	2.130	1.623	3.106	2.784	2.533	2.458	3.500
Mn	0.000	0.000	0.000	0.004	0.000	0.000	0.018	0.000
Mg	2.156	2.430	3.015	1.935	1.838	2.716	1.969	1.292
Ca	0.000	0.000	0.000	0.000	0.000	0.032	0.000	0 000
Na	0.056	0.093	0.156	0.081	0.060	0.100	0.012	0.056
K	1.843	1.804	1.554	1.866	1.882	1.752	1.896	1.798
Sum	15.457	15.479	15.327	15.599	15.542	15.671	15.476	15.589
Mg/(Fe+Mg)	0.485	0.533	0.650	0.384	0.398	0.517	0.445	0.270

Table A2.

Sample	90-185a	90-208b	91-250
Analysis	1,2,3	2	1
Location	matrix	matrix	matrix
n	6	3	1
SiO2	37.90	36.37	36.54
TiO2	2.01	4.10	5.42
Al2O3	15.19	15.00	14.19
FeO	14.91	16.87	15.65
MnO	0.55	0.09	0.00
MgO	14.50	12.89	14.53
CaO	0.00	0.00	0.00
Na2O	0.05	0.09	0.28
K2O	9.36	9.62	8.94
Total	94.47	95.03	95.55
Si	5.701	5.516	5.467
AlIV	2.299	2.484	2.500
AlVI	0.392	0.195	0.000
Ti	0.227	0.468	0.610
Fe	1.876	2.140	1.958
Mn	0.070	0.012	0.000
Mg	3.252	2.914	3.241
Ca	0.000	0.000	0.000
Na	0.015	0.026	0.081
K	1.796	1.861	1.706
Sum	15.628	15.616	15.563
Mg/(Fe+Mg)	0.634	0.577	0.623

Table A3. Plagioclase compositions used in thermobarometry. Formulae calculated on the basis of 8 oxygens.

Sample	88-3a	89-3	89-35	89-35	89-42c	D47a	89-67c	89-73a
Analysis	1,2	1,2,3	1,2	3	1,2,3	1,2	1,2,3	1,2,3,4,5
Location	rim	ave	rim	core	ave	ave	ave	ave
n	3	6	3	1	6	6	9	11
SiO2	57.65	65.20	61.17	61.36	62.06	62.88	63.47	59.13
Al2O3	26.66	21.87	24.16	24.85	23.23	23.53	22.89	25.83
FeO	0.23	0.03	0.00	0.00	0.05	0.07	0.10	0.11
CaO	8.49	2.85	6.27	6.74	4.95	4.76	4.59	7.66
Na2O	6.95	10.09	7.83	7.76	8.66	8.83	8.59	7.10
K2O	0.23	0.17	0.14	0.26	0.19	0.23	0.18	0.02
Total	100.21	100.21	99.57	100.97	99.14	100.30	99.82	99.85
Si	2.582	2 865	2.727	2.704	2.773	2.776	2.807	2.641
Al	1.406	1.132	1.268	1.289	1.222	1.223	1.192	1.359
Fe	0.009	0.001	0.000	0.000	0.002	0.003	0.004	0.004
Ca	0.407	0.134	0.299	0.318	0.237	0.225	0.218	0.367
Na	0.604	0.860	0.677	0.663	0.750	0.756	0.737	0.615
K	0.013	0.010	0.008	0.015	0.011	0.013	0.010	0.001
Sum	5.021	5.002	4.979	4.989	4.995	4.996	4.968	4.987
Ab	0.590	0.857	0.688	0.666	0.752	0.761	0.764	0.626
An	0.397	0.133	0.304	0.319	0.237	0.226	0.226	0.373
Or	0.013	0.010	0.008	0.015	0.011	0.013	0.010	0.001

Table A3.

Sample	89-88a	89-88a	89-88b	89-103a	89-103a	89-104d	89-108a	89-115b
Analysis	1,3,5,6	3,5,6	1	1,3	2,3	2	1,2	1,2,3
Location	rim	core	rim	core	ave	ave	rim	core
n	4	4	1	4	3	5	3	4
SiO2	58.70	58.69	59.37	62.33	62.30	64.95	60.10	62.16
Al2O3	26.33	26.45	25.35	23.45	24.04	22.21	25.46	24.03
FeO	0 06	0.06	0.49	0.00	0.40	0.19	0.15	0.22
CaO	7.79	7.63	6.90	4.83	5.52	3.21	7.05	5.72
Na2O	7.15	7.37	7.63	8.37	6.81	9.28	7.29	8.14
K2O	0.36	0.37	0.14	0.37	0.29	0.06	0.11	0.18
Total	100.39	100.57	99.88	99.35	99.36	99.90	100.16	100.45
Si	2.616	2.612	2.656	2.776	2.767	2.858	2.671	2.745
Al	1.382	1.386	1.335	1.230	1.257	1.151	1.332	1.250
Fe	0.002	0.002	0.018	0.000	0 015	0.007	0.006	0.008
Ca	0.372	0.364	0.331	0.230	0 263	0.151	0.336	0.271
Na	0.618	0.636	0.662	0.723	0 586	0.792	0.628	0.697
K	0.020	0.021	0.008	0.021	0.016	0.003	0.006	0.010
Sum	5.010	5.021	5.010	4.980	4.904	4.962	4.979	4.981
Ab	0.612	0.623	0.661	0.742	0.677	0.837	0.647	0.713
An	0.368	0.357	0.331	0.236	0.304	0.160	0.346	0.277
Or	0.020	0.021	0.008	0.022	0.018	0.003	0.006	0.010

Table A3.

Sample	89-115b	89-116c	89-116c	89-125	89-129b	89-155	89-185a	90-200f
Analysis	1,2,3	1	3	1,2,3	1,2,4	4	1,2,3	1,2,3
Location	rim	rim	inc/gt	rim	ave	rim	ave	ave
n	3	5	1	4	9	1	11	5
SiO2	63.46	63.13	64.37	60.52	63.29	63.38	63.42	56.24
Al2O3	23.27	23.32	23.09	24.55	23.00	22.57	23.03	27.24
FeO	0.06	0.16	0.46	0.39	0.06	0.00	0.07	0.24
CaO	4.80	4.88	3.95	6.10	3.86	3.71	4.33	9.63
Na2O	8.80	7.90	8.85	7.90	9.23	9.66	9.30	5.96
K2O	0.11	0.27	0.31	0.20	0.13	0.12	0.25	0.03
Total	100.50	99.66	101.03	99.66	99.57	99.44	100.40	99.34
Si	2.792	2.795	2.815	2.703	2.806	2.816	2.796	2.542
Al	1.205	1.216	1.189	1.291	1.201	1.181	1.196	1.450
Fe	0.002	0.006	0.017	0.015	0 002	0.000	0.003	0.009
Ca	0.226	0.231	0.185	0.292	0.183	0.177	0.205	0.466
Na	0.751	0.678	0.750	0.684	0.793	0.832	0.795	0.522
K	0.006	0.015	0.017	0.011	0.007	0.007	0.014	0.002
Sum	4.982	4.941	4.973	4.996	4.992	5.013	5.009	4.991
Ab	0.764	0.734	0.788	0.693	0.807	0.819	0.784	0.527
An	0.230	0.250	0.194	0.296	0.186	0.174	0.202	0.471
Or	0.006	0.016	0.018	0.011	0.007	0.007	0.014	0.002

Table A3.

Sample	90-208b	91-250
Analysis	2	2,3
Location	rim	ave
n	1	5
SiO2	55.89	63.94
Al2O3	27.48	22.19
FeO	0.24	0.10
CaO	9.90	3.74
Na2O	5.62	9.22
K2O	0.23	0.19
Total	99.36	99.38
Si	2.529	2.838
Al	1.465	1.160
Fe	0.009	0.004
Ca	0.480	0.178
Na	0.493	0.793
K	0.013	0.011
Sum	4.989	4.984
Ab	0.500	0.808
An	0.487	0.181
Or	0.013	0.011

Table A4. Muscovite compositions used in thermobarometry. Formulae calculated on the basis of 22 oxygens.

Sample	89-3	89-67c	89-115b	90-129b	90-155
Analysis	3	3	1	1,4	1,2,3,4
Location	int/bt	matrix	matrix	matrix	matrix
n	1	3	2	4	5
SiO2	46.64	47.08	47.85	46.75	45.53
TiO2	0.68	1.22	0.35	1.46	1.19
Al2O3	34.81	34.33	35.74	35.25	33.81
FeO	2.51	2.15	1.05	1.27	2.55
MnO	0.00	0.00	0.00	0.00	0.00
MgO	0.53	0.66	0.86	0.77	0.37
CaO	0.00	0.00	0.00	0.00	0.00
Na2O	0.51	0.36	0.36	0.38	0.42
K2O	9.04	8.77	8.51	9.07	9.29
Total	94.72	94.57	94.72	94.95	93.16
Si	5.653	5.692	5.718	5.619	5.633
AlIV	2.347	2.308	2.282	2.381	2.367
AlVI	2.622	2.580	2.748	2.609	2.559
Ti	0.062	0.111	0.031	0.132	0.111
Fe	0.254	0.217	0.105	0.128	0.264
Mn	0.000	0.000	0.000	0.000	0.000
Mg	0.096	0.119	0.153	0.138	0.068
Ca	0.000	0.000	0.000	0.000	0.000
Na	0.120	0.084	0.083	0.089	0.101
K	1.398	1.353	1.297	1.391	1.466
Sum	12.552	12.464	12.417	12.487	12.569
Mg/(Fe+Mg)	0.274	0.354	0.593	0.519	0.205

Table A5. Amphibole compositions used in thermobarometry. Formulae calculated on the basis of 23 oxygens using average of cations - (Na+K) = 15 and cations - (Ca+Na+K) = 13.

Sample	88-3a	89-73a	89-103a	89-116c	89-116c	89-125	90-185a	90-200f
Analysis	3,4	1,2	1	1	1,2,3	1	1,2,3	1,2,3
Location	matrix	matrix	ave	matrix	matrix	matrix	matrix	matrix
n	5	8	2	1	3	2	8	5
SiO2	42.71	43.66	42.40	41.18	41.35	41.88	44.39	42.63
TiO2	1.73	1.07	2.36	1.84	1.92	1.68	0.72	1.56
Al2O3	12.60	13.49	11.29	10.79	10.89	11.84	9.64	12.75
FeO	13.38	10.64	15.38	21.63	21.61	16.68	14.76	14.02
MnO	0.11	0.16	0.00	0.12	0.12	0.00	0.82	0.00
MgO	12.23	14.10	10.78	7.50	7.41	10.28	12.18	12.32
CaO	11.91	10.86	11.10	11.08	11.37	11.20	11.75	11.26
Na2O	1.52	2.15	1.53	1.93	1.75	1.93	1.60	2.64
K2O	1.23	0.11	1.65	1.39	1.46	1.29	1.08	0.00
Total	97.42	96.24	96.49	97.46	97.88	96.78	96.94	97.18
Si	6.344	6.411	6.430	6.391	6.388	6.371	6.676	6.331
AlIV	1.656	1.589	1.570	1.609	1.612	1.629	1.324	1.669
AlVI	0.548	0.744	0.446	0.363	0.370	0.492	0.383	0.571
Ti	0.193	0.118	0.269	0.215	0.223	0.192	0.081	0.174
Fe	1.662	1.306	1.951	2.808	2.792	2.122	1.857	1.741
Mn	0.014	0.020	0.000	0.016	0.016	0.000	0.104	0.000
Mg	2.708	3.087	2.437	1.735	1.707	2.331	2.731	2.728
Ca	1.896	1.709	1.803	1.842	1.882	1.825	1.894	1.792
Na	0.438	0.612	0.450	0.580	0.524	0.570	0.467	0.760
K	0.233	0.021	0.319	0.275	0.288	0.250	0.207	0.000
Sum	15.692	15.617	15.675	15.834	15.801	15.783	15.723	15.756
Fe3+	0.260	0.481	0.182	0.240	0.191	0.244	0.354	0.359
Fe2+	1.393	0.813	1.767	2.555	2.591	1.896	1.488	1.369

Table A5.

Sample	90-208b	91-250
Analysis	2	2,3
Location	matrix	matrix
n	2	4
SiO2	41.37	41.85
TiO2	1.33	2.47
Al2O3	13.22	11.88
FeO	16.05	14.81
MnO	0.25	0.00
MgO	10.09	11.40
CaO	11.88	10.93
Na2O	1.48	2.47
K2O	1.35	1.24
Total	97.02	97.05
Si	6.267	6.304
AlIV	1 733	1.696
AlVI	0.626	0.411
Ti	0.152	0.280
Fe	2.034	1.865
Mn	0.032	0.000
Mg	2.279	2.560
Ca	1.928	1.764
Na	0.435	0.721
K	0.261	0.238
Sum	15.746	15.840
Fe3+	0.298	0.207
Fe2+	1.723	1.658

Table A6. Orthopyroxene compositions used in thermobarometry. Formulae calculated on the basis of 6 oxygens.

Sample	88-3a	89-73a	89-88a	89-88a	89-88b	89-103a
Analysis	1,2	2,4	1	1,6	1	3
Location	matrix	matrix	rim	core	matrix	matrix
n	5	5	3	3	1	1
SiO2	51.12	52.49	52.90	53.25	52.12	52.44
TiO2	0.06	0.02	0.00	0.00	0.00	0.20
Al2O3	1.95	3.67	1.59	1.36	0.79	1.08
FeO	25.20	17.44	22.20	21.25	24.21	24.51
MnO	0.65	0.33	0.43	0.29	0.41	0.45
MgO	20.62	25.49	22.14	22.90	20.87	19.83
CaO	0.35	0.11	0.33	0.36	0.33	0.44
Na2O	0.04	0.00	0.31	0.28	0.28	0.39
Total	99.99	99.55	99.90	99.69	99.01	99.34
Si	1.924	1.912	1.965	1.973	1.973	1.988
AlIV	0.076	0.088	0.035	0.027	0.027	0.012
AlVI	0.010	0.069	0.035	0.033	0.008	0.036
Ti	0.002	0.001	0.000	0.000	0.000	0.006
Fe	0.793	0.531	0.690	0.659	0.767	0.777
Mn	0.021	0.010	0.014	0.009	0.013	0.014
Mg	1.157	1.384	1.226	1.265	1.178	1.120
Ca	0.014	0.004	0.013	0.014	0.013	0.018
Na	0.003	0.001	0.022	0.020	0.021	0.029
Sum	4.000	4.000	4.000	4.000	4.000	4.000
WO	0.711	0.222	0.676	0.734	0.679	0.926
EN	58.285	71.722	63.121	64.975	59.763	58.065
FS	41.004	28.056	36.203	34.291	39.558	41.009
Fe3+	0.065	0.017	0.022	0.014	0.039	0.000
Fe2+	0.728	0.514	0.668	0.645	0.728	0.777

Table A7. Clinopyroxene compositions used in thermobarometry. Formulae calculated on the basis of 6 oxygens.

Sample	89-88a	89-103a	89-125	90-200f	91-250
Analysis	1,6	2,3	1	1,2,3	1,2,3
Location	matrix	matrix	matrix	matrix	matrix
n	6	4	2	12	7
SiO2	53.23	52.67	52.80	51.02	52.28
TiO2	0.04	0.10	0.00	0.35	0.20
Al2O3	2.46	2.45	1.15	4.63	3.79
FeO	7.38	9.89	11.06	8.60	9.00
MnO	0.00	0.27	0.00	0.00	0.00
MgO	14.00	12.40	12.70	12.83	12.76
CaO	21.46	20.86	21.70	21.56	20.42
Na2O	0.84	0.90	0.78	1.09	1.49
Total	99.41	99.54	100.19	100.08	99.94
Si	1.975	1.974	1.972	1.885	1.933
AlIV	0.025	0.026	0.028	0.115	0.067
AlVI	0.082	0.082	0.023	0.086	0.098
Ti	0.001	0.003	0.000	0.010	0.006
Fe	0.229	0.310	0.345	0.265	0.278
Mn	0.000	0.009	0.000	0.000	0.000
Mg	0.774	0.693	0.707	0.707	0.703
Ca	0.853	0.838	0.868	0.853	0.809
Na	0.061	0.065	0.057	0.079	0.106
Sum	4.000	4.000	4.000	4.000	4.000
WO	45.953	45.302	45.205	46.743	45.178
EN	41.712	37.469	36.811	38.703	39.280
FS	12.335	17.228	17.984	14.554	15.542
Fe3+	0.001	0.003	0.062	0.087	0.065
Fe2+	0.228	0.307	0.284	0.179	0.213

Table A8. Spinel composition used in thermobarometry. Formula calculated on the basis of 4 oxygens.

Sample	90-42c
Analysis	1
Location	matrix
n	2
Al2O3	55.56
FeO	25.15
MgO	2.08
ZnO	16.69
Total	99.48
Al	1.943
Fe	0.625
Mg	0.092
Zn	0.370
Sum	3.030
Mg/(Mg+Fe)	0.128

APPENDIX B

Geochronology Sample Locations

Sample	Northing*	Easting*
GC89-73a	50453	5410
GC89-117	50476	5368
GC89-118	50464	5374
GC89-119	50449	5390
GC89-120	50440	5410
GC89-122	50428	5436
GC89-123	50412	5459
GC89-124	50386	5475
GC89-127	50389	5452
GC89-128	50425	5439
GC91-266	50459	5426
GC91-267a	50382	5416
GC91-269	50378	5420
GC91-270	50371	5424
LH89-11	50342	5660
LH89-12	50342	5660
TK84-91	50467	5513
TK84-92	50469	5510
DS-1	50349	5476
DS-3	50345	5474
DS-4	50392	5451

* See Fig. 5.1. for approximate sample locations. Sample coordinates reference a UTM grid (Zone 17) and are given in values of 100 metres. Sample locations can be determined from NTS 1:50,000 scale map sheets 41H/8 & 41H/7, 41H/9, and 41H/10.

APPENDIX C

Analytical Procedure For U-Pb Geochronology

All analytical work was carried out at the Jack Satterly Geochronology Laboratory, Royal Ontario Museum, Toronto. Stringent laboratory procedures for equipment and sample cleanliness were followed at all times to minimize the possibility of contamination.

Samples were reduced to a fine powder in a jaw crusher and disc mill which was divided into heavy and light mineral concentrates on a Wilfley Table. The heavy mineral concentrates were sieved through a 70 mesh screen prior to removal of strongly magnetic particles (e.g. magnetite) using a free-fall magnetic separation technique. Feldspar and quartz, where abundant, were removed from concentrates by a heavy liquid bromoform separation. The separates were passed 3-4 times at successively higher field strengths through a Frantz isodynamic separator at 10° side-tilt to remove biotite, garnet, amphibole, and other matrix phases. Apatite was removed from the least magnetic initial Frantz split using the heavy liquid methylene iodide. Final Frantzing at full-field strength was performed with decreasing angles of side-tilt (typically 5°, 3°, 1° and 0°) for each pass. At this stage heavy mineral concentrates of varying paramagnetic strength were available for selection of single- and multi-grain fractions for analysis .

All material for dating was hand-picked with tweezers under a binocular microscope from separates immersed in ethyl alcohol. Zircon was generally chosen from the least magnetic final Frantz split as this separate tends to yield the least discordant

analyses (Krogh 1982). Titanite was picked from initial Frantz magnetic splits at 1-1.7 A, and rutile was chosen from final Frantz magnetic fractions at 1°, 3° and 5° side-tilt. In all cases multi-grain fractions were selected based on similarities in grain morphology, size, colour and transparency. Where possible, grains with cracks, alteration, inclusions, core-rim relationships and other irregularities were avoided. All zircon fractions were abraded following the method of Krogh (1982) to minimize discordancy caused by surficial lead loss and to break-up and eliminate the most highly-cracked grains. Further hand-picking after abrasion served to increase the overall quality of the zircon fractions. Several of the titanite fractions were abraded but for a shorter time period (~ 20 minutes) than for zircon (~20-30 hours) and without a pyrite buffering agent. Rutile was not abraded.

Zircon was washed in 4N nitric acid, weighed, and dissolved in a 50% HF-8N HNO_3 (15:1) solution in sealed Teflon capsules at 220°C for approximately 5 days. Titanite and rutile were washed in 2N nitric acid, weighed, and dissolved in an identical acid mixture in Savillex Teflon capsules at 100°C for 5 days. A precise amount of mixed ^{205}Pb-^{235}U tracer was added prior to dissolution (Krogh and Davis 1975) so that concentrations could be determined by isotope dilution. Isolation of Pb and U by anion exchange chromatography generally followed the method of Krogh (1973). For zircon, however, ion exchange columns an order of magnitude smaller than those described by Krogh (1973) were used, and for titanite and rutile, extraction of Pb and U was performed using an HBr chemistry procedure (Corfu and Stott 1986) and involved an additional

purification of U. The total blanks for these procedures are typically 0.5-2 pg U and 2-5 pg Pb for zircon, and 5 pg U and 15 pg Pb for titanite and rutile.

Uranium and lead were combined in a silica gel - H_3PO_4 mixture (Cameron et al. 1969) and loaded on single outgassed Re filaments. Isotopic ratios were determined at 1440-1630°C with a VG-354 thermal ionization mass spectrometer in single collector mode. A Faraday collector was used for all ratio measurements except those including ^{204}Pb and other isotopes in low concentration; for these ratios a Daly photomultiplier detector was used. In general, however, the critical $^{207}Pb/^{206}Pb$ ratio could be measured using the more accurate Faraday collector. All isotopic data were corrected for mass discrimination by a factor of +0.13%/amu determined from replicate analyses of NBS-SRM 981 common Pb and NBS-SRM U 500 standards. Daly detector measurements were further corrected by a Daly-Faraday empirical correction factor of +0.35%/amu. Two-sigma analytical uncertainties due to measurement errors were generally <0.1% for the $^{207}Pb/^{206}Pb$ ratio and <0.5% for the Pb/U ratios.

Initial common Pb corrections were made by subtracting the amount and isotopic composition of procedural blank Pb from the measured Pb/U and Pb/Pb ratios (already corrected for fractionation and the ^{205}Pb-^{235}U spike). The remaining ^{204}Pb was applied to isotopic ratios for common lead calculated with the model of Stacey and Kramers (1975) at the estimated time of initial Pb retention. This allowed amounts of common ^{206}Pb, ^{207}Pb and ^{208}Pb incorporated during mineral growth to be estimated and corrected for. Where applicable, linear regressions and concordia intercept ages and errors (95% confidence level) were determined following the procedure of Davis (1982). The U decay constants

and isotopic abundance ratio used were: $^{238}U = 1.55125 \times 10^{-10}$ yr^{-1}, $^{235}U = 9.8485 \times 10^{-10}$ yr^{-1}, $^{238}U/^{235}U = 137.88$ (Steiger and Jäger 1977).

References

Abassi, M.R., and Mancktelow, N.S. 1990. The effect of initial perturbation shape and symmetry on fold development. Journal of Structural Geology, **12**: 273-282.

Andersen, T.B., and Jamtveit, B. 1990. Uplift of deep crust during orogenic extensional collapse: a model based on field studies in the Sogn-Sunnfjord region of western Norway. Tectonics, **9**: 1097-1111.

Anovitz, L.M., and Essene, E.J. 1990. Thermobarometry and pressure-temperature paths in the Grenville Province of Ontario. Journal of Petrology, **31**: 197-241.

\shwal, L.D., and Wooden, J.L. 1989. River Valley pluton, Ontario: A late Archean/early Proterozoic anorthositic intrusion in the Grenville Province. Geochimica et Cosmochimica Acta, **53**: 633-641.

Beach, A. 1976. The interrelationships of fluid transport, deformation, geochemistry and heat flow in early Proterozoic shear zones in the Lewisian complex. Philosophical Transactions of the Royal Society of London, **A280**: 569-604.

Bell, T.H., Rubenach, M.J., and Fleming, P.D. 1986. Porphyroblast nucleation, growth and dissolution in regional metamorphic rocks as a function of deformation partitioning during foliation development. Journal of Metamorphic Geology, **4**: 37-64.

Berman, R.G. 1988. Internally consistent thermodynamic data for minerals in the system Na_2O-K_2O-CaO-MgO-FeO-Fe_2O_3-Al_2O_3-SiO_2-TiO_2-H_2O-CO_2. Journal of Petrology, **29**: 445-522.

Berman, R.G. 1990. Mixing properties of Ca-Mg-Fe-Mn garnets. American Mineralogist, **75**: 328-344.

Berman, R.G. 1991. Thermobarometry using multiequilibrium calculations: a new technique, with petrological applications. Canadian Mineralogist, **29**: 833-855.

Berthé, D., Choukroune, P., and Jegouzo, P. 1979. Orthogneiss, mylonite and non-coaxial deformation of granites: the example of the South Armorican Shear Zone. Journal of Structural Geology, **1**: 31-42.

Best, M.G. 1982. Igneous and metamorphic petrology. W.H. Freeman and Company, New York, New York.

Bethune, K.M. 1989. Deformation, metamorphism, diabase dykes, and the Grenville Front southwest of Sudbury, Ontario. *In* Current research. Geological Survey of Canada, Paper 89-1C, pp. 19-28.

Bethune, K.M. 1991. Fate of the Sudbury dykes in the Tyson Lake area south of Sudbury, Ontario: implications for Grenville Front history and the origin of coronites of high-grade terranes. Geological Association of Canada - Mineralogical Association of Canada Annual Meeting, Program with Abstracts, **16**: A11.

Bethune, K.M. 1993. Evolution of the Grenville Front in the Tyson Lake area, southwest of Sudbury, Ontario, with emphasis on the tectonic significance of the Sudbury diabase dykes. Ph.D. thesis, Queen's University, Kingston, Ontario.

Bethune, K.M., and Davidson, A. 1988. Diabase dykes and the Grenville Front southwest of Sudbury, Ontario. *In* Current research. Geological Survey of Canada, Paper 88-1C, pp.151-159.

Bethune, K.M., Davidson, A., and Dudás, F.Ö. 1990. Structure and metamorphism of the Sudbury dykes: constraints on tectonic evolution of the Grenville Front south of Sudbury, Ontario. Geological Association of Canada - Mineralogical Association of Canada Annual Meeting, Program with Abstracts, **15**: A10.

Bickford, M.E., van Schmus, W.R., and Zietz, I. 1986. Proterozoic history of the midcontinent region of North America. Geology, **14**: 492-496.

Brodie, K.H., and Rutter, E.H. 1995. On the relationship between deformation and metamorphism, with special reference to the behaviour of basic rocks. *In* Metamorphic Reactions: Kinetics, Textures and Deformation. *Edited by* A.B. Thompson and D.C. Rubie. Advances in Physical Geochemistry, vol. 4., pp. 138-179.

Brown, R.L., and Journeay, J.M. 1987. Tectonic denudation of the Shuswap metamorphic terrane of southeastern British Columbia. Geology, **15**: 142-146.

Brown, T.H., Berman, R.G., and Perkins, E.H. 1988. GEO-CALC: software package for calculation and display of temperature-pressure-composition phase diagrams using an IBM or compatible personal computer. Computers and Geoscience, **14**: 279-289.

Buick, I.S., and Holland, T J.B. 1989. The P-T-t path associated with crustal extension, Naxos, Cyclades, Greece. *In* Evolution of Metamorphic Belts. *Edited by* J.S. Daly, R.A. Cliff, and B.W D Yardley. Geological Society Special Publication no. 43, pp. 365-369.

Burchfiel, B.C., and Royden, L.H. 1985. North-south extension within the convergent Himalayan region. Geology, **13**: 679-682.

Bussy, F., Krogh, T.E., Schwerdtner, F., and Klemens, W.P. 1993. Metadiabase record the time of metamorphic transformation. Lithoprobe Abitibi-Grenville Project, Report no. 33, p.1.

Cameron, A.E., Smith, D.E., and Walker, R.L. 1969. Mass spectrometry of nanogram size samples of lead. Analytical Chemistry, **41**: 525-526.

Carlson, K.A., van der Pluijm, B.A., and Hanmer, S. 1990. Marble mylonites of the Bancroft shear zone: evidence for extension in the Canadian Grenville. Geological Society of America Bulletin, **102**: 174-181.

Carmichael, D.M. 1969. On the mechanism of prograde metamorphic reactions in quartz-bearing pelitic rocks. Contributions to Mineralogy and Petrology, **20**: 244-267.

Carmichael, D.M. 1978. Metamorphic bathozones and bathograds: a measure of the depth of post-metamorphic uplift and erosion on the regional scale. American Journal of Science, **278**: 769-797.

Chakraborty, S., and Ganguly, J. 1990. Compositional zoning and cation diffusion in garnets. *In* Diffusion, Atomic Ordering, and Mass Transport. Selected Topics in Geochemistry. *Edited by* J. Ganguly. Advances in Physical Geochemistry, vol. 8, pp. 120-175

Chen, Y.D., Krogh, T.E., and Lumbers, S.B. 1993. U/Pb geochronological studies on the orthogneiss from the region west of Lake Nippissing, Ontario. Geological Association of Canada - Mineralogical Association of Canada Annual Meeting, Program and Abstracts, **18**: A18.

Ciesielski, A., and Parent, M. 1992. The Archean parautochthon in the Lake Temiscaming area, with reference to the Grenville Front and Abitibi-Grenville Lithoprobe line 15. Lithoprobe Abitibi-Grenville Project, Report no. 33, pp. 3-6.

Coney, P.J. 1973. Non-collision tectonogenesis in western North America. *In* Implications of Continental Drift to the Earth Sciences. *Edited by* D.H. Tarling and S.H. Runcorn. Academic Press, New York, pp. 713-717.

Coney, P.J. 1980. Cordilleran metamorphic core complexes: an overview. Geological Society of America, Memoir 153, pp. 7-31.

Connelly, J.N., and Heaman, L.M. 1993. U-Pb geochronological constraints on the tectonic evolution of the Grenville Province, western Labrador. Precambrian Research, **63**: 123-142.

Connelly, J.N., van Gool, J., Rivers, T., and James, D.T. 1993. Field guide to the geology of the Grenville Province of western Labrador. Friends of the Grenville, Field Trip Guidebook, 96pp.

Corfu, F. 1988. Differential response of U-Pb systems in coexisting accessory minerals, Winnipeg River Subprovince, Canadian Shield: implications for Archean crustal growth and stabilization. Contributions to Mineralogy and Petrology, **98**: 312-325.

Corfu, F., and Stott, G.M. 1986. U-Pb ages for late magmatism and regional deformation in the Shebandowan belt, Superior Province, Canada. Canadian Journal of Earth Sciences, **23**: 1075-1082.

Corrigan, D 1990. Geology and U-Pb geochronology of the Key Harbour area, Britt domain, southwest Grenville Province. M.Sc. thesis, Dalhousie University, Halifax, Nova Scotia.

Corrigan, D., Culshaw, N.G , and Mortensen, J.K 1994. Pre-Grenvillian evolution and Grenvillian overprinting of the Parautochthonous Belt in the Key Harbour area, Ontario; U-Pb and structural constraints. Canadian Journal of Earth Sciences, **31**: 583-596.

Cosca, M.A., Sutter, J.F., and Essene, E.J. 1991. Cooling and inferred uplift/erosion history of the Grenville orogen, Ontario: constraints from $^{40}Ar/^{39}Ar$ thermochronology. Tectonics, **10**: 959-977.

Cosca, M.A., Essene, E.J., Kunk, M.J., and Sutter, J.F. 1992. Differential unroofing within the Central Metasedimentary Belt of the Grenville orogen: constraints from $^{40}Ar/^{39}Ar$ thermochronology. Contributions to Mineralogy and Petrology, **110** 211-225.

Coward, M.P. 1984. Major shear zones in the Precambrian crust; examples from NW Scotland and southern Africa and their significance. *In* Precambrian Tectonics Illustrated. *Edited by* A. Kröner and R. Greiling. E. Schweizerbart'sche Verlagsbuchhandlung, Stuttgart, pp. 207-235.

Coward, M.P., and Potts, G J. 1983. Complex strain patterns developed at the frontal and lateral tips to shear zones and thrust zones. Journal of Structural Geology, **5**. 383-399.

Culshaw, N.G. 1987. Microstructure, c-axis pattern, microstrain and kinematics of some S-C mylonites in Grenville gneiss Journal of Structural Geology, 9: 299-311.

Culshaw, N.G., Davidson, A., and Nadeau, L. 1983. Structural subdivisions of the Grenville Province in the Parry Sound-Algonquin region, Ontario. *In* Current research. Geological Survey of Canada, Paper 83-1B, pp. 243-252.

Culshaw, N.G., Corrigan. D., Drage, J., and Wallace, P. 1988. Georgian Bay geological synthesis: Key Harbour to Dillon, Grenville Province of Ontario. *In* Current research. Geological Survey of Canada, Paper 88-1C, pp. 129-133.

Culshaw, N.G., Check, G., Corrigan, D., Drage, J., Gower, R., Haggart, M.J., Wallace, P., and Wodicka, N. 1989. Georgian Bay geological synthesis: Dillon to Twelve Mile Bay, Grenville Province of Ontario. *In* Current research. Geological Survey of Canada, Paper 89-1C, pp. 157-163.

Culshaw, N.G., Jamieson, R., Corrigan, D., Ketchum, J., Reynolds, P.H., Wodicka, N., Heaman, L, and Krogh, T. 1990. History of the Central Gneiss Belt, Grenville Province, along Georgian Bay, Ontario. Lithoprobe Abitibi-Grenville Project, Workshop Report 3, pp. 73-76.

Culshaw, N.G., Corrigan, D., Jamieson, R.A., Ketchum, J., Wallace, P., and Wodicka, N. 1991*a*. Traverse of the Central Gneiss Belt, Grenville Province, Georgian Bay. Geological Association of Canada - Mineralogical Association of Canada Annual Meeting, Field Trip B3: Guidebook, 32pp.

Culshaw, N.G., Reynolds, P.H., and Check, G. 1991*b*. A $^{40}Ar/^{39}Ar$ study of post-tectonic cooling in the Britt domain of the Grenville Province, Ontario. Earth and Planetary Science Letters, **105**: 405-415.

Culshaw, N.G., Ketchum, J.W.F., Wodicka, N., and Wallace, P. 1994. Ductile extension following thrusting in the southwestern Grenville Province, Ontario. Canadian Journal of Earth Sciences, **31**: 160-175.

Culshaw, N.G., Heaman, L.M., Ketchum, J.W.F., Krogh, T.E., Kwok, Y.Y., and Moore, M. In preparation. Constraints from U-Pb geochronology for the timing of geological events in the southern Britt domain, Grenville Province, Ontario.

Cumming, G.L., and Krstic, D. 1991. Geochronology at the Namew Lake Ni-Cu orebody, Flin Flon area, Manitoba, Canada: thermal history of a metamorphic terrane. Canadian Journal of Earth Sciences, **28**: 309-325.

Cygan, R., and Lasaga, A.C 1982. Crystal growth and the formation of chemical zoning in garnets. Contributions to Mineralogy and Petrology, **79**: 187-200.

Davidson, A. 1984*a*. Identification of ductile shear zones in the southwestern Grenville Province of the Canadian Shield. *In* Precambrian Tectonics Illustrated. *Edited by* A.

Kröner and R. Greiling. E. Schweizerbart'sche Verlagsbuchhandlung, Stuttgart, pp. 263-279.

Davidson, A. 1984*b*. Tectonic boundaries within the Grenville Province of the Canadian Shield. Journal of Geodynamics, **1**: 433-444.

Davidson, A. 1990. Evidence for eclogite metamorphism in the southwest Grenville Province, Ontario. *In* Current research. Geological Survey of Canada, Paper 90-1C, pp. 113-118.

Davidson, A. 1991. Metamorphism and tectonic setting of gabbroic and related rocks in the Central Gneiss Belt, Grenville Province, Ontario. Geological Association of Canada - Mineralogical Association of Canada Annual Meeting, Field Trip A2: Guidebook, 57pp.

Davidson, A., and Morgan, W.C. 1981. Preliminary notes on the geology east of Georgian Bay, Grenville Structural Province, Ontario. *In* Current research. Geological Survey of Canada, Paper 81-1A, pp. 291-298.

Davidson, A., and Grant, S.M. 1986. Reconnaisssance geology of western and central Algonquin Park and detailed study of coronitic olivine metagabbro, Central Gneiss Belt, Grenville Province of Ontario. *In* Current research. Geological Survey of Canada, Paper 86-1B, pp. 837-848.

Davidson, A., and Bethune, K.M. 1988. Geology of the north shore of Georgian Bay, Grenville Province of Ontario. *In* Current research. Geological Survey of Canada, Paper 88-1C, pp. 135-144.

Davidson, A., and van Breemen, O. 1988. Baddeleyite-zircon relationships in coronitic metagabbro, Grenville Province, Ontario: implications for geochronology. Contributions to Mineralogy and Petrology, **100**: 291-299.

Davidson, A., Culshaw, N.G., and Nadeau, L. 1982. A tectono-metamorphic framework for part of the Grenville Province, Parry Sound region, Ontario. *In* Current research. Geological Survey of Canada, Paper 82-1A, pp. 175-190.

Davidson, A., Nadeau, L., Grant, S.M., and Pryer, L.L. 1985. Studies in the Grenville Province of Ontario. *In* Current research. Geological Survey of Canada, Paper 85-1A, pp. 463-483.

Davidson, A., Carmichael, D.M., and Pattison, D.R.M. 1990. Metamorphism and geodynamics of the southwestern Grenville Province, Ontario. International Geological Correlation Program, Projects 235/304, Field Trip no. 1, Guidebook.

Davidson, A., van Breemen, O., and Sullivan, R.W. 1992. Circa 1.75 Ga ages for plutonic rocks from the Southern Province and adjacent Grenville Province: what is the expression of the Penokean orogeny? *In* Radiogenic Age and Isotopic Studies: Report 6. Geological Survey of Canada, Paper 92-2, pp. 107-118.

Davis, D.W. 1982. Optimum linear regression and error estimation applied to U-Pb data. Canadian Journal of Earth Sciences, **19**: 2141-2149.

Davis, G.A., and Lister, G.S. 1988. Detachment faulting in continental extension; perspectives from the southwestern U.S. Cordillera. Geological Society of America Special Paper 218, pp. 133-159.

Davis, G.A., Lister, G.S., and Reynolds, S.J. 1986. Structural evolution of the Whipple and South mountains shear zones, southwestern United States. Geology, **14**: 7-10.

Davis, G.H. 1983. Shear-zone model for the origin of metamorphic core complexes. Geology, **11**: 342-347.

Dewey, J.F. 1988. Extensional collapse of orogens. Tectonics, **7**: 1123-1139.

Dickin, A.P., and Higgins, M.D. 1992. Sm/Nd evidence for a major 1.5 Ga crust-forming event in the central Grenville Province. Geology, **20**: 137-140.

Dickin, A.P., and McNutt, R.H. 1989. Nd model age mapping of the southeast margin of the Archean foreland in the Grenville province of Ontario. Geology, **17**: 299-302.

Dickin, A.P., and McNutt, R.H. 1990. Nd model-age mapping of Grenville lithotectonic domains: mid-Proterozoic crustal evolution in Ontario. *In* Mid-Proterozoic Laurentia-Baltica. *Edited by* C.F. Gower, T. Rivers, and B. Ryan. Geological Association of Canada, Special Paper 38, pp. 79-94.

Doig, R. 1977. Rb-Sr geochronology and evolution of the Grenville Province in northwestern Quebec, Canada. Geological Society of America Bulletin, **88**: 1843-1856.

Easton, R.M. 1986. Geochronology of the Grenville Province. *In* The Grenville Province. *Edited by* J.M. Moore, A. Davidson, and A.J. Baer. Geological Association of Canada, Special Paper 31, pp. 127-173.

Easton, R.M. 1992. The Grenville Province and the Proterozoic history of central and southern Ontario. *In* Geology of Ontario. *Edited by* P.C. Thurston, H.R. Williams, R.H. Suttcliffe and G.M. Stott. Ontario Geological Survey, Special Volume 4, Part 2, pp. 715-904.

Emslie, R.F., and Hunt, P.A. 1990. Age and petrogenetic significance of igneous mangerite-charnockite suites associated with massif anorthosites, Grenville Province. Journal of Geology, **98**: 213-231.

England, P.C., and Houseman, G.A. 1988. The mechanics of the Tibetan plateau. Royal Society of London Philosophical Transactions, **A326**: 301-320.

England, P., and Molnar, P. 1993. The interpretation of inverted metamorphic isograds using simple physical calculations. Tectonics, **12**: 145-157.

England, P., and Richardson, S.W. 1977. The influence of erosion upon the mineral facies of rocks from different metamorphic environments. Journal of the Geological Society of London, **134**: 201-214.

Essene, E.J. 1989. The current status of thermobarometry in metamorphic rocks. *In* Evolution of Metamorphic Belts. *Edited by* J.S. Daly, R.A. Cliff and B.W. Yardley. Geological Society Special Publication 43, pp. 1-44.

Fahrig, W.F., and West, T.D. 1986. Diabase dyke swarms of the Canadian Shield. Geological Survey of Canada, Map 1627A.

Fossen, H., and Rykkelid, E. 1992. Postcollisional extension of the Caledonide orogen in Scandinavia: structural expressions and tectonic significance. Geology, **20**: 737-740.

Foster, C.T. 1991. The role of biotite as a catalyst in reaction mechanisms that form sillimanite. Canadian Mineralogist, **29**: 943-963.

Frost, B.R., and Tracy, R.J. 1991. P-T paths from zoned garnets: some minimum criteria. American Journal of Science, **291**: 917-939.

Fuhrman, M.L., and Lindsley, D.H. 1988. Ternary feldspar modeling and thermometry. American Mineralogist, **73**: 201-216.

Ghosh, S.K., and Chatterjee, A. 1985. Patterns of deformed early lineations over later folds formed by buckling and flattening. Journal of Structural Geology, **7**: 651-666

Ghosh, S.K., and Sengupta, S. 1987. Progressive development of structures in a ductile shear zone. Journal of Structural Geology, **9**: 277-287.

Gower, C.F. 1990. Mid-Proterozoic evolution of the eastern Grenville Province, Canada Geologiska Föreningens i Stockholm Förhandlingar, vol. 112, part 2, pp. 127-139

Gower, C.F. 1993. Syntectonic minor intrusions or syn-emplacement deformation? Canadian Journal of Earth Sciences, **30**: 1674-1675.

Gower, C.F., and Owen, J.V. 1984. Pre-Grenvillian and Grenvillian lithotectonic regions of eastern Labrador - correlation with the Sveconorwegian orogenic belt in Sweden. Canadian Journal of Earth Sciences, **21**: 678-693.

Gower, R J.W. 1992. Nappe emplacement direction in the Central Gneiss Belt, Grenville Province, Ontario, Canada: evidence for oblique collision. Precambrian Research, **59**: 73-94.

Grant, S.M. 1987. The petrology and structural relations of metagabbros from the western Grenville Province, Canada. Ph.D. thesis, University of Leicester, Leicester, U.K.

Grant, S.M. 1989. Tectonic implications from sapphirine-bearing lithologies, south-west Grenville Province, Canada. Journal of Metamorphic Geology, **7**: 583-598.

Grasemann, B., and Mancktelow, N.S. 1993. Two-dimensional thermal modelling of normal faulting: the Simplon Fault Zone, Central Alps, Switzerland. Tectonophysics, **225**. 155-165.

Green, A.G., Milkereit, B., Davidson, A., Spencer, C., Hutchinson, D.R., Cannon, W.F., Lee, M.W., Agena, W.F., Behrendt, J.C., and Hinze, W.J. 1988. Crustal structure of the Grenville front and adjacent terranes. Geology, **16**: 788-792.

Grocott, J. 1979. Controls of metamorphic grade in shear belts. Rapport Grønlands Geologiske Undersøgelse, **89**: 47-62.

Gromet, L.P. 1991. Direct dating of deformational fabrics. *In* Applications of Radiogenic Isotope Systems to Problems in Geology. *Edited by* L. Heaman and J. Ludden. Mineralogical Association of Canada, Short Course Handbook, vol. 19, pp. 167-189.

Haggart, M.J. 1991. Thermal history of the Grenville Front Tectonic Zone, central Ontario. M.Sc. thesis, Dalhousie University, Halifax, Nova Scotia.

Haggart, M.J., Jamieson, R.A., Reynolds, P.H., Krogh, T.E., Beaumont, C., and Culshaw, N.G. 1993. Last gasp of the Grenville orogeny - thermochronology of the Grenville Front Tectonic Zone near Killarney, Ontario. Journal of Geology, **101**: 575-589.

Hanmer, S. 1986. Asymmetrical pull-aparts and foliation fish as kinematic indicators. Journal of Structural Geology, **8**: 111-122.

Hanmer, S. 1988. Ductile thrusting at mid-crustal level, southwestern Grenville Province. Canadian Journal of Earth Sciences, **25**: 1049-1059.

Hanmer, S. 1990. Natural rotated inclusions in non-ideal shear. Tectonophysics, **176**: 245-255.

Hanmer, S., and Ciesielski, A. 1984. A structural reconnaissance of the northwest boundary of the Central Metasedimentary Belt, Grenville Province, Ontario and Quebec. *In* Current research. Geological Survey of Canada, Paper 84-1B, pp. 121-131.

Hanmer, S., and McEachern, S. 1992. Kinematical and rheological evolution of a crustal-scale ductile thrust zone, Central Metasedimentary Belt, Grenville orogen, Ontario. Canadian Journal of Earth Sciences, **29**: 1779-1790.

Hanmer, S., and Passchier, C. 1991. Shear-sense indicators: a review. Geological Survey of Canada, Paper 90-17, 72pp.

Heaman, L.M., and Parrish, R.R. 1991. U-Pb geochronology of accessory minerals *In* Applications of Radiogenic Isotope Systems to Problems in Geology. *Edited by* L. Heaman and J. Ludden. Mineralogical Association of Canada, Short Course Handbook, vol. 19, pp. 59-102.

Heaman, L.M., and LeCheminant, A.N. 1993. Paragenesis and U-Pb systematics of baddeleyite (ZrO_2). Chemical Geology, **110**: 95-126.

Hill, E.J., and Baldwin, S.L. 1993. Exhumation of high-pressure metamorphic rocks during crustal extension in the D'Entrecasteaux region, Papua New Guinea. Journal of Metamorphic Geology, **11**: 261-277.

Hobbs, B.E., Means, W.D., and Williams, P.F. 1976. An outline of structural geology. John Wiley and sons, New York.

Hodges, K.V., and Silverberg, D.S. 1988. Thermal evolution of the greater Himalaya, Garhwal, India. Tectonics, **7**: 583-600.

Hodges, K.V., and Royden, L. 1984. Geologic thermobarometry of retrograded metamorphic rocks: an indication of the uplift trajectory of a portion of the northern Scandinavian Caledonides. Journal of Geophysical Research, **89**: 7077-7090

Hoffman, P.F. 1989. Speculations on Laurentia's first gigayear (2.0 to 1.0 Ga) Geology, **17**: 135-138.

Houseman, G.A., and England, P.C. 1986. Finite strain calculations of continental deformation. I. Method and general results for convergent zones. Journal of Geophysical Research, **91**: 3651-3663.

Hubbard, M.S. 1989. Thermobarometric constraints on the thermal history of the Main Central Thrust zone and the Tibetan slab, eastern Nepal, Himalaya Journal of Metamorphic Geology, 7: 19-30

Indares, A. 1993. Eclogitized gabbros from the eastern Grenville Province: textures, metamorphic context, and implications. Canadian Journal of Earth Sciences, **30**: 159-173.

Indares, A., and Martignole, J. 1989. The Grenville Front south of Val-d'Or, Quebec. Tectonophysics, **157**: 221-239.

Indares, A., and Martignole, J. 1990*a*. Metamorphic constraints on the evolution of the gneisses from the parautochthonous and allochthonous polycyclic belts, Grenville Province, western Quebec. Canadian Journal of Earth Sciences, **27**: 357-370.

Indares, A., and Martignole, J. 1990*b*. Metamorphic constraints on the tectonic evolution of the allochthonous monocyclic belt of the Grenville Province, western Quebec. Canadian Journal of Earth Sciences, **27**: 371-386.

Jamieson, R.A. 1988. Textures, sequences of events, and assemblages in metamorphic rocks. *In* Short Course on Heat, Metamorphism, and Tectonics. *Edited by* E.G. Nisbet and C.M.R. Fowler. Mineralogical Association of Canada, Short Course, Vol. 14. pp. 189-212.

Jamieson, R.A., Culshaw, N.G., Wodicka, N., Corrigan, D., and Ketchum, J.W.F. 1992. Timing and tectonic setting of Grenvillian metamorphism - constraints from a transect along Georgian Bay, Ontario. Journal of Metamorphic Geology, **10**: 321-332.

Jamieson, R.A., Culshaw, N.G., and Corrigan, D 1995. Northwest propagation of the Grenville orogen: Grenvillian structure and metamorphism near Key Harbour, Georgian Bay, Ontario. Journal of Metamorphic Geology, **13**: 1-23.

John, B.E. 1987. Geometry and evolution of a mid-crustal extensional fault system: Chemehuevi Mountains, southeastern California. *In* Continental Extensional Tectonics. *Edited by* M.P. Coward, J.F. Dewey, and P.L. Hancock. Special Publication of the Geological Society of London, 28: 313-335.

Kamo, S.L , Heaman, L.M., and Lumbers, S.B. 1989. Age for a lamprophyre dyke, Callander Bay, Ontario: use of Ti-bearing minerals as a potential geochronometer. Geological Association of Canada - Mineralogical Association of Canada Annual Meeting, Program with Abstracts, **14**: A41.

Kamo, S.L., Kumarapeli, P.S., and Krogh, T.E. 1991. Further constraints on the opening of the Iapetus ocean: U-Pb ages for rift-related igneous activity from the Ottawa graben. International Geological Correlation Program Meeting, Project 257, Abstracts, Sao Paulo, Brazil.

Ketchum, J.W.F., Culshaw, N.G., Heaman, L.M., and Krogh, T.E. 1993*a*. U-Pb constraints on the late orogenic extensional and thermal history of the Central Britt shear zone, an allochthon-parautochthon boundary in the Central Gneiss Belt, Ontario. Lithoprobe Abitibi-Grenville Project, Report no. 33, pp. 161-164.

Ketchum, J.W.F., Culshaw, N.G., Heaman, L.M., Krogh, TE., and Jamieson, R.A. 1993*b*. Late orogenic ductile extension in the Middle Proterozoic Grenville orogen: an example from Ontario, Canada. *In* Late Orogenic Extension in Mountain Belts. *Edited by* M. Séranne and J. Malavielle. Bureau de Recherches Géologiques et Minières (France), Document no. 219, pp. 108-109.

Ketchum, J.W.F., Jamieson, R.A., Heaman, L.M., Culshaw, N.G., and Krogh, T.E. 1994. 1.45 Ga granulites in the southwestern Grenville Province: Geologic setting, P-T conditions, and U-Pb geochronology. Geology, **22**: 215-218.

Klemens, W.P., and Schwerdtner, W.M. 1991. Structural analysis of the Allochthon Boundary in westernmost Grenville Province: progress report. Lithoprobe Abitibi-Grenville Transect, Report No. 25, pp. 125-127.

Kretz, R. 1983. Symbols for rock-forming minerals. American Mineralogist, **68**: 277-279.

Krogh, T.E. 1973. A low-contamination method for hydrothermal decomposition of zircon and extraction of U and Pb for isotopic age determinations. Geochimica et Cosmochimica Acta, **37**: 485-494.

Krogh, T. E. 1982. Improved accuracy of U-Pb zircon ages by the creation of a more concordant system using an air abrasion technique. Geochimica et Cosmochimica Acta, **46**: 637-649.

Krogh, T.E. 1989. U-Pb systematics of zircon and titanite in metasediments and gneisses near the Grenville Front, Ontario. Geological Association of Canada - Mineralogical Association of Canada Annual Meeting, Program with Abstracts, **14**: A52.

Krogh, T.E. 1991. U-Pb zircon gochronology in the western Grenville Province. Lithoprobe Abitibi - Grenville Project, Workshop III, Program with Abstracts.

Krogh, T.E., and Davis, G.L. 1969. Geochronology of the Grenville Province. Carnegie Institute of Washington Yearbook, **67**: 224-230.

Krogh, T.E , and Davis, G.L. 1970*a*. Metamorphism 1700 ± 100 M.y. and 900 ± 100 M.y ago in the northwest part of the Grenville Province in Ontario. Carnegie Institute of Washington Yearbook, **68**: 308-309.

Krogh, T.E., and Davis, G.L. 1970*b*. Isotopic ages along the Grenville Front in Ontario. Carnegie Institute of Washington Yearbook, **68**: 309-313.

Krogh, T.E., and Davis, G.L. 1971. Paragneiss studies in the Georgian Bay area 90 km southeast of the Grenville Front. Carnegie Institute of Washington Yearbook, **69**: 339-341.

Krogh, T.E., and Davis, G.L. 1973. The effect of regional metamorphism on U-Pb systems in zircon and comparison with Rb-Sr systems in the same whole rock. Carnegie Institute of Washington Yearbook, **72**: 601-610.

Krogh, T.E., and Davis, G.L. 1974. Orogenic structural and metamorphic overprints: Archean intrusive and metamorphic rocks within a region of 1000 m.y. deformation and migmatization. Carnegie Institute of Washington Yearbook, **73**: 569-573.

Krogh, T.E., and Davis, G.L. 1975. The production and preparation of ^{205}Pb for use as a tracer for isotope dilution analyses. Carnegie Institute of Washington Yearbook, **74**: 416-417.

Krogh, T.E., and Wardle, R. 1984. U-Pb isotopic ages along the Grenville Front. Geological Association of Canada - Mineralogical Association of Canada, Annual Meeting, Program with Abstracts, **9**: 80.

Krogh, T.E., Davis, G.L., and Frarey, M.J. 1971. Isotopic ages along the Grenville Front in the Bell Lake area, southwest of Sudbury, Ontario. Carnegie Institute of Washington Yearbook, **69**: 337-339.

Krogh, T.E., Corfu, F., Davis, D.W., Dunning, G.R., Heaman. L.M., Kamo, S.L., and Machado, N. 1987. Precise U-Pb isotopic ages of diabase dykes and mafic to ultramafic rocks using trace amounts of baddeleyite and zircon. *In* Mafic Dyke Swarms. *Edited by* H.C. Halls and W.F. Fahrig. Geological Association of Canada, Special Paper 34, pp. 147-152.

Krogh, T.E., Chen, Y., Culshaw, N., and Ketchum, J. 1992. Terrane identification within the Grenville Province. Lithoprobe Abitibi-Grenville Project, Workshop IV, Program with Abstracts.

Krogh, T.E., Culshaw, N.G., and Ketchum, J. 1993*a*. Multiple ages of deformation and metamorphism in the Parry Sound - Pointe-au-Baril area. Lithoprobe Abitibi-Grenville Project, Report no. 33, p. 39.

Krogh, T.E., Kamo, S., and Nunn, G. 1993*b*. Dating the first metamorphic and frontal thrust near Killarney, Sudbury, North Bay (Ontario), Chibougamau (Quebec) and

Churchill Falls (Labrador). Lithoprobe Abitibi-Grenville Project, Report no. 33, p 165.

Kumarapeli, P.S. 1993. A plume-generated segment of the rifted margin of Laurentia, southern Canadian Appalachians, seen through a completed Wilson cycle. Tectonophysics, **219**: 47-55.

Le Fort, P. 1975. Himalayas, the collided range: present knowledge of the continental arc American Journal of Science, **A275**: 1-44.

Lister, G.S., and Price, G.P. 1978. Fabric development in a quartz-feldspar mylonite. Tectonophysics, **49**: 37-78.

Lister, G.S., and Davis, G.A. 1989. The origin of metamorphic core complexes and detachment faults formed during Tertiary continental extension in the northern Colorado River region, U.S.A. Journal of Structural Geology, **11**: 65-94.

Lumbers, S.B. 1971. Geology of the North Bay area, Districts of Nipissing and Parry Sound. Ontario Division of Mines, Geological Report 94, 104 pp.

Lumbers, S.B. 1975. Geology of the Burwash area, Districts of Nipissing, Parry Sound and Sudbury. Ontario Division of Mines, Geological Report 116, 158 pp.

Lumbers, S.B., Wu, Tsai Way, Heaman, L.M., Vertolli, V.M., and MacRae, N.D. 1991. Petrology and age of the A-type Mulock Batholith, northern Grenville Province. Precambrian Research, **53**: 199-231.

Macfie, R.I., and Dixon, J.M. 1992. New U-Pb ages for rocks of Parry Sound domain, southwest Central Gneiss Belt: some preliminary results. Lithoprobe Abitibi - Grenville Project, Workshop IV, Program with Abstracts.

Mader, U.K., and Berman, R.G. 1992. Amphibole thermobarometry: a thermodynamic approach. *In* Current research. Geological Survey of Canada, Paper 92-1E, pp 393-400.

Malavieille, J. 1987. Extensional shearing deformation and kilometer-scale "a"-type folds in a Cordilleran metamorphic core complex (Raft River mountains, northwestern Utah). Tectonics, **6**: 423-448.

Mancktelow, N.S., and Pavlis, T.L. 1994. Fold-fault relationships in low-angle detachment systems. Tectonics, **13**: 668-685.

Martignole, J. 1986. Some questions about crustal thickening in the central part of the Grenville Province. *In* The Grenville Province. *Edited by* J.M. Moore, A. Davidson, and A.J. Baer. Geological Association of Canada, Special Paper 31, pp. 327-340.

Martignole, J., and Pouget, P. 1993. Contrasting zoning profiles in high-grade garnets: evidence for the allochthonous nature of a Grenville Province terrane. Earth and Planetary Science Letters, **120**: 177-185.

McDougall, I., and Harrison, T.M. 1988. Geochronology and thermochronology by the $^{40}Ar/^{39}Ar$ method. Oxford University Press, New York, 212pp.

McEachern, S.J., and van Breemen, O. 1993. Ages of deformation within the Central Metasedimentary Belt boundary thrust zone, southwest Grenville Orogen: constraints on the collision of the mid-Proterozoic Elzevir terrane. Canadian Journal of Earth Sciences, **30**: 1155-1165.

McMullin, D.W.A., Berman, R.G., and Greenwood, H.J. 1991. Calibration of the SGAM thermobarometer for pelitic rocks using data from phase-equilibrium experiments and natural assemblages. Canadian Mineralogist, **29**: 889-908.

Mezger, K., Hanson, G.N., and Bohlen, S.R. 1989*a*. U-Pb systematics of garnet: dating the growth of garnet in the late Archean Pikwitonei granulite domain at Cauchon and Natawahunan Lakes, Manitoba, Canada. Contributions to Mineralogy and Petrology, **101**: 136-148.

Mezger, K., Hanson, G.N., and Bohlen, S.R. 1989*b*. High-precision U-Pb ages of metamorphic rutile: application to the cooling history of high-grade terranes. Earth and Planetary Science Letters, **96**: 106-118.

Mezger, K., Rawnsley, C.M., Bohlen, S.R., and Hanson, G.N. 1991*a*. U-Pb garnet, sphene, monazite, and rutile ages: implications for the duration of high-grade metamorphism and cooling histories, Adirondack Mts., New York. Journal of Geology, **99**: 415-428.

Mezger, K., van der Pluijm, B.A., Essene, E.J., and Halliday, A.N. 1991*b*. Synorogenic collapse: a perspective from the middle crust, the Proterozoic Grenville orogen. Science, **254**: 695-698.

Mezger, K., Essene, E.J., van der Pluijm, B.A., and Halliday, A.N. 1993. U-Pb geochronology of the Grenville orogen of Ontario and New York: constraints on ancient crustal tectonics. Contributions to Mineralogy and Petrology, **114**: 13-26.

Miller, E.L., Gans, P.B., and Garing, J. 1983. The Snake range décollement: an exhumed mid-Tertiary brittle-ductile transition. Tectonics, **2**: 239-263.

Moore, J.M. 1986. Introduction: the 'Grenville problem' then and now. *In* The Grenville Province. *Edited by* J.M. Moore, A. Davidson, and A.J. Baer. Geological Association of Canada, Special Paper 31, pp. 1-11.

Moore, J.M., and Thompson, P.H. 1980. The Flinton Group: a late Precambrian metasedimentary succession in the Grenville Province of eastern Ontario. Canadian Journal of Earth Sciences, **17**: 1686-1707.

Mueller, R.F. 1967. Mobility of the elements in metamorphism. Journal of Geology, **75**: 565-581.

Nadeau, L. 1990. Tectonic, thermal and magmatic evolution of the Central Gneiss Belt, Huntsville region, southwestern Grenville orogen. Ph.D. thesis, Carleton University, Ottawa, Ontario.

Nadeau, L., and Hanmer, S. 1992. Deep-crustal break-back stacking and slow exhumation of the continental footwall beneath a thrusted marginal basin, Grenville orogen, Canada. Tectonophysics, **210**: 215-233.

Nadeau, L., and van Breemen, O. 1993. The Montauban Group and La Bostonnais complex: arc magmatism ca. 1.4 Ga in the Grenville Province, Quebec. Geological Survey of Canada Current Activities Forum, Program with Abstracts, p. 5.

Needham, T.W. 1987 Geological setting of two metagabbroic bodies, central Britt domain, southwestern Grenville Province, Ontario. *In* Current research. Geological Survey of Canada, Paper 87-1A, pp. 597-603.

Needham, T.W. 1992. The metamorphic evolution of the Frederick Inlet metagabbros, southwestern Grenville Province, Ontario, Canada. M.Sc. thesis, Queens University, Kingston, Ontario.

Newton, R.C. 1983. Geobarometry of high-grade metamorphic rocks. American Journal of Science, **A283**: 1-28.

Nier, A.O., Thompson, R.W., and Murphy, B.F. 1941. The isotopic constitution of lead and the measurement of geologic time III. Physical Review, **60**: 112-116.

Nyman, M.W., Karlstrom, K.E., Kirby, E., and Graubard, C.M. 1994. Mesoproterozoic contractional orogeny in western North America: evidence from ca. 1.4 Ga plutons. Geology, **22**: 901-904.

Owen, J.V., Rivers, T., and Gower, C.F. 1986. The Grenville Front on the Labrador coast. *In* The Grenville Province. *Edited by* J.M. Moore, A. Davidson, and A.J. Baer. Geological Association of Canada, Special Paper 31, pp. 95-106.

Parrish R.R. 1990. U-Pb dating of monazite and its application to geological problems. Canadian Journal of Earth Sciences, **27**: 1431-1450.

Passchier, C.W., and Simpson, C. 1986. Porphyroclast systems as kinematic indicators. Journal of Structural Geology, **8**: 831-843.

Passchier, C.W., Myers, J.S., and Kroner, A. 1990. Field geology of high-grade gneiss terrains. Springer-Verlag, New York, New York.

Passchier, C.W., ten Brink, C.E., Bons, P.D., and Sokoutis, D. 1993. δ objects as a gauge for stress sensitivity of strain rate in mylonites. Earth and Planetary Science Letters, **120**: 239-245.

Pattison, D.R.M., and Bégin, N.J. 1994. Zoning patterns in orthopyroxene and garnet in granulites: implications for geothermometry. Journal of Metamorphic Petrology, **12**: 387-410.

Petrakakis, S. 1986. Metamorphism of high-grade gneisses from the Moldanubian zone, Austria, with particular reference to the garnets. Journal of Metamorphic Geology, **4**: 323-344.

Platt, J.P. 1983. Progressive refolding in ductile shear zones. Journal of Structural Geology, **5**: 619-622.

Platt, J.P., and Vissers, R.L.M. 1989. Extensional collapse of thickened continental lithosphere: a working hypothesis for the Alboran Sea and Gibraltar arc. Geology, **17**: 540-543.

Poldervaart, A. 1956. Zircon in rocks. 2. Igneous rocks. American Journal of Science, **254**: 521-554.

Prevec, S.A. 1992. U-Pb age constraints on early Proterozoic mafic magmatism from the southern Superior and western Grenville Provinces, Ontario. *In* Radiogenic Age and Isotopic Studies: Report 6. Geological Survey of Canada, Paper 92-2, pp. 97-106.

Ramsay, J G 1967. Folding and fracturing of rocks. McGraw-Hill Book Company, New York, New York, 568pp.

Ramsay, J G. 1980. Shear zone geometry: a review. Journal of Structural Geology, **2**: 83-99.

Reinhardt, J., and Kleeman, U 1994. Extensional unroofing of granulitic lower crust and related low-pressure, high-temperature metamorphism in the Saxonian Granulite Massif, Germany. Tectonophysics, **238**: 71-94.

Reynolds, S.J., and Lister, G.S. 1987. Structural aspects of fluid-rock interactions in detachment zones. Geology, **15**: 362-366.

Ridley, J. 1986. Parallel stretching lineations and fold axes oblique to a shear displacement direction - a model and observations. Journal of Structural Geology, **8**: 647-653.

Ridley, J. 1989. Vertical movement in orogenic belts and the timing of metamorphism relative to deformation. *In* Evolution of Metamorphic Belts. *Edited by* J.S. Daly, R.A. Cliff, and B.W.D. Yardley. Geological Society Special Publication, no. 43, pp. 103-115.

Ridley, J., and Casey, M. 1989. Numerical modeling of folding in rotational strain histories: Strain regimes expected in thrust belts and shear zones. Geology, **17**: 875-878.

Rivers T., and Nunn, G.A.C. 1985. A reassessment of the Grenvillian orogeny in western Labrador. *In* The Deep Proterozoic Crust in the North Atlantic Provinces. *Edited by* A.C. Tobi and J.L.R. Touret. NATO Advanced Studies Institute, Series C, vol. 158, pp. 163-174.

Rivers, T., and Chown, E.H. 1986. The Grenville orogen in eastern Quebec and western Labrador - definition, identification and tectonometamorphic relationships of autochthonous, parautochthonous, and allochthonous terranes. *In* The Grenville Province. *Edited by* J.M. Moore, A. Davidson, and A.J. Baer. Geological Association of Canada, Special Paper 31, pp. 31-50.

Rivers, T., Martignole, J., Gower, C.F., and Davidson, A. 1989. New tectonic divisions of the Grenville Province, southeast Canadian Shield. Tectonics, **8**: 63-84.

Rivers, T., van Gool, J.A.M., and Connelly, J.N. 1993. Contrasting tectonic styles in the northern Grenville Province: implications for the dynamics of orogenic fronts. Geology, **21**: 1127-1130.

Sanderson, D.J. 1982. Models of strain variation in nappes and thrust sheets. a review. Tectonophysics, **88**: 201-233.

Sanderson, D.J., and Marchini, W.R.D. 1984. Transpression. Journal of Structural Geology, **6**: 449-458

Schärer, U., Krogh, T.E., and Gower, C.F. 1986. Age and evolution of the Grenville Province in eastern Labrador from U-Pb systematics in accessory minerals. Contributions to Mineralogy and Petrology, **94**: 438-451.

Schau, M., Davidson, A., and Carmichael, D.M. 1986. Granulites and granulites. Geological Association of Canada - Mineralogical Association of Canada Annual Meeting, Field Trip 6: Guidebook, 36 pp.

Schwerdtner, W.M. 1987. Interplay between folding and ductile shearing in the Proterozoic crust of the Muskoka- Parry Sound region, central Ontario. Canadian Journal of Earth Sciences, **24**: 1507-1525.

Schwerdtner, W.M., and Waddington, D.H. 1978. Structure and lithology of Muskoka - southern Georgian Bay region, central Ontario. *In* Toronto '78 Field Trips Guidebook. *Edited by* A.L. Currie and W.O. Mackasey. Geological Association of Canada - Mineralogical Association of Canada Annual Meeting, pp. 204-212.

Scott, D.J., Machado, N., Hanmer, S., and Gariépy, C. 1993. Dating ductile deformation using U-Pb geochronology: examples from the Gilbert River Belt, Grenville Province, Labrador, Canada. Canadian Journal of Earth Sciences, **30**: 1458-1469.

Searle, M.P., and Rex, A.J. 1989. Thermal model for the Zanskar Himalaya. Journal of Metamorphic Geology, **7**: 127-134.

Selverstone, J., and Chamberlain, C.P. 1990. Apparent isobaric cooling paths from granulites: two counterexamples from British Columbia and New Hampshire. Geology, **18**: 307-310.

Shillibeer, H.A., and Cumming, G.L. 1956. The bearing of age determinations on the relation between the Keewatin and Grenville Provinces. *In* The Grenville Problem. *Edited by* J.E. Thomson. Royal Society of Canada, Special Publication 1, pp. 54-73.

Silver, L.T. 1969. A geochronological investigation of the anorthosite complex, Adirondack Mountains, New York. *In* Origin of Anorthosite and related Rocks. *Edited by* Y.W. Isachsen. New York State Museum and Science Service, Memoir 18, pp. 233-251.

Simpson, C., and Schmid, S.M. 1983. An evaluation of criteria to deduce the sense of movement in sheared rocks. Geological Society of America Bulletin, **94**: 1281-1288.

Spear, F.S., Hickmott, D.D., and Selverstone, J. 1990. Metamorphic consequences of thrust emplacement, Fall Mountain, New Hampshire. Geological Society of America Bulletin, **102**: 1344-1360.

Spotts, J.H. 1962. Zircon and other accessory minerals in the Coast Range Batholith, California. Geological Society of America Bulletin, **73**: 1221-1240.

Stacey, J.S., and Kramers, J.D. 1975. Approximation of terrestrial lead isotope evolution by a two-stage model. Earth and Planetary Science Letters, **26**: 207-221.

Steiger, R.H., and Wasserburg, G.J. 1969. Comparative U-Th-Pb systematics in 2.7 x 10^9 yr. plutons of different geologic histories. Geochimica et Cosmochimica Acta, **33**: 1213-1232.

Steiger, R.H., and Jäger, E. 1977. Subcommission on geochronology: conventions on the use of decay constants in geo- and cosmochronology. Earth and Planetary Science Letters, **36**: 359-362.

Stockwell, C.H. 1982. Proposal for time classification and correlation of Precambrian rocks and events in Canada and adjacent areas of the Canadian Shield; Part 1: A time classification of Precambrian rocks and events. Geological Survey of Canada, Paper 80-19, 135 pp.

Thomas, A., Nunn, G.A.C., and Krogh, T.E. 1986. The Labradorian Orogeny: evidence for a newly identified 1600 to 1700 Ma orogenic event in Grenville Province crystalline rocks from central Labrador. *In* The Grenville Province. *Edited by* J.M. Moore, A. Davidson, and A.J. Baer. Geological Association of Canada, Special Paper 31, pp. 107-117.

Thompson, A.B., and Ridley, J.R. 1987. Pressure-temperature-time (P-T-t) histories of orogenic belts. *In* Tectonic Settings of Regional Metamorphism. *Edited by* E R Oxburgh, B.W.D. Yardley, and P.C. England. Philosophical Transactions of the Royal Society, London, **A321**, pp. 27-45.

Tilton, G.R., Wetherill, G.W., Davis, G.L., and Bass, M.N 1960. 1000 million year old minerals from the eastern United States and Canada. Journal of Geophysical Research, **65**: 4173-4179.

Tracy, R.J. 1982. Compositional zoning and inclusions in metamorphic minerals. *In* Characterization of Metamorphism through Mineral Equilibria. *Edited by* J.M. Ferry. Mineralogical Society of America, Reviews in Mineralogy, vol. 10, pp. 355-397.

Tracy, R.J., Robinson, P., and Thompson, A.B. 1976. Garnet composition and zoning in the determination of temperature and pressure of metamorphism, central Massachusetts. American Mineralogist, **61**: 762-775.

Treloar, P.J., Broughton, R.D., Williams, M.P., Coward, M.P., and Windley, B.F. 1989. Deformation, metamorphism and imbrication of the Indian plate, south of the Main Mantle Thrust, north Pakistan. Journal of Metamorphic Geology, **7**: 111-125.

Tuccillo, M.E., Essene, E.J., and van der Pluijm, B.A. 1990. Growth and retrograde zoning in garnets from high-grade metapelites: implications for pressure-temperature paths. Geology, **18**: 839-842.

Tuccillo, M.E., Mezger, K., Essene, E.J., and van der Pluijm, B.A. 1992. Thermobarometry, geochronology and the interpretation of P-T-t data in the Britt domain, Ontario Grenville orogen, Canada. Journal of Petrology, **33**: 1225-1259.

Tucker, R.D., Råheim, A., Krogh, T.E., and Corfu, F. 1987. Uranium-lead zircon and titanite ages from the northern portion of the Western Gneiss Region, south-central Norway. Earth and Planetary Science Letters, **81**: 203-211.

van Breemen, O., and Davidson, A. 1988. Northeast extension of Proterozoic terranes of mid-continental North America. Geological Society of America Bulletin, **100**: 630-638.

van Breemen, O., and Davidson, A. 1990. U-Pb zircon and baddeleyite ages from the Central Gneiss Belt. *In* Radiogenic Age and Isotopic Studies: Report 3. Geological Survey of Canada, Paper 89-2, pp. 85-92.

van Breemen, O., and Hanmer, S. 1986. Zircon morphology and U-Pb geochronology in active shear zones: studies on syntectonic intrusions along the northwest boundary of the Central Metasedimentary Belt, Grenville Province, Ontario. *In* Current research. Geological Survey of Canada, Paper 86-1B, pp. 775-784.

van Breemen, O., Davidson, A., Loveridge, W.D., and Sullivan, R.W. 1986. U-Pb zircon geochronology of Grenville tectonites, granulites and igneous precursors, Parry Sound, Ontario, *In* The Grenville Province. *Edited by* J.M. Moore, A. Davidson, and A.J. Baer. Geological Association of Canada, Special Paper 31, pp. 191-207.

van Breemen, O., Henderson, J.B., Loveridge, W.D., and Thompson, P.H. 1987. U-Pb zircon and monazite geochronology and zircon morphology of granulites and granite from the Thelon Tectonic Zone, Healey Lake and Artillery Lake map areas, N.W.T. *In* Current research, part A. Geological Survey of Canada, Paper 87-1A, pp. 783-801.

van der Pluijm, B.A., and Carlson, K.A. 1989. Extension in the Central Metasedimentary Belt of the Ontario Grenville: timing and tectonic significance. Geology, **17**: 161-164.

van Schmus, W.R., Bickford, M.E., and Turek, A. 1993. Middle Proterozoic basement of the eastern mid-continent. American Association of Petroleum Geologists Hedberg Research Conference, Ann Arbor, Michigan, Program with Abstracts, pp. 131-133.

Vernon, R.H. 1977. Relationships between microstructures and metamorphic assemblages. Tectonophysics, **39**: 439-452.

Wanless, R.K., and Lowdon, J.A. 1961. Isotopic age measurements on coeval minerals and mineral pairs. *In* Age Determinations by the Geological Survey of Canada; Report 2, Isotopic Ages. Geological Survey of Canada, Paper 61-17, pp. 119-124.

Wardle, R.J., Rivers, T., Gower, C.F., Nunn, G.A.C., and Thomas, A. 1986. The northeastern Grenville Province: new insights. *In* The Grenville Province. *Edited by* J.M. Moore, A. Davidson, and A.J. Baer. Geological Association of Canada, Special Paper 31, pp. 13-29.

Wasserburg, G.J., and Hayden, R.J. 1955. A^{40}-K^{40} dating. Geochimica et Cosmochimica Acta, **7**: 51-60.

Watson, E.B., and Harrison, T.M. 1983. Zircon saturation revisited: temperature and composition effects in a variety of crustal magma types. Earth and Planetary Science Letters, **64**: 295-304.

Wayne, D.M., and Sinha, A.K. 1988. Physical and chemical response of zircons to deformation. Contributions to Mineralogy and Petrology, **98**: 109-121.

We nicke, B. 1985. Uniform-sense normal simple shear of the continental lithosphere. Canadian Journal of Earth Sciences, **22**: 108-125.

Wheeler, J. 1987. The determination of true shear senses from the deflection of passive markers in shear zones. Journal of the Geological Society of London, **144**: 73-77.

Wheeler, J., and Butler, R.W.H. 1994. Criteria for identifying structures related to true crustal extension in orogens. Journal of Structural Geology, **16**: 1023-1027.

White, D.J., Easton, R.M., Culshaw, N.G., Milkereit, B., Forsyth, D.A , Carr, S., Green, A.G., and Davidson, A. 1994. Seismic images of the Grenville orogen in Ontario. Canadian Journal of Earth Sciences, **31**: 293-307.

White, J.C., and Flagler, P.A. 1992. Deformation within part of a major crustal shear zone, Parry Sound, Ontario: structure and kinematics. Canadian Journal of Earth Sciences, **29**: 129-141.

White, S.H., Burrows, S.E., Carreras, J., Shaw, N.D., and Humphreys, F.J. 1980. On mylonites in ductile shear zones. Journal of Structural Geology, **2**: 175-188.

Whitney, P.R., and McLelland, J.M. 1973. Origin of coronas in metagabbros of the Adirondack Mts., N.Y. Contributions to Mineralogy and Petrology, **39**: 81-98.

Willett, S., Beaumont, C., and Fullsack, P. 1993. Mechanical model for the tectonics of doubly vergent compressional orogens. Geology, **21**: 371-374.

Windley, B.F. 1986. Comparative tectonics of the western Grenville and the western Himalayas. *In* The Grenville Province. *Edited by* J.M. Moore, A. Davidson, and A.J. Baer. Geological Association of Canada, Special Paper 31, pp. 341-348.

Windley, B.F. 1989. Anorogenic magmatism and the Grenvillian orogeny. Canadian Journal of Earth Sciences, **26**: 479-489.

Wodicka, N. 1994. Middle Proterozoic evolution of the Parry Sound domain, southwest Grenville orogen, Ontario: structural, metamorphic, U/Pb, and $^{40}Ar/^{39}Ar$ constraints. Ph.D. thesis, Dalhousie University, Halifax, Nova Scotia.

Wynne-Edwards, H.R. 1972. The Grenville Province. *In* Variations in Tectonic Styles in Canada. *Edited by* R.A. Price, and R.J.W. Douglas. Geological Association of Canada, Special Paper 11, pp. 263-334.

Yoder, H.S., and Tilley, C.E. 1962. Origin of basalt magmas: an experimental study of natural and synthetic rock systems. Journal of Petrology, **3**: 342-352.